Statistical Modeling of Extreme Rainfall Processes in British Columbia

SUN-HEE LIM

Department of Civil Engineering & Applied Mechanics

McGill University, Montreal

May 2016

A thesis submitted to McGill University in partial fulfillment of the requirements of the degree of Master of Engineering in Civil Engineering

Table of Contents

ABSTRACT

Millions of people are still exposed to unanticipated extreme rainfall events, and their devastating effects extend from communities to the surrounding environment. The impact extends across borders, to both developed and developing nations, causing massive casualties and financial loss. Accurate estimation of such events, however, requires an elaborated investigation covering different parameters, since precipitation patterns can be so diverse depending on the regional Topographical condition and even more so with progressive climate change.

Prediction of extreme precipitations has been extensively studied and improved in recent years by various specialists from science and engineering. In particular, in current engineering practices for the estimation of extreme rainfall for design purposes, many probability models have been proposed for describing the distribution of this random variable. However, there is no general agreement as to which distribution should be used to provide the most accurate and most reliable design rainfall estimate.

In view of the above-mentioned issues, the overall objective of the present research is therefore to propose a general procedure for assessing the descriptive and predictive abilities of ten probability distributions that have been used in extreme rainfall frequency analyses. The feasibility of the proposed procedure was tested using available 5-minute, 1-hour, and 24-hour annual maximum rainfall data from a network of 11 raingage stations located in the British Columbia region in Canada. Two commonly used methods, the maximum likelihood and L-moment methods, were used for estimating the parameters of the selected probability models. On the basis of the assessment of the descriptive and predictive abilities of each model, the GNO, PE3 and GEV models were found the best choice for the selected daily and sub-daily annual maximum rainfalls. Despite the popular use of GEV in Canada, the GNO distribution was found to have more robust and accurate descriptive and predictive ability from this study. However, no one distribution consistently outperformed the others among those distributions, and it is impossible to choose one distribution as the best to represent the versatile rainfall pattern of BC.

The performance of the distribution models was not consistent with either the topographical or climatological condition of study stations. Yet it was evident that most distributions performed poorly with data sets with high skewness. However, it was difficult to define a pattern of skewness in data, as skewness can vary without relation to rainfall durations and climatological or Topographical condition. Using the proposed procedure for selecting the best distribution, the GNO, GEV and PE3 were found the best overall choice for its descriptive and predictive ability with annual maximum rainfall data in British Columbia.

RÉSUMÉ

De nos jours, des millions de personnes sont encore exposés à des événements climatiques extrêmes non-anticipés, et leurs effets dévastateurs affectent tout aussi bien les populations locales que leur milieu environnant. Leurs impacts s'étendent au delà des frontières, causant d'importants dégâts et de nombreuses victimes dans les pays en voie de développement autant que dans les pays développés. Une estimation exacte de tels événements requiert cependant un examen détaillé de nombreux paramètres à cause de la diversité du régime de précipitation qui dépend des conditions topographiques et également des effets croissants du changement climatique.

La prédiction des précipitations extrêmes a été largement étudiée et améliorée ces dernières années par de nombreux spécialistes, issus tout aussi bien du milieu de la recherche académique que des études d'ingénieurs. En particulier, dans le cadre des estimations de précipitations extrêmes pour le travail de conception en pratique, de nombreux modèles probabilistes ont été proposés afin de décrire au mieux la distribution de cette variable aléatoire. Il est cependant à noter qu'aucun consensus général n'existe quant à la meilleure distribution qui devrait être utilisée afin d'obtenir les estimations de précipitations les plus précises et fiables.

En vue des limites actuelles mentionnées ci-dessus, l'objectif principal de ce projet de recherche est de proposer une procédure générale pour évaluer des capacités descriptive et prédictive de dix distributions probabilistes qui sont fréquemment utilisées dans l'analyse fréquentielle des précipitations extrêmes. L'applicabilité de la procédure ainsi proposée a été évaluée en utilisant les séries annuelles de précipitation maximale disponibles (maximum 5-minutes, 1-heure, 24-

heures) d'un réseau de 11 stations météorologiques situées dans la région de la Colombie Britannique au Canada. Deux méthodes d'estimation populaires – le maximum de vraisemblance et les L-moments – ont été utilisées afin d'estimer les paramètres des modèles probabilistes retenus. Suite à l'évaluation de la capacité descriptive et prédictive de chaque modèle, les modèles GNO, PE3 et GEV ont été

identifiés comme étant les plus performants en utilisant les données climatiques journalières et de durées plus courtes. Malgré l'usage répandu du modèle GEV au Canada, il a été constaté que le modèle GNO produisait généralement de meilleurs résultats descriptifs et prédictifs. Il est cependant à noter, qu'aucune distribution ne s'est distinguée systématiquement des autres, il est donc impossible de considérer l'une de ces distributions comme étant la meilleure pour décrire globalement les précipitations en Colombie Britannique.

Il a également été constaté que la performance des différents modèles de précipitation n'était pas corrélée aux conditions climatiques ou topographiques des stations météorologiques étudiées. Il a été toutefois évident, que la plupart des modèles étaient peu performants lorsque les échantillons présentaient une forte asymétrie. A noter qu'il a été impossible d'identifier un modèle qui serait mieux à même de décrire de tels échantillons, les variations de l'asymétrie n'étant pas corrélées aux durées de précipitation, ou aux conditions climatiques et topologiques.

En se basant sur la procédure proposée afin de sélectionner la meilleure distribution, les modèles GNO, GEV et PE3 ont été reconnus comme étant les plus performants tout aussi bien dans leur adéquation descriptive que prédictive avec les données de pluies annuelles maximales en Colombie Britannique.

ACKNOWLEDGEMENT

I spent more than half of my life at school as a student so far, but it was nothing compare to past two years in McGill where I was constantly challenged and defeated many times. It was a tough journey that I couldn’t drag myself this far without help of my supervisor and colleagues.

With a profound respect, I sincerely appreciate the great support and advices from Professor Nguyen who would guide me to improve and focus on the thesis, when it seemed impossible to finish the work for me. He understood my needs when I was struggling, and allowed me to join a wonderful group of compassionate and intelligent colleagues, Huy, Sarah and Myeong-Ho. Working and studying with them inspired me and guided me to understand the various aspects of this topic.

I also want to thank the people in my office (MD398), who would welcome and help me no matter how rarely I appear to the office. Having them was enriching my days in school with the cultural and intellectual interactions we had.

Outside of school life, I would like to express my sincere appreciation to my close group of friends for always being there and hearing me out. I was truly a lucky girl to live in the beautiful Montreal with them.

And thanks to my family for their unconditional love and support for every steps I made in my life.

I would also like to express my sincere gratitude to *mon ami* DMJ for translating the Abstract for this thesis, and encouraging me to believe in myself.

Last but not least, thanks to my Mango the ginger tabby for being there for me, rain or shine.

ABBREVIATION

AMP	Annual Maximum Precipitation
BEK	Beta-K
BEP	Beta-P
GEV	Generalized Extreme Value
GLO	Generalized Logistic
GNO	Generalized Normal
GPA	Generalized Pareto
GUM	Gumbel
LP3	Log-Pearson Type III
PE3	Pearson Type III
WAK	Wakeby
RMSE	Root Mean Square Error
RRMSE	Relative Root Mean Square Error
MAE	Maximum Absolute Error
CC	Correlation of Coefficient

SUMMARY OF FIGURES

SUMMARY OF TABLES

I. INTRODUCTION

Over the years, it has been observed that the frequency and intensity of severe storms have increased over many different regions in the world, and this increasing trend is expected to continue as the effects of climate change become more pronounced (Canada 2013). Information on the variability of precipitation amounts and frequency of occurrences is hence critical that can help mitigate the impacts caused by storms and floods in many different sectors such as agriculture, economic, environmental regimes, public health, etc. The estimation of extreme rainfalls or flood peak discharges, consequently, has been extensively investigated based on statistical frequency analysis of maximum precipitations or maximum streamflow records.

1.1 Statement of Problems

The challenge of estimating extreme events in hydrology comes from the problems in interpretation of historical records of hydrologic events in terms of future probabilities of occurrence. Model projections of future precipitations can vary greatly, depending on the quality of the data used to estimate the frequency and intensity of extreme precipitations and the length of the available historical rainfall record. Uncertainty of data samples usually involves the quality of data, including missing data, inadequate record length or no data at ungauged sites. Data quality is of less concern with the improvement in technology, yet can be a critical drawback for developing nations.

From an engineering stand point, the main problem is to determine a suitable probability model that could accurately describe the distribution of existing extreme rainfall values and could provide the most accurate prediction of future extreme rainfall estimates. Despite the long history of investigation and various distribution models introduced, there is no single generally accepted model. This is only natural, as rainfall patterns can vary even within the same region depending on its topographical and climatic conditions. Therefore, it is necessary to compare the performance of various available distributions for a given region and for different local climatic features.

1.2 Current Practice

In order to perform rainfall frequency analysis, extreme rainfall events are first extracted from the available historical rainfall time series. Generally, there are two common methods for this extraction (WMO 2009a, 2009b): annual maximum series (AMS) and partial duration series (PDS). The AMS are obtained by extracting only the maximum extreme value of each year, while the PDS (also known as peaks over threshold data) are achieved by extracting all the extreme values exceeding a certain selected threshold. The PDS model often covers a wider range of extreme events and offers a more complete description of the rainfall process since it relies on the analysis of both the magnitude and the time of arrival of peaks compared to the AMS model (Lang et al. 1999). However, difficulties are present regarding the subjective choice of the threshold value and also the arrival pattern of the extreme events. Hence, the AMS models are more popular in practice due to its simpler structure and can be constructed in an objective manner (Lang et al. 1999). The present research thus deals with the AMS only.

A number of different probability distributions and parameter estimation methods have been used and proposed in the past for representing extreme rainfalls (Chow 1964, Hosking et al. 1997, Rao et al. 2000, Stedinger et al. 1993, WMO 2009a). However, there is still no general agreement as to which distribution(s) should be used. The selection of a proper model thus depends mainly on the characteristics of observed rainfall data at a particular site. In practice, a number of popular distributions are often selected and compared for their performances by different studies for different regions. As the choice varies, each country adopts different distribution models for describing extreme rainfall distribution such as: Gumbel for Canada, GLO for the UK and PE3 for the US.

1.3 Outline of the Thesis

General assessment procedure is presented to investigate and compare the performance of ten different probability models in order to determine the best model that could provide the most accurate estimates of extreme rainfall. In detail, Beta-K (BEK), Beta-P (BEP), Generalized Extreme Value (GEV), Generalized Logistic (GLO), Generalized Normal (GNO), Generalized Pareto (GPA), Gumbel (GUM), Log-Pearson Type III (LP3), Pearson Type III (PE3), and Wakeby (WAK), are assessed in terms of their descriptive and predictive abilities to represent the distribution of annual maximum rainfall. In Chapter 2, the basic statistical theory was described for the selected distributions based on the literature reviews. Various graphical and numerical criteria were introduced in Chapter 3 as the methodology of this study for evaluating the performance of the probability models. Those methods were chosen to measure the descriptive and predictive ability of each distribution model to the data. Chapter 4 presents the application of the suggested procedure to a total of 33 AMP datasets for 5-minute, 1-hour, and 24-hour rainfall durations, from a network of 11 raingages located in British Columbia in Canada. Analysis was conducted focusing on the descriptive and predictive ability of each distribution, and the result was presented and discussed in Chapter 5. In particular, their performance on the right tail region was the major concern, since it contains the key information for engineering design and practice (El Adlouni et al. 2008). The conclusion and recommendations are presented in Chapter 6.

II. LITERATURE REVIEW

2.1 Probability Distributions and Parameter Estimation Methods

In hydrology, many random variables correspond to maximum rainfall or flood years must be considered, in order to find the distribution that can most closely describe the variability of rainfall pattern. Unfortunately, there is no one dominant distribution that can globally fit the precipitation pattern of any locations. Every region has a different climate pattern with various geographic and atmospheric conditions, which consequently cause an extensive range of rainfall patterns. Hence, the investigation has become more regional, and each region has applied different distribution models for its engineering practice. For instance, Canada and Australia have implemented GEV distribution for the precipitation frequency analysis; the US has been using Log-Pearson type 3 distribution; and the UK has been using Generalized Logistics distribution. In this study, 10 distribution models were grouped based on the nature of each distribution as proposed by Rao et al. (2000).

2.1.1 Generalized Normal Distribution

From the Normal and related distributions family, the Generalized Normal distribution (GNO) was investigated with the L-moments proposed by Hosking et al. (1997). It is the re-parameterized version of the three-parameter log-normal distribution (LN3). The log-normal distribution is one of the widely used distributions with a long history of use in water resources. Yet the logarithms of random variables are generally not normally distributed. The location factor is introduced, hence, with which the distribution performs more flexibly to fit with the data. Unfortunately, the log-normal distribution has its limit on fitting expectations in real situations where many times the data could show different trends (Martin et al. 2009). Still the fitting methods of the log-normal distribution are found robust and reliable, especially when the distribution of the logarithms departs from normality (Stedinger 1980). The modified version has several advantages over the LN3 since it includes both LN3 distribution with positive and negative skewness and the normal distribution as the special case with zero skewness (Hosking et al. 1997).

2.1.2 Gamma Family : Pearson type 3 and Log-Pearson type 3

Most popular distribution models in the Gamma family are the Pearson type-3 (PE3) and Log-Pearson type-3 (LP3) distributions, particularly for hydrological frequency analysis. The PE3 is also known as three-parameter gamma distribution, and it was the first skewed distribution applied in hydrology for extreme events. The LP3 has been extensively used as a base method for flood frequency analysis in the US. Performance of LP3 can widely vary depending on the parameter estimation applied. The LP3 has a tendency to give low upper bounds of the precipitation magnitude, which is undesirable for analyzing maximum events (Cunnane 1978). Their statistical behavior was compared by Bobee et al. (1977) using several long-term records of annual flood flows. In their study, LP3 was preferred, when the L-moments was applied; yet PE3 was preferred with the method of moments (MOM). Matalas et al. (1973) found that the method of maximum likelihood estimation (MLE) is less biased and viable than MOM estimates.

2.1.3 Extreme value distribution : Gumbel and Generalized Extreme Value

Gumbel (GUM) is known as a type I extreme value (EV) distribution with two parameters, as its shape factor is zero. It can be introduced especially when an independent set of daily rainfall data is with the exponential like upper tail. As shown in Table 1, the density function of GUM is similar to that of the log-normal distribution. GEV is an incorporated general mathematical form of type I, II and III extreme value distributions for maxima. GEV requires the location factor, which describes the shift of a distribution in a given direction on the horizontal axis. The shape of the GEV distribution depends on the value of the shape factor (k). It is similar to that of GUM when $|k|<0.3$; it has a thicker right hand tail when $k<0$; and it has a thinner right hand tail when $k>0$. As described in the equation in Table 1, the shape factor is expressed with the skewness of a data set, which indicates where the data are concentrated. The

GEV distribution has been commonly used to describe the probability distribution of annual extreme rainfall events, and for the construction of IDF curves (Schaefer 1990).

2.1.4 Generalized Logistic Distribution

The Generalized Logistic (GLO) distribution is a three-parameter distribution introduced by Hosking et al. (1997). Its parameterization and behaviour on tails with large values are similar to the GEV distribution. The distribution has been used for flood frequency analysis in the United Kingdom since Robson et al. (1999) suggested.

2.1.5 Wakeby distributions: Wakeby (5) and Generalized Pareto

The Wakeby distribution (WEK) has five parameters, and was first introduced by Houghton (1978) to be used for the flood frequency analysis. His interpretation was that the conventionally used three-parameter distributions lack in kurtosis for any given skew (Houghton 1978). Cunnane (1978) explained that distributions with two parameters have smaller standard error, but larger bias than distributions with three or higher number of parameters, especially in a small sample size. However, distributions with higher number of parameters, such as Wakeby, often have large standard errors which result in wide confidence intervals for the quantile estimates (Ahmad et al. 1988). Furthermore, the distribution function doesn't have an explicit form, which causes problems in parameter estimation by MLE methods (Öztekin 2011). In this study, the L-moments method was used for the WEK distribution as proposed by (Hosking et al. 1997). The Generalized Pareto Distribution (GPA) is a special case of WEK and exponential distribution with three-parameters. It has a good potential for the analysis of flood peaks because of its inherent properties (Öztekin 2005). It has been studied by many scholars, and applied to the distribution of peaks over thresholds of rainfall series using the maximum likelihood method for estimation. Yet Hosking et al. (1987) found either MOM or PWM was more reliable than the MLE estimates for Generalized Pareto. GPA was found to give a better fit to large peaks, which is why it performed well for modeling the data from the peaks over threshold series. It is especially useful for describing events that exceed a specified lower bound, such as all floods above a threshold or daily flows above zero.

2.1.6 Generalized Beta-Distributions : Beta-K and Beta-P

Beta-K (BEK) and Beta-P (BEP) are two distinct special cases of Generalized Beta distribution. These distributions appear to provide reasonable descriptions of commonly encountered types of measurements, and to possess desirable computational properties. BEK is a re-parameterized version of a distribution termed the Kappa distribution (Mielke et al. 1974). BEK was found to provide an excellent computational facility with order statistic distributions. The two alike distributions could be distinguished by the specific restriction on the parameter γ as shown in Table 1. BEK is suggested to be the best fit to annual data on extreme events but BEP is better fit to partial-duration data (Wilks 1993). In this study, the maximum likelihood method is applied for the parameter estimation of both BEK and BEP.

Table 1 Summary of distributions

No	Distribution	PDF $f(x)$ and CDF $F(x)$	Parameters and Parameter Estimates
1	**GNO**	$f(x) = \frac{e^{ky - \frac{y^2}{2}}}{\alpha\sqrt{2\pi}}; \quad y = \begin{cases} -\frac{1}{k}\log\left[1 - \frac{k(x-\xi)}{\alpha}\right]; k \neq 0 \\ \frac{x-\xi}{\alpha}; k = 0 \end{cases}$	$\alpha = \frac{\lambda_2 k e^{-k^2/2}}{1-2\phi\left(-\frac{k}{\sqrt{2}}\right)}; \xi = \lambda_1 - \frac{\alpha}{k}\left(1 - e^{k^2/2}\right)$ $\phi(x) = \sqrt{\frac{1}{2\pi}} e^{-1/2 x^2}$; [1]k= $-\tau_3 \times \frac{E_0 + E_1\tau_3^2 + E_2\tau_3^4 + E_3\tau_3^6}{1 + F_1\tau_3^2 + F_2\tau_3^4 + F_3\tau_3^6}$
2, 3	**PE3 & LP3**	$\gamma = 0$, then the distribution is Normal and $-\infty \le x < \infty$, $f(x) = \phi\left(\frac{x-\mu}{\sigma}\right); \ F(x) = \Phi\left(\frac{x-\mu}{\sigma}\right)$ $\gamma > 0$, then $\xi \le x < \infty$, $f(x) = \frac{(x-\xi)^{\alpha-1} e^{-\frac{x-\xi}{\beta}}}{\beta^\alpha \Gamma(\alpha)}; F(x) = G(\alpha, \frac{x-\xi}{\beta})/\Gamma(\alpha)$ $\gamma < 0$, then $-\infty \le x < \xi$, $f(x) = \frac{(x-\xi)^{\alpha-1} e^{-\frac{\xi-x}{\beta}}}{\beta^\alpha \Gamma(\alpha)}; F(x) = 1 - G(\alpha, \frac{\xi-x}{\beta})/\Gamma(\alpha)$	If $\gamma \neq 0$: $\alpha = \frac{4}{\gamma^2}, \beta = \frac{1}{2}\sigma\lvert\gamma\rvert, \xi = \mu - \frac{2\sigma}{\gamma}$ Re-parameterized by Hosking and Wallis (1997) : $\gamma = 2\alpha^{-1/2} sign(\tau_3), \ \mu = \lambda_1 ; \sigma = \lambda_2 \pi^{1/2} \alpha^{-1/2} \Gamma(\alpha)/\Gamma\left(\alpha + \frac{1}{2}\right)$ If $0 < \lvert\tau_3\rvert < \frac{1}{3}$, let $z = 3\pi{\tau_3}^2$: $\alpha \approx \frac{1 + 0.2906z}{z + 0.1882z^2 + 0.0442z^3}$ If $\frac{1}{3} \le \lvert\tau_3\rvert < 1, let\ z = 1 - \lvert\tau_3\rvert$: $\alpha \approx \frac{0.36067z - 0.59567z^2 + 0.25361z^3}{1 - 2.78861z + 2.56096z^2 - 0.77045z^3}$

----

[1] This approximation of the shape parameter k has relative accuracy of about 2.5×10^{-6} for $\lvert\tau_3\rvert \le 3$. Note that k is a function of τ_3 only. E and F are coefficients of approximation given by (Hosking et al. 1997).

4, 5	**GEV, GUM**	$f(x)=\frac{1}{\alpha}e^{-(1-k)y-e^{-y}};\ y=\begin{cases}-\frac{1}{k}\log\left[1-\frac{k(x-\xi)}{\alpha}\right]; & k\neq 0\\ \frac{x-\xi}{\alpha} \quad ; & k=0\end{cases}$ $x(F)=\begin{cases}\xi+\dfrac{\alpha[1-(-\log F)^k]}{k}; & k\neq 0\\ \xi-\alpha\log(-\log F) \quad ; & k=0\end{cases}$	$k=7.8590c+2.9554c^2\ ;\ \alpha=\frac{\lambda_2 k}{(1-2^{-k})\Gamma(1+k)}$ $\xi=\lambda_1-\frac{\alpha[1-\Gamma(1+k)]}{k}\ ;\ c=\frac{2}{3+\tau_3}-\frac{\log 2}{\log 3}$
6	**GLO**	$f(x)=\dfrac{\alpha^{-1}e^{-(1-k)y}}{(1+e^{-y})^2},\ y=\begin{cases}-k^{-1}log\left\{1-\dfrac{k(x-\xi)}{\alpha}\alpha\right\}, & k\neq 0\\ \dfrac{x-\xi}{\alpha}\alpha, & k=0\end{cases}$ $F(x)=\frac{1}{(1+e^{-y})}\ ;\ x(F))=\begin{cases}\xi+\alpha\frac{\{(1-F)/F\}^k}{k}, & k\neq 0\\ \xi-\alpha log\left\{\frac{(1-F))}{F}\right\}, & k=0\end{cases}$	$k=-\tau_3\ ;\ \alpha=\frac{\lambda_2 sing(k\pi)}{k\pi}$ $\xi=\ \lambda_1-\ \alpha\left(\dfrac{1}{k}-\dfrac{\pi}{\sin\,(k\pi)}\right)$
7	**GPA**	$f(x)=\dfrac{1}{\alpha}e^{-(1-k)y}, \qquad y=\begin{cases}-\dfrac{1}{k}\log\left(1-\dfrac{k(x-\xi)}{\alpha}\right); & k\neq 0\\ \dfrac{x-\xi}{\alpha}\ ; & k=0\end{cases}$ $F(x)=1-e^{-y};\ x(F)=\begin{cases}\xi+\frac{\alpha[1-(1-F)^k}{k}\ ; & k\neq 0\\ \xi-\alpha\log(1-F); & k=0\end{cases}$ Range: $\xi\leq x\leq\xi+\frac{\alpha}{k}$ if $k>0$; $\xi\leq \mathrm{x}<\infty$ if $\mathrm{k}\leq 0$	$k=\dfrac{1-3\tau_3}{1+\tau_3}$ $\alpha=(1+k)(2+k)\lambda_2$ $\xi=\lambda_1-(2+k)\lambda_2$

8	**WAK**	$x(F) = \xi + \frac{\alpha}{\beta}\{1-(1-F)^{\beta}\} - \frac{\gamma}{\beta}\{1-(1-F)^{-\delta}\}$ $\begin{cases} \xi \le x < \infty \; if \; \delta \ge 0 \; and \; \gamma > 0 \\ \xi \le x \le \xi + {}^{\alpha}/_{\beta} - {}^{\gamma}/_{\delta} \; if \; \delta < 0 \; or \; \gamma = 0 \end{cases}$	[2]β and γ are the roots of a quadratic equation: $\alpha = \frac{(1+\beta)(2+\beta)(3+\beta)\{(1+\delta)\lambda_2 - (3-\delta)\lambda_3\}}{4(\beta+\delta)}$ $\gamma = -\frac{(1-\delta)(2-\delta)(3-\delta)\{(1-\beta)\lambda_2 - (3+\beta)\lambda_3\}}{4(\beta+\delta)}$ $\xi = \lambda_1 - \frac{\alpha}{(1+\beta)} - \frac{\gamma}{(1-\delta)}$
9	**BEK**	$f(x) = \left(\frac{\alpha\theta}{\beta}\right)\left(\frac{x}{\beta}\right)^{\alpha\theta-1}\left[1+\left(\frac{x}{\beta}\right)^{\theta}\right]^{-(\alpha+1)}$; $(x > 0, \alpha > 0, \beta > 0, \theta > 0)$; $x(F) = \beta[\frac{F^{1/\alpha}}{(1-F^{1/\alpha})}]^{1/\theta}$	$\alpha_j = n\left\{\sum_{i=1}^{n} \ln[1+\left(\frac{x_i}{\beta_{j-1}}\right)^{-\theta_{j-1}}]\right\}^{-1}$; $\beta_j = \frac{1}{n}(1+\alpha_j{}^{-1})\beta_{j-1}\sum_{i=1}^{n}[1+\left(\frac{x_i}{\beta_{j-1}}\right)^{-\theta_{j-1}}]^{-1}$ $\theta_j = n\left\{\sum_{i=1}^{n}\frac{[\left(\frac{x_i}{\beta_j}\right)^{\theta_{j-1}} - \alpha_j\Big]\ln(\frac{x_i}{\beta_j})}{1+(\frac{x_i}{\beta_j})^{\theta_{j-1}}}\right\}^{-1}$
10	**BEP**	$f(x) = \left(\frac{\alpha\theta}{\beta}\right)\left(\frac{x}{\beta}\right)^{\theta-1}\left[1+\left(\frac{x}{\beta}\right)^{\theta}\right]^{-(\alpha+1)}$ $(x > 0, \alpha > 0, \beta > 0, \theta > 0)$ $x(F) = \beta[(1-F))^{-\frac{1}{a}a} - 1]^{1/\theta}$	$\alpha_j = n\left\{\sum_{i=1}^{n} \ln[1+\left(\frac{x_i}{\beta_{j-1}}\right)^{-\theta_{j-1}}]\right\}^{-1}$ $\beta_j = \frac{1}{n}(1+\alpha_j)\beta_{j-1}\sum_{i=1}^{n}[1+\left(\frac{x_i}{\beta_{j-1}}\right)^{-\theta_{j-1}}]^{-1}$

----

[2] $\beta \; and - \delta$ are the roots of the following quadratic equation; β being the larger of the 2 roots:

$(N_2C_3 - N_3C_2)z^2 + (N_1C_3 - N_3C_1)z + (N_1C_2 - N_2C_1) = 0$

		$\theta_j = n\left\{\sum_{i=1}^{n}\frac{\left[\alpha_j\left(\frac{x_i}{\beta_j}\right)^{\theta_{j-1}}-1\right]\ln\left(\frac{x_i}{\beta_j}\right)}{1+\left(\frac{x_i}{\beta_j}\right)^{\theta_{j-1}}}\right\}^{-1}$
[3]**L-moments**	$\lambda_1 = L1 = M_{100}$ $\lambda_2 = L2 = 2M_{110} - M_{100}$ $\lambda_3 = L3 = 6M_{120} - 6M_{110} + M_{100}$ $\lambda_4 = L4 = 20M_{130} - 30M_{120} + 12M_{110} - M_{100}$	$L - CV : \tau_2 = \frac{L2}{L1}$

----

[3] The following L-moments are defined in Cunnane C. (1989).

2.2 Summary of Parameter Estimation Methods

The performance of each distribution varies depending on the parameter estimation method used. Historically, various parameter estimation methods have been applied and investigated. Regarding the estimation of the distribution parameters, some common procedures include the method of moments, the maximum likelihood method, the method of L-moments (Chow, 1964; Kite, 1977; Hosking, 1990; Stedinger et. al., 1993; Hosking and Wallis, 1997; and Rao and Hamed, 2000), and the method of non-central moments (NCMs; Nguyen et al., 2002b). These approaches differ in the weights they give to different elements in the selected data set. The moments or cumulants from an observed data set have been commonly used to summarize the statistical characteristics. Despite its long establishment in statistics, however, it is still difficult to explain how moments of third and higher order describe the shape of a distribution (Hosking 1989). In this research, two common parameter estimation methods were used for the 10 distribution models selected, namely the maximum likelihood method and L-moments. Method of moments is still used in some practices, but it is often less accurate than other estimation methods.

2.2.1 L-moments

L-moments were derived from Probability Weighted Moments (PWM) and defined by Cunnane (1989) as shown in *Table 1* of this report. Vogel (1995) emphasized the significant impact of the theory of L-moments on the overall understanding of extreme events. L-moments is unbiased way of parameter estimation, and it was possible to discriminate against the behaviour of skewed hydrologic data regardless of the biased parent population (Vogel 1995). Hosking et al. (1997) successfully proved the advantage of L-moments over conventional moments for its ability to characterize a wider range of distributions, and to be more robust to the presence of outliers in the data. Hence, L-moments is the main parameter estimation method adopted and applied for 8 distribution models in this research. There are additional theoretical advantages in Lmoments compared to the other conventional moments methods suggested by Hosking et al. (1997):

i) L-moments can characterize a wider range of distributions;
ii) It can be more robust to the presence of outliers in the data;
iii) It is less subject to bias in estimation;
iv) It approximates their asymptotic normal distribution more closely in finite samples; and
v) L-moments can be more accurate in small samples than the maximum likelihood methods.

2.2.2 Maximum Likelihood Method (MLE)

The maximum likelihood method yields asymptotically optimal estimators of the parameters for some distributions; however, it often involves tedious computation, and is sensitive to computational techniques. Moment-based parameter estimation methods were investigated for BEK and BEP by Murshed et al. (2011). It was found that MLE was an effective parameter estimation method for light-tailed samples, whereas L-moments was effective for small and skewed samples. For extreme precipitations, it is rare to find low skewed data sets. However, the performance of both MLE and L-moments was similar when the sample data was moderate and high in numbers (Murshed et al. 2011). Considering the findings of Murshed et al. (2011), L-moments is preferred for its more tractable and less frequent recourse to iterative procedures, but the approach for BEK and BEP requires tedious calculations. Therefore, in this research, the maximum likelihood method was used with the computation procedure established by Mielke et al. (1974).

III. METHODOLOGY

Assessing the descriptive ability of a distribution is an important step to evaluate the suitability of a probability distribution for describing the observed data. There are various criteria to evaluate the descriptive ability of a probability distribution such as graphical display and statistical goodness-of-fit tests. The predictive ability of the distribution is a vital characteristic to be evaluated, as the accuracy of rainfall prediction depends on it. Often it is known that the more parameters a distribution has, the better it will fit to the data. As mentioned in section 2.2, however, parameter estimation can be challenging when distribution parameters are more than three, like Wakeby. The extrapolation could result in a critically inaccurate prediction, as the distribution may be too rigid (Vogel 1995). A nonparametric data resampling scheme is required in order to evaluate the predictive ability of distributions (Tao et al. 2002).

3.1 Evaluation of the Probability Distribution Descriptive Ability

3.1.1 Graphical Display

Graphical display is a simple yet effective way to compare the observed and theoretical values. In this report, the quantile-quantile (Q-Q) plots and L-moment ratio diagrams are adopted to visualize the adequacy of the fitted distributions.

3.1.1.1 Quantile-Quantile Plot

The Q-Q plot is a plot of the quantiles of the observed (x_i) and the theoretical (y_i) values. In order to produce the theoretical values, the plotting position and CDF of the observed values were computed. The plotting position of the non-exceedence probability ($p_{i:n}$) was computed for each observed value (x_i). Cunnane (1978) introduced a plotting position formula similar to that of Blom; which was acceptable for normal probability plots. It was widely used for plotting flow duration and flood-frequency curves, and by Canadian and some European hydrologists (Helsel et al. 2002). The Cunnane plotting position formula was implemented for this report for its ability to yield approximately unbiased quantiles for a wide range of distributions (Cunnane 1978).

$$p_{i:n} = (i - 0.4)/(n + 0.2) \tag{3.1}$$

Afterwards, an assumed cumulative distribution function (CDF) was applied to the plotting positions for each distribution. The theoretical values (y_i) were computed from the CDF as follows:

$$y_{i:n} = F^{-1}(p_{i:n)}) \tag{3.2}$$

The Q-Q plot was plotted with the observed values (x_i) against the theoretical values (y_i) on normal graph with a 1:1 straight line extending from the origin. In theory, all points should fall on the 1:1 line if the assumed CDF perfectly replicated the distribution pattern of the observed data.

3.1.1.2 L-moment Ratio Diagram

Another way to measure goodness-of-fit is to construct an L-moment ratio diagram. L-moment ratio diagrams allow simple comparison between the sample estimates of L-skewness and L-kurtosis and their theoretical counterparts from selected distributions (Asquith 1998). Both L-skewness and L-kurtosis are expressed with L-moments as shown in equation 3.3 and 3.4 below.

$$L - Skewness: \ \tau_3 = \frac{L3}{L2} \tag{3.3}$$

$$L - Kurtosis: \ \tau_4 = \frac{L4}{L2} \tag{3.4}$$

L-moment ratio diagram is a plot of L-skewness against L-Kurtosis of the sample data set, which is plotted using continuous lines and points of known statistical distributions of interest. Some statistical distributions have predetermined relationships between L-Skewness and L-Kurtosis. In this method, the average ratio of study stations is assumed as representing the all station. The lines closest to the average ratio could be interpreted as the best fit distributions. However, the average ratio of study stations could not be always confirmed as a representative ratio to decide the best fit distribution. Another drawback of this method is that the predetermined ratio line is not available for all distribution models.

3.1.2 Numerical Assessment

Four numerical assessment criterias were considered in this study as graphical analysis cannot precisely describe the statistical significance of the fit, particularly with the large number of distribution models to compare. The following notations are used for this section:

$$\begin{cases} n = number\ \ of\ data \\ m = number\ \ of\ parameters \end{cases} \qquad \begin{cases} x_i = observed\ value \\ y_i = theoretical\ value \\ \bar{x} = average\ of\ observed\ value \\ \bar{y} = average\ of\ theoretical\ value \end{cases}$$

3.1.2.1 Root-mean-square error

The root-mean-square error (RMSE) is a popular method to measure the differences between observed and theoretical values, which are called residuals. As expressed in the formula below, RMSE represents the sample standard deviation of the differences between the observed and theoretical values. Hence, RMSE could be a good measure of accuracy to compare forecasting errors of different models for a particular variable (Hyndman et al. 2006).

$$RMSE = \left\{\sum \frac{(x_i - y_i)^2}{(n-m)}\right\}^{1/2} \tag{3.5}$$

However, RMSE gives heavy weighting to large errors that can obscure the true picture of the fit of a distribution. In hydrologic analysis, the right tail area can be sensitive to errors, resulting in a high RMSE, even though there is a good fit for the left and center areas of the distribution (Tao et al. 2002).

3.1.2.2 *Relative Root-mean-square error*

The relative root-mean-square error (RRMSE) is based on the relative errors between the observed and theoretical values, unlike RMSE. For RRMSE, each error is calculated in proportion to the size of the observations, hence reducing the influence of outliers and providing better picture of the overall fit of a distribution than RMSE (Tao et al. 2002). The magnitude of RRMSE tends to decrease with increasing sample size (Yu et al. 1994).

$$RRMSE = \left[\frac{1}{(n-m)}\sum\left\{\frac{(x_i-y_i)}{x_i}\right\}^2\right]^{1/2} \tag{3.6}$$

3.1.2.3 *Maximum Absolute Error*

The maximum absolute error (MAE) represents the largest absolute difference between the observed and computed values. Unlike the relative error, the absolute error describes how large the error is independent of the observed value. The formula of MAE is closely related to the Kolmogorov – Smirnov statistics test (Tao D.Q. et al. 2002).

$$MAE = \max\left(|x_i - y_i|\right) \tag{3.7}$$

3.1.2.4 *Correlation of Coefficient*

The correlation coefficient (CC) indicates the strength of the linear relationship between the observed and theoretical values. It has a range between -1 and 1; -1 indicates a perfect positive linear relationship, +1 indicates a perfect negative linear relationship, and 0 indicates no linear relationship. The reliability of the CC is questionable if the underlying relationship between observed and theoretical values is non-linear. The formula of CC used for the report is as follows:

$$CC = \frac{\sum\{(x_i - \bar{x})(y_i - \bar{y})\}}{\{\sum(x_i - \bar{x})^2 \sum(y_i - \bar{y})^2\}^{1/2}} \tag{3.8}$$

3.1.2.5 *Evaluation of Numerical Assessment (Ranking Scheme)*

After computing the four statistical tests, a ranking scheme is utilized to rank all the selected distributions. Ranking scores are assigned to each distribution according to the value computed for each criterion. The distribution with the lowest RMSE, RRMSE, MAE or highest CC is given a rank of 1 for this assessment category. In case of a tie, equal ranks are given to those corresponding distributions. Furthermore, for each numerical criterion, the overall rank associated with each distribution is computed by summing the individual ranks obtained for each of the study stations.

3.2 Evaluation of The Probability Distribution Predictive Ability

3.2.1 Bootstrap Method

One of main objectives of rainfall frequency analysis is in the prediction of future rainfall extremes by extrapolating beyond the existing data. In particular, the behavior of distributions for the extreme right tail area is important since it has the great impact on the accuracy of the prediction. The bootstrap method, first introduced by Efron et al. (1994) is a nonparametric approach of resampling technique. Underlying idea behind this method is that observed data, or the sample values, is the best resources to depend on, if the uncertainty could be estimated with statistical sampling procedure. The bootstrap model yields multiple synthetic samples, which are the same sizes as the observations (Efron et al. 1994). Most attractive feature of this method is that it is a powerful tool to describe the behavior of distribution only with the obtained sample values, even when the information about the true distribution is lacking. Moreover, the bootstrap method could conveniently assess the sampling uncertainty. Vogel (1995) found that the distribution of sample statistics computed from the bootstrap samples is a good representation of the respective distribution of the observed statistics. Hence, the bootstrap method was applied in this study in order to investigate the predictive ability of each distribution model, especially for the extreme values.

The method repeatedly draws, with replacement, n observations from the available data set of size N (N>n) and estimates the empirical distribution of sample statistic over all the subsamples. The basis of the bootstrap is that the batch to batch variations exhibited by different samples from a parent population can be simulated by repeatedly treating a single available a batch of data in a way that mimics the process of sampling from the parent population (Tao et al. 2002). It is found that the distribution of sample statistics computed from the bootstrap samples is a good representation of the respective distribution of the observed statistics (Vogel 1995).

In this study, the sampling characteristics of extrapolated right-tail quantiles were investigated using the bootstrap procedure. A total of one thousand bootstrap samples of size approximately half of the actual sample size were drawn with replacement form the observations. Each candidate distribution was fitted to the bootstrap samples and used to extrapolate the right-tail quantiles corresponding to the four largest observed precipitation amounts in the full data set.

3.2.2 Boxplots of Extrapolated Right Tail Quantiles

A boxplot is a concise graphical display depicting groups of numerical data through their quantiles. It effectively summarizes the distribution of a data set, such as central tendency, variability, symmetry and presence of outliers. Boxplots are often put side-by-side to visually compare and contrast groups of data. In this report, the modified boxplot was used. The size of the box indicates the robustness of each distribution's extrapolative ability. Large box height or whiskers imply high uncertainty in the estimation of these extreme values. If the observed values fall outside the box, then the distribution fitted to the bootstrap samples has overestimated or underestimated the true values and is therefore not reliable. The modified boxplots used for this report provide visual summaries of:

i) The middle line of the box (the sample mean);
ii) Half of box height (the standard deviation);
iii) Upper and lower whisker ends (the maximum and minimum of the sample);
iv) Red (x) marks indicating the four largest observed values.

IV. CASE STUDY (11 STATIONS IN BC)

4.1 DATA DESCRIPTION

4.1.1 Selection of Stations and Data

The study site was limited to the British Columbia (BC) area, where a total of 129 raingage stations are operated under the supervision of the Environment Canada. From these, 11 stations were selected for three rainfall durations: 5 minutes, 1 hour and 24 hours. In total, 33 datasets of annual maximum rainfall were analyzed for this study. The stations and data were selected from the archive of the Engineering Climate Datasets program under the Environment Canada, based on quality of the historical data and its length (Canada 2013). Adequate length of the data for over 40 years was adopted for this study to obtain reliable rainfall extremes. From previous studies on the frequency analysis of extreme rainfall events, 20 years of minimum data length was proposed as sufficient to determine a representative distribution by Vogel (1995).

Three rainfall durations were selected for their common use in both extreme event analysis and intensity duration frequency (IDF) analysis. Out of 11 study stations, four stations are located in the Victoria island; three stations are within the Greater Vancouver area; and the remaining four stations are scattered around the south of BC. Among all study stations, seven raingage stations are from airports. Raingages from airports are maintained well, so that result a good data quality with sufficient data length. Total number of missing data per stations ranged from none to one per dataset as summarized in Table 2 below.

TABLE 2 NUMBER OF MISSING DATA PER DATASET

	5min	1hr	24hr
Blue River A	0	0	1
Comox A	1	1	0
Mission West Abbey	0	0	0
Penticton A	1	0	0

Pitt Polder.	0	0	0
Prince George A	0	0	1
Terrace PCC	1	1	0
Tofino A	0	0	0
Vancouver Intl A	1	0	0
Victoria Intl A	0	0	0
Victoria Gonzales HTS	0	0	0

Table 3 below shows the name of each station with its corresponding Topographical coordination provided by the Environment Canada. The location of every station in BC is visually presented using QGIS with the geographic information provided by the GeoGratis (2014) in the map of Figure 1.

TABLE 3 LOCATION OF THE 11 CLIMATOLOGICAL STATIONS

Station No.	Climate ID	Station Name	Latitude	Longitude
1	1160899	Blue River A	52.12	-119.28
2	1021830	Comox A	49.72	-124.90
3	1105192	Mission West Abbey	49.15	-122.27
4	1126150	Penticton A	49.47	-119.60
5	1106180	Pitt Polder.	49.27	-122.63
6	1096450	Prince George A	53.88	-122.68
7	1068131	Terrace PCC	54.50	-128.62
8	1038205	Tofino A	49.08	-125.77
9	1108395	Vancouver Intl A	49.18	-123.18
10	1018621	Victoria Intl A	48.15	-123.43
11	1018610	Victoria Gonzales HTS	48.42	-123.33

4.1.2 Data Summary

Annual Maximum Precipitation (AMP) data of three durations are summarized for all 11 stations in Table 4. The data length of the 33 AMP data sets varied from 40 to 61 for each duration, and the average length of observations was around 46 years. The longest observation period was 61 years from Victoria Intl. A for both 1hr and 24hr durations; whereas the shortest observation period was 40 years from Tofino A. In total, 8 years of data were missing from 33 AMP data sets. The details of the annual maximum rainfall data for 11 raingage stations are summarized and presented in from Table 15 to 26 of Appendix 1.

TABLE 4 SUMMARY OF AMP DATA (5MIN, 1HR AND 24HR)

		5min	1hr	24hr
Maximum AMP	Station	Prince George A	Vancouver A	Tofino A
	Amount (mm)	15.2	38.6	228
Minimum AMP	Station	Terrace & Victoria G.	Terrace PCC	Penticton A
	Amount (mm)	1.0	3.6	15
Maximum Observation Period (years)		60	61	61
Minimum Observation Period (years)		40	40	41

The maximum AMP was from Prince George A for 5 min duration; Vancouver A for 1 hr; and Tofino A for 24hr. The minimum AMP was found from Terrace PCC and Victoria Gonzales HTC for 5 min duration; Terrace PCC for 1hr; and Penticton for 24hr. Meanwhile, the highest mean was from Prince George A for 5min, Tofino A for both 1hr and 24hr. There is no clear trend in skewness of the data sets, either by rainfall duration or locations of stations as shown in Table 5 below. The skewness of datasets increased with increase of duration for 6 stations, but the following 5 stations showed the largest skewness with 1hr dataset: Comox A, Terrace PCC, Tofino A, Vancouver Intl. A, and Victoria Gonzales HTS. The overall largest skewness was from Vancouver Intl. A for 1hr duration. And the lowest skewness was from Pit Polder for 24hr duration.

TABLE 5 SUMMARY OF THE SKEWNESS OF 33 AMP DATA SETS

	5min	1hr	24hr
Blue River A	2.93	1.69	0.53
Comox A	1.07	1.69	1.02
Mission West Abbey	1.19	1.18	0.75
Penticton A	1.91	1.64	1.37
Pitt Polder.	1.90	0.44	0.14
Prince George A	1.89	1.19	1.09
Terrace PCC	1.14	1.82	0.75
Tofino A	1.09	1.35	0.76
Vancouver Intl A	0.70	3.23	1.10
Victoria Intl A	1.13	1.50	1.85
Victoria Gonzales HTS	1.49	2.85	1.50
Average	**1.49**	**1.68**	**0.98**

*skewness above the average are marked in red.

4.1.3 Climate Classification of Stations

Climate classification of each station was investigated in relation to its precipitation pattern and Topographical condition (Climate-Data). In this report, the four Köppen Geiger classifications were used in order to summarize the climate patterns of the study sites as shown in Table 6: Continental, Mediterranean, Oceanic and Semi-arid Climate zones. The classification criteria were adopted by the Environment Canada. It is one of the most widely used climate classification systems based on the concept that the native vegetation is the best expression of climate. As shown in Table 6, it includes average temperature and precipitation of every station, as well as the seasonality of the precipitation.

Continental climate zone (DFb) includes the Blue River, Prince George and Terrace PCC, and it has about 5°C lower than other stations with less average precipitation amount. Penticton is classified as a semi-arid or stepped climate zone (Bsk), which is a region that generally receives precipitation below potential evaporation. This station had warm average temperature (9°C), but its average precipitation amount is the lowest among all stations (306mm). Oceanic Climate zone (Cfb) includes four following stations: Tofino A, Vancouver Intl A, Victoria Intl A and Victoria Gonzales HTS. All four stations in this zone have warm average temperatures, above 9°C, and their average precipitations ranges from 718mm to 1307mm. Oceanic Climate zone include Tofino A, Mission West Abbey and Pit Polder, which have similar average temperature as ones from Mediterranean Climate zone. However, their average precipitation amounts are much higher as ranging from 1488mm to 3160mm. Different precipitation and temperature pattern of each climate zone can be explained in relation to the topographical condition of study stations in BC in following section.

Table 6 Köppen Geiger Climate Classification and Weather Pattern (11 stations)

City	Station Name	Climate Classification		Avg. Temp.	Avg. Prep.	Driest month	Highest month
Blue River	Blue River A	**Dfb**[4]	Cold and temperate	4.5 °C	840 mm	April (44 mm)	December (96 mm)
Comox	Comox A	**Csb**[5]	Warm and temperate	9.4 °C	1307 mm	July (37 mm)	December (213 mm)
Mission	Mission West Abbey	**Cfb**[6]	Warm and temperate	9.6 °C	1721 mm	July (53 mm)	December (243 mm)
Penticton	Penticton A	**BSk**[7]	Cold and Stepped climate	9.0 °C	306 mm	October (17 mm)	June (33 mm)
Pitt Meadows	Pitt Polder	**Cfb**[6]	Mild, warm and temperate	9.7 °C	1488 mm	July (43 mm)	December (221 mm)
Prince George	Prince George A	**Dfb**[4]	Cold and temperate	4.1 °C	621 mm	April (27mm)	August (64 mm)
Terrace	Terrace PCC	**Dfb**[4]	Cold and temperate	6.4 °C	1458 mm	June (50 mm)	October (236 mm)
Tofino	Tofino A	**Cfb**[6]	Warm and temperate	9.4 °C	3160 mm	July (76 mm)	November (434 mm)
Vancouver	Vancouver Intl A	**Csb**[5]	Warm and temperate	9.9 °C	1283 mm	July (36 mm)	December (198 mm)
Victoria (city)	Victoria Intl A Victoria Gonzales	**Csb**[5]	Warm and temperate	9.8 °C	718 mm	July (17 mm)	December (212 mm)

[4] Cold (continental), without dry season, warm summer (continental or hemi-boreal climates)
[5] Temperate, Dry and warm Summer, (Mediterranean climates)
[6] Temperate, without dry season, warm summer (Maritime temperate climates or oceanic climates)
[7] Semi-Arid, steppe, cold

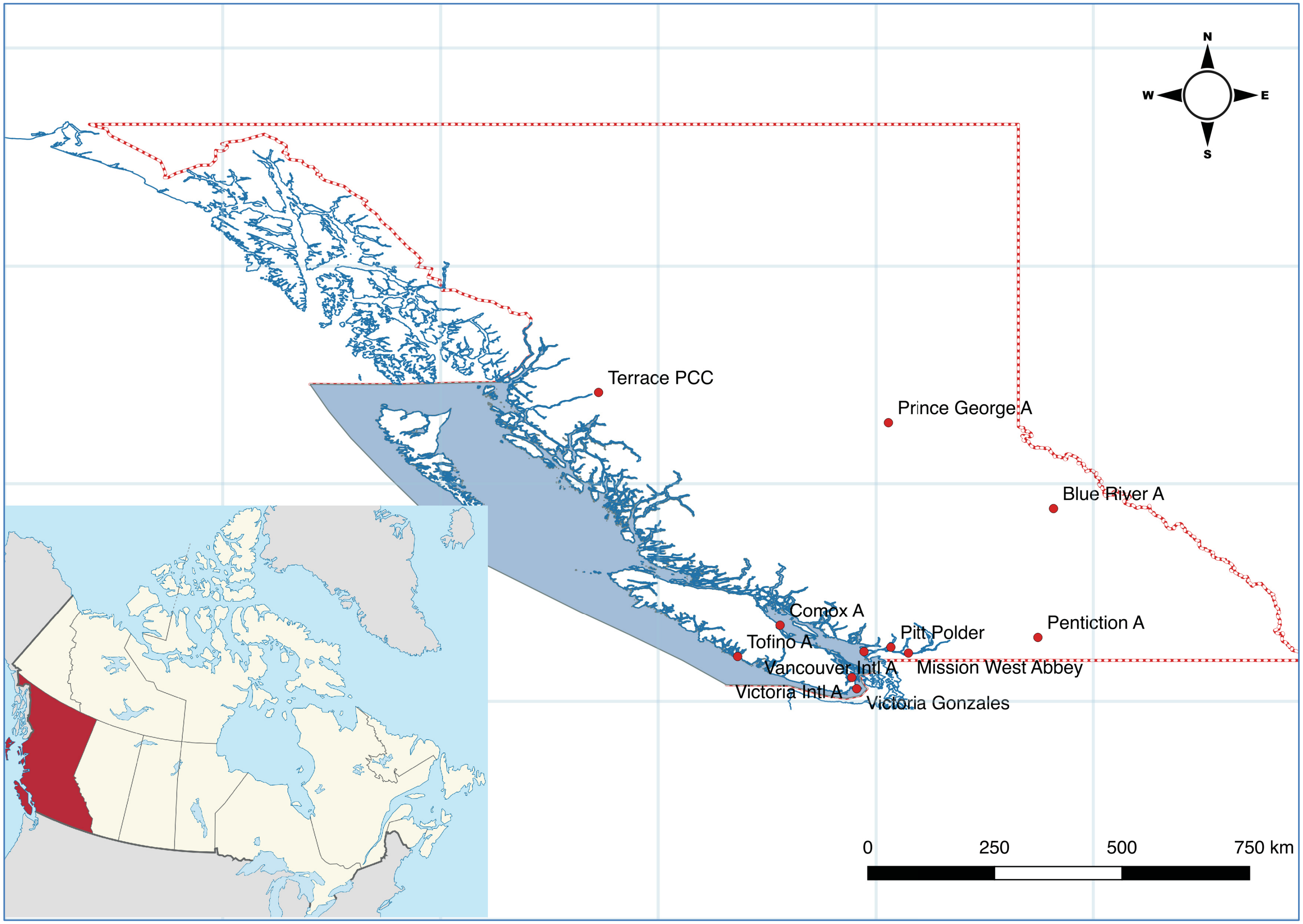

FIGURE 1 *LOCATION MAP OF CLIMATOLOGICAL STATION*

4.1.4 Topographical Conditions of BC in Relation to Rainfall Pattern

British Columbia could be divided into six distinctive areas as shown in Figure 2 below: South Coast, Tompson-Okanagan, Kootenays and Columbias, Central and Northern Interior and Northeast BC as described in (Klock et al. 2001). Among 11 study stations, 7 stations are in the South Coast area, 1 station each in the North Coast area, the Central & Northern Interior area, the Thompson-Okanagan area, and the Kootenays & Columbias. The topographical condition of each area is a vital piece of information to understand the precipitation pattern of each station along with its climate classification.

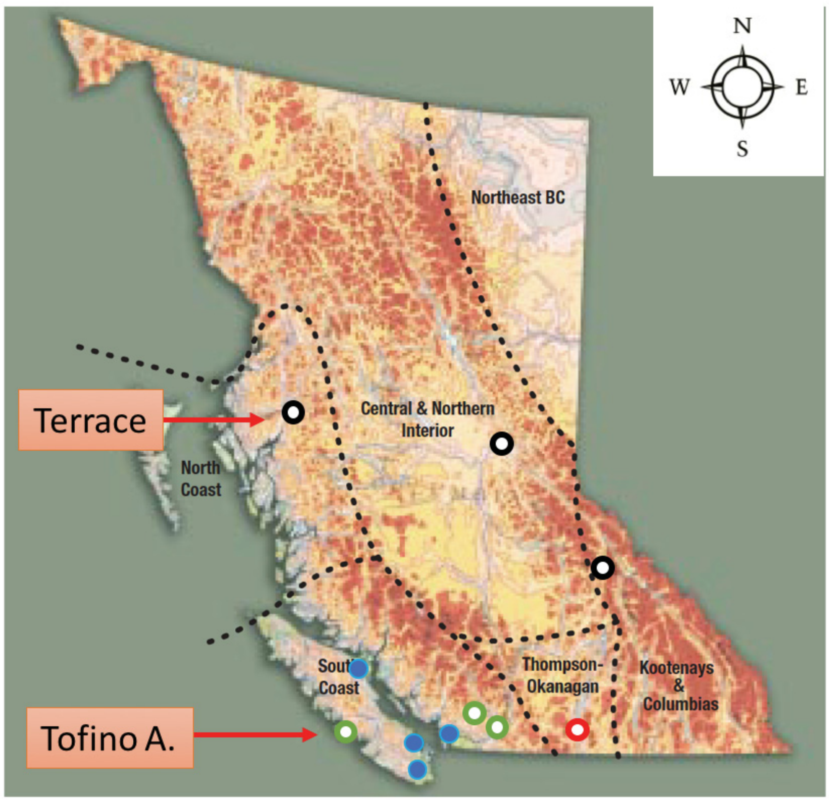

FIGURE 2 TOPOGRAPHY OF BRITISH COLUMBIA

Following the climate classifications from section 4.1.2, it is clear that Mediterranean and Oceanic Climate zones are the dominant climate patterns in the South Coast region as summarized in Table 7 below. Although the stations from these two climate zones are located close to each other, their precipitation pattern and amount are different from each other.

TABLE 7 GEOLOGICAL CONDITION OF STUDY STATIONS

Area	Stations	Climate Classification	
South Coast	Tofino A Mission West Abbey Pitt Polder	Cfb Cfb Cfb	Maritime temperate/Oceanic
	Comox A Vancouver Intl A Victoria Intl A Victoria Gonzales HTS	Csb Csb Csb Csb	Mediterranean
North Coast	Terrace PCC	Dfb	Continental
Central & Northern Interior	Prince George A	Dfb	Continental
Thompson-Okanagan	Penticton A	Bsk	Semi-arid, stepped
Kootenays & Columbias	Blue River A	Dfb	Continental

As shown in Figure 3, the weather pattern of this area is significantly affected by the mountains. The ocean edge of the South Coast is itself dominated by the Coast Mountains that seem to rise right out of the sea, and divide the moist coastal environment from the dry environment of the interior (Klock et al. 2001). The rainfall pattern of Vancouver Island is also affected by the Vancouver Island Mountains, which divide the east and west of the island. The total rainfall amount is two times higher in the west than east. It explains why the total rainfall amount significantly higher at the study stations in this region compared to the rest.

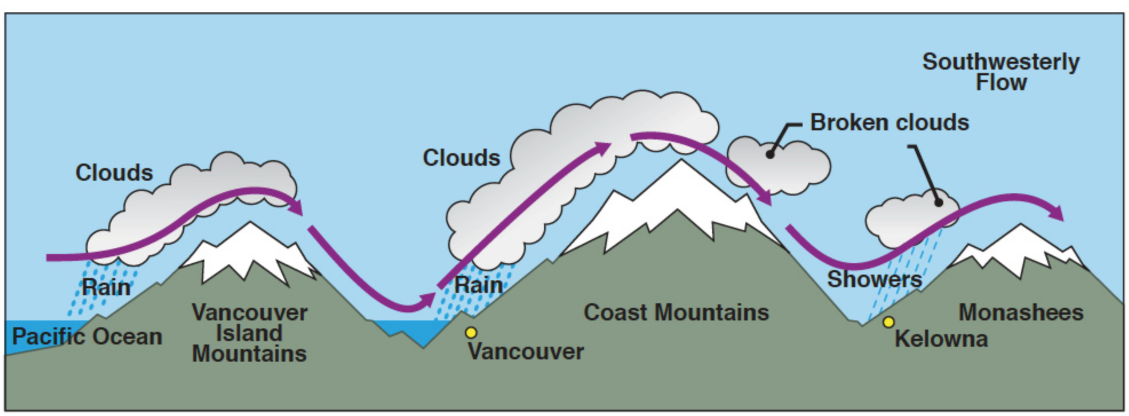

FIGURE 3 EFFECT OF TOPOGRAPHICAL CONDITION ON PRECIPITATION (BC)

The stations classified as Continental or Semi-arid Climate zones are located inland with less influence from the Pacific Ocean. Topographical conditions can vary depending on locations of each stations, even when they are classified as in a same climate zone as shown in Table 7. In particular, three stations from Continental Climate zone are scattered around to the North Coast, Central & Northern Interior and Kootenays & Columbias, where the Topographical condition can be very different. The North Coast, where Terrace PCC is located, is influenced by the ocean moderating the coastal temperature, but it can easily get cold due to outflow winds through the inland valleys, unlike the South Coast. During the winter, the clash between warmer coastal air and cold air flowing out of the interior can cause the extremely variable precipitation types. However, the Thompson-Okanagan area has a mixture of mountain and valleys, and its weather is controlled by the Coast Mountains located on the west of the area as shown in Figure 3. As most precipitation falls before the mountains, this area has a rather arid or semi-arid climate. During the summer, however, the Pacific High breaks down and widespread thunderstorms occur along the ridges. In Kootenays & Columbias area, the most prominent feature is the Rocky Mountains trench, where the low-lying areas tend to allow cold air to drain into them, creating high occurrences of fog. In the Central and Northern Interior area, the Central Interior Plateau has flattened terrain right next to the Rocky Mountains. This particular plateau can develop a significant convection. Therefore, moderate to heavy thunderstorms are common, especially in the Prince George area.

4.2 Data Analysis

4.2.1 Graphical Analysis

In this section, the standard boxplot, known as Tukey's schematic plot, was used to visualize the rainfall pattern. Boxplots are often put side-by-side to visually compare and contrast groups of data. It provides visual summaries of:

- The centerline of the box (the median)
- The box height (interquartile range)

- The relative size of box halves (quantile skew)
- The presence or absence of unusual values (“outside” and “far outside” values)

The particular feature of this version is that outlying values are distinguished from the rest of the plot. Interquartile range defines the box, and the whiskers are only extended to the last observation within one step beyond either end of the box (known as adjacent values). One step is 1.5 times the interquartile range or the height of the box (Helsel et al. 2002). Observations beyond the whisker lengths are marked with a red cross (+).

4.2.2 Analysis of Seasonality and Variability

Seasonality and variability of rainfall pattern is analyzed in this section for each station in relation to its topographical and climatological conditions discussed in previous section. In order to visualize the rainfall patterns of the 33 AMP data sets, the total monthly and annual precipitation data are presented in standard boxplot format as shown in Figure 6 and 7, respectively. For the visual comparison between stations, the Normals (or averages) of the monthly and annual total precipitation data for 30 years (1971-2000) are plotted and shown in Figure 4 and 5. The Normals are used as a reference for the seasonal monitoring of precipitation for basic public interest by the Government of Canada. The World Meteorological Organization recommends to countries to prepare the official 30 years normal periods and update it at the end of every decade (Canada 2013).

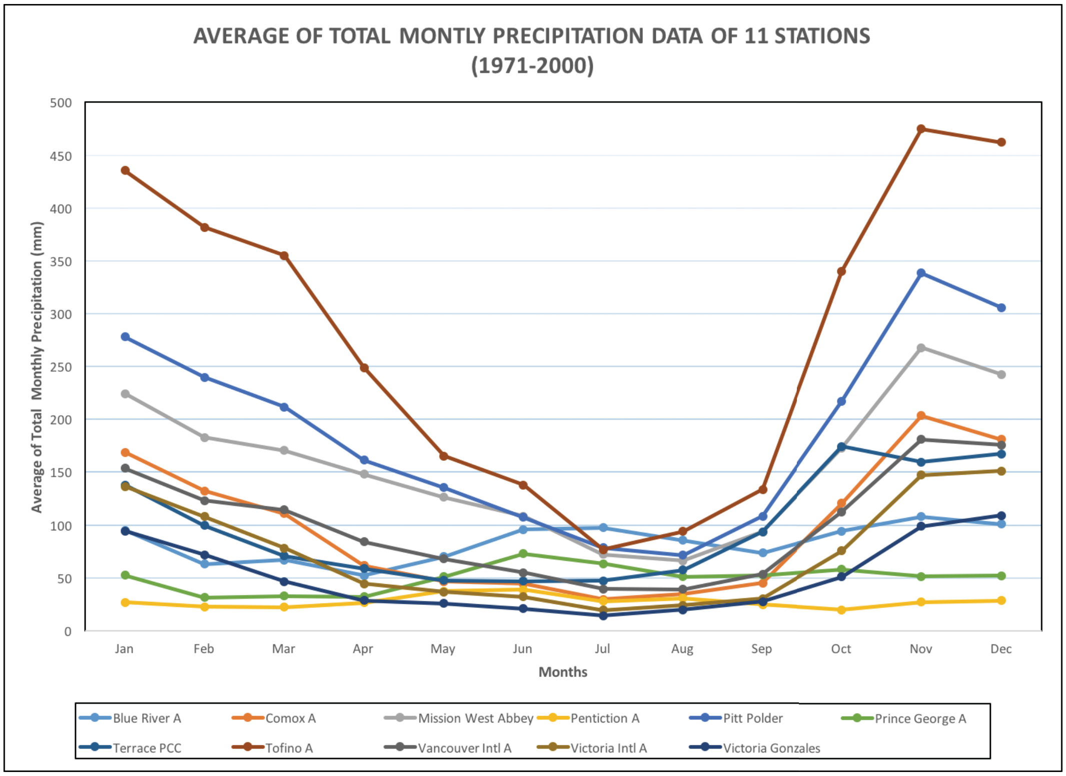

FIGURE 4 AVERAGE OF TOTAL MONTHLY PRECIPITATION DATA OF 11 STATIONS (1971-2000)

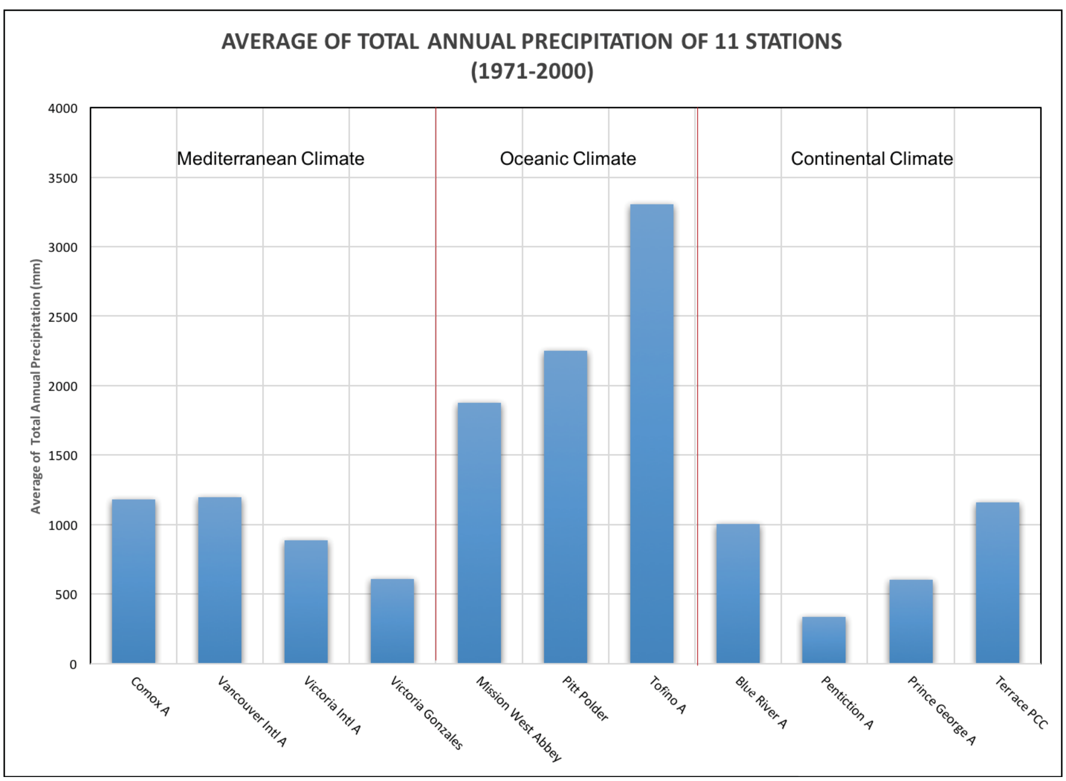

FIGURE 5 AVERAGE OF TOTAL ANNUAL PRECIPITATIONS OF 11 STATIONS (1971-2000)

The rainfall amount of most stations decreased from winter to summer as shown in Figure 6. However, three particular stations, Penticton A, Prince George A and Blue River A, showed the opposite trend with low average rainfall amounts; it increased until summer with a maximum in June or July. This pattern can be found from stations from Continental Climate zone located inland surrounded by mountains, with less influence from the Pacific Oceanic. The maximum annual total precipitation amount was found from Tofino A, where the variability was the largest. The large variability in rainfall amount can be explained by the location of the station, that is facing the Pacific Ocean with the Vancouver Island Mountains behind. Other stations from Oceanic Climate zone like Tofino, also showed much larger variability in monthly rainfall amounts. These stations showed higher rainfall in winter than summer as shown in Figure 6. While, stations from Mediterranean Climate zone showed similar seasonal rainfall pattern similar to the ones from Oceanic Climate zone with dry summer, yet their variability of monthly rainfall amount was much less. The similarity in seasonality and difference in variability of two climate zones could be explained by the topographical condition detailed in Figure 3 from previous section.

The minimum annual total precipitation amount was found from Penticton A, which had the smallest seasonality and variability. The rainfall pattern of Penticton A is due to its particular Topographical condition, that is a plateau to the west of the Rocky Mountains and to the east of the Coast Mountains, as described in Section 4.1.4. Stations inland showed inconsistent rainfall patterns, and it depended on the topographical condition of the area: flat terrain, near mountains or near the shore.

With the analysis above, the study stations can be categorized into three groups based on their climate classification and rainfall pattern as shown in Table 8 below. Group 1 includes the cities located nearby the Pacific Ocean mostly with Mediterranean climate; Group 2 includes the cities with large rainfall all year around yet more in winter than summer due to its Oceanic climate; while Group 3 includes cities with Continental climate with less overall rainfall and heavier rainfall in summer than winter. Terrace PCC showed a similar rainfall pattern as other cities in Group 1, although it is classified as a continental climate zone. And Penticton A is in Group 3 for its similar rainfall seasonality and variability as other stations in this group.

TABLE 8 STATION GROUPS BASED ON THE RAINFALL PATTERN

Group	Cities	Rainfall pattern	Climate class
Group 1	Comox A Victoria Intl. A Victoria Gonzales HTC Vancouver A	Overall moderate rainfall Heavy in winter Low in summer	Mediterranean climate
Group 2	Mission West Abbey Pitt Polder Tofino A	Overall heavy rainfall Heavy in winter Low in Summer	Oceanic/Maritime climate
Group 3	Blue River A Penticton A Prince George A Terrace PCC	Overall low rainfall amount Heavy in summer Low in Winter	Continental climate

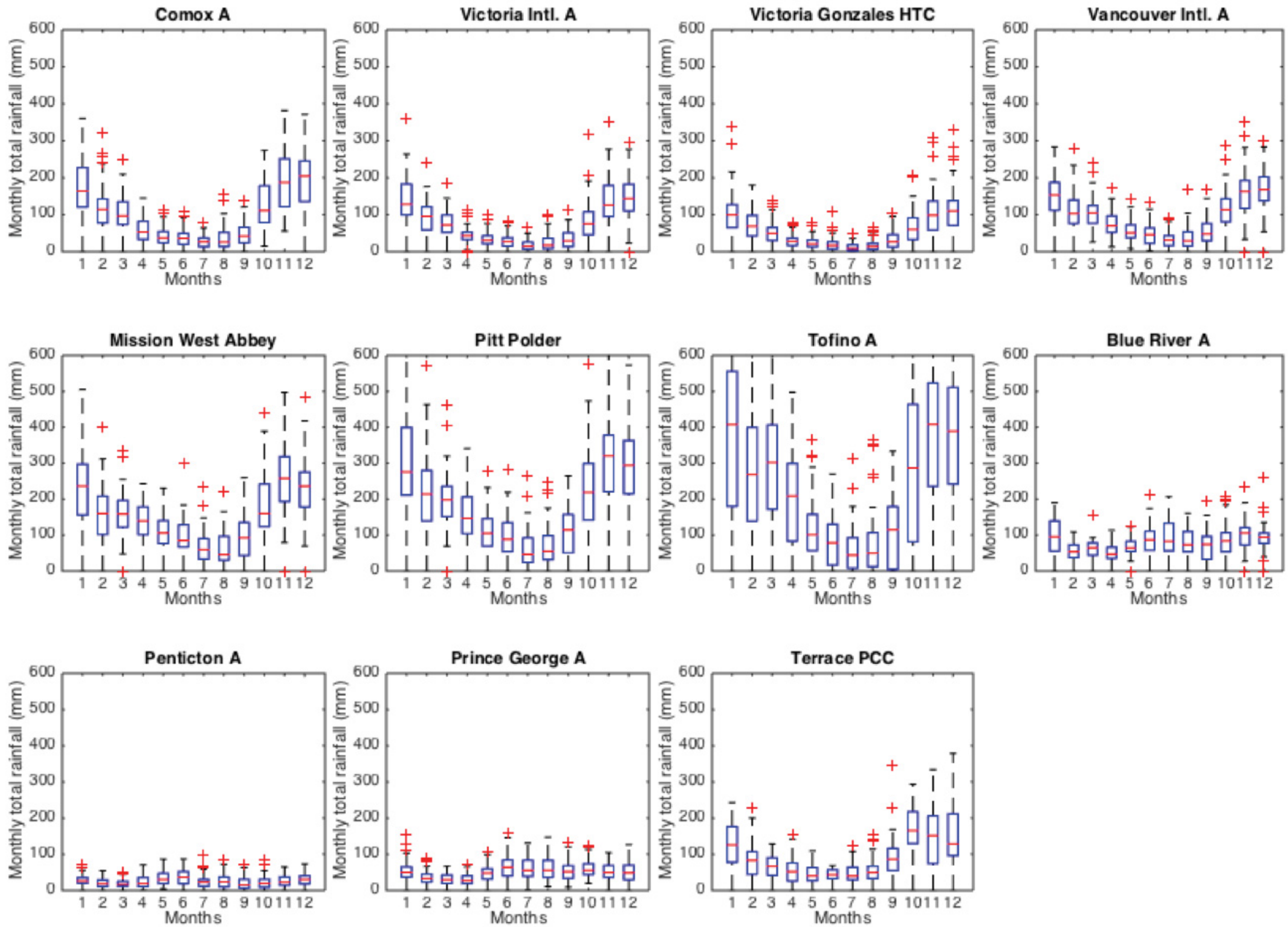

FIGURE 6 BOXPLOTS OF TOTAL MONTHLY PRECIPITATION (11 STATIONS)

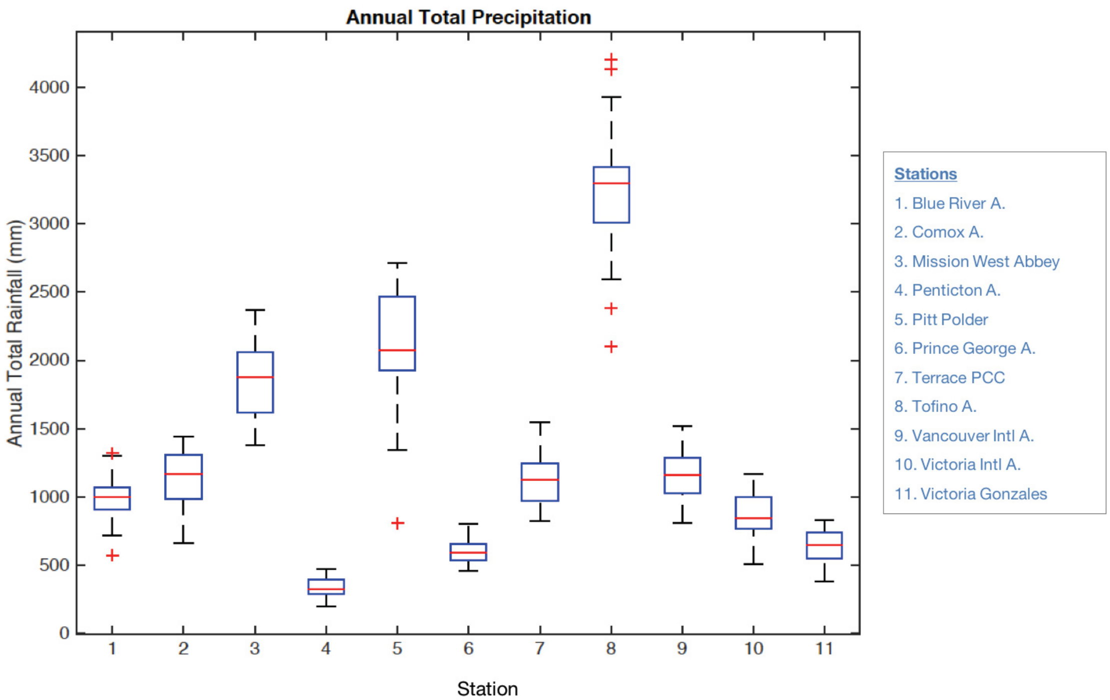

FIGURE 7 BOXPLOTS OF ANNUAL TOTAL PRECIPITATION

4.2.3 Analysis of Outliers and Extreme Values

Hydrologic historical data is a time series that usually shows stochastic, nonlinear, nonstationary, and multi-temporal scale characteristics. So it is important to detect any abnormality or disturbances that can cause difficulties in fitting a frequency distribution to the sample (Yu et al. 2014). Those errors could be due to the malfunctioning of instruments, inherent data change, operation error or other possible influencing factors. In order to detect those outliers and extremes, the standard box plot was used in this section. A value is referred to as an outlier if the following conditions hold (Mendenhall et al. 1991):

$$P^{75th} + 1.5\times(H\ spread) < X_{high\ outlier} < P^{75th} + 3.0\times(H\ spread) \quad (4.1)$$

$$P^{25th} - 1.5\times(H\ spread) < X_{high\ outlier} < P^{25th} - 3.0\times(H\ spread) \quad (4.2)$$

The *H spread* is equivalent to the interquantile range, or the difference between the 75th percentile and 25th percentile. One step is 1.5 times the interquantile range, and the outliers are outside of the whisker length, or one step away from the *H-spread.* The extremes are the ones beyond two steps away from the *H-spread*, and the following conditions hold:

$$X_{high\ extreme} > P^{75th} + 3.0\times(H\ spread) \tag{4.3}$$

$$X_{high\ extreme} < P^{25th} - 3.0\times(H\ spread) \tag{4.4}$$

The AMP of 11 study stations are presented in the standard boxplot format for 5min, 1hr and 24hr accumulation period in *Figure 8, 9 and 10*. The outliers are marked as the red cross (+), and the extremes are flagged with the red dot on top of the red cross. The boxplots for 5min and 1hr have many outliers, yet only one extreme is found from the 1hr boxplot from Vancouver Intl A. The 24hr boxplots has two extremes: one from Victoria Intl A and another from Victoria Gonzales HTS. It is evident that the stations in the Mediterranean climate zone located near the shore have the tendency of having more unexpected extreme rainfall events with larger skewness. The detected outliers and extremes were not discarded, since they might be valid data carrying important hydrologic information.

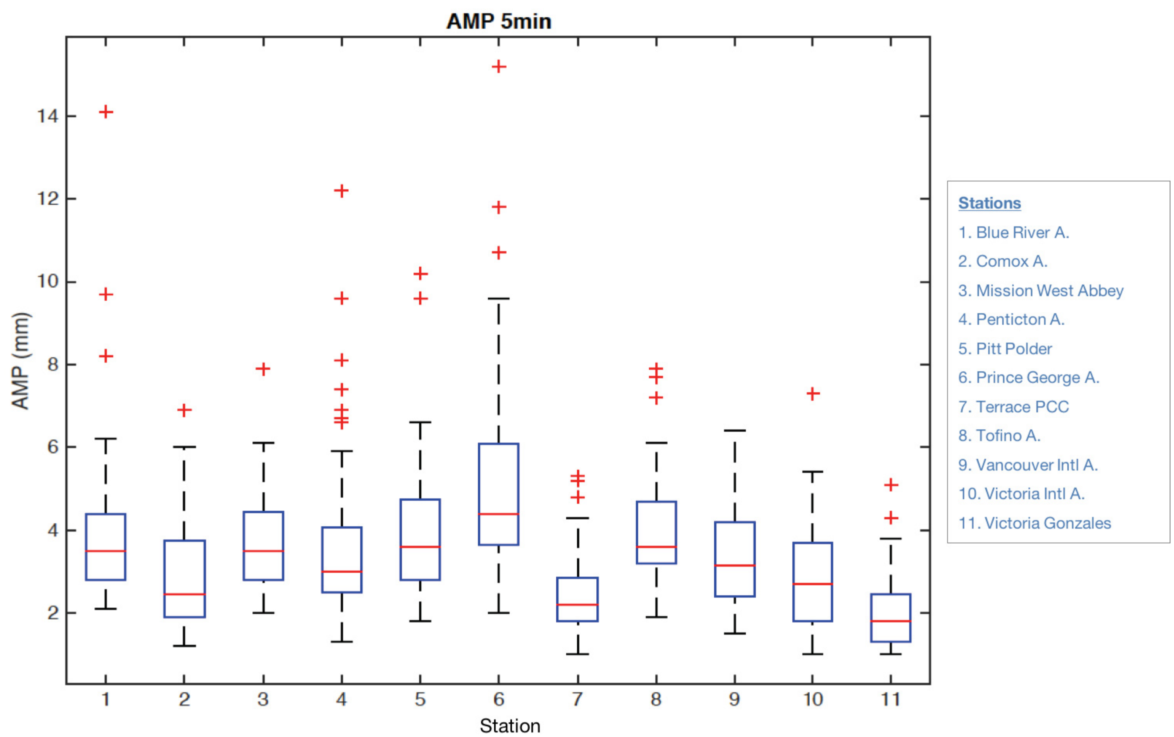

FIGURE 8 5MIN AMP FOR 11 STATIONS

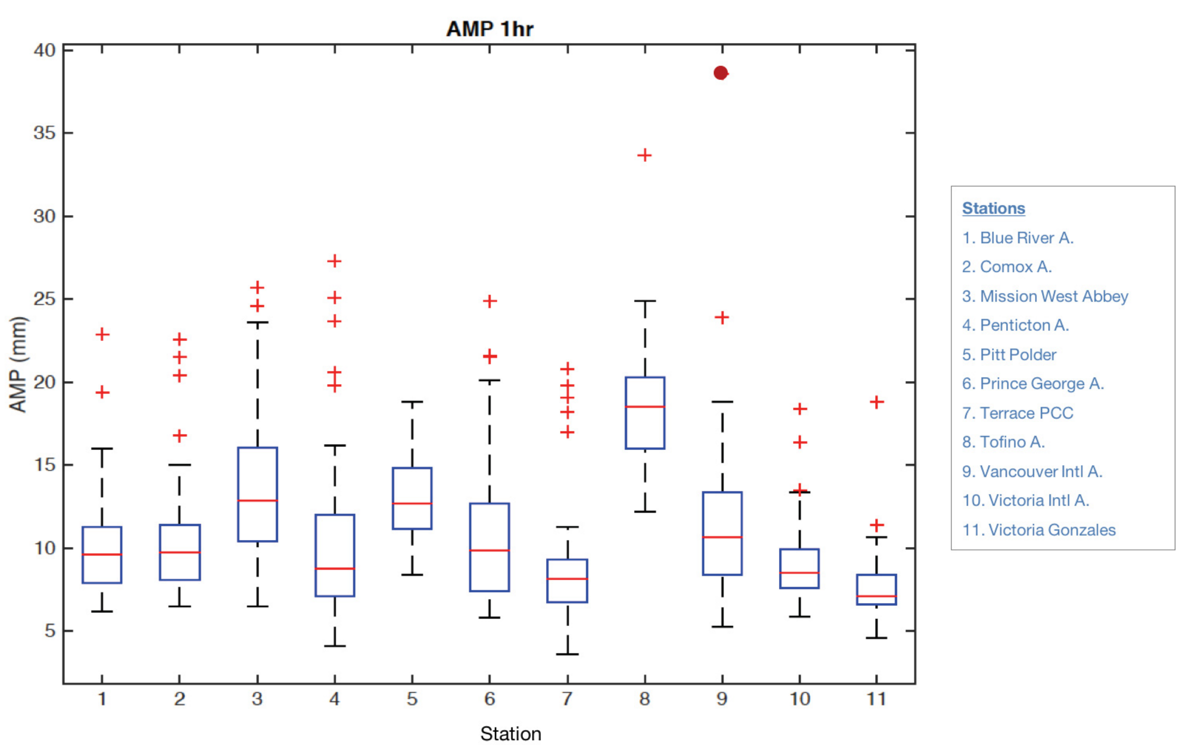

FIGURE 9 1 HR AMP FOR 11 STATIONS

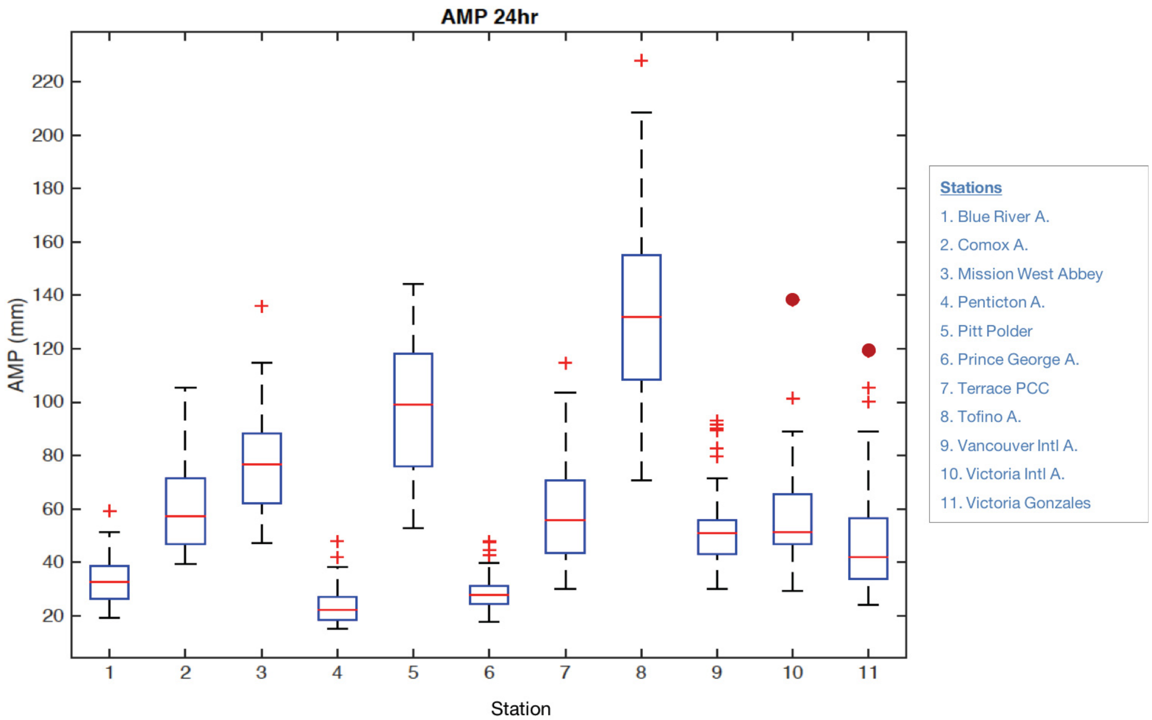

FIGURE 10 24HR AMP FOR 11 STATIONS

V. RESULT AND DISCUSSION

5.1 Probability Distribution Descriptive Ability Assessment Result

5.1.1 Graphical Assessment

5.1.1.1 Q-Q plots

The Q-Q plots of all 33 AMP series closely described the left tail and central part. The fitting of the right tail, however, varied depending on which distribution model was used. Often the values on this area can be overestimated, under estimated or well estimated. The challenge is to find the distribution model that can well describe the right tail area. Unfortunately, it was difficult to detect the best performing distribution models, since the Q-Q plots results were not showing visible differences in their performance in right tail area. Most distributions performed equally poor for stations with highly skewed data sets, but better with data sets with low skewness. Vancouver Intl A was a good example to confirm this pattern, since its data sets from all three rainfall durations (ie, 5min, 1hr & 24hr) had different skewness causing different performances of study distribution models. Figure 11 below shows the dataset with low skewness from Vancouver Intl A. Yet there was no relation between skewness of study stations with their climatological conditions. Therefore, it was difficult to investigate the preferred distribution models for each climate classification. With the BC AMP data, it was easier to detect the distributions with poor performance, such as GUM, BEK, BEP, LP3 and GLO, which showed inconsistent and poor performance with extreme values.

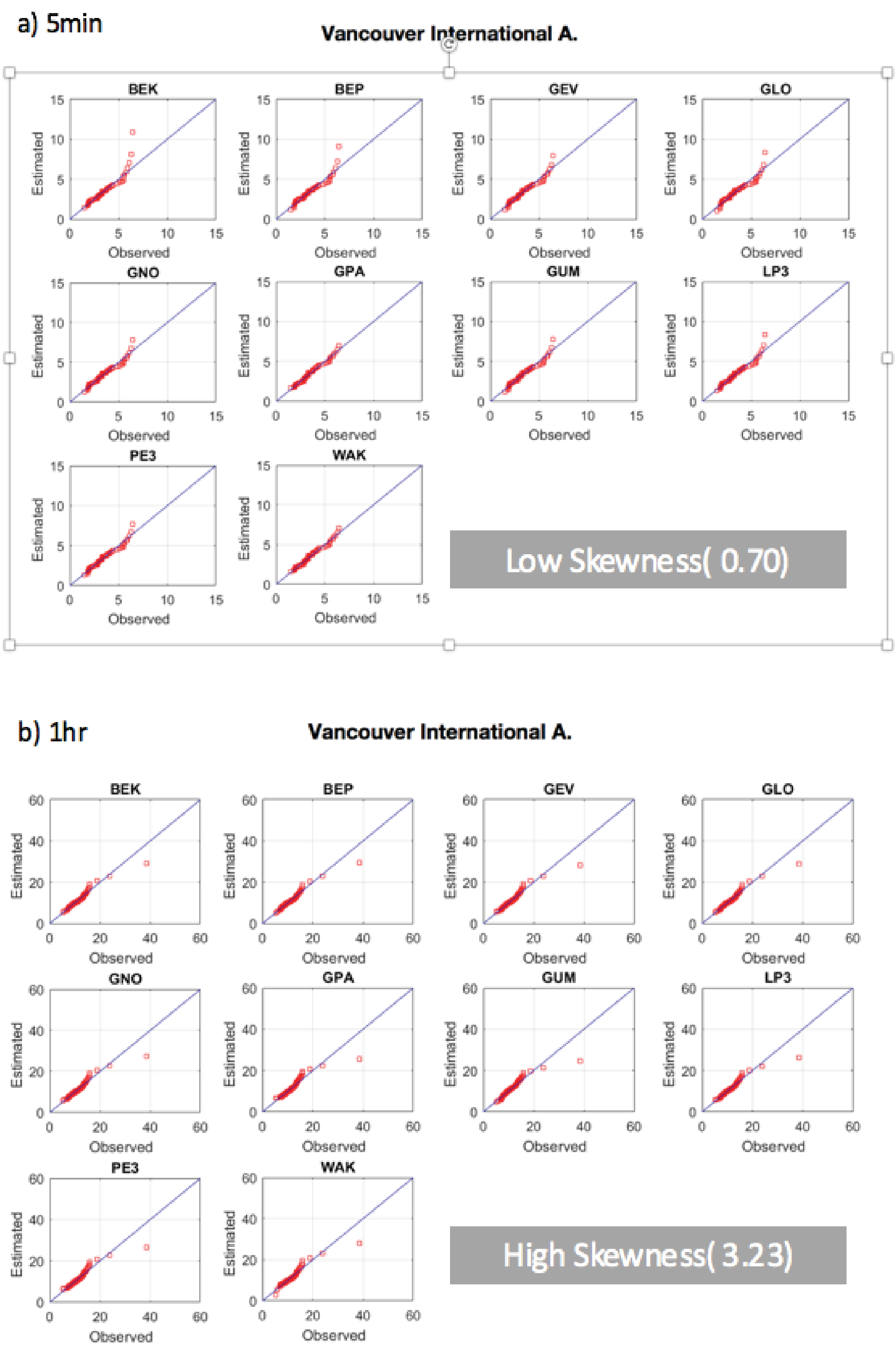

FIGURE 11 QUANTILE-QUANTILE PLOTS FOR VANCOUVER INTL A STATION

5.1.1.2 L-moment Ratio Diagram

The L-moment ratio diagrams of all 33 AMP are presented by each rainfall duration in Figure 12. As shown in Figure 12, there are the ratio lines for the following distribution models: GLO, GEV, LN3, GPA and PE3. The small blue dots in the diagrams represent the ratio of observed data for 11 study stations, and the blue cross (+) represents the average ratio of all study stations. The ratio lines that fell close to the average ratio were considered to describe the historical rainfall pattern better than the others. In Figure 12, the ratio lines that fell close to the average ratio were LN3 and GEV for 5min; GEV and GLO for 1 hr; and LN3 and GEV for 24 hr.

However, it is not logical to conclude that the average ratio (blue cross (+)) can represent the entire study area without knowing the homogeneity of the selected raingage stations. It is acknowledged that one can go further by conducting the discordancy measure test to group stations within homogeneous regions. With this test the average points fall close to the representative distribution(s) for those distinct delineated homogeneous regions.

Moreover, using this approach, some distributions including BEK and BEP could not be investigated, as the MLE was used for the parameter estimation of those distributions due to their complexity in computation of Lmoments. In addition, the performances of the predictive ability of different distributions could not be investigated using the L-moment ratio diagram. This section presents an illustrative application of the proposed procedure presented in section 3 to select the most appropriate distribution(s) for the BC AMP datasets.

In general, the significance of the differences among most distribution models was too difficult to judge solely based on the visual inspection due to the minor differences. A more objective evaluation using numerical comparison criteria was performed as described in the following sections.

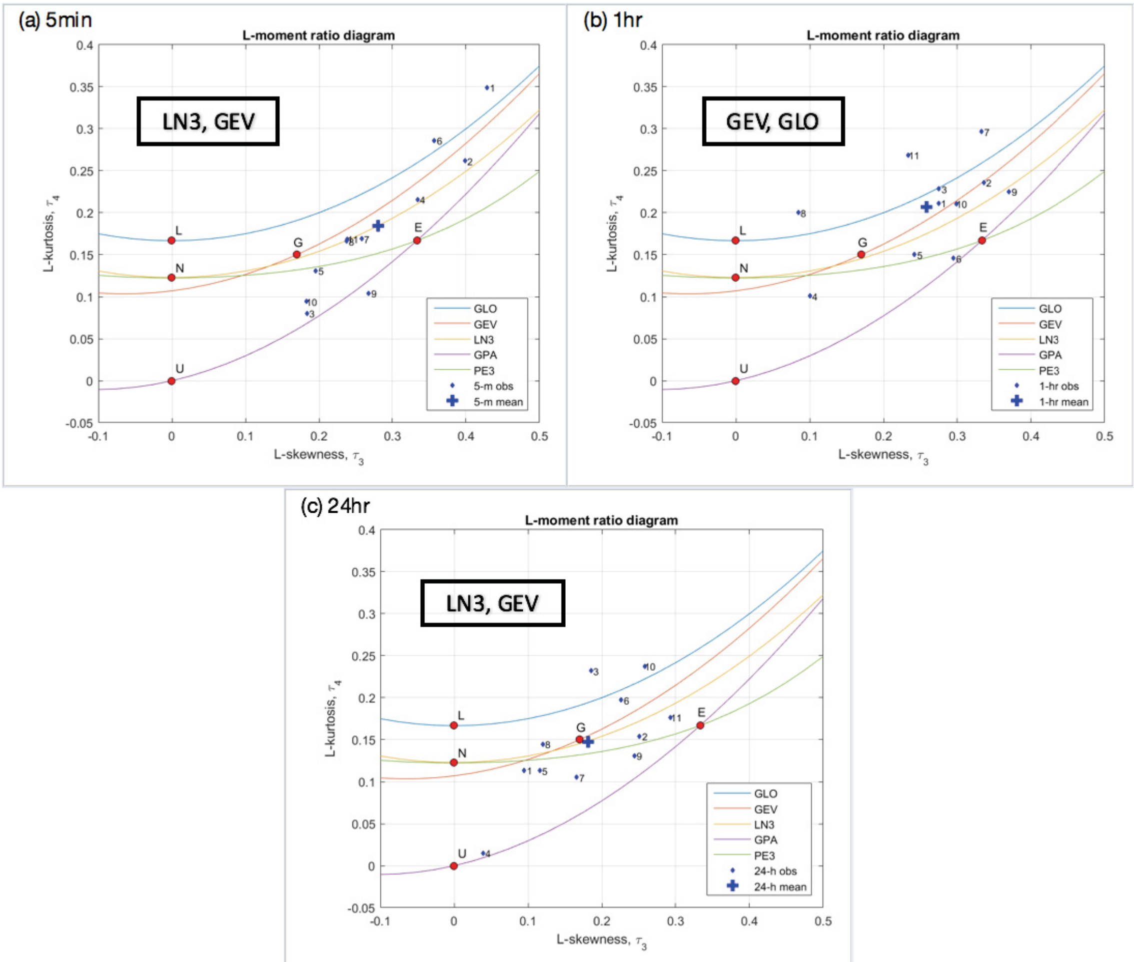

FIGURE 12 L-MOMENT RATIO DIAGRAM (A) 5MIN, (B) 1HR & (C) 24HR

5.1.2 Numerical Assessment

The overall result of goodness-of-fit tests was summarized by the ranking scheme described in section 3.1.2.5, as the numerical assessment on the performance of distribution models. Unlike the graphical assessment, the ranking scheme provided a more objective assessment of the descriptive ability of each distribution model. The top three best performing distribution models are listed in Table 27 of Appendix 2 for all study stations, and the overall rank-sum result is shown in Table 9 below, for each goodness-of-fit criterion.

5.1.2.1 Assessment Result in relation to rainfall-durations

The results reveal that no unique distribution ranks consistently best at all locations nor for all three rainfall durations. This agrees well with the preliminary investigation using the L-moment ratio diagram presented in section 5.1.1.2 above, since the preferred distributions were different for each rainfall duration. As explained in section 3.1.2.5, the overall rank associated with each distribution is computed by summing the individual ranks obtained for each of the study stations. Then, the rank-sum results are sorted for each rainfall duration for each goodness-of-fit test from lowest to highest rank-sum amount, and presented in Table 9 below. Therefore, the highest ranked distribution is with the lowest rank-sum amount for each case.

As shown in Table 9(a), both GNO and WAK outperformed the others in describing the distribution of 5min AMP, and ranked mostly high with their lower rank-sum amount. Yet GNO showed a slightly better result than WAK, since it ranked mostly within top three except for the MAE test. The GEV, LP3 and PE3 models also proved their performance by their close scores to the highly ranked distributions. It was also noticed that PE3 and LP3 performed slightly better than GEV.

However, the longer durations showed slightly different results. For instance, WAK and PE3 showed better performance than GNO for 1hr AMP data as shown in Table 9(b). The LP3 showed a rather poor result in this case, and the GPA performed much better than it did with 5min AMP. The GUM, GPA, and BEK models ranked consistently poorly compared to the others.

Meanwhile, WAK and PE3 ranked high for 24 hr AMP data, and GNO ranked as second best for all four tests as shown in Table 9(c). Those three models ranked highly with 5 min AMP data too. This results shows that GNO performed better than PE3 with a longer rainfall period. Other models like GEV and or GPA did not make it to the top three with 24hr AMP data, yet stayed in the fourth and fifth for most cases. The GUM, BEK and BEP showed the poorest prediction most of time for all rainfall durations. And GLO joined this lowest ranking group with 24 hr AMP data.

TABLE 9 *RANK-SUM OF GOODNESS-OF-FIT TEST RESULTS (A) 5MIN, (B) 1HR & (C) 24HR*

(a) 5min

Rank	RMSE		RRMSE		MAE		CC	
1	36	GNO	37	LP3	44.5	PE3	40.5	GNO
2	47	LP3	41.5	GEV	45.5	WAK	42	WAK
3	48	WAK	42	GNO	46	GPA	47	GEV
4	49.5	PE3	49.5	PE3	47	GNO	50	LP3
5	50	GEV	64.5	GLO	56	LP3	54	PE3
6	53	GPA	65	WAK	58	GEV	58.5	GPA
7	75	GLO	68	BEK	65	GLO	67.5	GLO
8	75.5	BEP	71	GPA	74	GUM	78	GUM
9	76	GUM	73.5	BEP	77	BEP	80	BEP
10	95	BEK	93	GUM	92	BEK	87.5	BEK

(b) 1hr

Rank	RMSE		RRMSE		MAE		CC	
1	40.5	WAK	41.5	GEV	34.5	WAK	36	WAK
2	45.5	PE3	43	GNO	42.5	PE3	45.5	PE3
3	46.5	GNO	46	LP3	50	GNO	48.5	GNO
4	51.5	GPA	53	GLO	50	GPA	54.5	GPA
5	56	GEV	57	BEK	58.5	GEV	58	GEV
6	65	GLO	62	WAK	68	GLO	65.5	LP3
7	65	LP3	62.5	BEP	71	LP3	66.5	BEK
8	72	BEP	68.5	PE3	75.5	GUM	67.5	GLO
9	74.5	BEK	80.5	GPA	76	BEP	72.5	BEP
10	88.5	GUM	91	GUM	79	BEK	90.5	GUM

(c) 24hrs

Rank	RMSE		RRMSE		MAE		CC	
1	45.5	PE3	43	LP3	43	WAK	41.5	WAK
2	46	GNO	48	GNO	47	GNO	45.5	GNO
3	46	WAK	49.5	PE3	49	PE3	48.5	PE3
4	54.5	LP3	51	GEV	54	GPA	49.5	GEV
5	55	GEV	53	WAK	56	GEV	53.5	LP3
6	63	GPA	67	BEK	65	GLO	65.5	GPA
7	66	GUM	69.5	GUM	65	GUM	70	GLO
8	72	GLO	71	GPA	65	LP3	71.5	GUM
9	77	BEP	75	GLO	80	BEP	77.5	BEP
10	80	BEK	78	BEP	81	BEK	82	BEK

5.1.2.2 *Assessment Result in relation to Climate Classification*

The result was also presented according to the climate classification to see whether certain climate patterns could indicate a preferred distribution over the others. The overall rank associated with each distribution and rainfall duration was computed by summing the individual ranks obtained for each of the study station, which were grouped by its climate classification. The sorted rank-sum results for each rainfall duration for corresponding climate classifications are presented in Table 26, 27 and 28 of Appendix 2. Then, the ranks for all three durations were summed up per climate classification, and sorted as shown in Table 10 below for Continental, Mediterranean and Oceanic Climate.

In general, it is not to identify a preferred distribution model for a given climate classification. However, it can be observed that the GNO, WAK, GEV and PE3 were within the top 3 best-fit distributions for most of time as shown in Table 10. In particular, the GNO was outperforming for Continental and Oceanic Climates, and less preferred for Mediterranean Climate yet still within top 5. The GEV, PE and WAK was less preferred, and their performance too varied without clear pattern to identify their preference of climate classifications.

In addition, the GUM, BEK and BEP constantly ranked very low for all three climate classifications regardless of the rainfall durations, yet particularly low for Continental and Mediterranean Climates. Its poor performance could be explained that GUM naturally has a weaker descriptive ability than GNO or other distributions with three or more parameters, because it lacks a shape parameter. Regarding BEK and BEP distributions, simulation results of many stations showed that it tended to over-estimate the right-tail part, and this lead to poor results in the goodness-of-fit test.

TABLE 10 RANK-SUM OF GOODNESS-OF-FIT TEST RESULTS (A) CONTINENTAL, (B) MEDITERRANEAN & (C) OCEANIC CLIMATE

(a) Continental Climate

Rank	RMSE		RRMSE		MAE		CC	
1	42	PE3	42	LP3	41	GNO	41	WAK
2	43	GNO	43.5	GEV	41	PE3	45.5	GNO
3	48	GPA	52	GNO	43	GPA	48.5	PE3
4	48	WAK	61.5	BEK	48.5	WAK	52.5	GPA
5	56	LP3	68.5	PE3	61	GEV	53	GEV
6	59	GEV	70.5	GLO	68	LP3	60.5	LP3
7	86	BEP	71	WAK	79.5	GUM	83.5	GLO
8	88	GLO	71.5	BEP	86	GLO	88	BEK
9	94	BEK	81	GPA	94	BEP	93	BEP
10	94	GUM	98.5	GUM	98	BEK	94.5	GUM

(b) Mediterranean Climate

Rank	RMSE		RRMSE		MAE		CC	
1	48	GNO	51	GEV	39	WAK	46.5	WAK
2	53	PE3	52.5	GLO	49	GPA	50	GNO
3	53	WAK	52.5	LP3	49	PE3	55.5	GEV
4	55	GEV	54	GNO	52	GNO	57.5	PE3
5	64	LP3	56.5	BEK	59	GEV	64	LP3
6	67	GPA	60	BEP	71	GLO	67	GPA
7	69	GLO	74.5	WAK	81	LP3	68	GLO
8	76	BEP	75.5	PE3	83	BEP	75	BEK
9	81	GUM	81	GPA	88	BEK	79.5	BEP
10	91	BEK	102.5	GUM	89	GUM	97	GUM

(c) Oceanic Climate

Rank	RMSE		RRMSE		MAE		CC	
1	34.5	GNO	31	GEV	28	WAK	23.5	WAK
2	37.5	PE3	32	GNO	47	GLO	40	GNO
3	40.5	WAK	32	LP3	47	PE3	43.5	GEV
4	41	LP3	43.5	PE3	47.5	GPA	46	PE3
5	42.5	GPA	49.5	WAK	48	GNO	47	LP3
6	44	GEV	54	GLO	49	LP3	53.5	GLO
7	59	GLO	55.5	BEK	53.5	GEV	55.5	GPA
8	62.5	GUM	61.5	GUM	55	GUM	60	GUM
9	64	BEP	62.5	BEP	58	BEP	60.5	BEP
10	67.5	BEK	73.5	GPA	62	BEK	65.5	BEK

5.1.2.3 Overall Numerical Assessment Result

Each goodness-of-fit criterion indicates the best distribution for all 11 stations and for all rainfall durations considered. As discussed in section 3, the absolute error describes the amount of error, not relative to the observed value; which is a reliable measure to assess extreme events. With the precipitation frequency analysis, the large absolute error was common due to the behavior of extreme events on the right tail area. Whereas, the relative error reduced the influence of outliers and provided a better indication for the overall fit of a distribution, as it was calculated in proportion to the size of the observations (Tao et al. 2002). Therefore, it was important to combine the result of four goodness-of-fit test result to find the distribution with the best descriptive ability.

The overall numerical assessment result is summarized and presented in table 11 and in the bar graph of Figure 13 for more thorough performance measure of each distribution for each goodness-of-fit test. The length of each bar indicates the rank-sum of each distribution model, and the numbers on each bar indicates the exact amount of rank-sum. For instance, the WAK, PE3 and GNO performed better for RMSE and MAE, while the GNO, GEV and LP3 performed better for RRMSE and CC consistently. And it is easy to find that the BEK, BEP and GUM ranked the lowest for all four tests from the Figure 13.

Another bar charts were used in order to confirm the numerical assessment result in Figure 14 for 5min, Figure 17 for 1hr and Figure 18 For 24hr in Appendix 2. Each bar of the graph presents the rank-sum amount of each study station for each goodness-of-fit test result, and longer bar indicates the larger rank-sum amount indicating the poor performance for RMSE, RRMSE and MAE. Yet the shorter bar indicates the poor performance for CC, since it means lower correlation coefficient value. This can be due to the type of error assessed by each test, since RMSE and MAE are based on absolute errors, yet RRMSE and CC are based on relative errors. The poor performance of BEK, BEP and GUM can be easily detected in the bar chart shown in

Figure 14 (a), (b) and (c), for example, since their corresponding bars (blue, navy and orange) are sticking out of the crowd.

TABLE 11 SUMMARY OF NUMERICAL ASSESSMENT RESULT (BEST DISTRIBUTIONS)

Results by rainfall durations		Results by climate classifications	
5min	GNO, WAK,GEV	Continental	GNO, PE3, GEV
1hr	WAK, PE3, GNO, GEV	Mediterranean	GNO, WAK, GEV
24hr	WAK, PE3, GNO, GEV	Oceanic	PE3, GNO, WAK
Overall	**GNO, WAK, GEV, PE3**	**Overall**	**GNO, WAK, GEV, PE3**

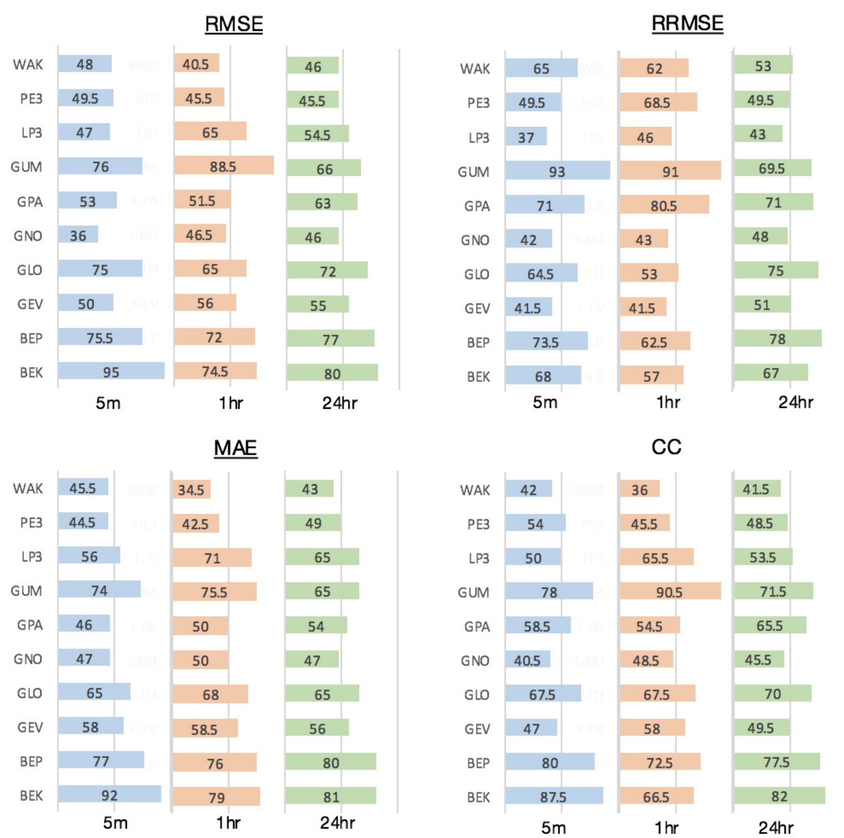

FIGURE 13 COMPARISON OF OF THE DESCRIPTIVE ABILITY OF DIFFERENT DISTRIBUTIONS ACCORDING TO DIFFERENT GOODNESS-OF-FIT CRITERIA FOR ALL RAINFALL DURATIONS AND FOR ALL 11 RAINGAGES

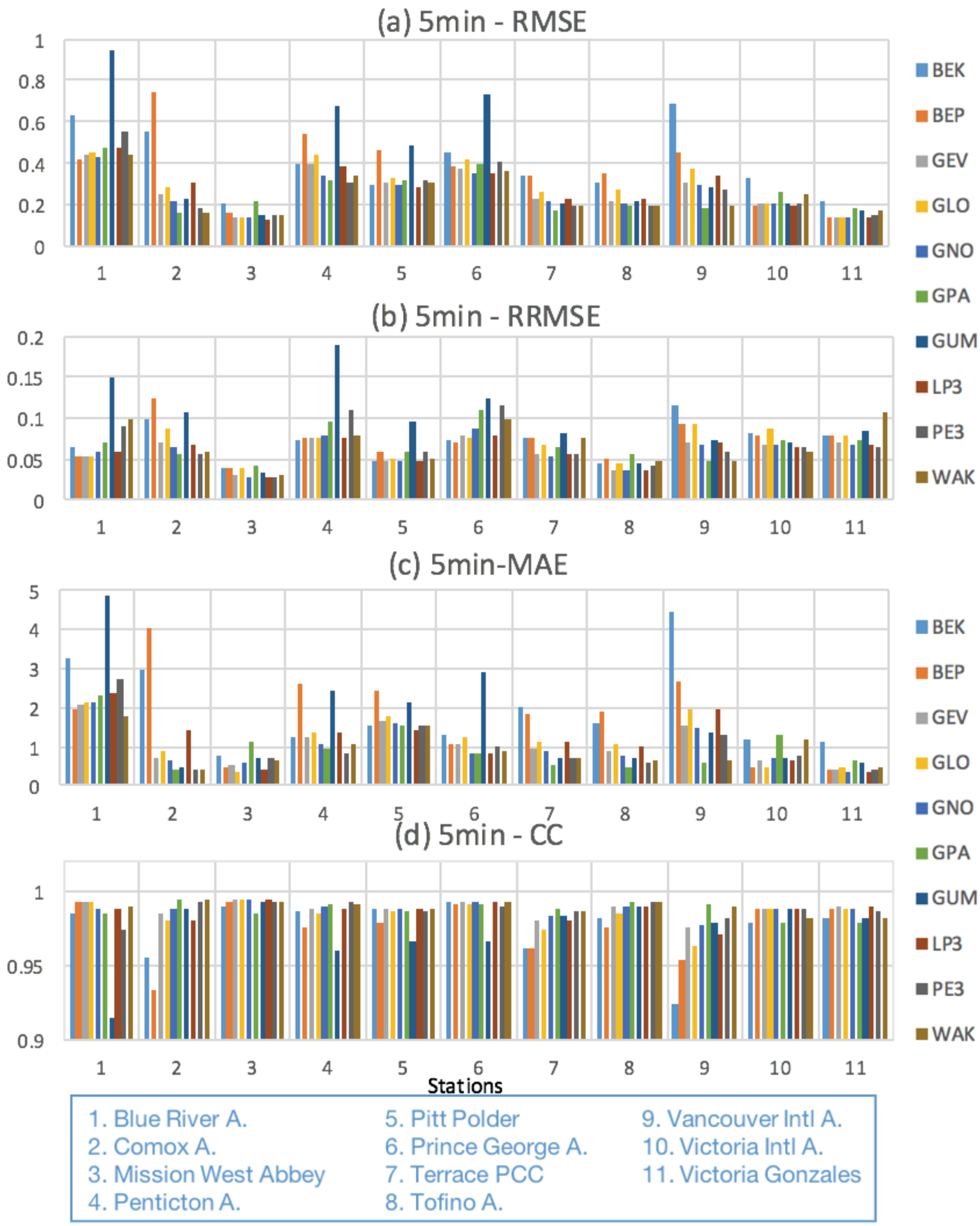

FIGURE 14 GOODNESS-OF-FIT ANALYSIS RESULT FOR 5-MIN RAINFALL DURATION AND FOR ALL 11 RAINGAGES

5.1.3 Summary of Graphical and Numerical Assessment

From the graphical analysis results (section 5.1.1), the Q-Q plots and L-moment ratio diagram were used to measure the descriptive ability of distributions. With the Q-Q plots, it was easier to detect the poorly performing distribution models, which were the GUM, BEK, BEP, LP3 and LGO, than the best ones. In general, the distributions accurately described the observed dataset, when it has low skewness. Whereas, it was more convenient to detect the distribution models with a good descriptive ability with L-moment ratio diagram, such as the LN3, GEV and GLO. The GEV was particularly preferred for all three rainfall durations. However, due to the lack of compatibility of both graphical methods, the numerical analysis was conducted.

In section 5.1.2, the result of the goodness-of-fit test was analyzed and discussed to draw an objective conclusion on which distributions could be the best to describe the historical rainfall pattern. Also, the result was sorted in two different ways as explained in section 5.1.2.1 and 5.1.2.2, in order to measure the effect of rainfall durations and climate classifications to the performance of distribution models. The effect of rainfall durations and climate classification were not evident according to the assessment results from this section. As summarized in Table 11 above, the GNO, WAK, GEV and PE3 were outperforming other distribution according to the numerical assessment result. And the BEK, BEP and GUM were ruled out for its lack of this ability. The performance of the predictive ability of each distribution is presented in the next section.

5.2 Probability Distribution Predictive Ability Assessment Results

As described in Section 3.2, to assess the predictive ability of a distribution, the boxplots for the estimation of the four largest predicted extreme rainfalls for all rainfall durations and for all 11 raingage stations were analyzed based on the width of the box, the whisker length, and the closeness of the observed value with the estimated median value inside the box. The large box width indicates a large uncertainty or the lack of robustness in the estimation of the extreme rainfall amount. The long whisker length was interpreted as containing a greater range of the overall samples, which was an indicator of highly probable values and larger variance among the extremes. The location of the observed rainfall value (marked as a red cross in the boxplots) was used to measure the bias; an extreme rainfall estimate is considered as reasonably accurate if the red cross position is located within the box. For purposes of illustration, Figure 15 shows the results for Vancouver International Airport. Similar results for other stations are presented in Appendix 3.

5.2.1 Graphical Assessment of the Modified Boxplots

In general, the BEK, BEP and GUM consistently performed poorly with high estimation variation and bias as indicated by the large box width and the long whiskers for all three rainfall durations. Also, the observed data often fell outside of the box for those three distributions as the prediction was overestimated or underestimated. The behaviors of the three models agreed with the results of the descriptive ability tests in Section 4.3, where they ranked consistently the lowest among all the goodness-of-fit test results. The WAK also showed the large box width and the long whiskers similar to the BEP and BEK, yet the observed value often fell within the box closer to the mean, exhibiting a small bias. In particular, the WAK consistently presented much longer whiskers than other models, which was the indicator of highly probable values due to the greater range of the overall sample This could be interpreted as there is larger variance among the estimated extreme rainfalls, yet the whisker length was less of concern than the tall box. The WAK model, with five parameters, can mimic many distributions and can fit close to any observed dataset. However, it can be a rigid model with its large number of parameters, and it cannot provide consistently predictive values, as presented by the whisker length and box height of its modified boxplots. In addition, results of modified boxplots reveal that, the LP3 model produced taller box heights with longer whisker lengths relative to the other distributions, yet it still performed better than BEK, BEP or WAK. Furthermore, the result showed that the GUM distribution exhibited the lowest estimation variation in most cases, though it tended to overestimate or underestimate the observed values most frequently.

The GEV, GLO, GNO, GPA and PE3 distributions outperformed other distribution models at most stations, where the box enclosed the observed right-tail values with a reasonable whisker spread and correlation with the observed values. The performance of the five distributions were investigated more in detail per stations for each rainfall duration and the results are presented in Table 12 below. The good performance was marked as check (√), and the poor ones were marked as red x (x). And the predictive ability of those five distribution models decreased as the rainfall duration increases, and this can be easily found with the total number of good performance in the last row of the Table 12. And the behavior of those five distributions was almost identical. Yet, GPA had the observed data (red cross in Figure 15) exactly on the mean line for 12 datasets out of total 33 AMP detasets, or the observed data would still stay close to the mean line within the box. PE3 produced slightly shorter boxes, upper whiskers, and slightly lower means.

Over and under-estimation of the largest rainfall amounts occurred for all distributions at most stations. The accuracy of the prediction was investigated from the modified boxplots results by locating the observed value (red cross). As discussed above, the BEK, BEP, GUM, WAK and LP3 were the least accurate distribution models, that over and under estimated the largest rainfall amount far away from the observed value. The GEV, GNO, GPA and PE3, however, predicted very closed to the observed value, and those four distribution models showed same prediction trend. The prediction trend of the GEV, GNO, GPA and PE3 was further investigated in detail, and presented in Table

13 in the next page. The exact estimation of largest rainfall amount was found for five stations with 5 min, yet less frequently found with longer rainfall durations such as one station with 1 hr and three stations with 24 hr. In short, the distributions showed no consistency at over or under representing the right-tail region.

TABLE 12 DETAIL INVESTIGATION OF THE PREDICTIVE ABILITY OF GEV, GLO, GNO, GPA AND PE3 FOR ALL 11 RAINGAGES

	5min					1hr					24hr				
	GEV	GLO	GNO	GPA	PE3	GEV	GLO	GNO	GPA	PE3	GEV	GLO	GNO	GPA	PE3
Blue River A	√	√	√	√	√	√	√	√	√	√	x	x	x	x	x
Comox A	√	√	√	√	√	x	x	x	x	x	x	x	x	x	x
Mission West Abbey	√	√	√	√	√	x	x	x	√	x	√	√	√	√	√
Penticton A	√	√	√	√	√	√	√	√	√	√	√	√	√	√	√
Pitt Polder.	x	x	x	x	x	√	√	√	√	√	x	x	x	x	x
Prince George A	√	√	√	√	√	x	x	x	x	x	√	√	√	√	√
Terrace PCC	√	√	√	√	√	√	√	√	√	√	x	x	x	x	x
Tofino A	√	√	√	√	√	√	√	√	√	√	√	√	√	√	√
Vancouver Intl A	√	√	√	√	√	x	x	x	x	x	x	x	x	x	x
Victoria Intl A	√	√	√	√	√	x	x	x	x	x	√	√	√	√	√
Victoria Gonzales HTS	√	√	√	√	√	√	√	√	√	√	x	x	x	x	x
Total Number of Good Performance	**10**	**10**	**10**	**10**	**10**	**6**	**6**	**6**	**5**	**5**	**5**	**5**	**5**	**5**	**5**

TABLE 13 ACCURACY OF THE LARGEST RAINFALL PREDICTIONS FROM THE BOXPLOT RESULTS (COMPARE TO THE OBSERVED DATA)

	5min	1hr	24hr
Blue River A	Under	Under	Exact
Comox A	Under	Over	Over
Mission West Abbey	Over	Over	Exact
Penticton A	Over	Exact	Over
Pitt Polder.	Exact	Over	Over
Prince George A	Exact	Over	Over
Terrace PCC	Exact	Over	Over
Tofino A	Exact	Under	Exact
Vancouver Intl A	Over	Under	Exact
Victoria Intl A	Under	Over	Under
Victoria Gonzales HTS	Exact	Under	Over

5.2.2 Graphical Assessment in relation to the Skewness of data

The performance of distribution models was compared in relations to the skewness of data sets, in order to measure their effects on the predictive ability of study distribution models. Poorly performing distribution models were showing in consistent result regardless of the skewness, for instance, BEK, BEP, LP3 would sometime show smaller box height for low skewed data. It was found that the performance of distribution was at its best when the skewness was low than high; most distribution showed taller box height and longer whisker for datasets with high skewness such as: Blue River_5min (2.93), Vancouver Intl A_1hr (3.23) and Victoria Gonzales HTS_2hr (2.85). GUM consistently showed smaller box height regardless of skewness, but the observed data was often not captured within the box. However, the predictive ability test results did not indicate a preferred particular distribution for a given climate region as defined according to the selected Climate Classification scheme. This result was expected since no connection was found between the estimated extreme rainfall skewness values and these defined climate regions.

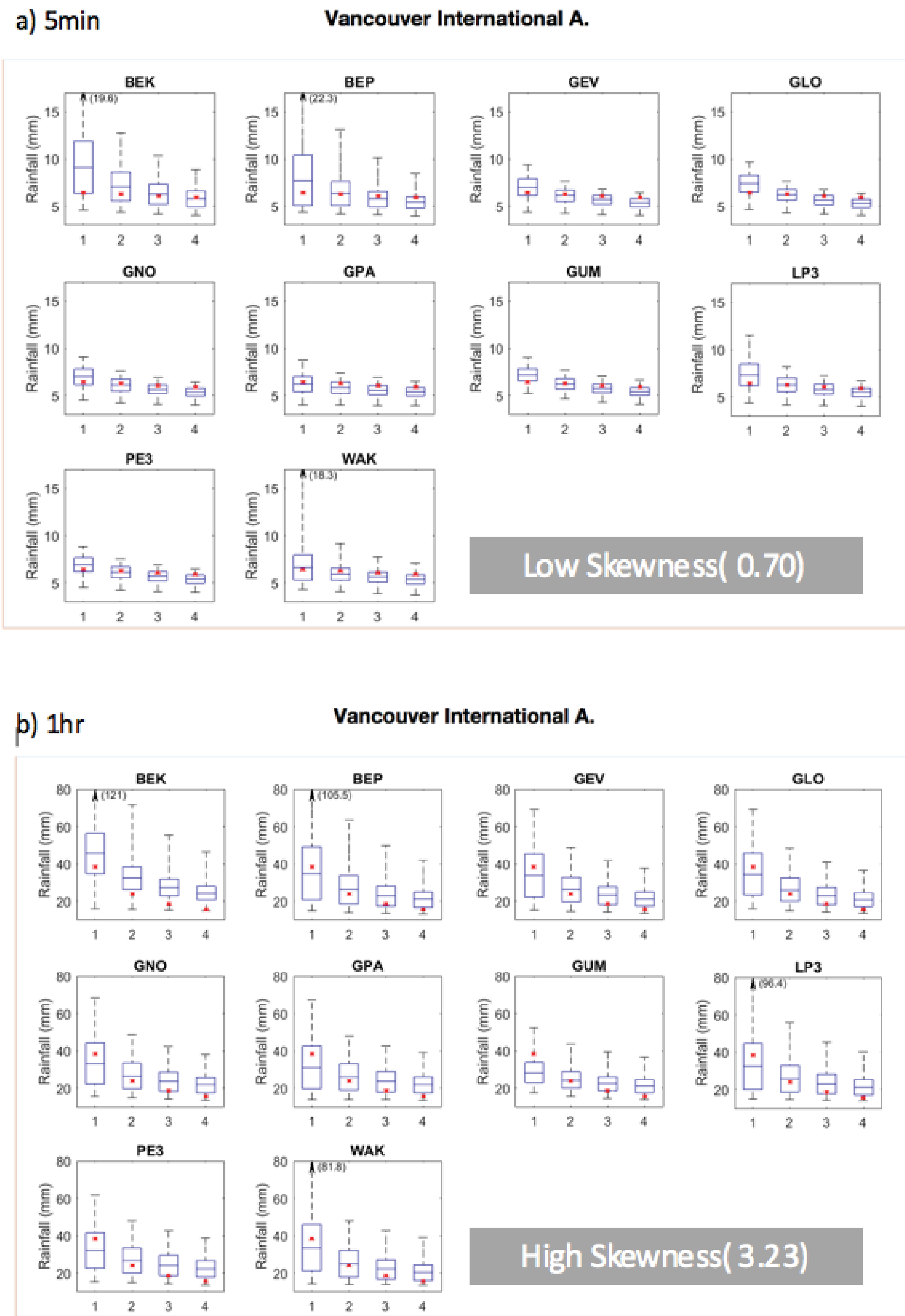

FIGURE 15 BOXPLOTS FOR VANCOUVER INTL A.

5.3 Selection of The Best Distribution Model for BC

Results of the numerical application using the annual maximum rainfall series for three durations (5 minutes, one hour and 24 hours) and for 11 raingages in BC have indicated that no unique distribution consistently performed best at every station for all three durations. The performance of a distribution model was not found affected by the climatological or topographical condition of a given station. However, most distribution models showed significantly less descriptive and predictive ability for extreme rainfall datasets with high skewness.

More specifically, for the best descriptive ability, the GNO, WAK, PE3 and GEV could provide the best fit to the observed data according to the graphical and numerical goodness-of-fit assessment results as discussed in section 5.1. In addition, for the best predictive ability, the GNO and PE3 showed quite similar predictive ability, and the PE3 in general had a smaller box height with the observed value (red cross) closer to the mean than the GNO. Again, their predictive abilities were better with less skewed data. Combining the result of both descriptive and predictive ability tests, the GNO and PE3 were competitive options, yet the GNO was slightly superior with its strong descriptive ability.

Considering the popular use of GEV for rainfall frequency analysis in Canada, the GEV was expected to more accurately describe and predict the extreme rainfall pattern, however, its performance was not exceptionally better than either GNO or PE3. Historically, the GEV was favoured for its simple computation for the parameter estimation compared to the more complicated computation of the GNO and PE3 distributions. As shown in Table 1, however, the probability density and cumulative distribution functions of both GEV and GNO is identical, and the parameter estimation process can be simplified by estimating the k-factor for both models as proposed by Hosking et al. (1997). The complicated computation can be easily handled by advanced software like Matlab. Therefore, the GNO and PE3 can be considered as the most suitable distribution for describing the annual maximum rainfalls in BC region. The best distribution selection process is summarized and presented in Figure 16.

FIGURE 16 SUMMARY DIAGRAM FOR THE SELECTION OF BEST DISTRIBUTIONS

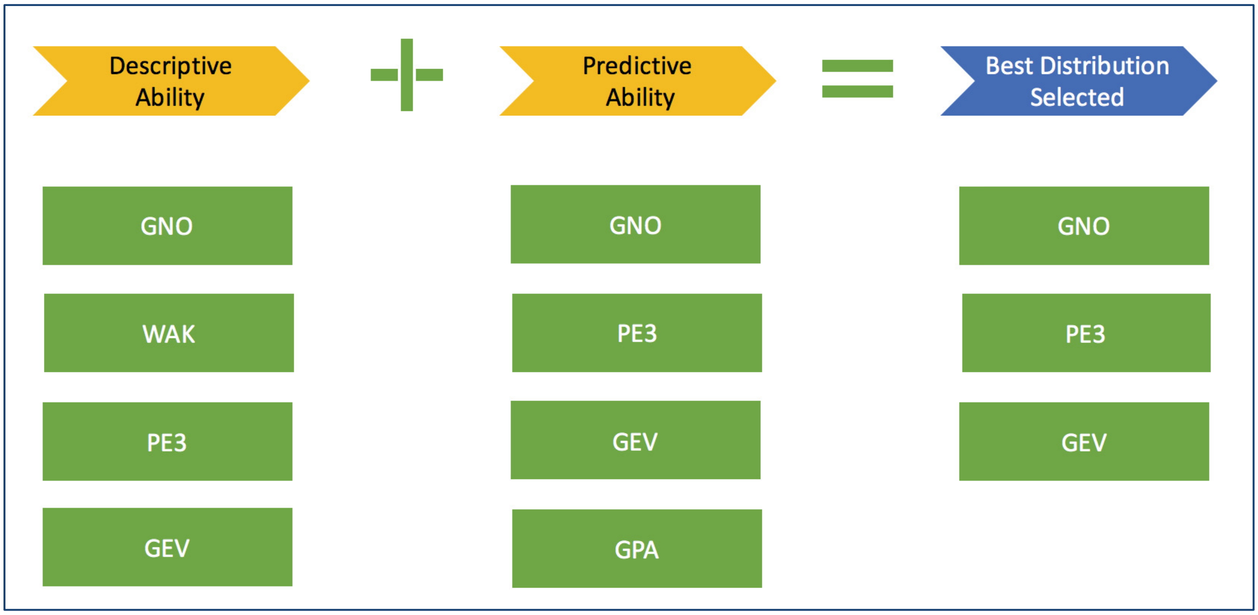

VI. SUMMARY AND CONCLUSION

5.1 CONCLUSION

Following a review of various probability distributions available in the literature, ten popular probability models were selected for evaluation. These models include the BEK, BEP, GEV, GLO, GNO, GPA, GUM, LP3, P3, and WAK distributions. The proposed procedure has been successfully applied to 5-min, 1-hour, and 24-hour annual maximum rainfall series from 11 raingages located in British Columbia.

The L-moment ratio was not an objective way to draw a conclusion, despite its wide use in the rainfall frequency analysis. It was not, first of all, applicable to distributions that could not use L-moments as the parameter estimation method. Then, L-moment ratio diagram was used under the assumption of homogeneity of all study stations, which must be confirmed by the discordancy measure first.

The Goodness-of-fit tests were an effective way to assess the descriptive ability of distributions for each rainfall, confirming the visual assessment from the quantile-quantile plots. Overall results confirmed GNO, WAK, PE3 and GEV as the best choices for their descriptive ability, although no distribution could be chosen as the one best option.

On basis of bootstrap sampling results, however, the WAK was ruled out due to its lack of predictive ability test. This additional test confirmed the extrapolative ability of GNO and GEV at predicting extreme right-tail values of the annual maximum rainfall. PE3 and GPA also exhibited fair predictability.

Recognizing distributions that perform less satisfactory was relatively easier than finding the best distribution, as the BEK, BEP, GUM and LP3 constantly showed poor performance for the descriptive and predictive tests.

The performance of the distribution models was not consistent with either the topographical or climatological condition of study stations. Yet it was evident that most distributions performed poorly with data sets with high skewness. However, it was difficult to define a pattern of skewness in data, as skewness can vary without relation to rainfall durations and climatological or Topographical condition. Using the proposed procedure for selecting the best distribution, the GNO, GEV and PE3 were found the best overall choice for its descriptive and predictive ability with annual maximum rainfall data in British Columbia.

5.2 Recommendations

1. For practical application purposes, the GEV is preferable in many research studies due to its more solid theoretical basis, relatively simpler parameter estimation method, and its recent applications in constructing climate-change-scenario IDF curves. However, from this study, both descriptive and predictive abilities of GEV were not exceptionally better than either GNO or PE3. Therefore, application of one distribution across Canada shall be re-investigated.

2. In this study, the length of data was limited to over 40 years, and only 33 datasets could be investigated for three rainfall durations. With this limitation, it was difficult to read the effect of topographic or climatological condition on the rainfall pattern. It is possible that some distributions could perform better than others in certain topographic or climatological condition. Also, the effect of rainfall duration could be further investigated with more datasets.

3. Rainfall pattern was found unpredictable since even stations located close to each would show different rainfall trends. Therefore, finding a way to grouping stations based on other information, such as occurrences of rainfall, can be a more accurate approach to conduct the regional rainfall frequency analysis rather than relying on climatological conditions of stations.

REFERENCE

Ahmad, M.I., Sinclair, C.D. and Werritty, A. (1988) Log-logistic flood frequency analysis. Journal of Hydrology 98, 20.

Asquith, W.H. (1998) Depth-Duration Frequency of Precipitation for Texas, U.S.G. Survey, Austin, Texas.

Bobee, B.B. and Robitaille, R. (1977) The use of the Pearson Type 3 and Log Pearson Type 3 Distribution revisited. Watre Resources Research 13(2).

Canada, E. (2013) Climate, http://climate.weather.gc.ca/.

Chow, V.t. (1964) Handbook of Applied Hydrology, McGraw-Hill, New York, USA.

Climate-Data Climate Data for Cities Worldwide, Gernsbach.

Cunnane, C. (1989) Statistical Distributions for Flood Frequency Analysis, World Meteorological Organization.

Cunnane, C. (1978) Unbiased plotting positions A review. Journal of Hydrology 37(3), 205-222.

Efron, B. and Tibshirani, R.J. (1994) An introduction to the bootstrap, Chapman & Hall, New York.

El Adlouni, S., Bobée, B. and Ouarda, T.B.M.J. (2008) On the tails of extreme event distributions in hydrology. Journal of Hydrology 355(1-4), 16-33.

GeoGratis (2014) GeoGratis API, Natural Resources Canada, Government of Canada, Canada.

Helsel, D.R. and Hirsch, R.M. (2002) Book 4, Hydrologic Analysis and Interpretation. Survey, U.S.G. (ed).

Hosking, J.R.M. (1989) L-moments: Analysis and Estimation of Distributions using Linear Combinations of Order Statistics. Journal of Royal Statistical Society 52(1), 20.

Hosking, J.R.M. and Wallis, J.R. (1987) Parameter and Quantile Estimation for the Generalized Pareto Distribtuion. American Statistical Association and the American Society for Quality Control 29(3).

Hosking, J.R.M. and Wallis, J.R. (1997) Regional Frequency Analysis, Cambridge University Press, Cambridge, UK.

Houghton, J.C. (1978) Birth of a parent: The Wakeby Distribution for modeling flood flows. Water Resources Research 14(6), 1105-1109.

Hyndman, R.J. and Koehler, A.B. (2006) Another look at measures of forecast accuracy. International Journal of Forecasting 22(4), 679-688.

Klock, R. and Mullock, J. (2001) The weather of British Columbia, NAV Canada, Canada (Government of Canada).

Lang, M., Quarda, T.B.M.J. and Bobee, B. (1999) Towards operational guidelines for over-threshold modeling. Journal of Hydrology 225(3-4), 14.

Martin, J. and Perez, C.J. (2009) Bayesian analysis of a generlized lognormal distribtuion. Computational Statistics and Data Anlaysis 53, 1377-1387.

Matalas, N.C. and Wallis, J.R. (1973) Eureka! Water Resources Research (9), 9.

Mendenhall, W. and Beaver, R.J. (1991) Introduction to probability and statistics, PWS-Kent Pub. Co., Boston.

Mielke, P.W.J. and Johnson, E.S. (1974) Some Generalized Beta Distributions of the Second Kind Having Desirable Application Features in Hydrology and Meteorology. Water Resources Research 10(2).

Murshed, M.S., Kim, S. and Park, J.-S. (2011) Beta-K distribution and its application to hydrologic events. Stoch Environ Res Risk Assess 25, 897-911.

Öztekin, T. (2005) Comparison of Parameter Estimation Methods for the Three Parameter Generalized Pareto Distribtuion. Turkish Journal of Agriculture and Foresty 29.

Öztekin, T. (2011) Estimation of the Parameters of Wakeby Distribtuion by a Numerical Least Squares Method and Applying it to the Annual Peak Flows of Turkish River. Water Resour MAnage 25.

Rao, A.R. and Hamed, K.H. (2000) Flood Frequency Analysis, CRC Press, Florida.

Robson, A.J. and Reed, D.W. (1999) Flood Estimation Handbook, Institute of Hydrology, Wallingford, UK.

Schaefer, M. (1990) Regional Analyses of Precipitation Annual Maxima in Washington State. Water Resources Research 26(1), 13.

Stedinger, J.R. (1980) Fitting Log Normal-Distributions to Hydrologic Data. Water Resources Research 16(3), 481-490.

Stedinger, J.R., Vogel, R.M. and Foufoula-Georgiou, E. (1993) Frequency Analysis of Extreme Events.

Tao D.Q., Nguyen V-T-V and Bourque, A. (2002) On selection of probability distributions for representing extreme precipitaitons in southern quebec. Annual Conference of the Canadian Society for Civil Engieering.

Tao, D.Q., Nguyen, V.-T.-V. and Bourque, A. (2002) On selection of probability distributions for representing extreme precipitaitons in southern quebec. Annual Conference of the Canadian Society for Civil Engieering.

Vogel, R.M. (1995) Recent advances and themes in hydrology. Reviews of Geophysics 33(S2), 933-936.

Wilks, D.S. (1993) Comparison of Three-Parameter Probability Distributions for Representing Annual Extreme and Partial Duration Precipitation Series. Water Resources Research 29(10), 3543-3549.

WMO (2009a) Guide to Hydrological Practices, Geneva, Switzerland.

WMO (2009b) Guidelines on Analysis of extremes in a changing climate in support of informed decisions for adaptation, World Meteorological Organization, Geneva, Switzerland.

Yu, F.X., Naghavi, B., Singh, V.P. and Wang, G.-T. (1994) MMO: An improved estimator for log-Pearson type-3 distribution. Stochastic Hydrology and Hydraulics 8(3), 219-231.

Yu, Y., Zhu, Y., Li, S. and Wan, D. (2014) Time Series Outlier Detection Based on Sliding Window Prediction. Mathematical Problems in Engineering 2014, 14.

APPENDIX

APPENDIX 1 ANNUAL MAXIMUM RAINFALL DATA FOR 11 STATIONS

TABLE 14 SUMMARY OF THE ANNUAL MAXIMUM RAINFALL DATA FOR 11 STATIONS

5min_ AMP

	Blue River A	Comox A	Mission West Abbey	Pentiction A	Pitt Polder	Prince George	Terace PCC	Tofino A	Vancouver Intl. A	Victoria Intl. A	Victoria Gonzales HTS
n	42	40	48	45	41	43	44	42	60	49	56
mean	4.03	2.94	3.70	3.78	4.01	5.20	2.48	4.05	3.44	2.86	2.00
sd	2.22	1.38	1.17	2.26	1.78	2.68	1.10	1.44	1.33	1.23	0.85
skewness	2.93	1.07	1.19	1.91	1.90	1.89	1.14	1.09	0.70	1.13	1.49
kurtosis	10.57	0.58	2.21	3.91	4.28	4.18	0.68	0.82	-0.50	2.10	2.93

1hr_AMP

	Blue River A	Comox A	Mission West Abbey	Pentiction A	Pitt Polder	Prince George	Terace PCC	Tofino A	Vancouver Intl. A	Victoria Intl. A	Victoria Gonzales HTS
n	42	40	48	46	41	43	44	42	61	49	56
mean	10.44	10.72	13.67	10.53	13.13	11.25	8.73	18.36	11.57	9.21	7.63
sd	3.44	4.00	4.41	5.39	2.67	4.86	3.62	3.92	4.86	2.67	2.11
skewness	1.69	1.69	1.18	1.64	0.44	1.19	1.82	1.35	3.23	1.50	2.85
kurtosis	3.77	2.37	1.07	2.36	-0.51	0.68	3.35	4.63	15.83	2.40	13.66

24hrs_AMP

	Blue River A	Comox A	Mission West Abbey	Pentiction A	Pitt Polder	Prince George	Terace PCC	Tofino A	Vancouver Intl. A	Victoria Intl. A	Victoria Gonzales HTS
n	41	41	48	46	41	42	45	42	61	49	56
mean	34.35	61.65	77.76	23.82	98.61	28.91	59.26	134.62	52.86	57.28	48.70
sd	9.07	17.71	18.05	7.08	26.48	7.45	21.91	31.89	14.85	19.46	20.65
skewness	0.53	1.02	0.75	1.37	0.14	1.09	0.75	0.76	1.10	1.85	1.50
kurtosis	0.19	0.26	1.02	2.30	-1.15	0.81	-0.12	1.00	1.27	5.46	2.36

TABLE 15 ANNUAL MAXIMUM RAINFALL DATA FOR BLUE RIVER A (1970-2011)

5min_AMP

Year	AMP	Year	AMP	Year	AMP	Year	AMP	Year	AMP
1970	2.3	1979	3.4	1988	3.7	1997	4.8	2006	5.8
1971	2.3	1980	8.2	1989	2.8	1998	3.1	2007	3.6
1972	3.3	1981	14.1	1990	4.4	1999	5	2008	2.3
1973	3.6	1982	2.1	1991	2.4	2000	3.3	2009	3.9
1974	2.5	1983	6.2	1992	3.3	2001	2.1	2010	5.5
1975	3.3	1984	2.3	1993	4.1	2002	3.4	2011	3
1976	2.8	1985	4.7	1994	4.7	2003	3.8		
1977	3.6	1986	2.7	1995	2.7	2004	3.6		
1978	3.2	1987	3.6	1996	9.7	2005	3.9		

1hr_AMP

Year	AMP	Year	AMP	Year	AMP	Year	AMP	Year	AMP
1970	6.6	1979	8.4	1988	7.8	1997	10.4	2006	19.4
1971	7.6	1980	9.6	1989	8.2	1998	7.5	2007	9.4
1972	8.4	1981	22.9	1990	6.2	1999	11.3	2008	7.9
1973	11.7	1982	6.3	1991	8.8	2000	11.1	2009	9.9
1974	6.9	1983	8.9	1992	7.6	2001	7.7	2010	13.6
1975	10.9	1984	10.4	1993	14	2002	16	2011	10.8
1976	10.9	1985	15.2	1994	9.7	2003	6.4		
1977	8.1	1986	10.7	1995	13.3	2004	9.1		
1978	10.1	1987	9.5	1996	12.2	2005	13.4		

24hrs_AMP

Year	AMP	Year	AMP	Year	AMP	Year	AMP	Year	AMP
1970	25.1	1979	23.2	1988	24.7	1997	38.7	2006	49
1971	26.2	1980	38.8	1989	30.9	1998	30.2	2007	48.5
1972	29.2	1981	41.6	1990	37.4	1999	45.7	2008	39.8
1973	33.5	1982	31.4	1991	30.6	2000	37.4	2009	25
1974	20.6	1983	38.7	1992	32.6	2001	59.3	2010	-99.9
1975	37.1	1984	36.3	1993	22.8	2002	37.6	2011	32.3
1976	38.6	1985	31.5	1994	28.1	2003	51.3		
1977	19.3	1986	21.2	1995	37.2	2004	41.9		
1978	43.9	1987	24.7	1996	25.9	2005	31.2		

TABLE 16 ANNUAL MAXIMUM RAINFALL DATA FOR COMOX A (1963-2006)

5min_AMP

Year	AMP	Year	AMP	Year	AMP	Year	AMP	Year	AMP
1963	5.1	1972	1.3	1981	2.3	1990	1.4	2001	2.4
1964	2	1973	1.8	1982	6	1992	2.3	2002	3.7
1965	4.1	1974	2.5	1983	3.1	1993	6.9	2003	1.9
1966	2.5	1975	4.3	1984	2	1994	4.1	2004	1.2
1967	1.8	1976	1.8	1985	1.8	1995	2.7	2006	-99.9
1968	5.1	1977	2.3	1986	3	1996	2.3		
1969	3.8	1978	1.9	1987	1.8	1997	3.6		
1970	1.5	1979	5	1988	3.7	1998	2.8		
1971	2	1980	4.8	1989	2.9	1999	1.9		

1hr_AMP

Year	AMP	Year	AMP	Year	AMP	Year	AMP	Year	AMP
1963	10.9	1972	7.9	1981	15	1990	7	2001	10
1964	8.1	1973	11.7	1982	8.7	1992	9.4	2002	13
1965	16.8	1974	8.6	1983	16.8	1993	22.6	2003	8.5
1966	8.1	1975	8.4	1984	9.8	1994	7.6	2004	10.2
1967	10.9	1976	6.9	1985	6.5	1995	7.3	2006	-99.9
1968	12.4	1977	7.4	1986	11.2	1996	8.1		
1969	8.9	1978	7.8	1987	8.6	1997	20.4		
1970	11.4	1979	9.9	1988	10.8	1998	21.5		
1971	7.9	1980	11.4	1989	10.8	1999	9.7		

24hrs_AMP

Year	AMP	Year	AMP	Year	AMP	Year	AMP	Year	AMP
1963	63.8	1972	62	1981	51.1	1990	85.8	2001	58.5
1964	46.5	1973	72.4	1982	71	1992	56.3	2002	46
1965	53.1	1974	72.6	1983	89.6	1993	43.6	2003	84.9
1966	63.5	1975	59.7	1984	54.3	1994	54.3	2004	51.6
1967	56.6	1976	41.9	1985	40	1995	78.7	2006	62.2
1968	85.3	1977	49	1986	105.6	1996	42.7		
1969	64.8	1978	47	1987	46.5	1997	98.9		
1970	47	1979	62.7	1988	55.3	1998	103.1		
1971	57.4	1980	46.2	1989	39.3	1999	58.8		

TABLE 17 ANNUAL MAXIMUM RAINFALL DATA FOR MISSION WEST ABBEY (1963-2010)

5min_AMP

Year	AMP	Year	AMP	Year	AMP	Year	AMP	Year	AMP
1963	3.6	1973	3.3	1983	3.5	1993	3.8	2003	3.5
1964	3.8	1974	2.5	1984	4.1	1994	3.4	2004	3.7
1965	2	1975	3	1985	3	1995	3.1	2005	3.7
1966	2.3	1976	2.8	1986	4.7	1996	3.9	2006	3.3
1967	6.1	1977	2.5	1987	2.6	1997	4.3	2007	5.2
1968	4.8	1978	5.6	1988	2.6	1998	4.3	2008	3.4
1969	2.8	1979	3	1989	3.6	1999	2.9	2009	4.6
1970	7.9	1980	2.7	1990	5.5	2000	2.8	2010	4.3
1971	2.8	1981	5.1	1991	2.3	2001	4.7		
1972	4.6	1982	2.1	1992	4.6	2002	2.7		

1hr_AMP

Year	AMP	Year	AMP	Year	AMP	Year	AMP	Year	AMP
1963	17.5	1973	10.9	1983	12.9	1993	9.9	2003	16.2
1964	16.8	1974	11.2	1984	17.7	1994	13.7	2004	15.4
1965	9.7	1975	10.2	1985	6.5	1995	12.8	2005	11.6
1966	15.5	1976	9.9	1986	25.7	1996	16	2006	11.4
1967	13	1977	14.2	1987	13.2	1997	15.4	2007	12
1968	23.6	1978	11.4	1988	12.2	1998	8.1	2008	9.8
1969	11.7	1979	16.1	1989	17.2	1999	9.6	2009	12.9
1970	24.6	1980	13.5	1990	21.5	2000	10.1	2010	10.9
1971	11.4	1981	23.6	1991	9.9	2001	15.7		
1972	17	1982	9.1	1992	10.6	2002	10.3		

24hrs_AMP

Year	AMP	Year	AMP	Year	AMP	Year	AMP	Year	AMP
1963	60.7	1973	55.9	1983	97.1	1993	65.9	2003	136
1964	61.7	1974	79.5	1984	97.2	1994	53.5	2004	85.9
1965	71.9	1975	87.9	1985	68.1	1995	86.1	2005	90.6
1966	69.3	1976	58.4	1986	97.7	1996	62.1	2006	95.8
1967	62.5	1977	64	1987	59.4	1997	79.2	2007	99.7
1968	103.9	1978	60.6	1988	75.1	1998	55.7	2008	47.3
1969	76.5	1979	89	1989	89.4	1999	80.1	2009	86.3
1970	57.7	1980	101.6	1990	114.7	2000	49.9	2010	77.6
1971	77.2	1981	74.4	1991	63.8	2001	78.9		
1972	85.3	1982	75.6	1992	70.1	2002	78.6		

Table 18 Annual Maximum Rainfall Data for Pentiction A (1953-2002)

5min_AMP

Year	AMP	Year	AMP	Year	AMP	Year	AMP	Year	AMP
1953	2.5	1963	1.8	1977	3	1987	3.2	1997	6.6
1954	2	1964	4.3	1978	2.2	1988	2.7	1998	5.9
1955	3	1965	2.5	1979	2.8	1989	12.2	1999	3
1956	1.3	1966	-99.9	1980	2.7	1990	4	2000	3.7
1957	3.6	1969	1.8	1981	2.9	1991	3	2001	2.6
1958	8.1	1972	4.6	1982	6.7	1992	2.3	2002	1.5
1959	2.3	1973	1.8	1983	5.6	1993	3.5		
1960	2.3	1974	6.9	1984	3.7	1994	3.1		
1961	3.6	1975	2.5	1985	9.6	1995	3		
1962	2.8	1976	2.5	1986	7.4	1996	3.2		

1hr_AMP

Year	AMP	Year	AMP	Year	AMP	Year	AMP	Year	AMP
1953	7.4	1963	7.4	1977	14.7	1987	6.9	1997	23.7
1954	7.4	1964	19.8	1978	5.9	1988	9.8	1998	10.3
1955	7.1	1965	10.2	1979	14.5	1989	27.3	1999	9.9
1956	4.6	1966	9.9	1980	11.1	1990	7.7	2000	8.2
1957	4.1	1969	8.6	1981	9	1991	5	2001	13
1958	25.1	1972	13.5	1982	16.2	1992	8.9	2002	5.5
1959	4.3	1973	8.1	1983	10.4	1993	8.5		
1960	5.6	1974	20.6	1984	6	1994	10.8		
1961	6.9	1975	7.6	1985	12.7	1995	8.9		
1962	6.3	1976	8.6	1986	12	1996	8		

24hrs_AMP

Year	AMP	Year	AMP	Year	AMP	Year	AMP	Year	AMP
1953	20.6	1963	19	1977	20.1	1987	31.5	1997	26.3
1954	25.7	1964	26.9	1978	18.8	1988	38.4	1998	30
1955	15.7	1965	17.8	1979	28.1	1989	47.8	1999	19.4
1956	15.7	1966	15.7	1980	18.6	1990	32.5	2000	22.4
1957	29	1969	18.3	1981	25.4	1991	18.3	2001	16.9
1958	25.4	1972	26.9	1982	41.8	1992	33	2002	16.8
1959	18	1973	23.9	1983	28.5	1993	27.3		
1960	15	1974	23.6	1984	22.8	1994	22		
1961	21.1	1975	17.8	1985	25.2	1995	21.6		
1962	19	1976	18.5	1986	21.4	1996	24.2		

Table 19 Annual Maximum Rainfall Data for Pitt Polder (1965-2007)

5min_AMP

Year	AMP	Year	AMP	Year	AMP	Year	AMP	Year	AMP
1965	2.5	1974	5.1	1983	3.4	1994	3.7	2003	3
1966	3	1975	4.1	1984	3.9	1995	3.2	2004	4
1967	2.5	1976	5.1	1985	3.2	1996	6.3	2005	3.6
1968	3.8	1977	2.3	1986	5.9	1997	4.9	2006	4.7
1969	2.5	1978	4.1	1987	2.7	1998	9.6	2007	2.6
1970	1.8	1979	2.4	1988	2.7	1999	2.8		
1971	5.1	1980	3.9	1989	4	2000	2.8		
1972	10.2	1981	6.6	1990	4.4	2001	3.6		
1973	2.8	1982	2.9	1993	5.9	2002	3		

1hr_AMP

Year	AMP	Year	AMP	Year	AMP	Year	AMP	Year	AMP
1965	11.4	1974	8.4	1983	14	1994	12.2	2003	14
1966	11.9	1975	15.5	1984	10.8	1995	18.4	2004	10.9
1967	11.4	1976	13.2	1985	16.7	1996	13	2005	11.2
1968	17.3	1977	10.2	1986	14.8	1997	15.7	2006	13.2
1969	12.4	1978	13.2	1987	8.7	1998	13.4	2007	17
1970	11.4	1979	11	1988	12	1999	9.6		
1971	16	1980	14.6	1989	14.9	2000	13.9		
1972	11.4	1981	18.1	1990	11.8	2001	8.6		
1973	12.7	1982	9.5	1993	18.8	2002	10.5		

24hrs_AMP

Year	AMP	Year	AMP	Year	AMP	Year	AMP	Year	AMP
1965	99.1	1974	95.8	1983	137.9	1994	71.5	2003	142.6
1966	99.6	1975	96.8	1984	116.7	1995	106.2	2004	77.9
1967	100.3	1976	77.2	1985	69.8	1996	70.8	2005	118.8
1968	144.3	1977	86.6	1986	135.9	1997	108.1	2006	111
1969	85.1	1978	83.2	1987	60.3	1998	89	2007	137.9
1970	70.1	1979	136.3	1988	69.6	1999	80.9		
1971	117.9	1980	109.9	1989	132.5	2000	52.9		
1972	122.2	1981	127.4	1990	101	2001	62.6		
1973	72.6	1982	88.5	1993	59.6	2002	117		

TABLE 20 ANNUAL MAXIMUM RAINFALL DATA FOR PRINCE GEORGE A (1960-2002)

5min_AMP

Year	AMP	Year	AMP	Year	AMP	Year	AMP	Year	AMP
1960	4.6	1969	10.7	1978	4	1987	3.4	1996	5.5
1961	5.1	1970	7.1	1979	3.2	1988	3.5	1997	4.4
1962	4.1	1971	2	1980	6.2	1989	4.5	1998	5.7
1963	4.3	1972	6.9	1981	5.2	1990	3.3	1999	4.2
1964	8.4	1973	8.6	1982	6.4	1991	9.6	2000	4
1965	15.2	1974	4.6	1983	11.8	1992	3.9	2001	3.5
1966	4.1	1975	3.6	1984	2.3	1993	4.4	2002	4.4
1967	3.8	1976	4.3	1985	3.3	1994	2.5		
1968	2	1977	4.3	1986	4.4	1995	6.5		

1hr_AMP

Year	AMP	Year	AMP	Year	AMP	Year	AMP	Year	AMP
1960	9.9	1969	10.9	1978	6.1	1987	6.8	1996	10.1
1961	5.8	1970	19	1979	12.7	1988	9.5	1997	11.6
1962	8.9	1971	7.4	1980	9.5	1989	14.8	1998	14.1
1963	20.1	1972	18.8	1981	10.8	1990	12.6	1999	8.7
1964	11.4	1973	21.6	1982	11.7	1991	15.4	2000	8.1
1965	24.9	1974	9.9	1983	21.5	1992	10.7	2001	7.4
1966	7.4	1975	6.3	1984	7.3	1993	9.6	2002	11
1967	6.9	1976	7.1	1985	6.2	1994	9		
1968	7.4	1977	10.4	1986	6.4	1995	16.9		

24hrs_AMP

Year	AMP	Year	AMP	Year	AMP	Year	AMP	Year	AMP
1960	39.6	1969	27.2	1978	19.4	1987	24.2	1996	24.8
1961	26.4	1970	27.9	1979	23.6	1988	24.8	1997	23.2
1962	39.6	1971	35.1	1980	30.1	1989	24.2	1998	-99.9
1963	32.5	1972	38.1	1981	25.7	1990	28.8	1999	27.8
1964	42.7	1973	24.6	1982	47.7	1991	19.4	2000	44.5
1965	47.8	1974	26.9	1983	31.3	1992	27.7	2001	28.9
1966	27.9	1975	18.5	1984	38.8	1993	30.3	2002	28.6
1967	25.9	1976	28.7	1985	21	1994	28.2		
1968	25.1	1977	26.7	1986	23	1995	17.9		

Table 21 Annual Maximum Rainfall Data for Terrace Pcc (1968-2013)

5min_AMP

Year	AMP	Year	AMP	Year	AMP	Year	AMP	Year	AMP
1968	2.5	1977	1.5	1987	3.8	1996	2.1	2005	1.9
1969	1.5	1979	2.7	1988	1.3	1997	4.8	2006	3.7
1970	1.3	1980	5.2	1989	3	1998	2.8	2007	2.9
1971	1	1981	2	1990	4.8	1999	2.1	2008	2.5
1972	1.3	1982	1.2	1991	2.7	2000	1.9	2009	-99.9
1973	2	1983	3.6	1992	5.3	2001	1.2	2010	2.2
1974	2.3	1984	2.5	1993	1.6	2002	2.2	2011	2
1975	1.8	1985	3.4	1994	1.8	2003	2	2012	2.3
1976	1.8	1986	4.3	1995	2.3	2004	2.5	2013	1.5

1hr_AMP

Year	AMP	Year	AMP	Year	AMP	Year	AMP	Year	AMP
1968	20.8	1977	9.7	1987	18.2	1996	6.9	2005	8.9
1969	6.6	1979	7.6	1988	9.2	1997	19.8	2006	11.2
1970	7.1	1980	19.1	1989	8.8	1998	9.4	2007	9.9
1971	8.1	1981	6.4	1990	7.7	1999	8.4	2008	6.1
1972	5.3	1982	6	1991	9.3	2000	7.2	2009	-99.9
1973	5.8	1983	8.2	1992	17	2001	4.9	2010	7.8
1974	8.4	1984	7.7	1993	9.1	2002	7.2	2011	8.1
1975	3.6	1985	11.3	1994	8.7	2003	7.5	2012	11
1976	5.1	1986	8.3	1995	5.3	2004	8.2	2013	5.1

24hrs_AMP

Year	AMP	Year	AMP	Year	AMP	Year	AMP	Year	AMP
1968	67.8	1977	34	1987	75.9	1996	37.4	2005	79.5
1969	65.8	1979	32.8	1988	97	1997	90.2	2006	88.9
1970	31	1980	57.6	1989	61	1998	51.5	2007	103.7
1971	44.7	1981	55.8	1990	68.2	1999	103.2	2008	53.8
1972	58.9	1982	40.6	1991	88.2	2000	57.9	2009	61.6
1973	31.2	1983	35.4	1992	114.7	2001	62	2010	60.7
1974	82.8	1984	55.9	1993	70.7	2002	42	2011	45.6
1975	30	1985	55	1994	71.4	2003	50.6	2012	45.2
1976	33.3	1986	44	1995	36.2	2004	54.7	2013	46.7

Table 22 Annual Maximum Rainfall Data for Tofino A (1970-2012)

5min_AMP

Year	AMP	Year	AMP	Year	AMP	Year	AMP	Year	AMP
1970	3	1980	5	1989	4.3	1998	3.2	2007	3.2
1971	3.3	1981	3.9	1990	4.1	1999	2.4	2008	2.8
1972	2.5	1982	1.9	1991	4.7	2000	3.3	2009	4.3
1973	5.8	1983	3.4	1992	5.2	2001	5.8	2010	2.2
1974	7.9	1984	5	1993	3.7	2002	4	2011	3.6
1975	2.5	1985	4	1994	3.6	2003	3.3	2012	3.6
1976	3.3	1986	2.7	1995	3.5	2004	4.4		
1977	6.1	1987	3.3	1996	6	2005	7.2		
1978	3	1988	2.7	1997	7.7	2006	4.6		

1hr_AMP

Year	AMP	Year	AMP	Year	AMP	Year	AMP	Year	AMP
1970	20.3	1980	17.5	1989	14.4	1998	13.5	2007	16
1971	20.3	1981	17.8	1990	15.6	1999	20.7	2008	18.7
1972	12.2	1982	19.8	1991	20.5	2000	18.9	2009	21.6
1973	22.1	1983	14.4	1992	18.1	2001	16.7	2010	12.6
1974	22.4	1984	15.7	1993	18.8	2002	33.7	2011	17.9
1975	18.8	1985	17.2	1994	18.1	2003	19.4	2012	24.9
1976	20.6	1986	16.2	1995	18.4	2004	13.8		
1977	21.8	1987	13.4	1996	18.6	2005	19.7		
1978	16.1	1988	12.9	1997	22.9	2006	20		

24hrs_AMP

Year	AMP	Year	AMP	Year	AMP	Year	AMP	Year	AMP
1970	85.6	1980	208.6	1989	102.4	1998	123.8	2007	156.5
1971	127	1981	141.7	1990	147.2	1999	145.6	2008	115.6
1972	149.6	1982	119	1991	139.8	2000	100.8	2009	186.1
1973	127.8	1983	108.6	1992	154.9	2001	109.6	2010	90.8
1974	139.7	1984	107.9	1993	163.3	2002	108.4	2011	102.4
1975	164.6	1985	70.8	1994	128.3	2003	118.6	2012	183.8
1976	102.6	1986	139.6	1995	115.2	2004	155		
1977	99.8	1987	136.7	1996	135.5	2005	228		
1978	160	1988	104.9	1997	157.1	2006	141.9		

TABLE 23 ANNUAL MAXIMUM RAINFALL DATA FOR VANCOUVER INTL A (1953-2013)

5min_AMP

Year	AMP	Year	AMP	Year	AMP	Year	AMP	Year	AMP	Year	AMP
1953	3.8	1964	3.3	1975	4.1	1986	3.1	1997	5.4	2008	2
1954	4.8	1965	1.8	1976	2	1987	2.8	1998	5.5	2009	2.9
1955	1.8	1966	1.5	1977	4.3	1988	2.8	1999	5.5	2010	3.2
1956	2.8	1967	3	1978	2.8	1989	3.4	2000	3.7	2011	2.2
1957	3.3	1968	3.3	1979	2.1	1990	2.5	2001	3.3	2012	1.9
1958	5.1	1969	1.8	1980	2.7	1991	2.2	2002	1.9	2013	6.1
1959	5.8	1970	2	1981	4.4	1992	3.7	2003	-99.9		
1960	6.3	1971	2.8	1982	2.8	1993	3.9	2004	6.4		
1961	2.5	1972	2.3	1983	1.9	1994	3	2005	5.5		
1962	3.8	1973	4.1	1984	3.1	1995	3.3	2006	5.9		
1963	3.3	1974	4.3	1985	2.9	1996	5.6	2007	2		

1hr_AMP

Year	AMP	Year	AMP	Year	AMP	Year	AMP	Year	AMP	Year	AMP
1953	16	1964	12.2	1975	13	1986	12.8	1997	13.4	2008	5.8
1954	11.9	1965	8.9	1976	8.4	1987	9.1	1998	16	2009	7.6
1955	8.4	1966	8.4	1977	10.7	1988	9.4	1999	23.9	2010	14.3
1956	10.4	1967	7.1	1978	7.7	1989	10.7	2000	10.2	2011	7.4
1957	6.9	1968	13.5	1979	9.6	1990	9.1	2001	11.1	2012	8
1958	18.8	1969	7.1	1980	10.1	1991	9.7	2002	5.3	2013	14.8
1959	11.2	1970	9.9	1981	14.1	1992	14.4	2003	15.2		
1960	12.7	1971	8.9	1982	7.5	1993	11.3	2004	38.6		
1961	13.2	1972	8.9	1983	7.6	1994	12.4	2005	13.4		
1962	15	1973	7.6	1984	7.4	1995	8.4	2006	13.6		
1963	12.7	1974	8.9	1985	11.3	1996	15.5	2007	12		

24hrs_AMP

Year	AMP	Year	AMP	Year	AMP	Year	AMP	Year	AMP	Year	AMP
1953	48	1964	53.6	1975	71.6	1986	59.6	1997	54.1	2008	40
1954	53.6	1965	38.4	1976	50.3	1987	47.8	1998	45.6	2009	41.3
1955	79.5	1966	47.2	1977	40.1	1988	53	1999	49.5	2010	55.9
1956	59.7	1967	54.9	1978	32.1	1989	65	2000	38.2	2011	35.3
1957	30.2	1968	82.8	1979	90.2	1990	48.6	2001	42.8	2012	36.1
1958	57.7	1969	42.4	1980	56	1991	55.8	2002	30.6	2013	46.6
1959	55.9	1970	33.3	1981	65.1	1992	48.6	2003	89.3		
1960	48	1971	51.8	1982	64.2	1993	33.3	2004	91.6		
1961	52.6	1972	93	1983	50.3	1994	52	2005	62.6		
1962	50.5	1973	54.4	1984	44.1	1995	43.1	2006	49.6		
1963	55.4	1974	53.8	1985	38.3	1996	53.5	2007	51.1		

TABLE 24 ANNUAL MAXIMUM RAINFALL DATA FOR VICTORIA INTL A (1965-2013)

5min_AMP

Year	AMP	Year	AMP	Year	AMP	Year	AMP	Year	AMP
1965	1.3	1975	3	1985	1.9	1995	3.4	2005	2.9
1966	1	1976	1.8	1986	5.4	1996	1.8	2006	2.7
1967	2.3	1977	1.8	1987	1.9	1997	7.3	2007	3
1968	2	1978	4.3	1988	4.4	1998	3.9	2008	1.8
1969	3.6	1979	3.8	1989	3.6	1999	3.7	2009	4.3
1970	2	1980	3.9	1990	1.8	2000	2.7	2010	2.4
1971	2.5	1981	3.2	1991	1.4	2001	2.6	2011	4.5
1972	1.8	1982	2.8	1992	3.5	2002	1.5	2012	1.7
1973	1.8	1983	2.7	1993	4.6	2003	1.9	2013	2.8
1974	1.5	1984	2.2	1994	3.7	2004	3.9		

1hr_AMP

Year	AMP	Year	AMP	Year	AMP	Year	AMP	Year	AMP
1965	8.4	1975	7.6	1985	6	1995	8.3	2005	5.9
1966	6.1	1976	6.9	1986	12.4	1996	8.6	2006	7.4
1967	7.9	1977	7.6	1987	8.8	1997	12.5	2007	13.3
1968	7.9	1978	8.9	1988	8.7	1998	8.4	2008	9.4
1969	13.5	1979	8.4	1989	10.5	1999	8.6	2009	8.8
1970	6.9	1980	8.5	1990	9.4	2000	6.6	2010	7.8
1971	7.6	1981	9	1991	6.8	2001	8.3	2011	18.4
1972	9.9	1982	7.5	1992	13.1	2002	6.9	2012	6.5
1973	7.6	1983	10	1993	16.4	2003	11.2	2013	9.3
1974	11.9	1984	9.4	1994	13.4	2004	7.5		

24hrs_AMP

Year	AMP	Year	AMP	Year	AMP	Year	AMP	Year	AMP
1965	47	1975	54.1	1985	49.8	1995	67	2005	39.6
1966	37.1	1976	49.3	1986	101.5	1996	49.1	2006	54.8
1967	74.2	1977	43.2	1987	71.8	1997	53.9	2007	88
1968	62.2	1978	35.4	1988	46.6	1998	47	2008	59.8
1969	29.2	1979	69.5	1989	40.1	1999	82.9	2009	63.7
1970	35.8	1980	73.3	1990	65.1	2000	32.8	2010	66
1971	49.3	1981	37.4	1991	53.2	2001	65	2011	45.7
1972	89.2	1982	48.8	1992	55.9	2002	70	2012	41.7
1973	50.5	1983	51.2	1993	50	2003	138.2	2013	57.5
1974	50.5	1984	47.2	1994	56.5	2004	48.9		

TABLE 25 ANNUAL MAXIMUM RAINFALL DATA FOR VICTORIA GONZALES HTS (1925-1988)

5min_AMP

Year	AMP	Year	AMP	Year	AMP	Year	AMP	Year	AMP	Year	AMP
1925	1	1941	5.1	1951	1	1962	1.3	1972	2.5	1983	2
1926	2.3	1942	1	1953	2.3	1963	4.3	1973	1.5	1984	2.5
1927	3.8	1943	1.3	1954	1.8	1964	1.3	1974	1	1985	1.4
1928	2	1944	1.3	1955	1.3	1965	1.3	1975	2.5	1986	2.4
1929	2.3	1945	1	1956	2.5	1966	1.8	1976	1.3	1987	1.7
1930	1.8	1946	2	1957	1.8	1967	2.8	1977	1.3	1988	1.8
1937	2	1947	1.3	1958	2.5	1968	1.3	1978	1.3		
1938	2.3	1948	2.5	1959	1.5	1969	1.8	1979	1.9		
1939	2.5	1949	2	1960	2.3	1970	2	1981	3.3		
1940	3.8	1950	1	1961	1.8	1971	2.8	1982	1.6		

1hr_AMP

Year	AMP	Year	AMP	Year	AMP	Year	AMP	Year	AMP	Year	AMP
1925	5.1	1941	8.6	1951	6.9	1962	10.2	1972	7.1	1983	6.3
1926	6.6	1942	6.6	1953	8.4	1963	8.1	1973	6.1	1984	6.8
1927	6.6	1943	6.3	1954	7.1	1964	8.1	1974	8.9	1985	5.7
1928	7.4	1944	4.8	1955	7.9	1965	6.9	1975	8.1	1986	10.1
1929	5.8	1945	7.1	1956	18.8	1966	6.6	1976	9.1	1987	6.5
1930	4.6	1946	6.9	1957	5.3	1967	6.9	1977	8.4	1988	8.9
1937	7.1	1947	6.6	1958	7.6	1968	5.6	1978	7		
1938	7.1	1948	8.6	1959	8.6	1969	5.6	1979	8.3		
1939	6.9	1949	8.1	1960	7.6	1970	6.9	1981	9.5		
1940	10.7	1950	5.1	1961	7.4	1971	11.4	1982	9.5		

24hrs_AMP

Year	AMP	Year	AMP	Year	AMP	Year	AMP	Year	AMP	Year	AMP
1925	25.9	1941	36.8	1951	39.1	1962	64.5	1972	70.1	1983	49.5
1926	41.9	1942	28.2	1953	50.3	1963	50	1973	31.5	1984	47.6
1927	47.5	1943	38.4	1954	38.4	1964	35.8	1974	51.8	1985	30
1928	53.1	1944	26.9	1955	89.2	1965	31.7	1975	72.1	1986	67.2
1929	44.2	1945	40.1	1956	118.9	1966	36.8	1976	58.4	1987	48.4
1930	29.7	1946	34	1957	29.5	1967	47.8	1977	29.7	1988	29.2
1937	67.3	1947	41.4	1958	54.9	1968	41.7	1978	38.4		
1938	70.1	1948	47	1959	49.3	1969	26.9	1979	100.2		
1939	38.4	1949	105.4	1960	33.8	1970	24.1	1981	25.7		
1940	35.3	1950	39.9	1961	57.9	1971	64	1982	78.4		

APPENDIX 2 GOODNESS-OF-FIT TESTS RESULTS

TABLE 26 TOP 3 DISTRIBUTIONS (A) 5MIN, (B) 1HR & (C) 24HR

(a) Top 3 Distributions for 5 min AMP

Stations	RMSE	RRMSE	MAE	CC
1	LP3,GEV,GNO	PE3,GNO,LP3	LP3,GNO,PE3	(GEV),(LP3),((BEP))
2	GPA,WAK,PE3	(GPA),(PE3),WAK	(GPA),(WAK),PE3	(GPA),(WAK),PE3
3	LP3,GEV,GNO	(LP3),(PE3),GNO	GLO,LP3,BEP	(GEV),(GLO),(GNO)
4	PE3,GPA,GNO	BEK,(BEP),(GEV)	PE3,GPA,WAK	PE3,(GPA),(WAK)
5	LP3,GNO,BEK	(BEK),(GEV),(LP3),	LP3,(GPA),(PE3)	(GEV),(GNO),(LP3)
6	LP3,GNO,WAK	BEP,BEK,GLO	GNO,GPA,LP3	(GEV),(GNO),(LP3)
7	GPQ,PE3,WAK	GNO,PE3,(GEV)	GPA,GUM,PE3	GPA,(PE3),(WAK)
8	(GPA),(PE3),WAK	(GEV),(GNO),(LP3)	GPA,PE3,WAK	(GPA),(PE3),(WAK)
9	GPA,WAK,PE3	(GPA),(WAK),PE3	GPA,WAK,PE3	GPA,WAK,PE3
10	BEP,LP3,GNO	WAK,(LP3),(PE3)	GLO,BEP,LP3	(BEP),(GNO),(LP3)
11	LP3,GEV,GNO	PE3,GNO,LP3	LP3,GNO,PE3	(GEV),(LP3),((BEP))

(b) Top 3 Distributions for 1 hr AMP

Stations	RMSE	RRMSE	MAE	CC
1	BEK,BEP,WAK	WAK,(GEV),(LP3)	BEP,BEK,LP3	WAK,(BEK),(BEP)
2	PE3,GPA,WAK	GNO,GPA,(LP3)	PE3,GPA,WAK	PE3,GPA,WAK
3	WAK,GPA,PE3	GEV,GNO,(GUM)	GPA,WAK,PE3	WAK,(GPA),(PE3)
4	PE3,GPA,GNO	(GEV),(LP3),GNO	PE3,GPA,GNO	(GPA),(PE3),GNO
5	GPA,GEV,PE3	(GEV),(GNO),(PE3)	GPA,WAK,(GEV)	(GEV),(GPA),(PE3)
6	GPA,WAK,PE3	GPA,(PE3),(WAK)	GPA,WAK,PE3	GPA,WAK,PE3
7	(GPA),(PE3),GNO	BEP,BEK,GLO	GPA,PE3,GNO	(GNO),(GPA),(PE3)
8	WAK,GLO,GUM	WAK,(BEP),(GLO)	GUM,WAK,GLO	WAK,(BEP),(GLO)
9	BEP,GLO,BEK	GLO,(BEK),(BEP)	BEP,BEK,GLO	BEP,GLO,BEK
10	GNO,LP3,PE3	(GEV),(GNO),(LP3)	PE3,WAK,LP3,	(GNO),(LP3),(PE3)
11	WAK,GLO,BEP	WAK,GLO,BEP	WAK,GLO,GEV	WAK,GLO,BEP

(c) Top 3 Distributions for 24 hrs AMP

Stations	RMSE	RRMSE	MAE	CC
1	WAK,LP3,PE3	WAK,LP3,PE3	PE3,GNO,GEV	WAK,(GEV),(GNO)
2	GPA,WAK,PE3	GPA,(PE3),(WAK)	GPA,GUM,WAK	GPA,WAK,PE3
3	WAK,LP3,GNO	WAK,(GEV),(GNO)	GLO,BEP,GUM	WAK,(GNO),(LP3)
4	LP3,GNO,GEV	PE3,(GNO),(LP3)	LP3,GNO,GEV	(GEV),(GNO),(LP3)
5	GPA,WAK,GEV	GPA,WAK,LP3	WAK,GPA,BEP	(GPA),(WAK),GEV
6	GPA,PE3,GUM	(GEV),(GUM),((BEK))	GPA,GUM,PE3	(GPA),(GUM),(PE3)
7	GPA,PE3,WAK	GPA,PE3,LP3	GPA,PE3,WAK	GPA,(PE3),(WAK)
8	BEK,GLO,BEP	(BEK),(BEP),(GLO)	BEK,GLO,WAK	(BEK),(BEP),(GLO)
9	GUM,GEV,GNO	(BEK),(GLO),(GUM)	GPA,PE3,GNO	(GEV),(GNO),(GUM)
10	BEP,WAK,GLO	(BEP),(WAK),GLO	BEP,WAK,GLO	(BEP),(GLO),WAK
11	PE3,GPA,WAK	PE3,GNO,LP3	WAK,GPA,PE3	PE3,(GNO),(GPA)

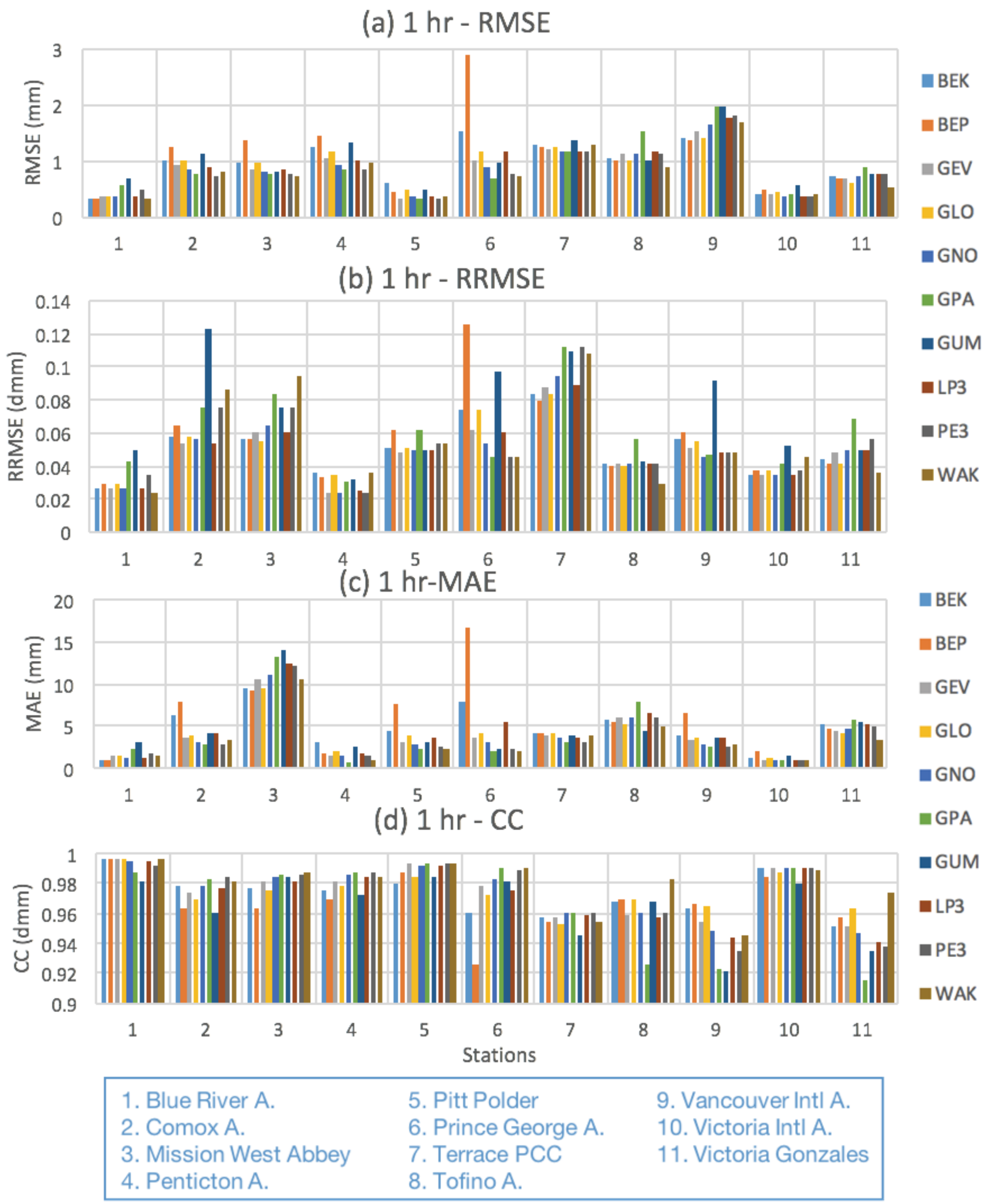

FIGURE 17 GOODNESS-OF-FIT ANALYSIS RESULT FOR 1HR RAINFALL DURATION AND FOR ALL 11 RAINGAGES

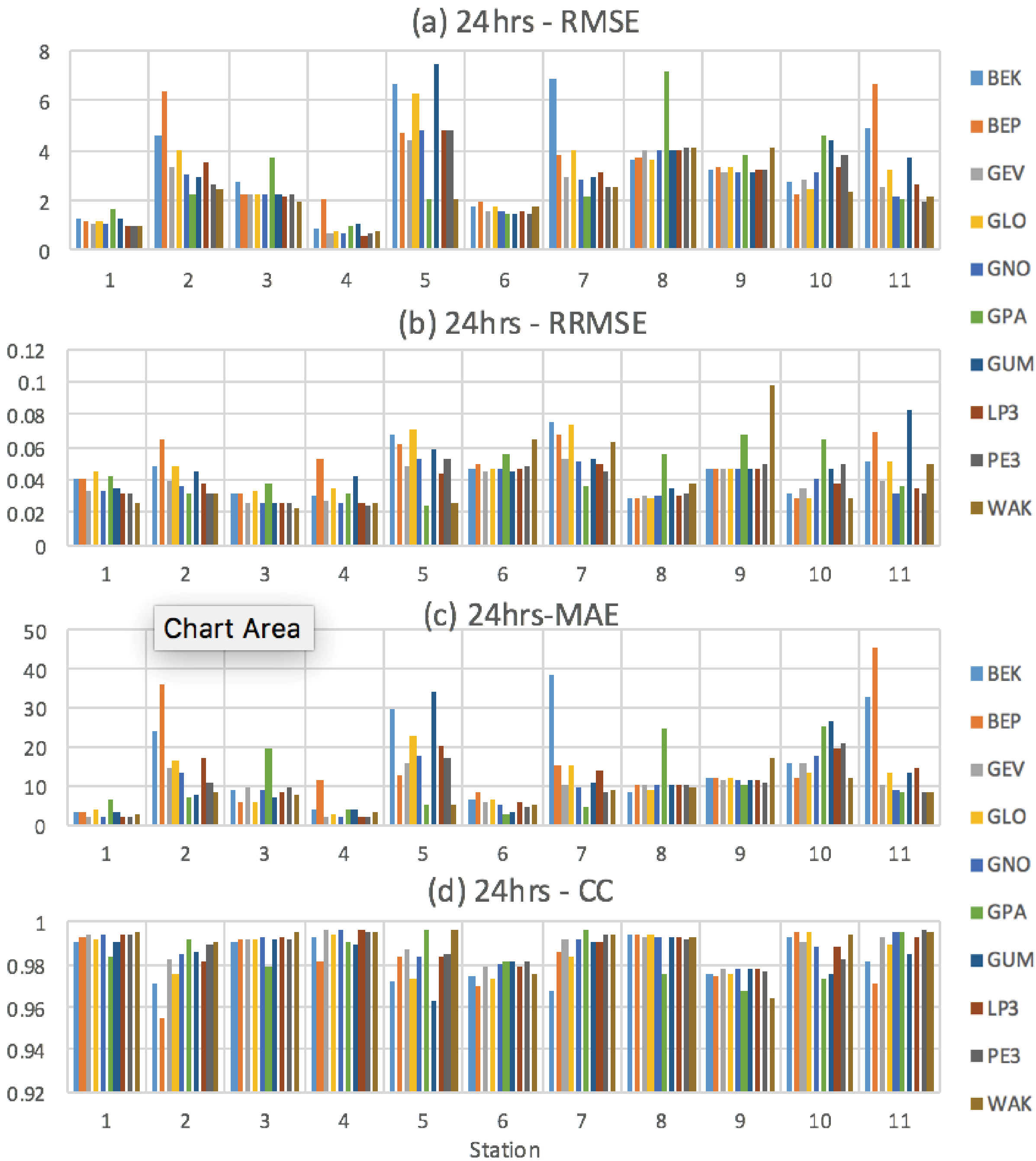

1. Blue River A.	5. Pitt Polder	9. Vancouver Intl A.
2. Comox A.	6. Prince George A.	10. Victoria Intl A.
3. Mission West Abbey	7. Terrace PCC	11. Victoria Gonzales
4. Penticton A.	8. Tofino A.	

FIGURE 18 GOODNESS-OF-FIT ANALYSIS RESULT FOR 24HR RAINFALL DURATION AND FOR ALL 11 RAINGAGES

Table 27 Rank-Sum Test Results for Continental Climate (a) 5min, (b) 1hr & (c) 24hr

(a) Continental Climate - 5min

Rank	RMSE		RRMSE		MAE		CC	
1	12	GNO	12.5	GEV	11	GPA	11.5	WAK
2	14	WAK	14	BEP	12	WAK	16	GNO
3	15	GPA	16	BEK	14	GNO	16.5	GEV
4	18	PE3	16	GLO	17	PE3	18	GPA
5	19	GEV	16	LP3	21	GEV	20.5	LP3
6	20	LP3	19	GNO	26	LP3	21.5	PE3
7	24	BEP	28	GPA	27	GLO	25	GLO
8	29	GLO	28	PE3	28	BEP	28	BEP
9	34	GUM	30.5	WAK	31	GUM	28.5	BEK
10	35	BEK	40	GUM	33	BEK	34.5	GUM

(b) Continental Climate – 1hr

Rank	RMSE		RRMSE		MAE		CC	
1	13	GPA	9	LP3	12	GNO	7	WAK
2	13	PE3	10	GEV	12	GPA	11.5	GPA
3	17	GNO	11.5	GNO	12	PE3	12.5	PE3
4	17	WAK	12.5	WAK	12	WAK	13.5	GNO
5	21	GEV	16.5	BEK	16	GEV	15.5	GEV
6	21	LP3	17.5	GPA	19	LP3	18.5	GLO
7	26	BEK	18	PE3	20	BEK	18.5	LP3
8	28	BEP	18.5	GLO	20	GLO	20.5	BEK
9	28	GLO	22.5	BEP	21	BEP	23.5	BEP
10	34	GUM	29	GUM	21	GUM	24	GUM

(c) Continental Climate – 24hr

Rank	RMSE		RRMSE		MAE		CC	
1	11	PE3	12	LP3	10	PE3	12.5	PE3
2	14	GNO	13	PE3	12	GNO	14	GNO
3	15	LP3	15.5	GNO	17	GEV	15	WAK
4	17	WAK	17	GEV	19	GPA	15.5	GEV
5	19	GEV	21	WAK	19	LP3	17.5	LP3
6	20	GPA	21.5	GUM	19	WAK	21	GPA
7	26	GUM	26	GPA	22	GUM	26	GUM
8	31	GLO	27	BEK	31	GLO	31	GLO
9	33	BEK	33	GLO	35	BEK	33.5	BEK
10	34	BEP	34	BEP	36	BEP	34	BEP

TABLE 28 RANK-SUM TEST RESULTS FOR MEDITERRANEAN CLIMATE (A) 5MIN, (B) 1HR & (C) 24HR

(a) Mediterranean Climate – 5min

Rank	RMSE		RRMSE		MAE		CC	
1	13	GPA	9	LP3	12	GNO	7	WAK
2	13	PE3	10	GEV	12	GPA	11.5	GPA
3	17	GNO	11.5	GNO	12	PE3	12.5	PE3
4	17	WAK	12.5	WAK	12	WAK	13.5	GNO
5	21	GEV	16.5	BEK	16	GEV	15.5	GEV
6	21	LP3	17.5	GPA	19	LP3	18.5	GLO
7	26	BEK	18	PE3	20	BEK	18.5	LP3
8	28	BEP	18.5	GLO	20	GLO	20.5	BEK
9	28	GLO	22.5	BEP	21	BEP	23.5	BEP
10	34	GUM	29	GUM	21	GUM	24	GUM

(b) Mediterranean Climate – 1hr

Rank	RMSE		RRMSE		MAE		CC	
1	15	GNO	15	GNO	11	PE3	13	GNO
2	16	WAK	16	GEV	15.5	WAK	13	PE3
3	19	GEV	16	LP3	16	GPA	18	GPA
4	19	GLO	16.5	BEK	18	GNO	18.5	BEK
5	19	PE3	16.5	GLO	22	GEV	19	LP3
6	22	LP3	18	BEP	22	LP3	21.5	GEV
7	23	BEP	27.5	PE3	27	GLO	23.5	WAK
8	24	BEK	28.5	GPA	28	BEK	26.5	BEP
9	25	GPA	30	WAK	30	BEP	27	GLO
10	38	GUM	36	GUM	30.5	GUM	40	GUM

(c) Mediterranean Climate – 24hr

Rank	RMSE		RRMSE		MAE		CC	
1	4.5	GPA	15.5	GEV	7	WAK	5.5	WAK
2	7.5	PE3	16.5	GNO	19.5	PE3	20	PE3
3	11.5	GNO	18	GLO	20	GNO	21	GEV
4	13	GEV	19.5	WAK	20.5	GEV	22	GLO
5	14.5	WAK	21	LP3	21	GLO	22	GNO
6	17	LP3	22	BEP	22	GPA	22.5	BEP
7	23	BEP	23	PE3	24	GUM	25	GPA
8	23	GLO	24	BEK	25	BEP	26.5	GUM
9	23.5	GUM	26	GUM	30	LP3	27.5	BEK
10	27.5	BEK	34.5	GPA	31	BEK	28	LP3

TABLE 29 RANK-SUM TEST RESULT FOR OCEANIC CLIMATE (A) 5MIN, (B) 1HR & (C) 24HR

(a) Oceanic Climate – 5min

Rank	RMSE		RRMSE		MAE		CC	
1	11	PE3	12	LP3	10	PE3	12.5	PE3
2	14	GNO	13	PE3	12	GNO	14	GNO
3	15	LP3	15.5	GNO	17	GEV	15	WAK
4	17	WAK	17	GEV	19	GPA	15.5	GEV
5	19	GEV	21	WAK	19	LP3	17.5	LP3
6	20	GPA	21.5	GUM	19	WAK	21	GPA
7	26	GUM	26	GPA	22	GUM	26	GUM
8	31	GLO	27	BEK	31	GLO	31	GLO
9	33	BEK	33	GLO	35	BEK	33.5	BEK
10	34	BEP	34	BEP	36	BEP	34	BEP

(b) Oceanic Climate – 1hr

Rank	RMSE		RRMSE		MAE		CC	
1	16	PE3	18.5	GNO	13	GPA	17	GNO
2	17	WAK	19.5	LP3	16	WAK	17	PE3
3	18	GEV	20	WAK	17	PE3	18	WAK
4	18	GNO	20.5	PE3	18	GNO	19	GEV
5	22	GPA	21	GLO	20	GEV	21.5	LP3
6	22	GUM	21.5	GEV	23	GLO	23	GLO
7	24	LP3	22	BEK	24	GUM	23	GPA
8	25	GLO	24	GPA	29	LP3	23.5	GUM
9	28	BEK	26	BEP	30	BEK	28.5	BEK
10	29	BEP	27	GUM	30	BEP	29.5	BEP

(c) Oceanic Climate – 24hr

Rank	RMSE		RRMSE		MAE		CC	
1	12	WAK	11.5	LP3	8	WAK	8.5	WAK
2	14	BEP	12	WAK	11	GLO	14	BEP
3	14	GNO	12.5	GEV	14	BEP	14.5	GNO
4	15	LP3	14	GNO	16	BEK	14.5	LP3
5	16	GLO	16	PE3	17	GNO	15	GEV
6	18	GEV	18	BEK	17	LP3	16	GLO
7	18	GUM	18	BEP	19	GEV	19	PE3
8	18	PE3	21	GLO	19	GUM	20	BEK
9	19	BEK	21	GPA	22	GPA	21.5	GPA
10	21	GPA	21	GUM	22	PE3	22	GUM

APPENDIX 3 QUANTILE-QUANTILE PLOTS FOR THE DISTRIBUTIONS

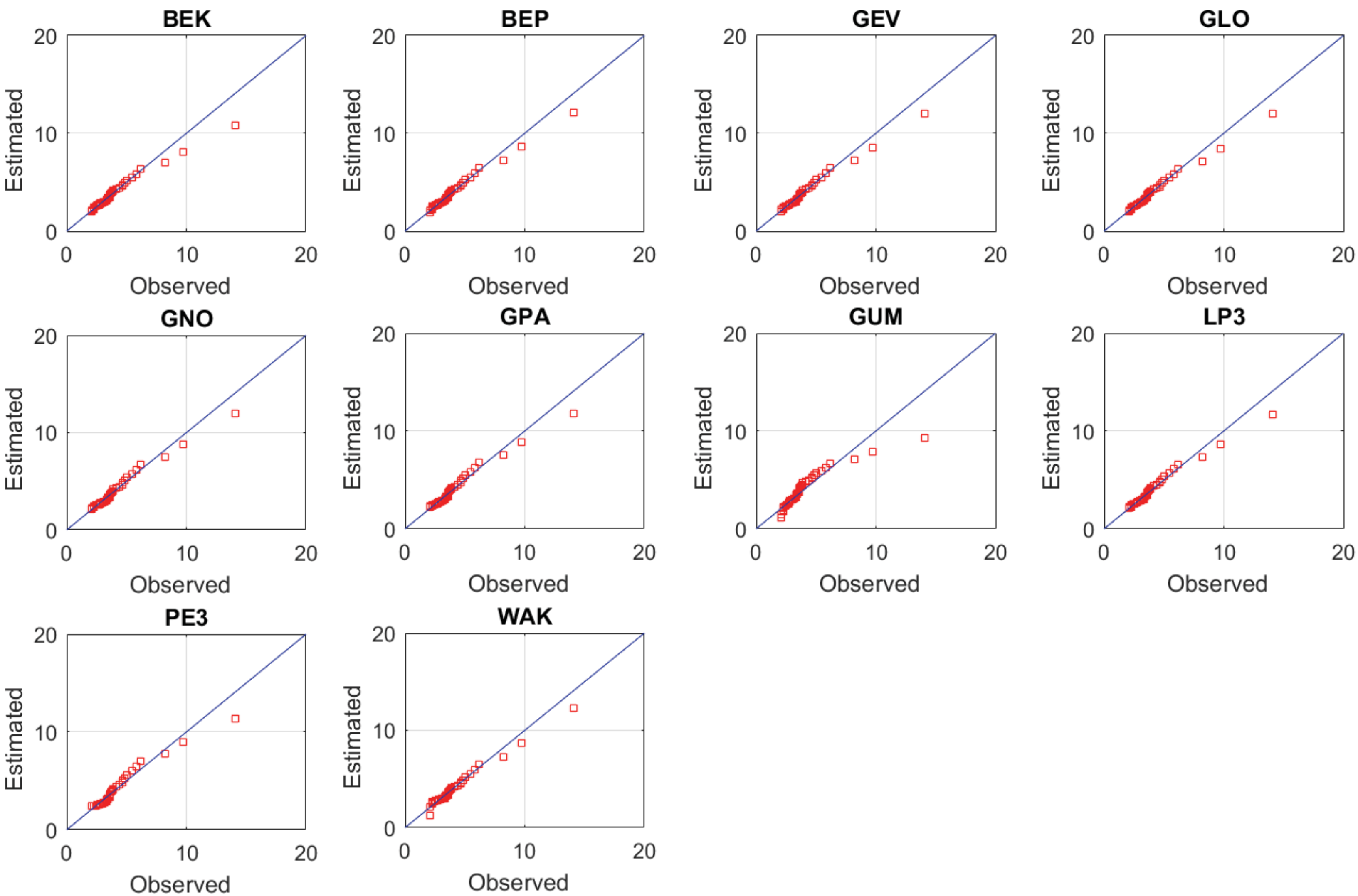

FIGURE 19 Q-Q PLOTS FOR 5MIN RAINFALL DATA OF BLUE RIVER A

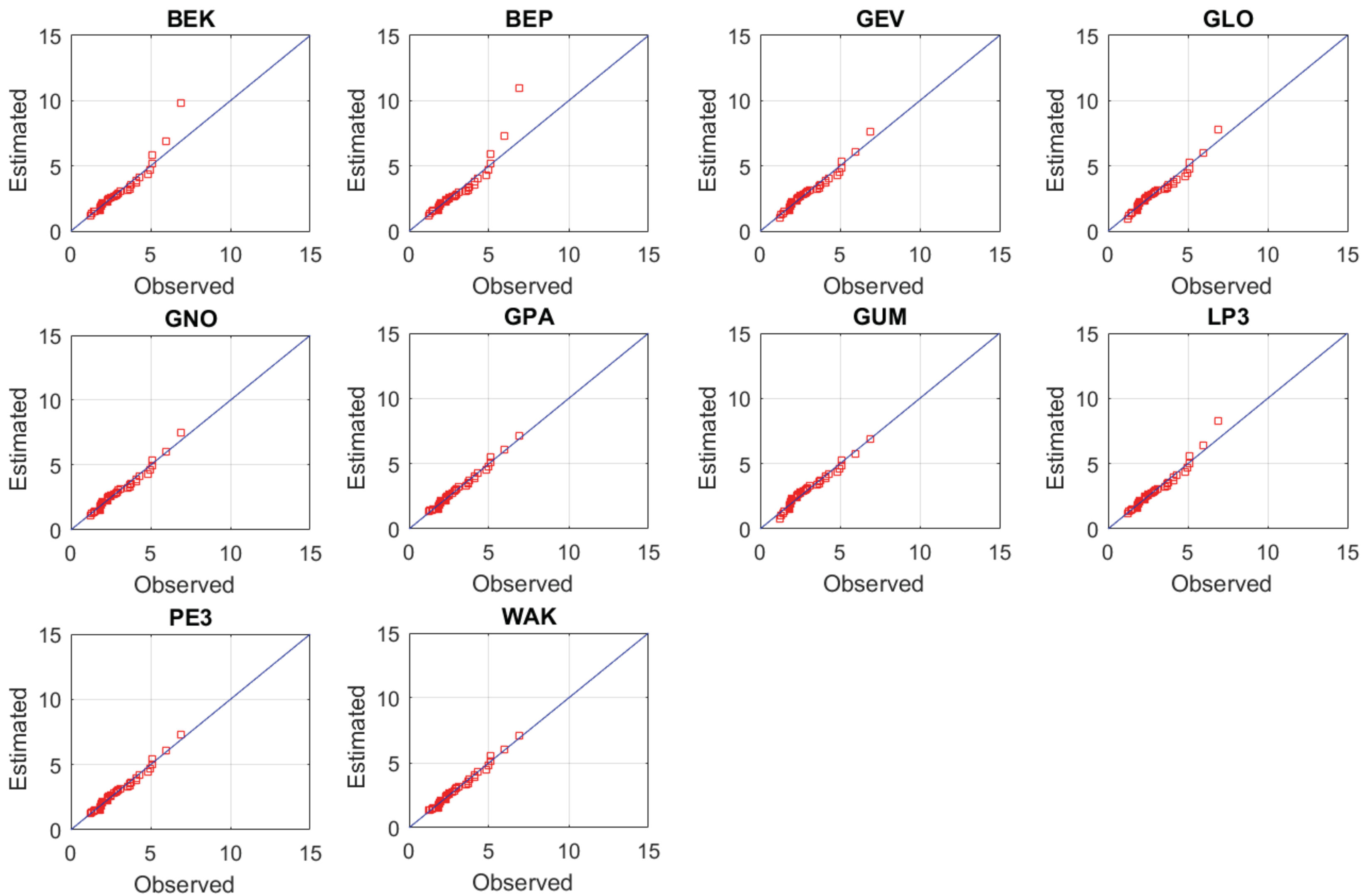

FIGURE 20 Q-Q PLOTS FOR 5MIN RAINFALL DATA OF COMOX A

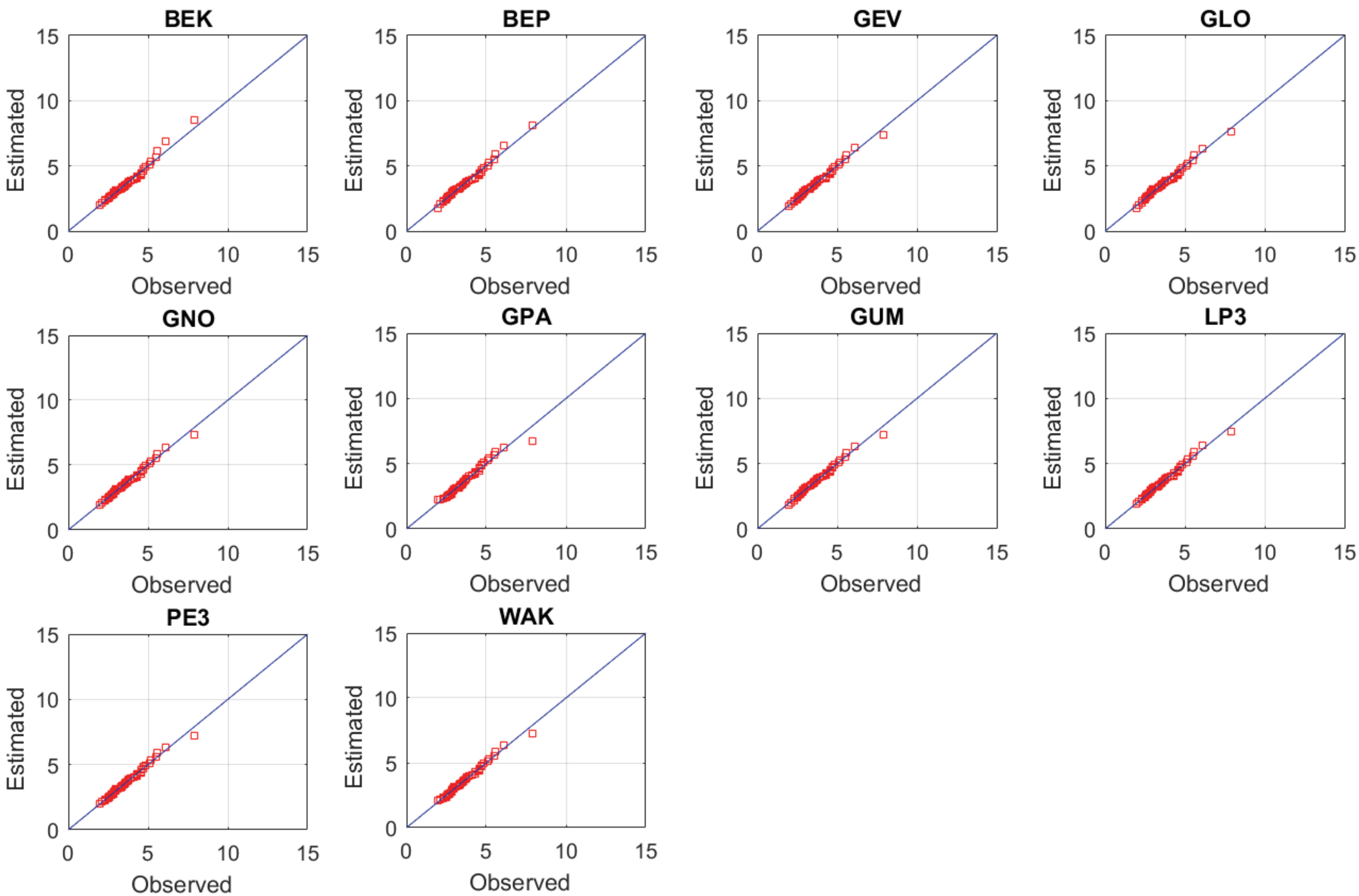

FIGURE 21 *Q-Q PLOTS FOR 5MIN RAINFALL DATA OF MISSION WEST ABBEY*

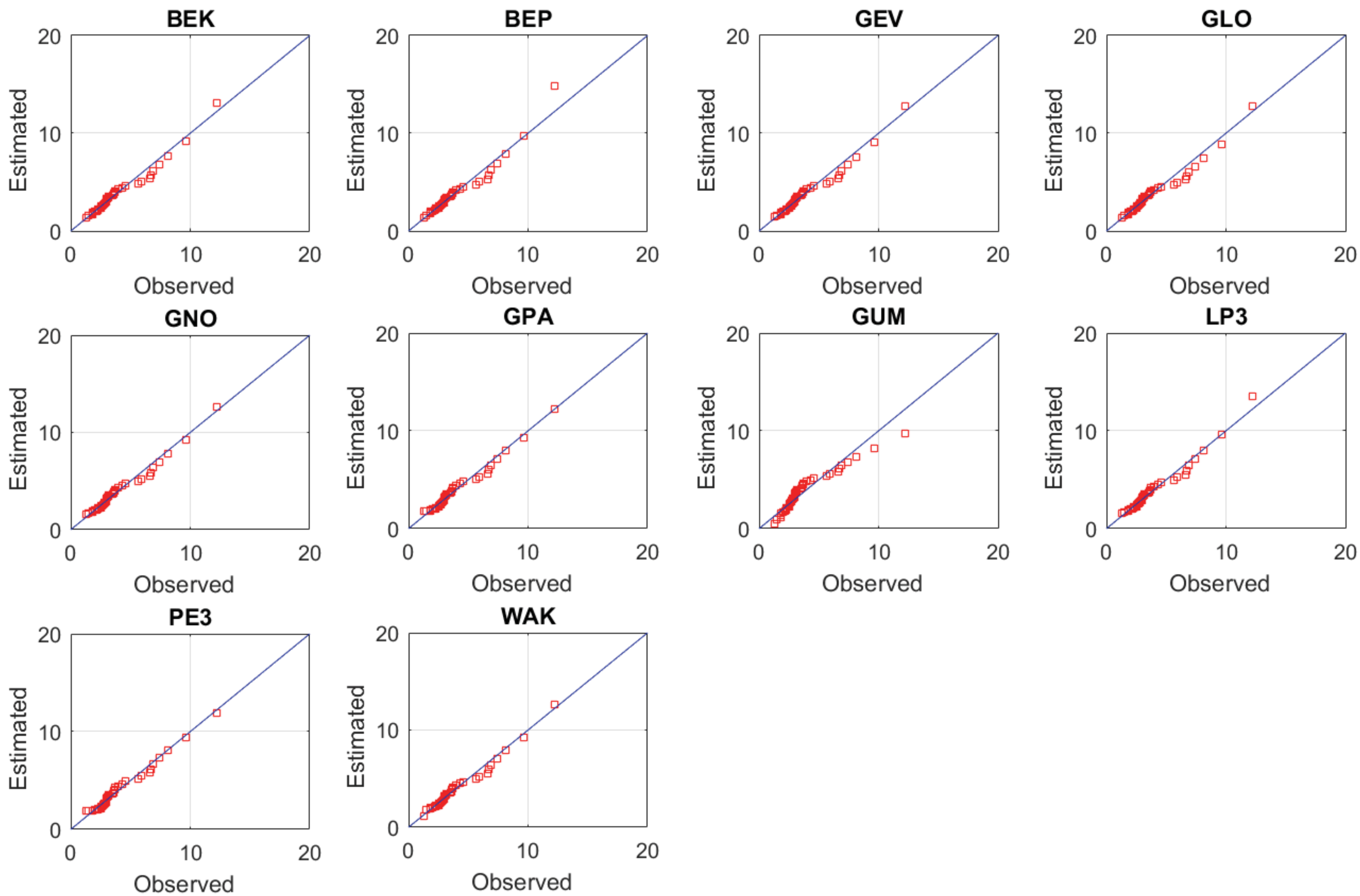

FIGURE 22 Q-Q PLOTS FOR 5MIN RAINFALL DATA OF PENTICTION A

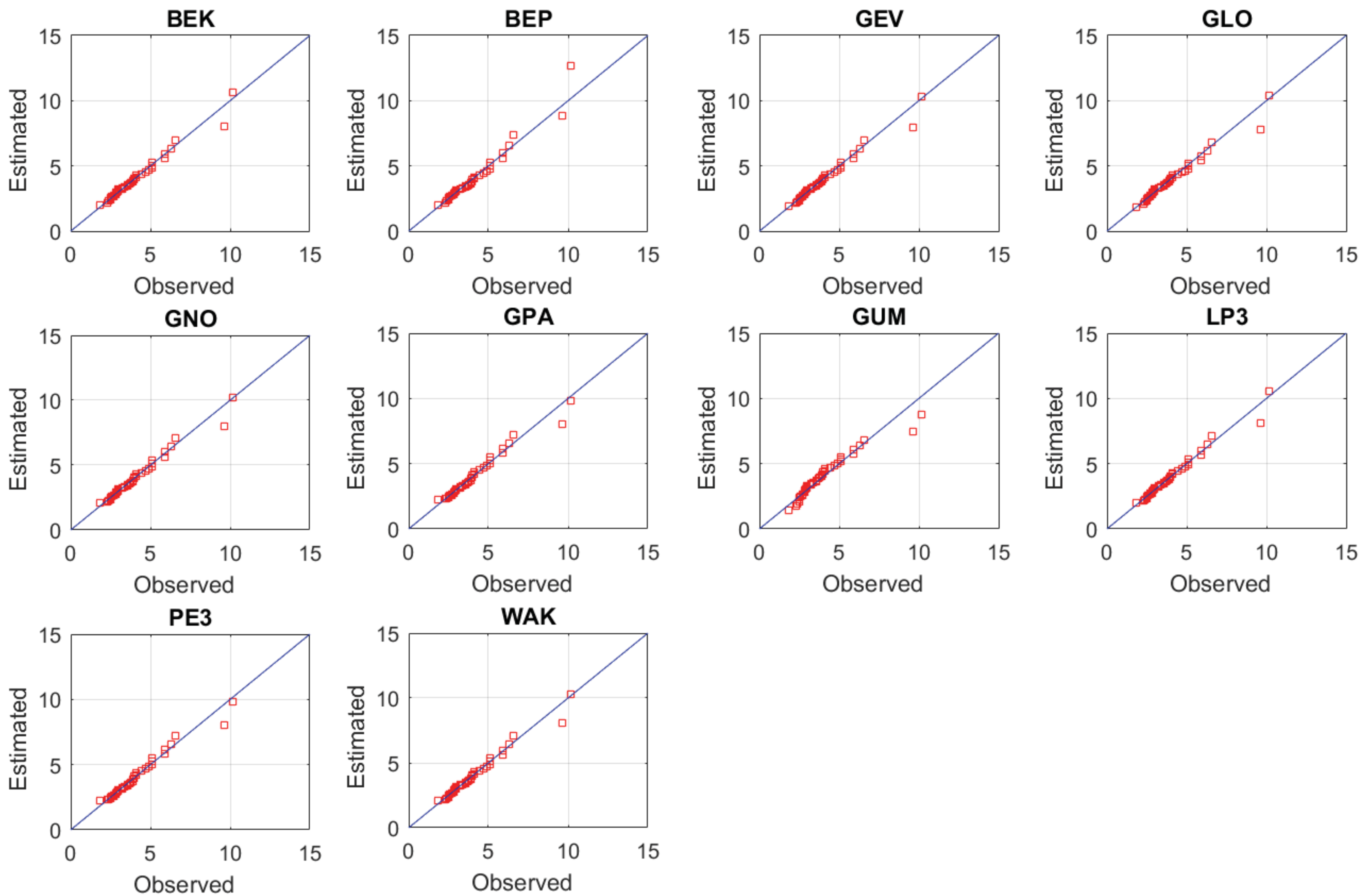

FIGURE 23 Q-Q PLOTS FOR 5MIN RAINFALL DATA OF PITT POLDER

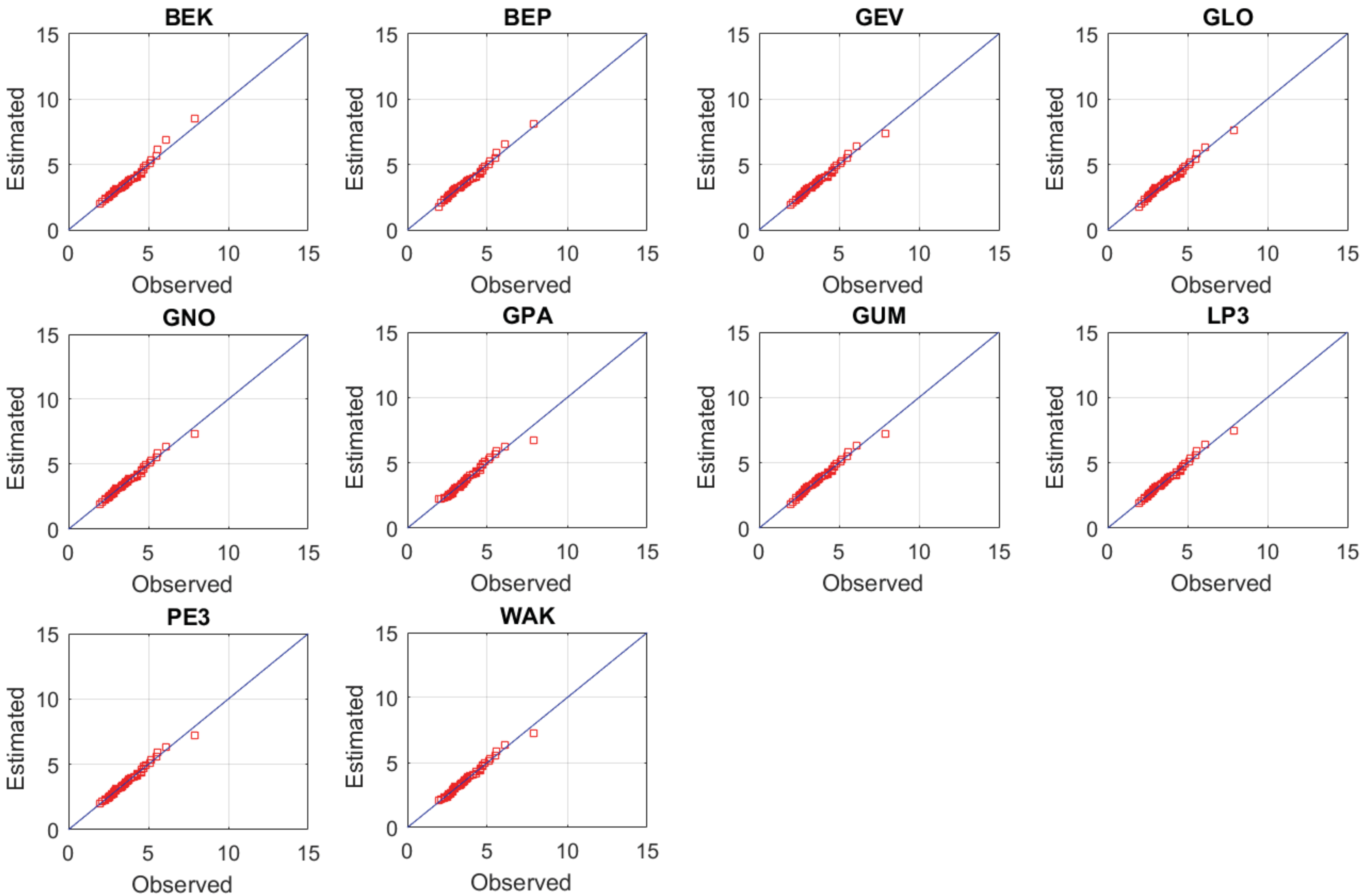

FIGURE 24 Q-Q PLOTS FOR 5MIN RAINFALL DATA OF PRINCE GEORGE A

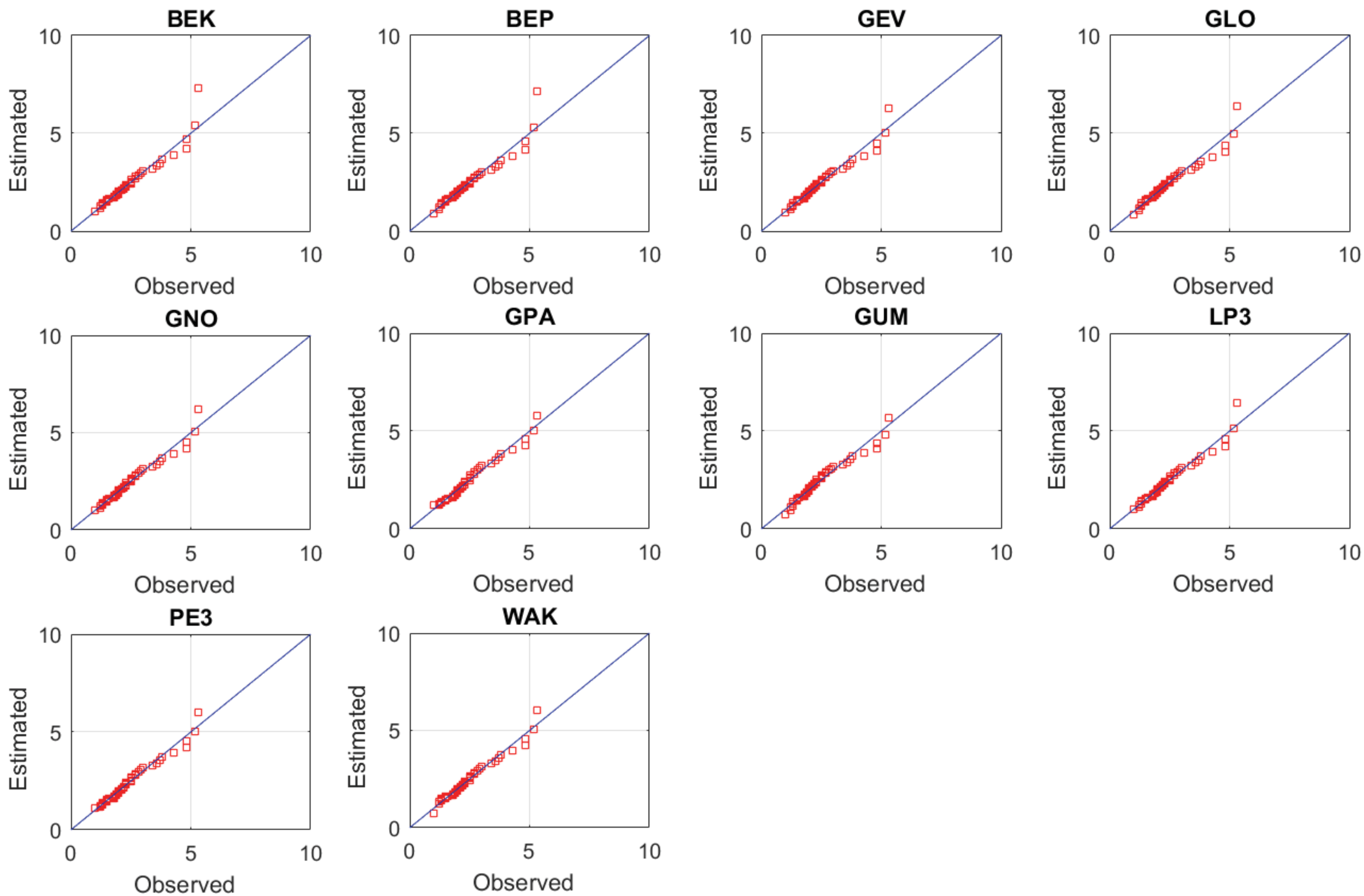

FIGURE 25   Q-Q PLOTS FOR 5MIN RAINFALL DATA OF TERRACE PCC

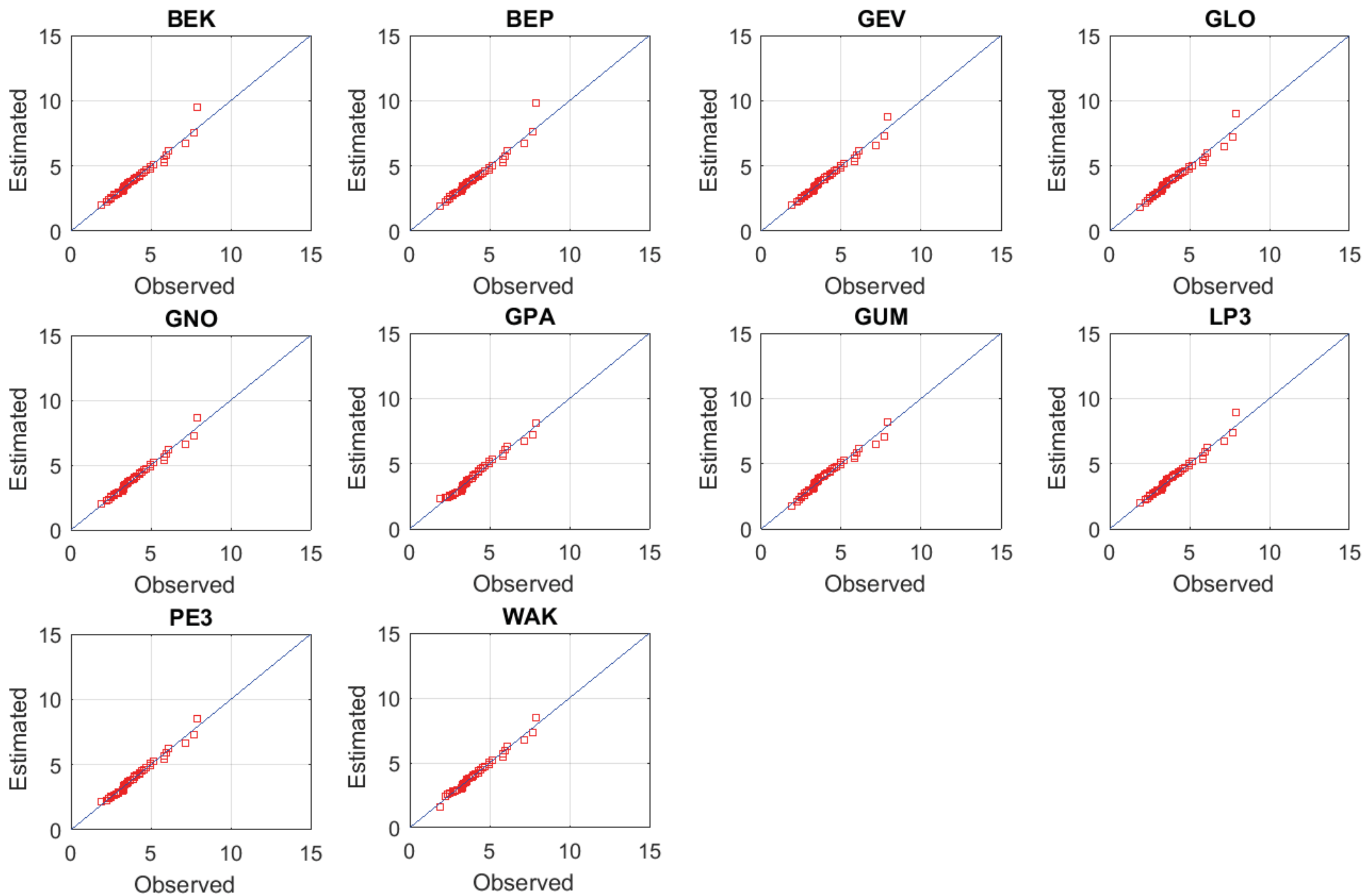

FIGURE 26 Q-Q PLOTS FOR 5MIN RAINFALL DATA OF TOFINO A

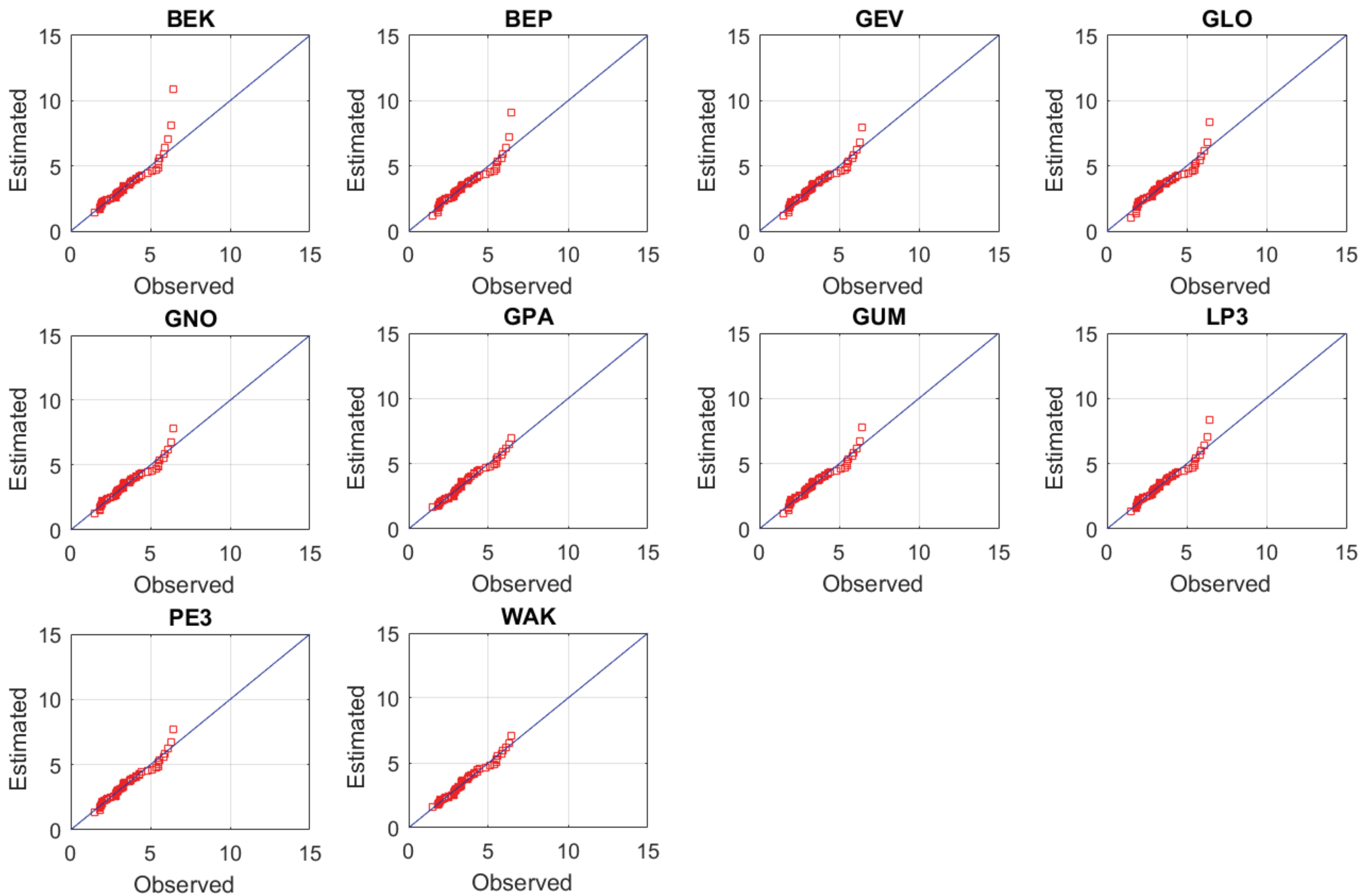

FIGURE 27 Q-Q PLOTS FOR 5MIN RAINFALL DATA OF VANCOUVER INTL A

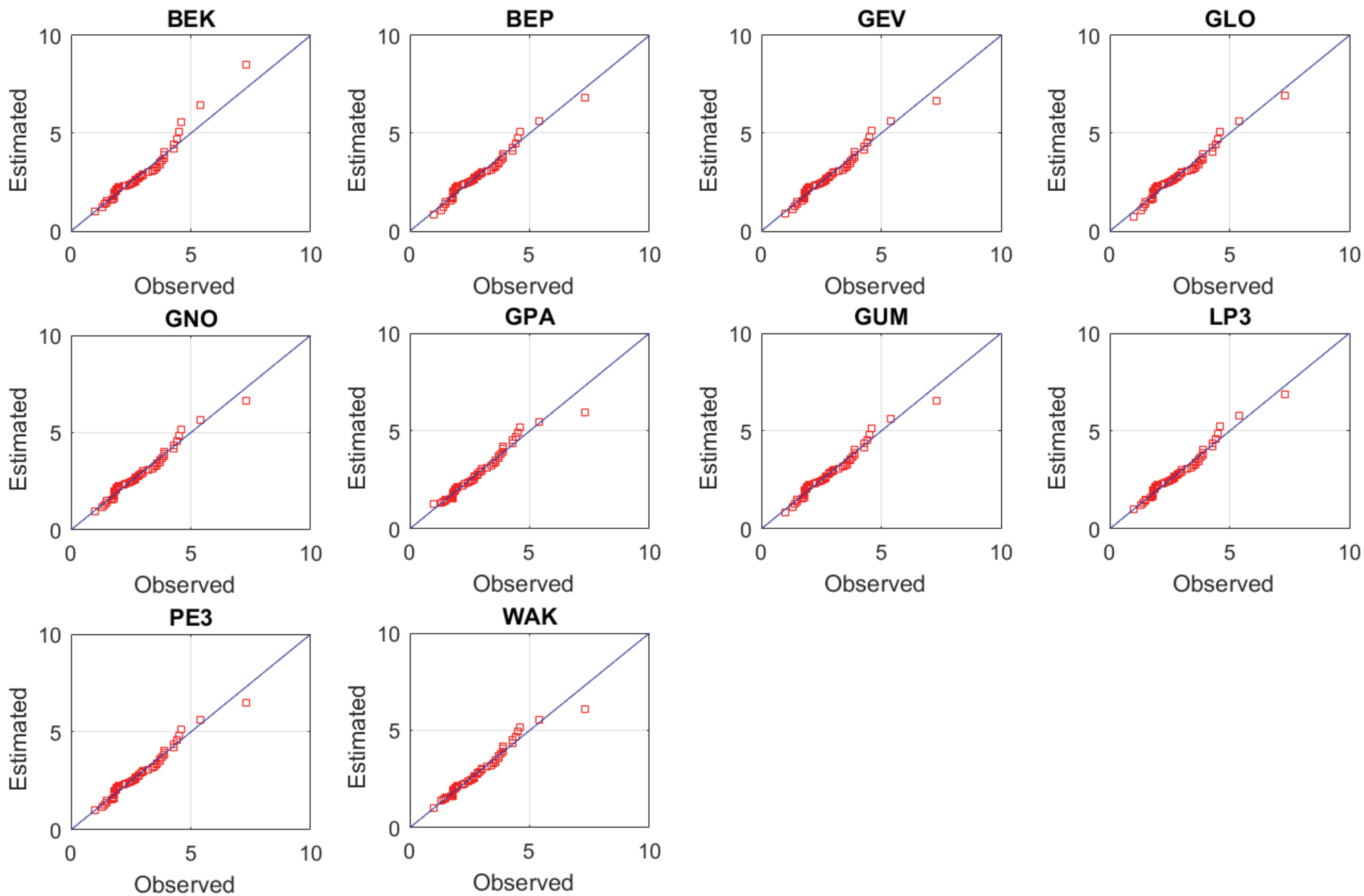

FIGURE 28 Q-Q PLOTS FOR 5MIN RAINFALL DATA OF VICTORIA INTL A

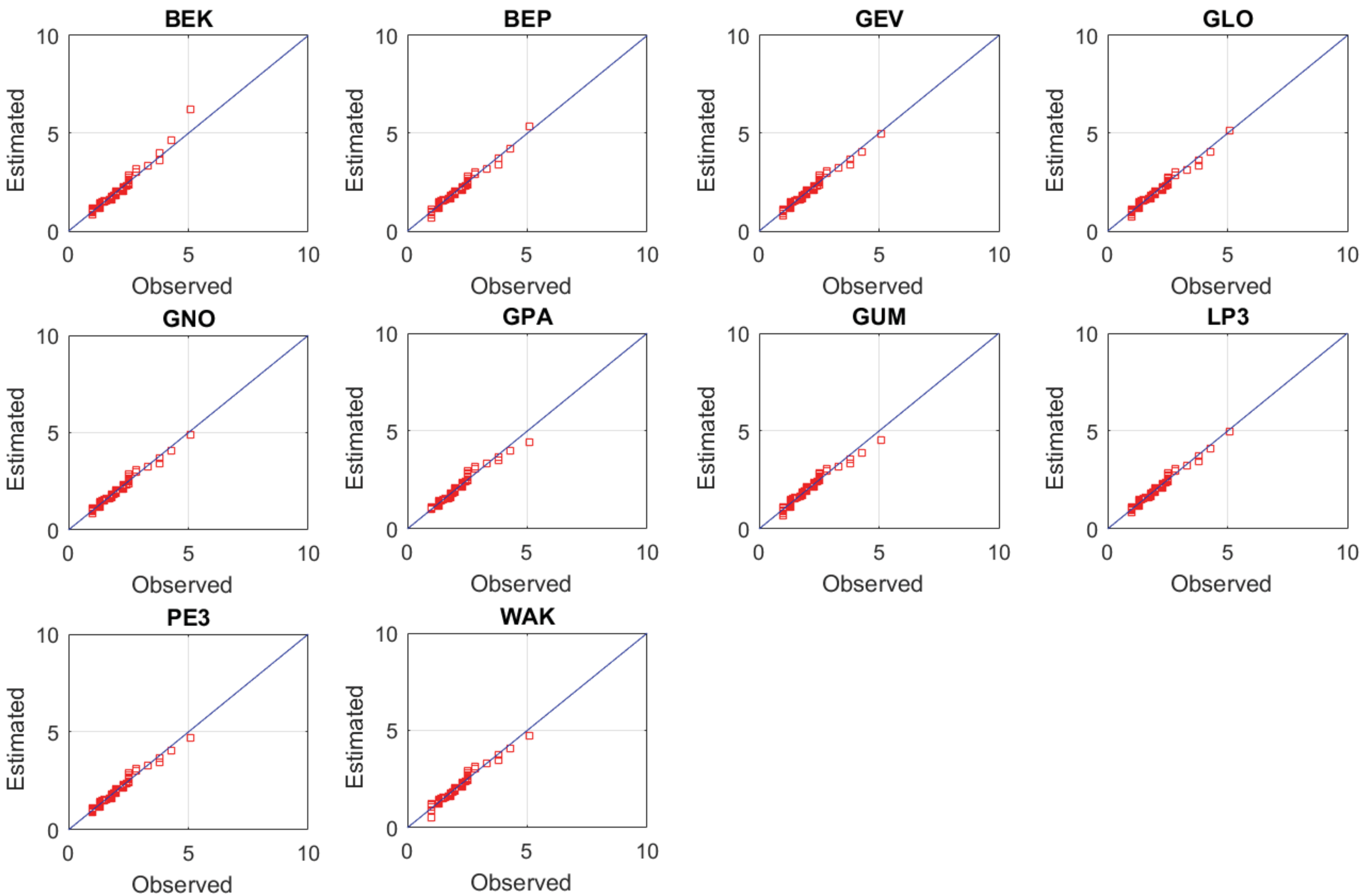

FIGURE 29 Q-Q PLOTS FOR 5MIN RAINFALL DATA OF VICTORIA GONZALES HTS

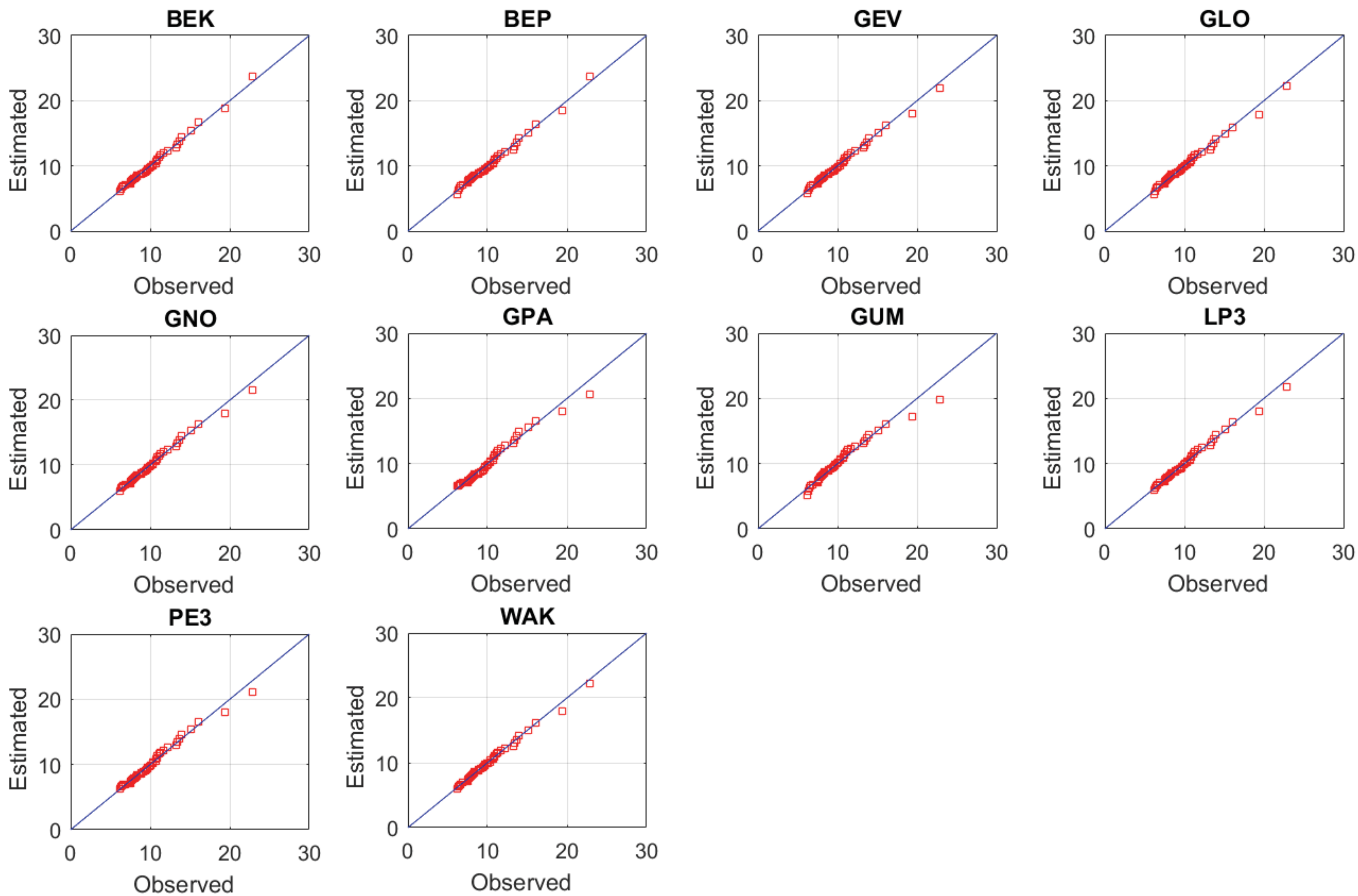

Figure 30 Q-Q Plots for 1hr Rainfall Data of Blue River A

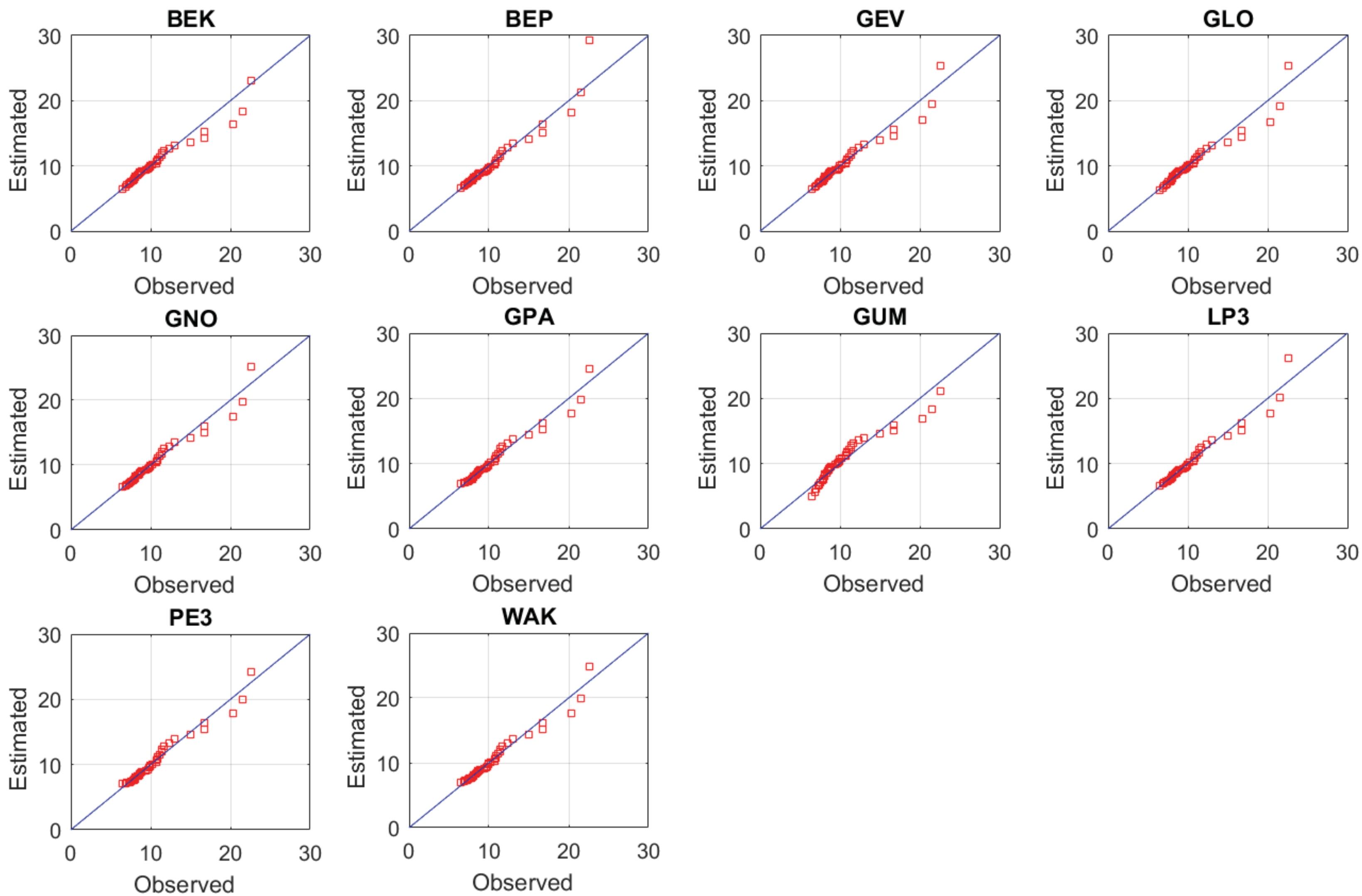

FIGURE 31 Q-Q PLOTS FOR 1HR RAINFALL DATA OF COMOX A

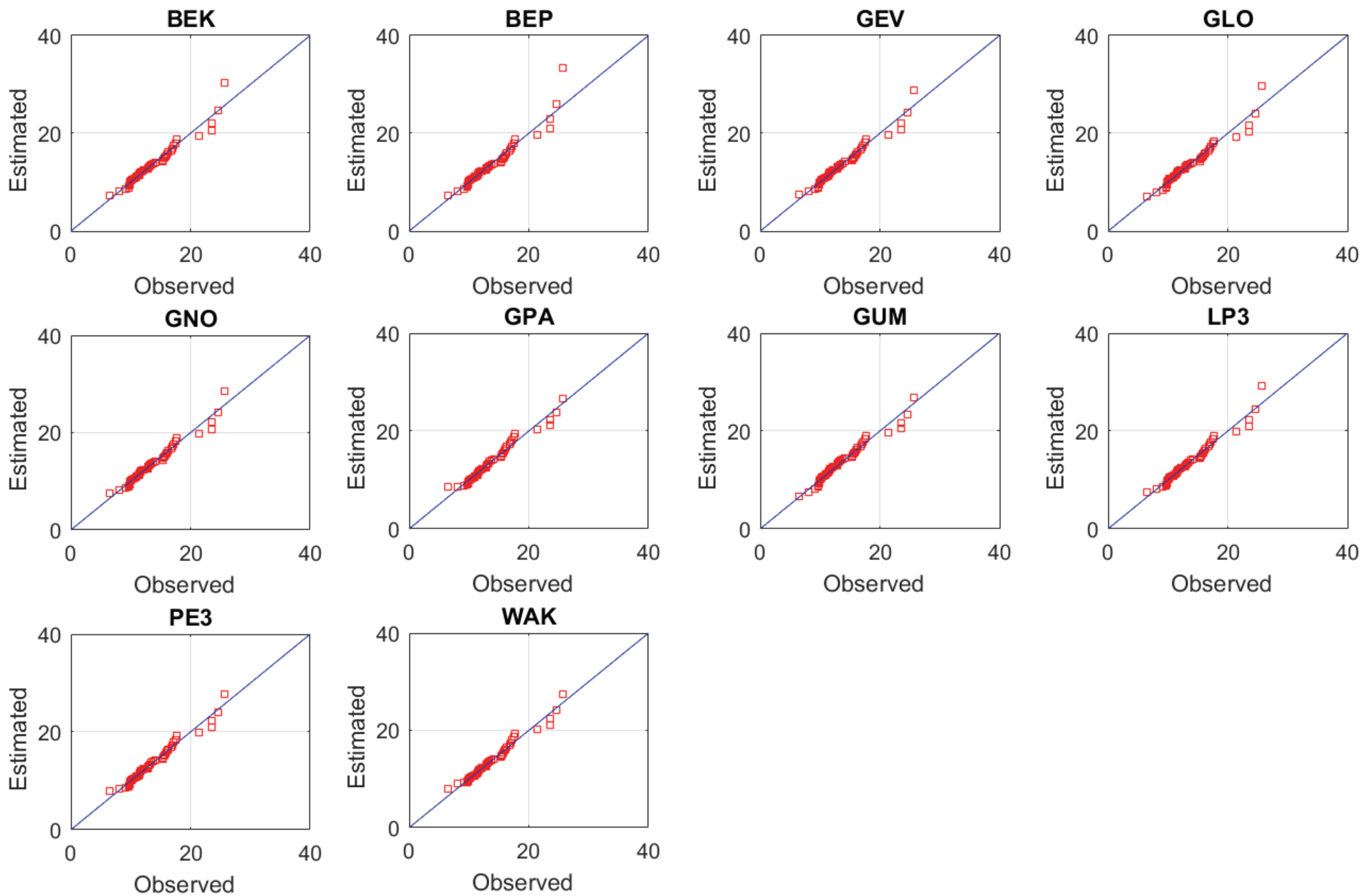

FIGURE 32 Q-Q PLOTS FOR 1HR RAINFALL DATA OF MISSION WEST ABEY

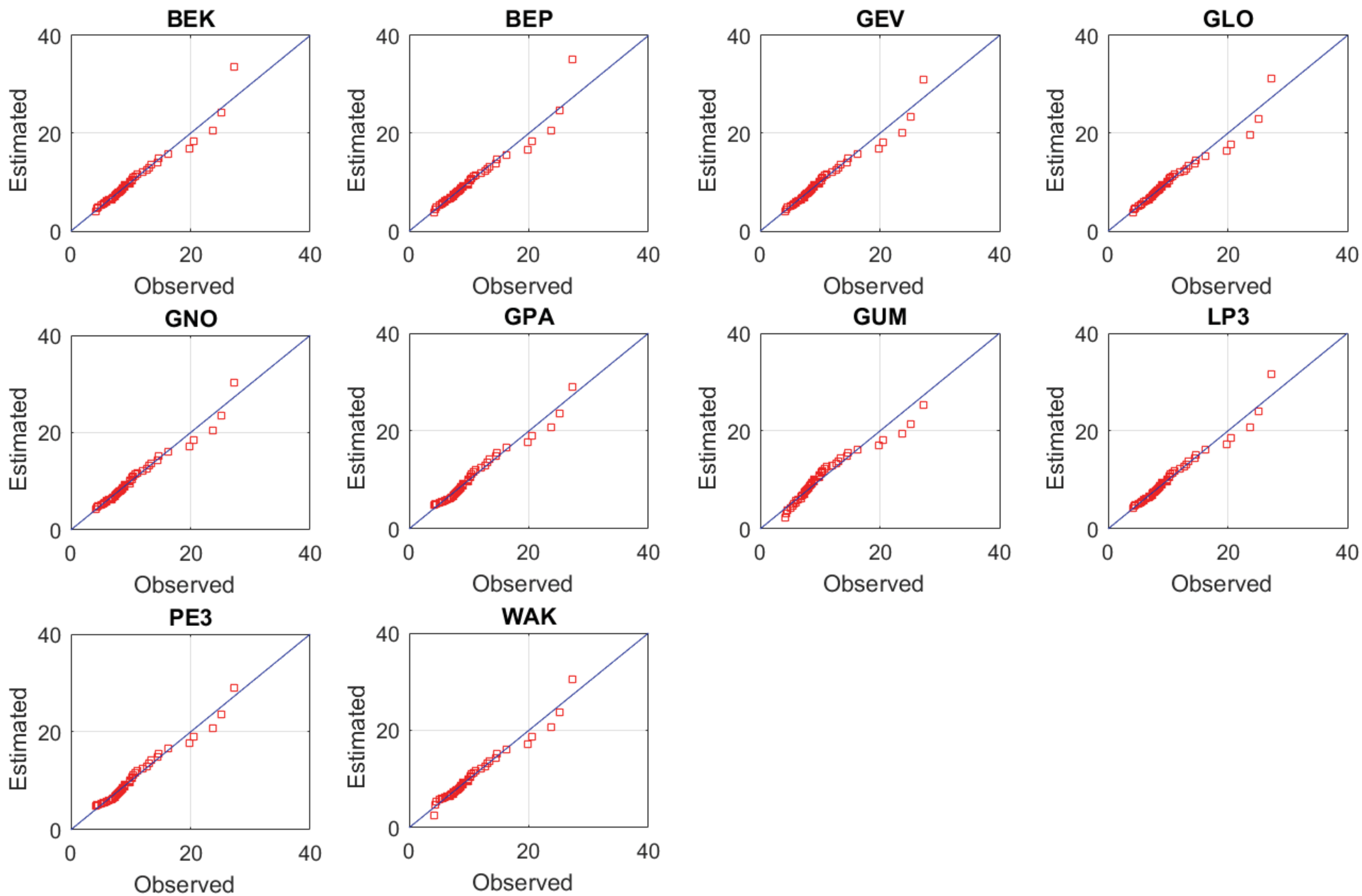

Figure 33 Q-Q Plots for 1hr Rainfall Data of Penticton A

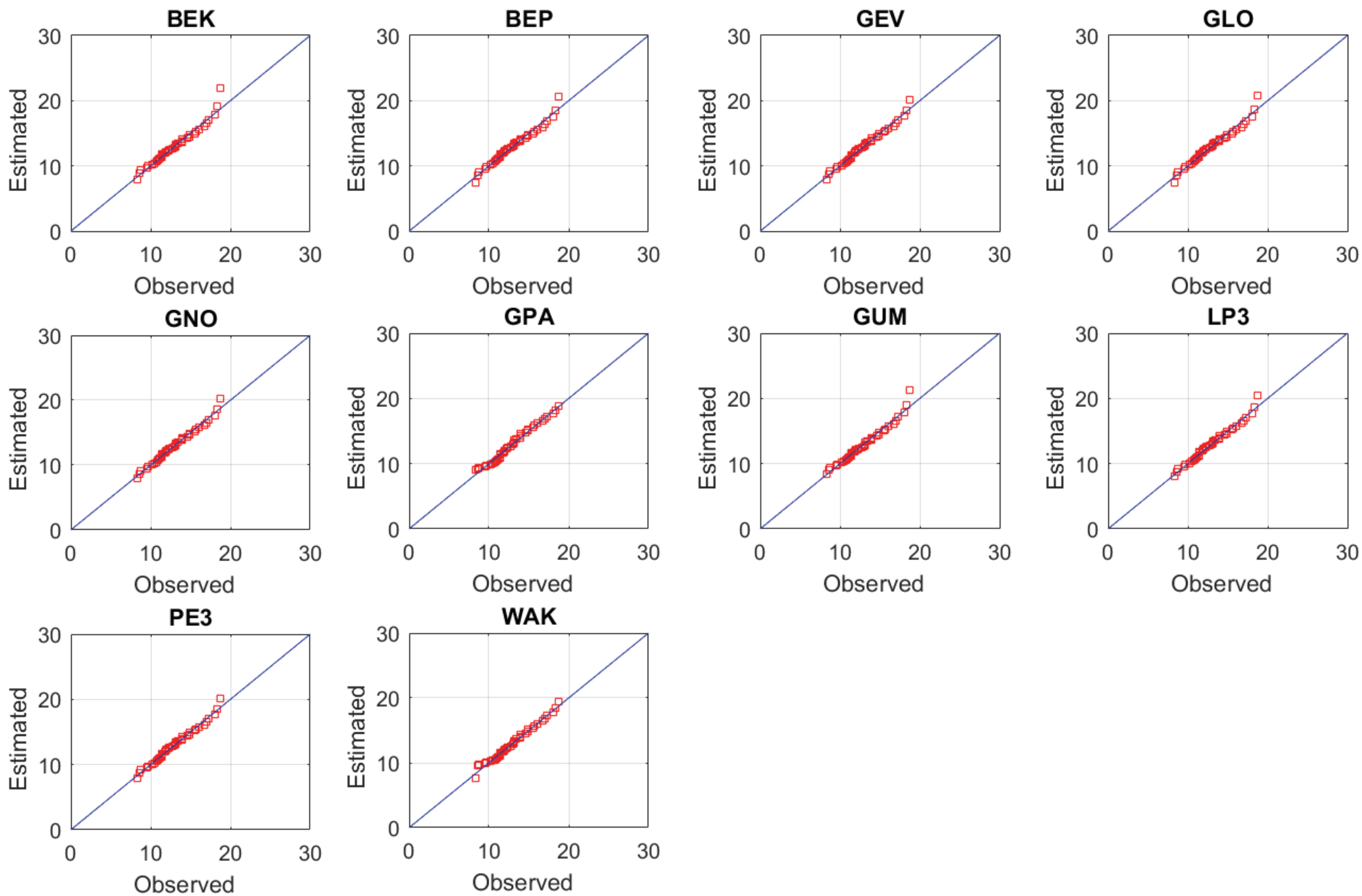

FIGURE 34 Q-Q PLOTS FOR 1HR RAINFALL DATA OF PITT POLDER

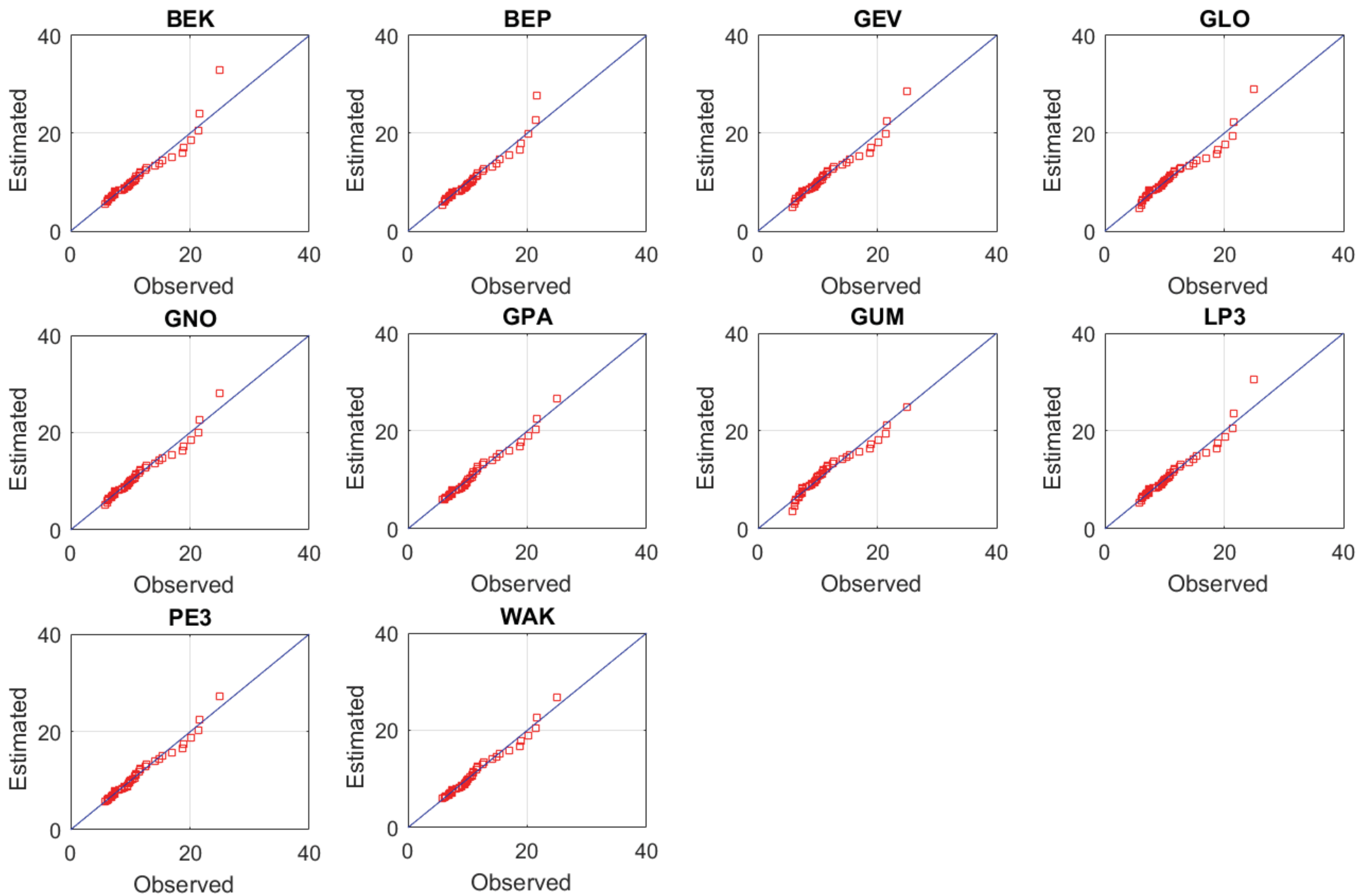

FIGURE 35 Q-Q PLOTS FOR 1HR RAINFALL DATA OF PRINCE GEORGE A

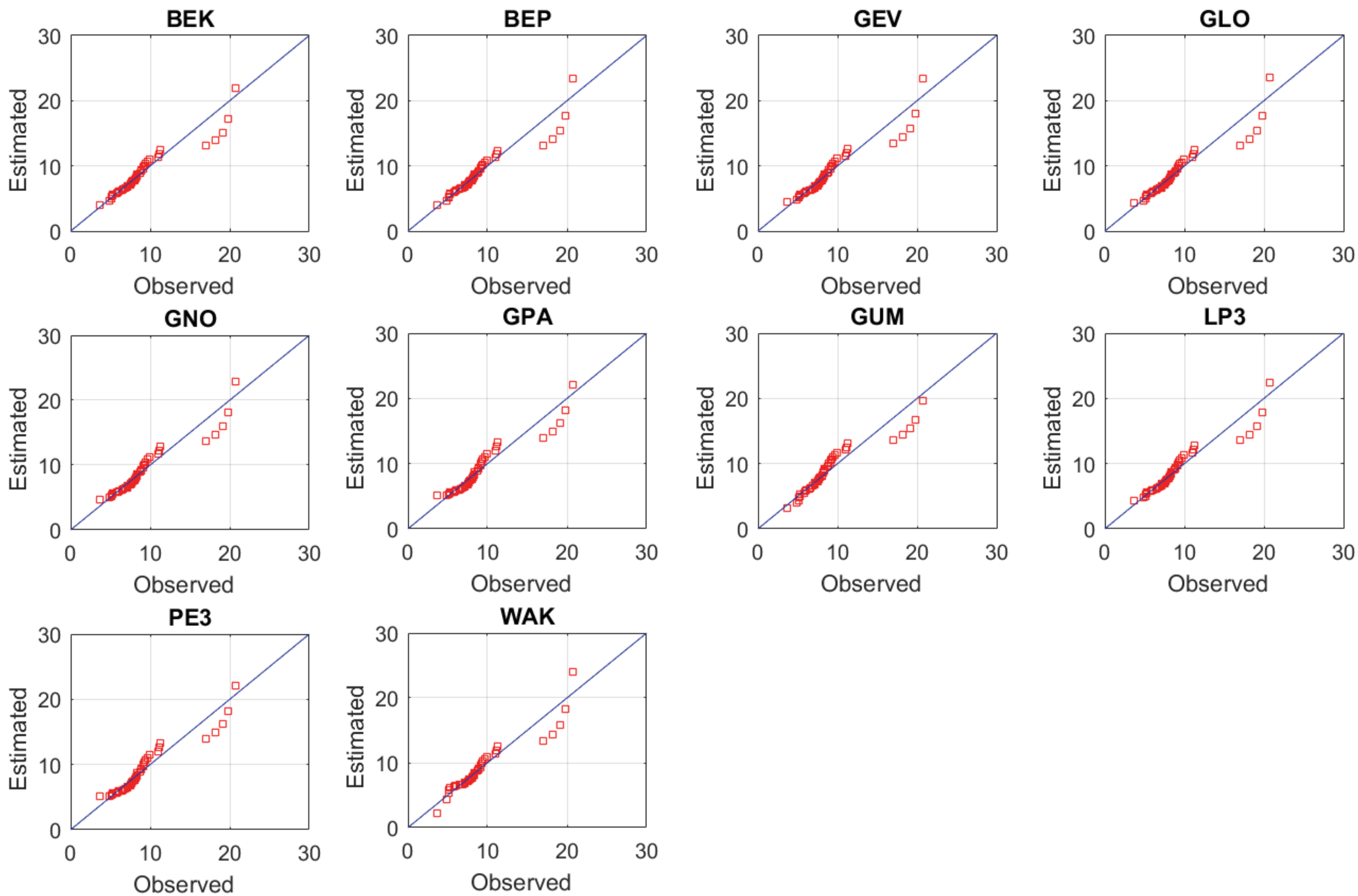

FIGURE 36 Q-Q PLOTS FOR 1HR RAINFALL DATA OF TERRACE PCC

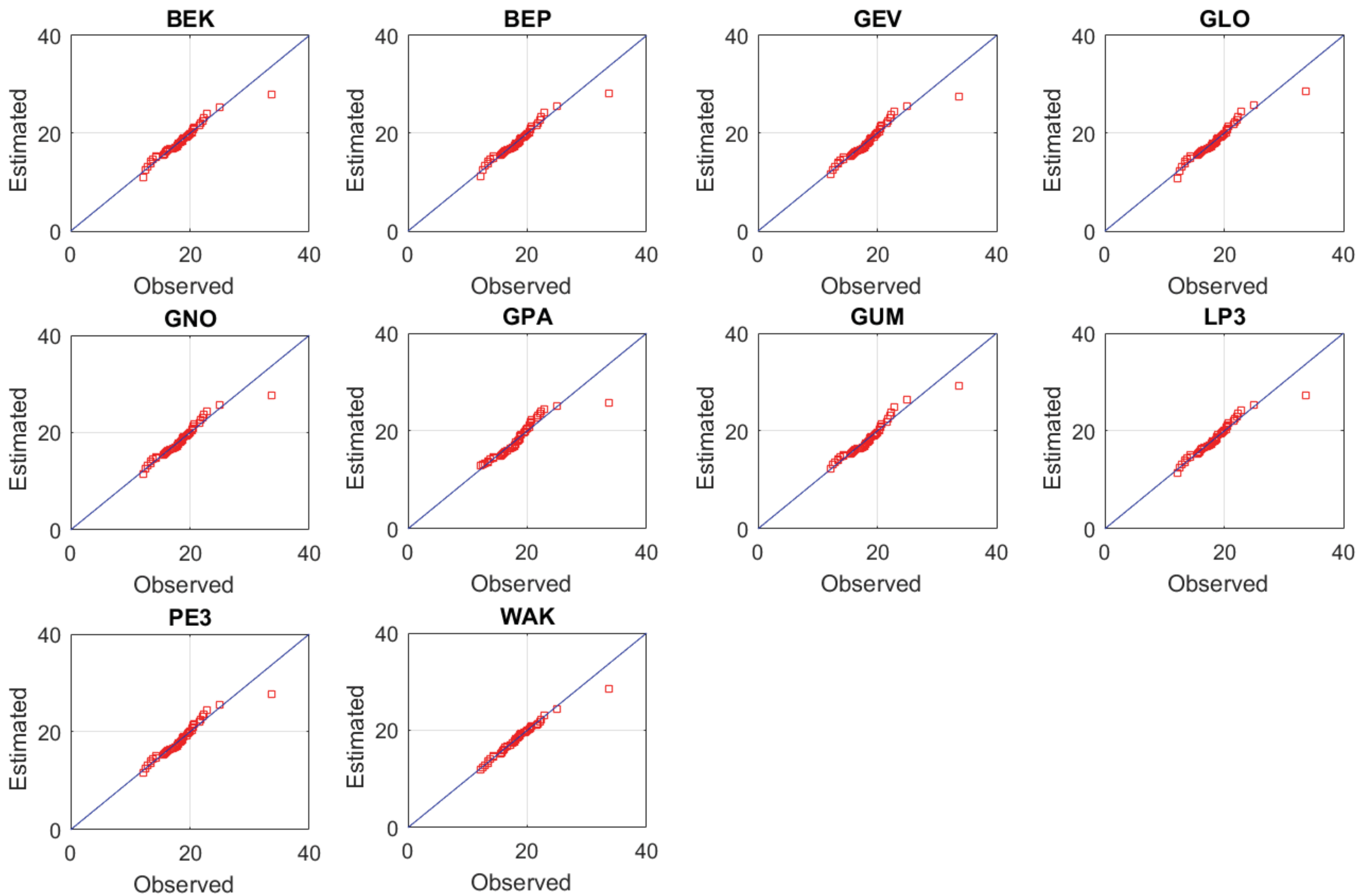

FIGURE 37 Q-Q PLOTS FOR 1HR RAINFALL DATA OF TOFINO A

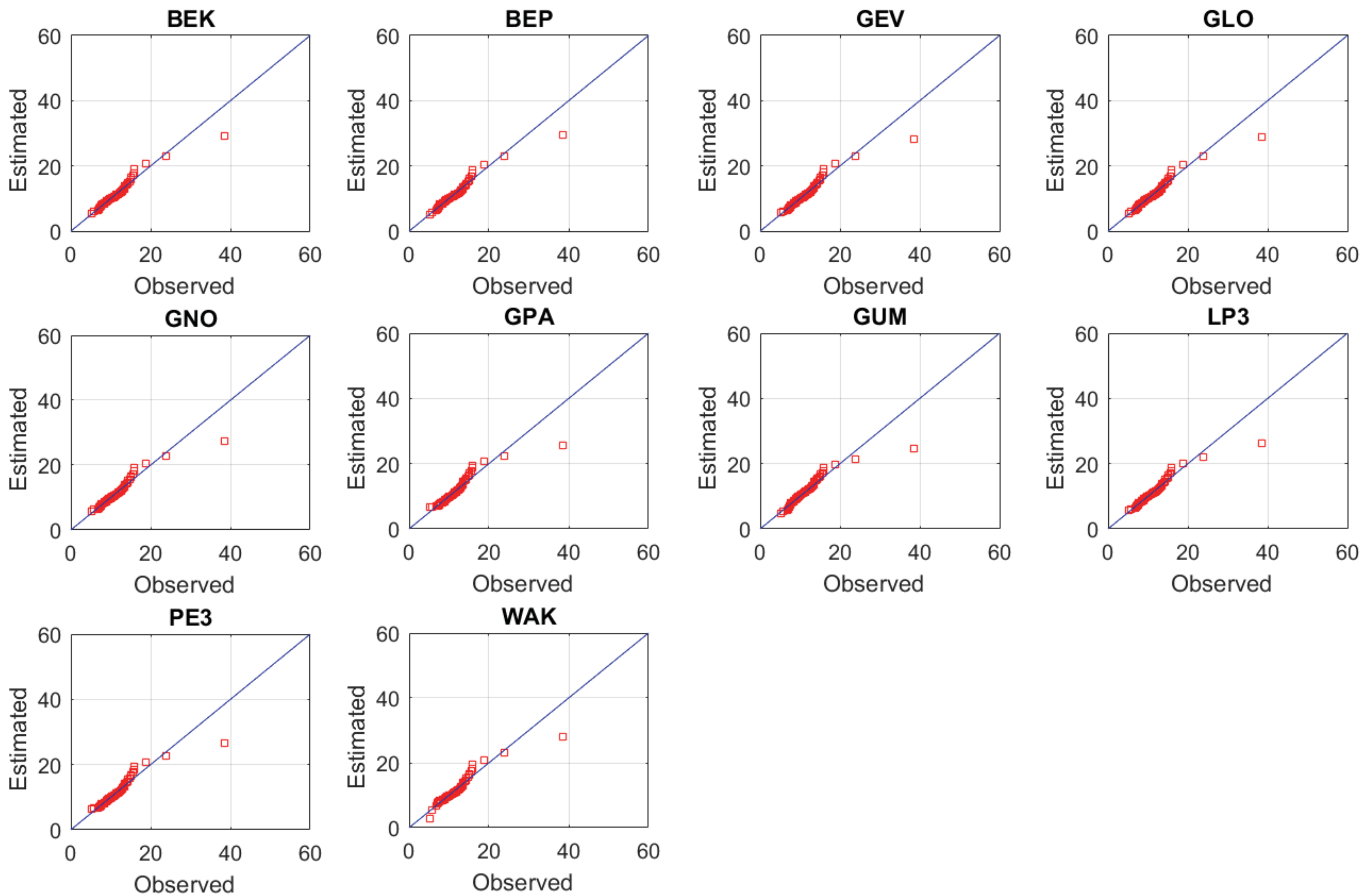

FIGURE 38 Q-Q PLOTS FOR 1HR RAINFALL DATA OF VANCOUVER INTL A

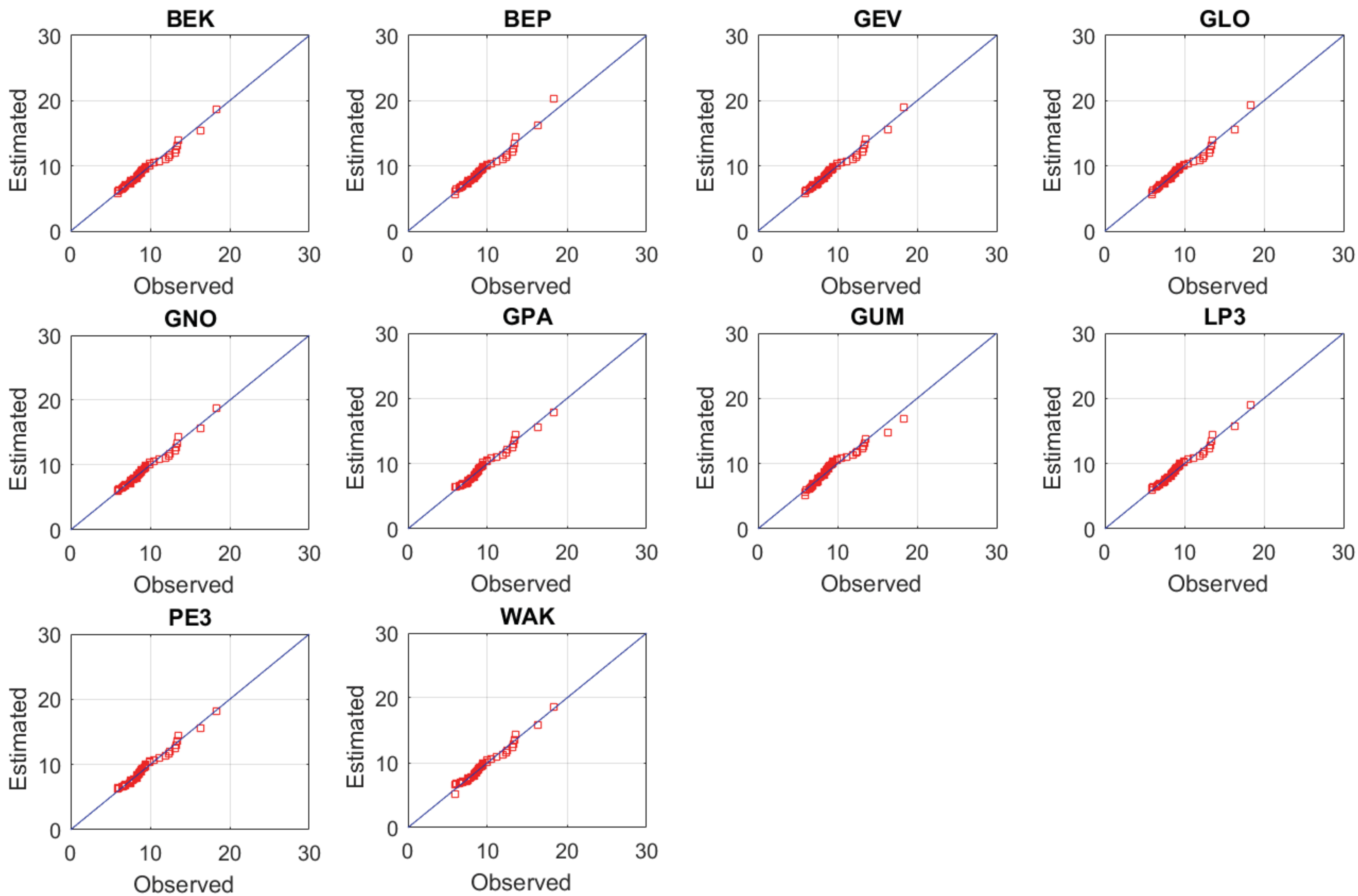

FIGURE 39 Q-Q PLOTS FOR 1HR RAINFALL DATA OF VICTORIA INTL A

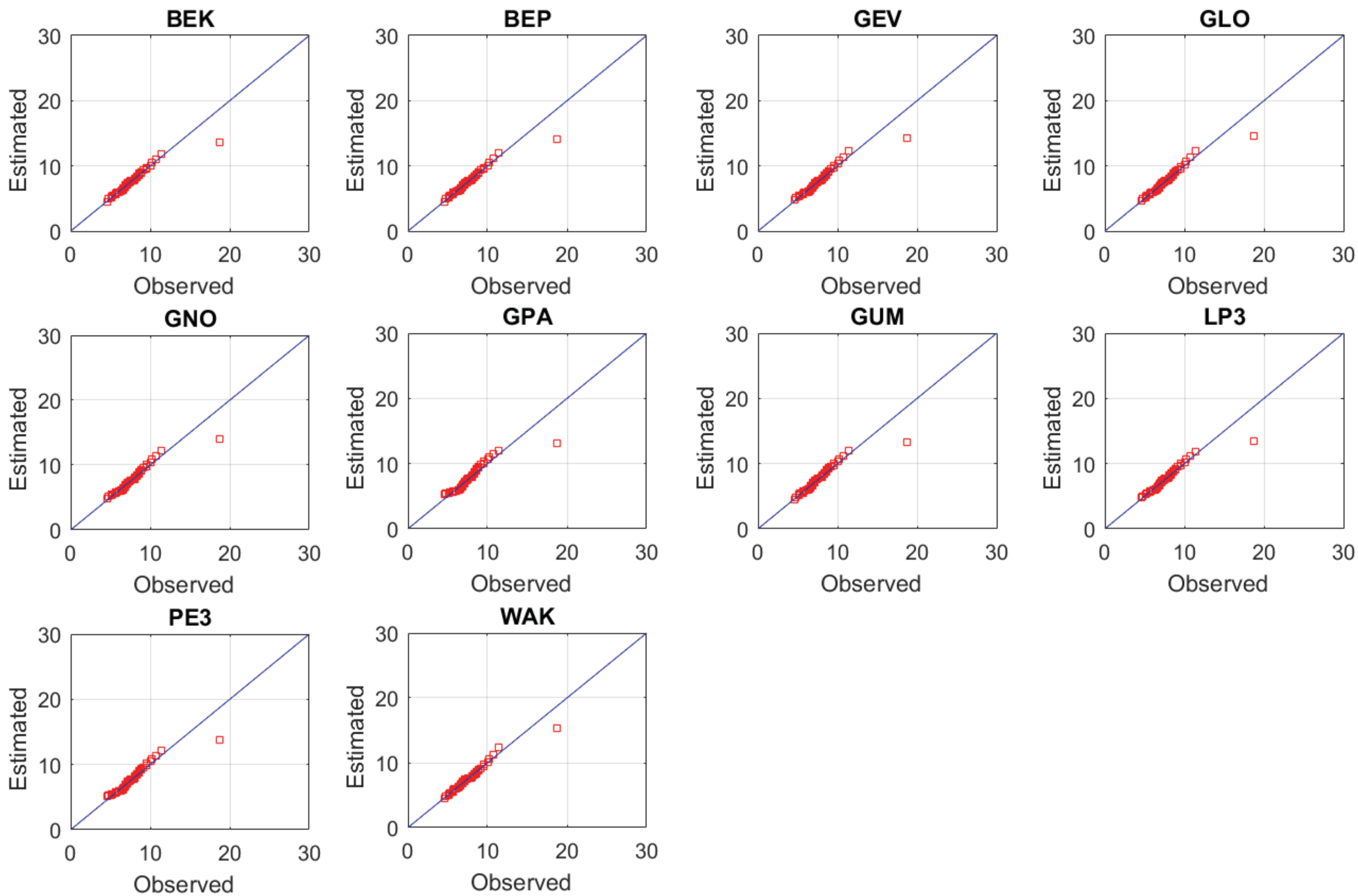

Figure 40 Q-Q Plots for 1hr Rainfall Data of Victoria Gonzales HTS

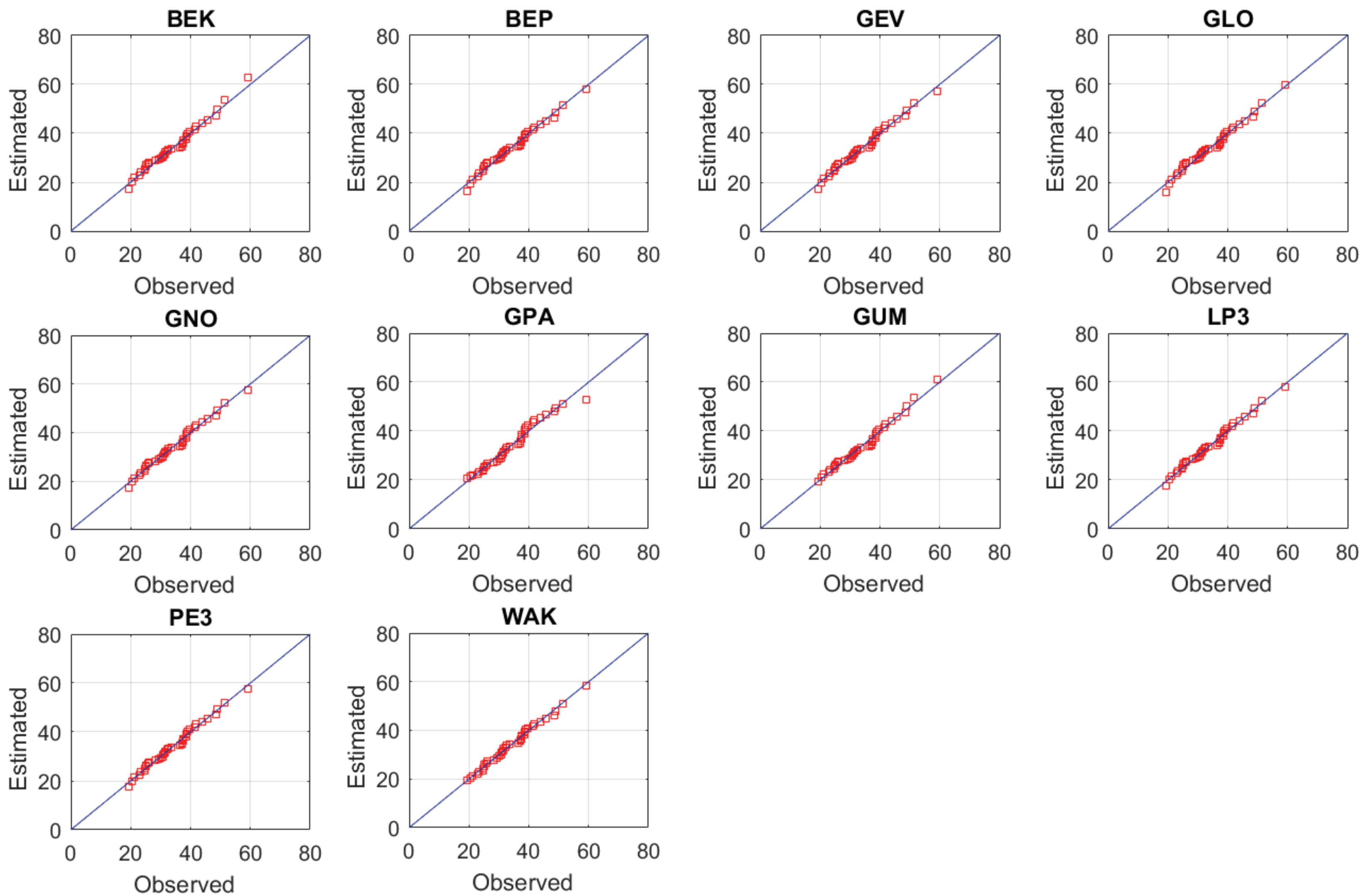

FIGURE 41 Q-Q PLOTS FOR 24HR RAINFALL DATA OF BLUE RIVER A

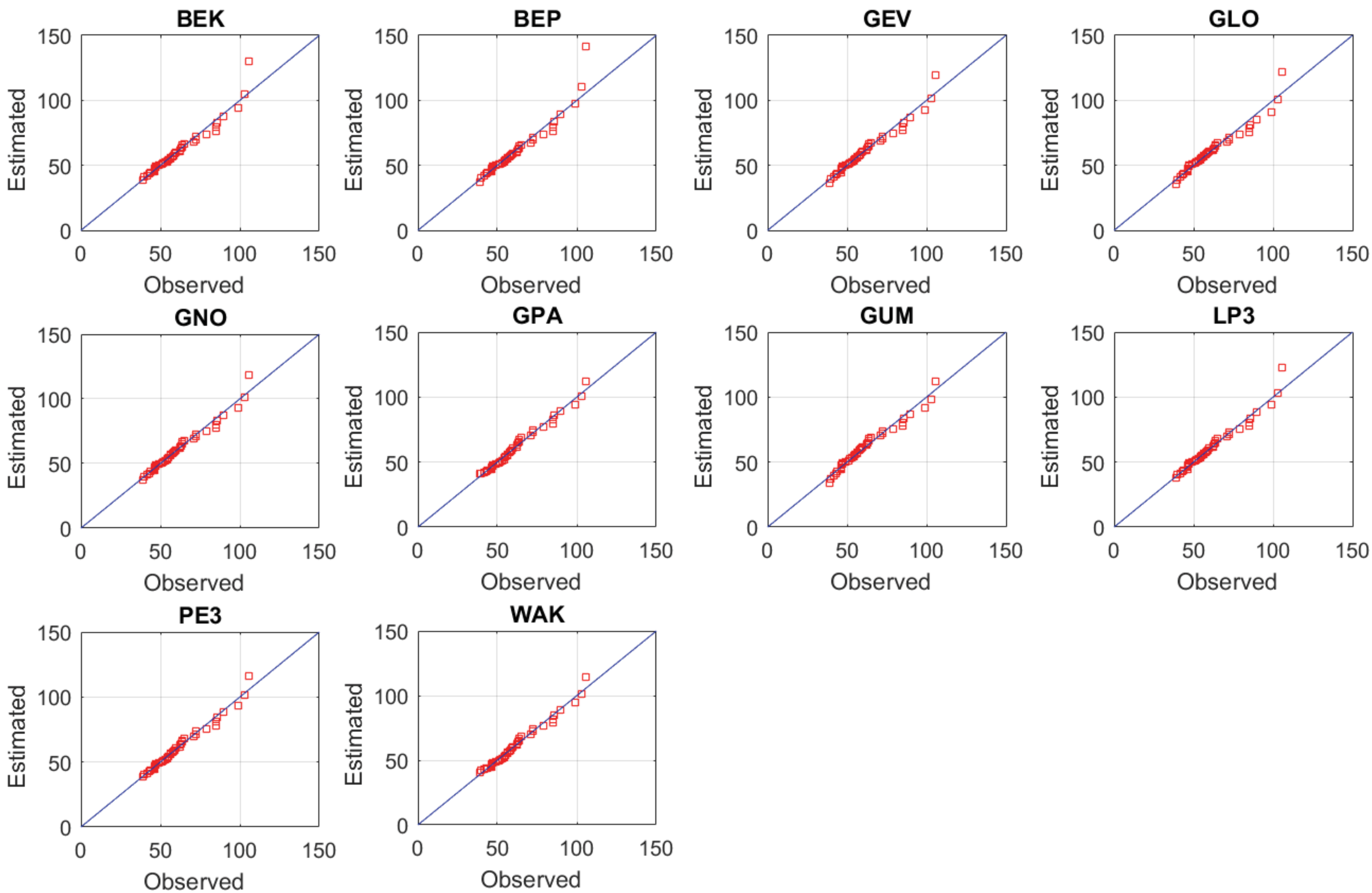

FIGURE 42 Q-Q PLOTS FOR 24HR RAINFALL DATA OF COMOX A

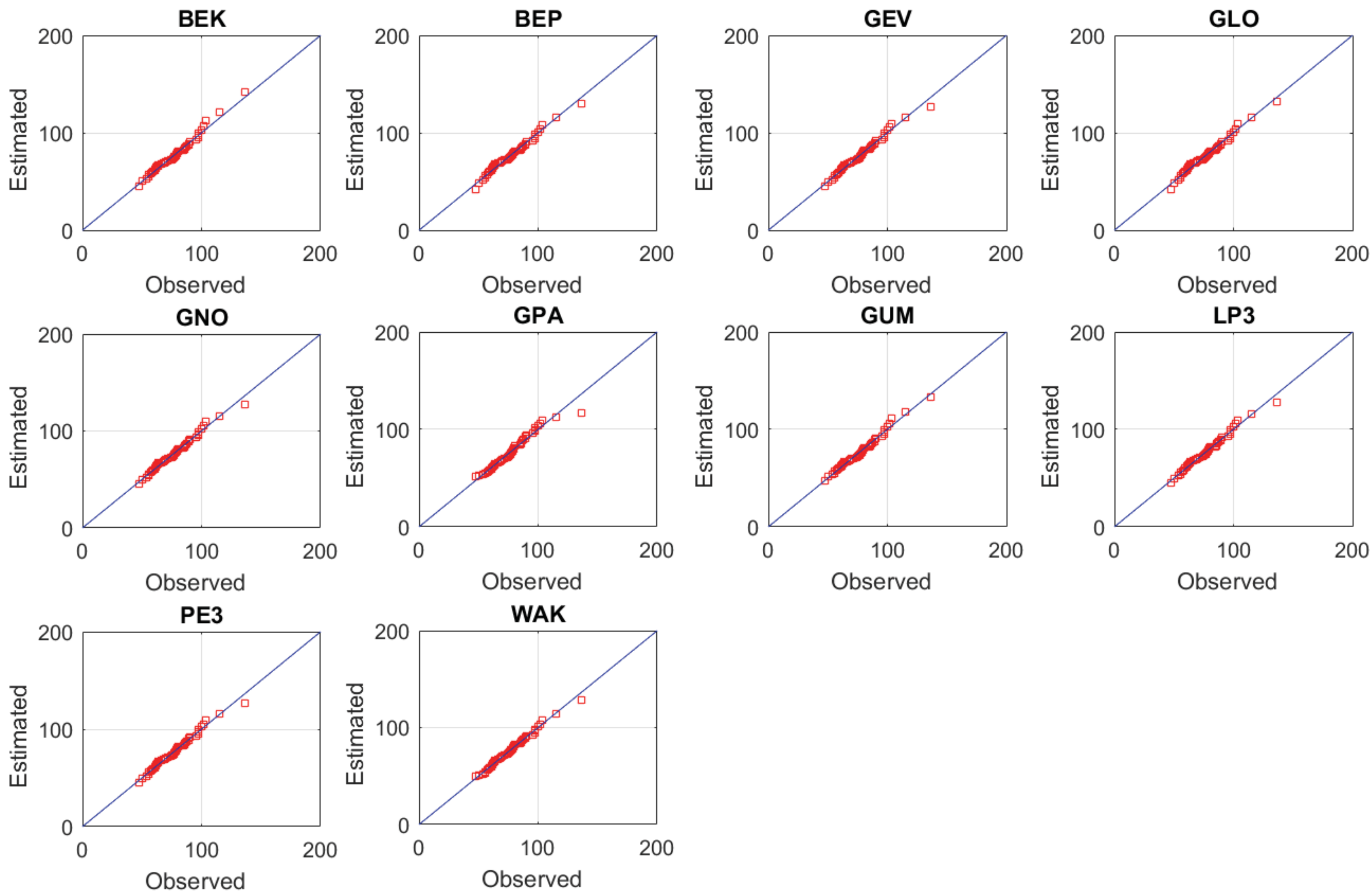

FIGURE 43 Q-Q PLOTS FOR 24HR RAINFALL DATA OF MISSION WEST ABBEY

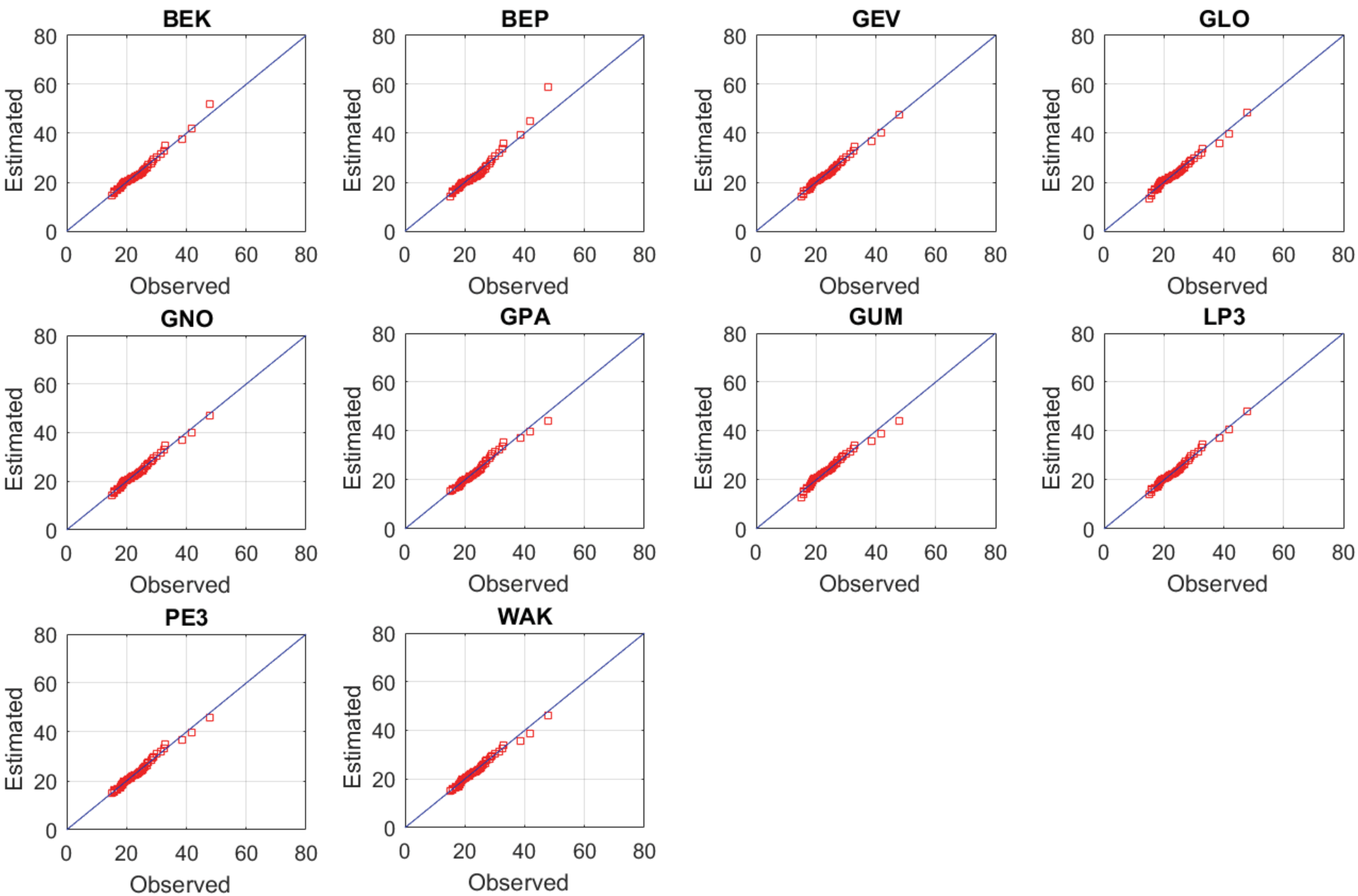

FIGURE 44 Q-Q PLOTS FOR 24HR RAINFALL DATA OF PENTICTON A

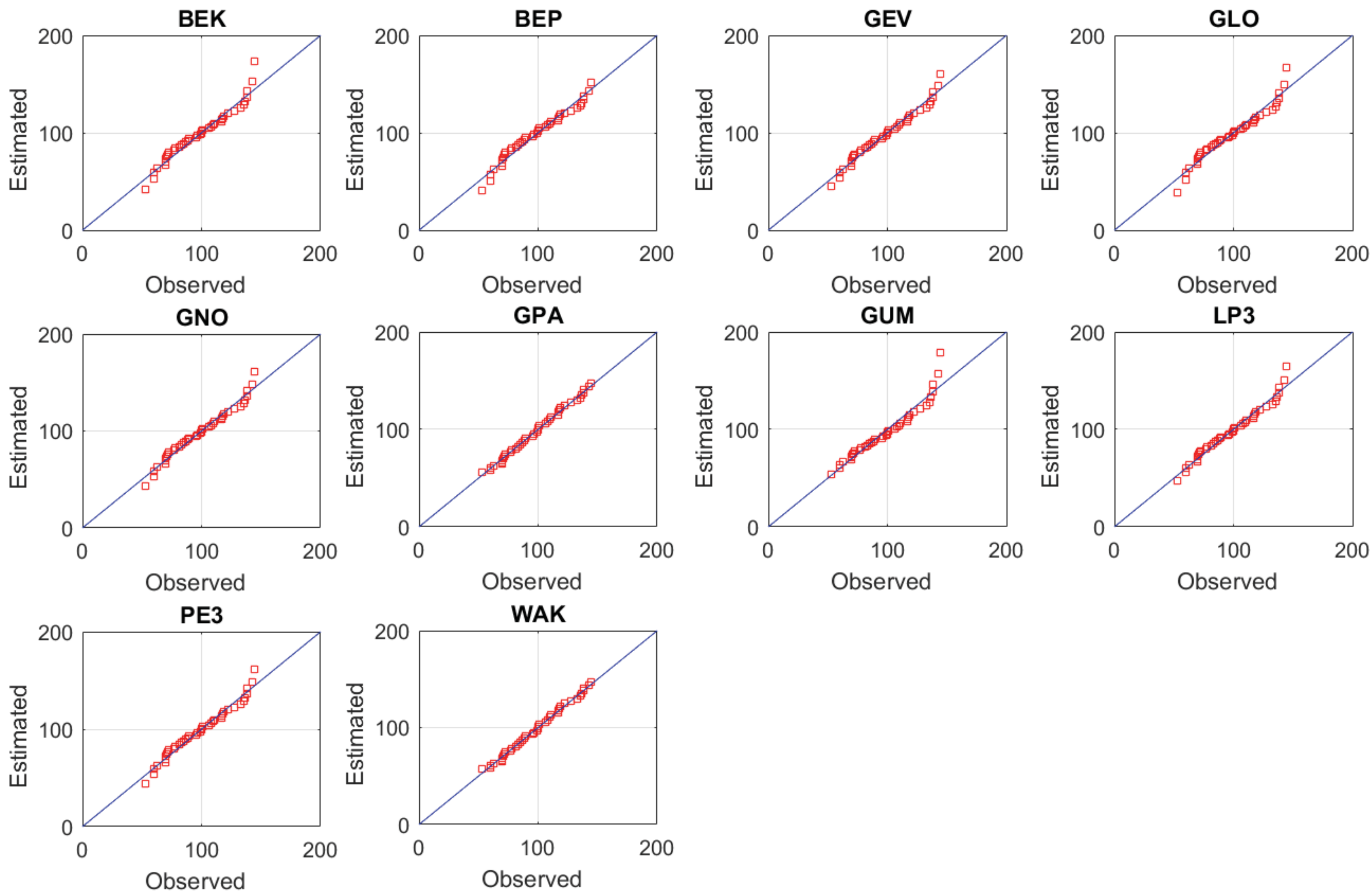

FIGURE 45 Q-Q PLOTS FOR 24HR RAINFALL DATA OF PITT POLDER

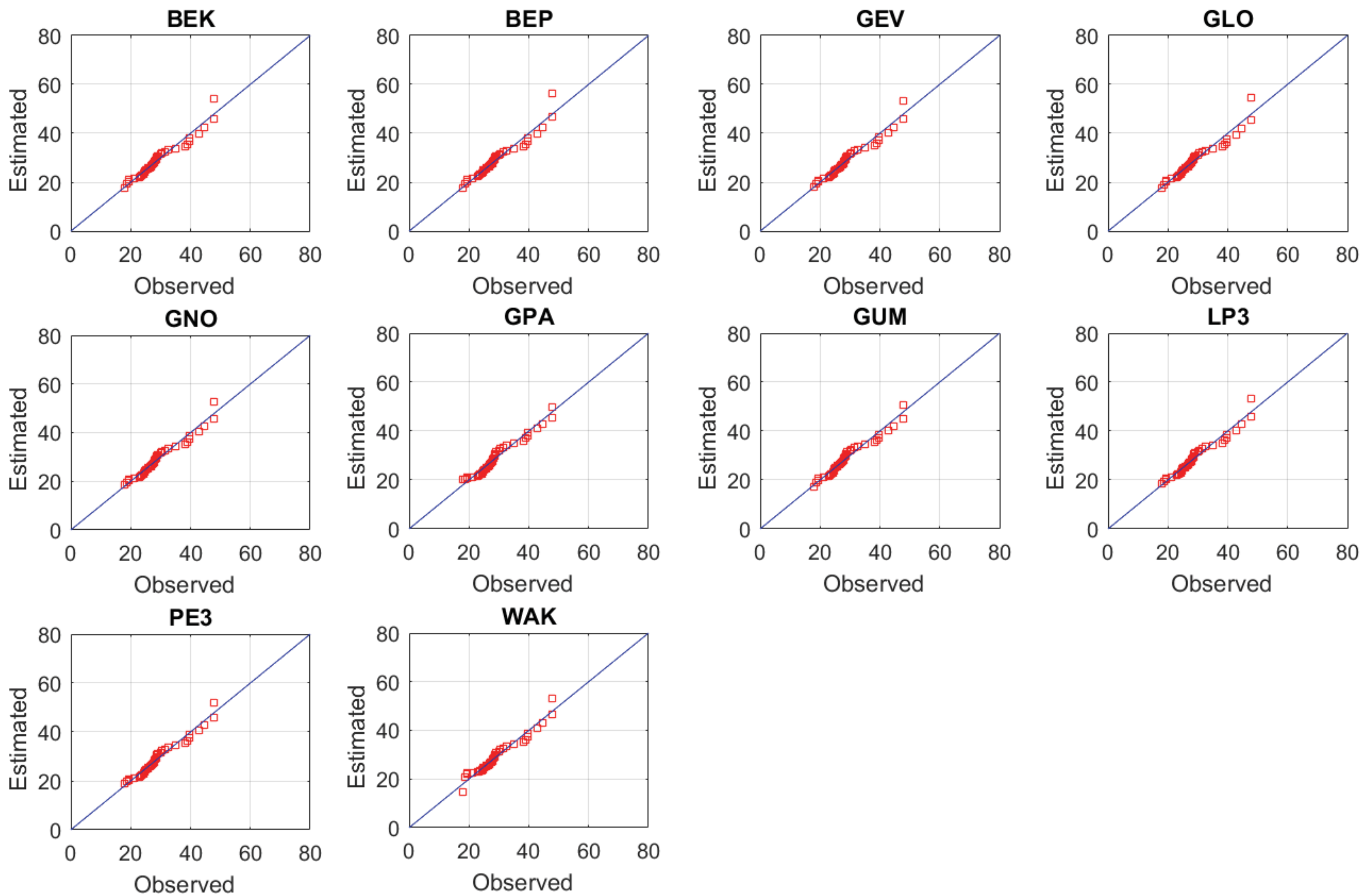

FIGURE 46 Q-Q PLOTS FOR 24HR RAINFALL DATA OF PRINCE GEORGE A

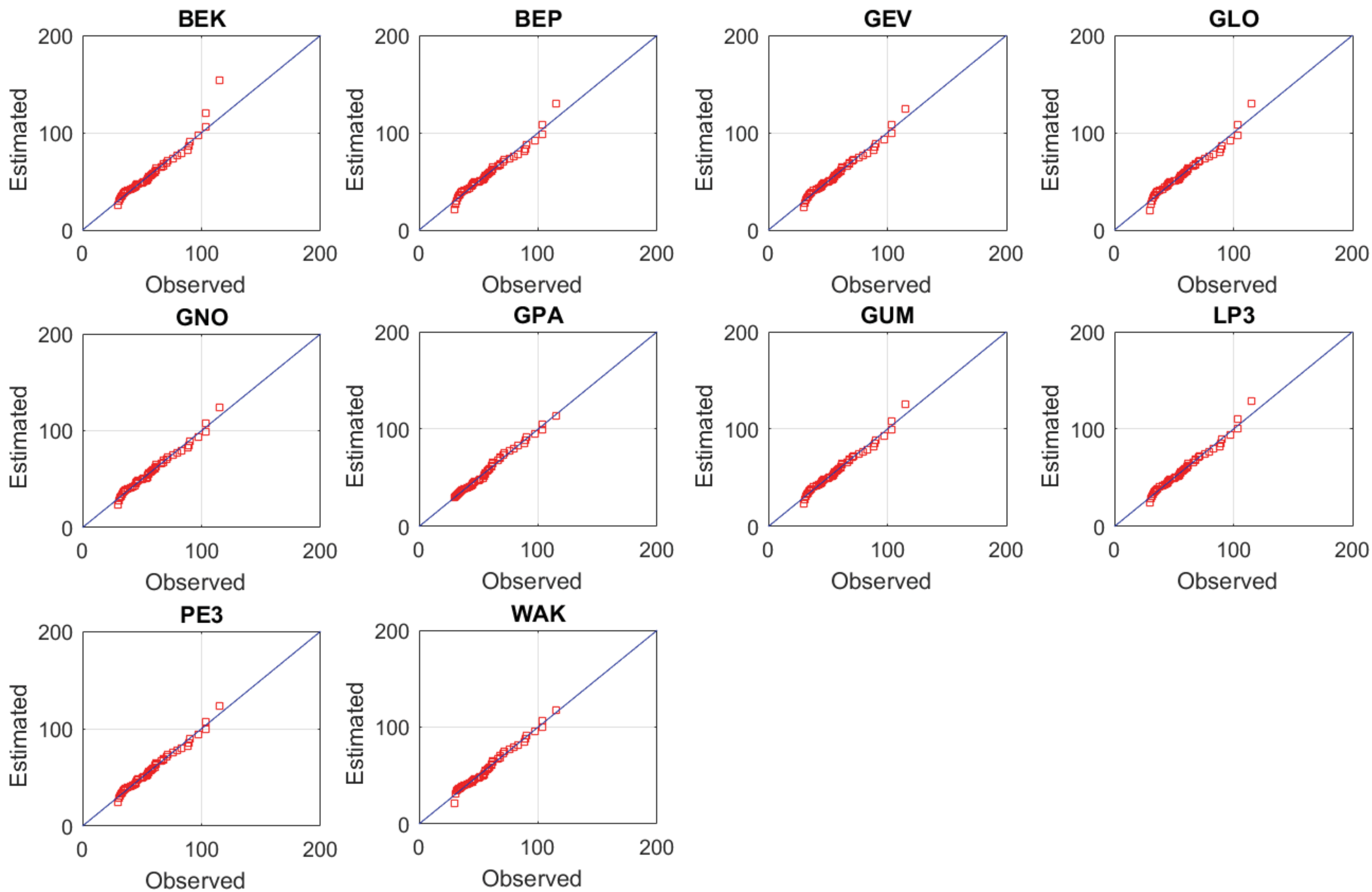

FIGURE 47 Q-Q PLOTS FOR 24HR RAINFALL DATA OF TERRACE PCC

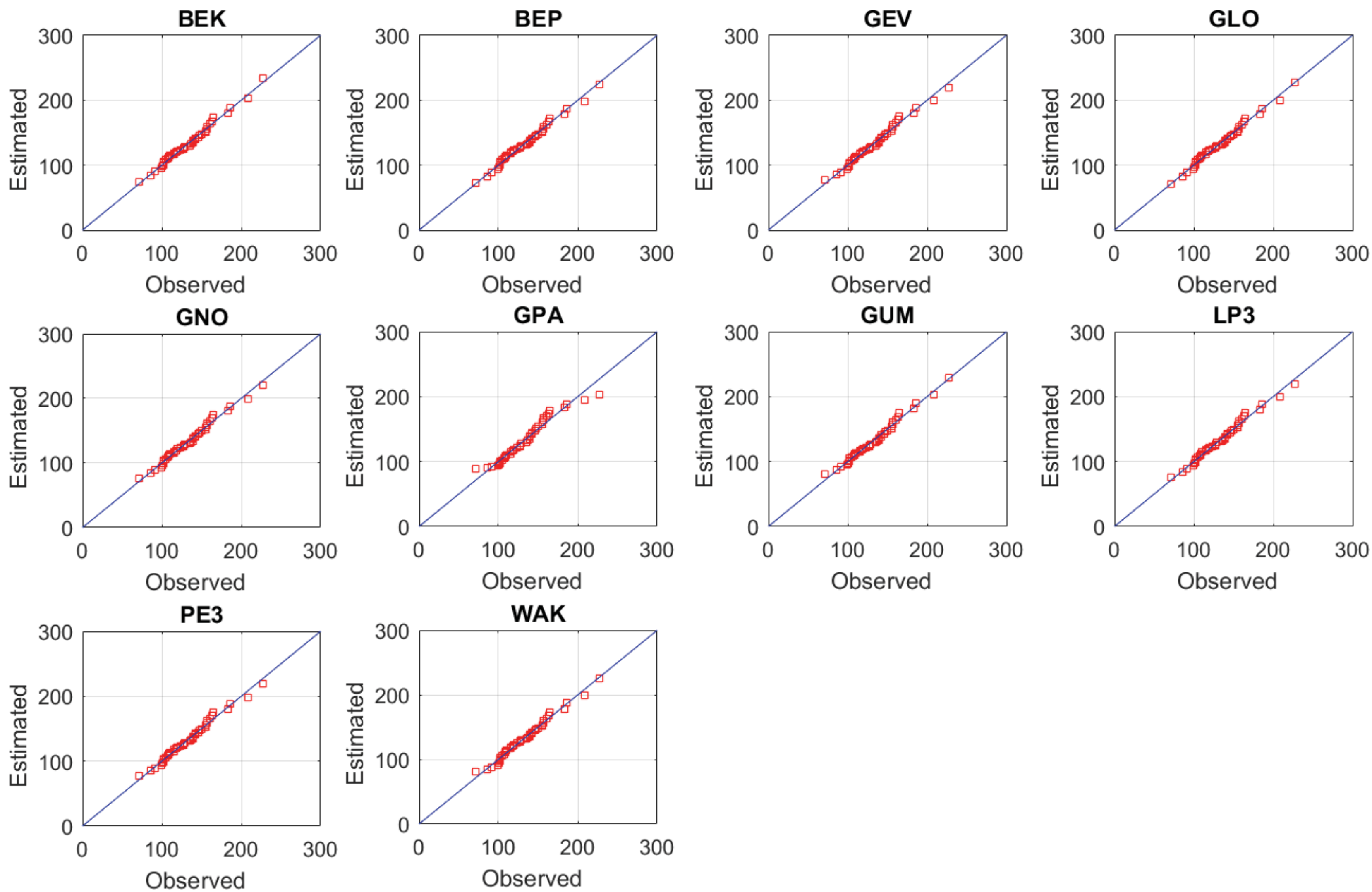

FIGURE 48 Q-Q PLOTS FOR 24HR RAINFALL DATA OF TOFINO A

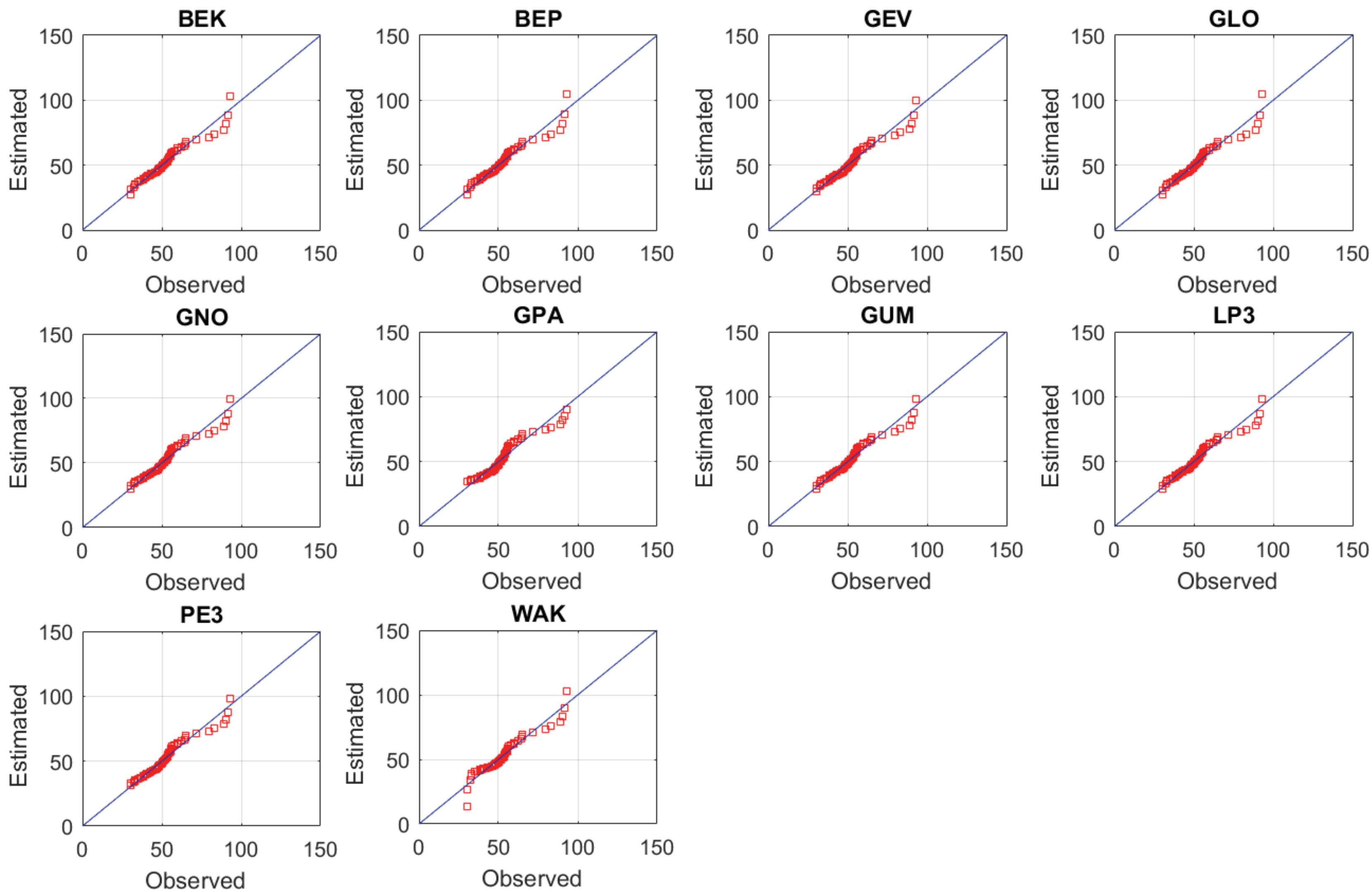

FIGURE 49 Q-Q PLOTS FOR 24HR RAINFALL DATA OF VANCOUVER INTL A

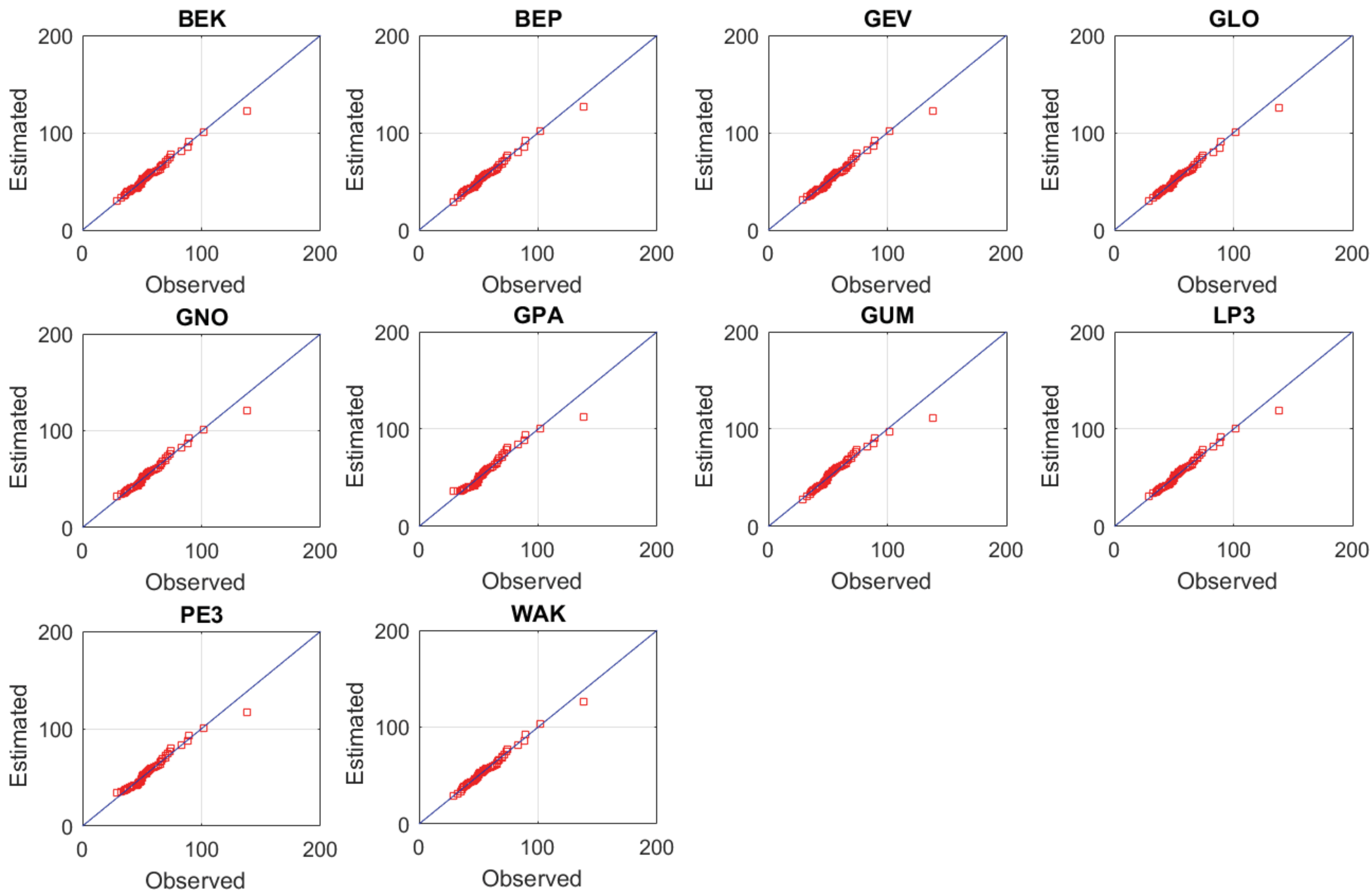

FIGURE 50 Q-Q PLOTS FOR 24HR RAINFALL DATA OF VICTORIA INTL A

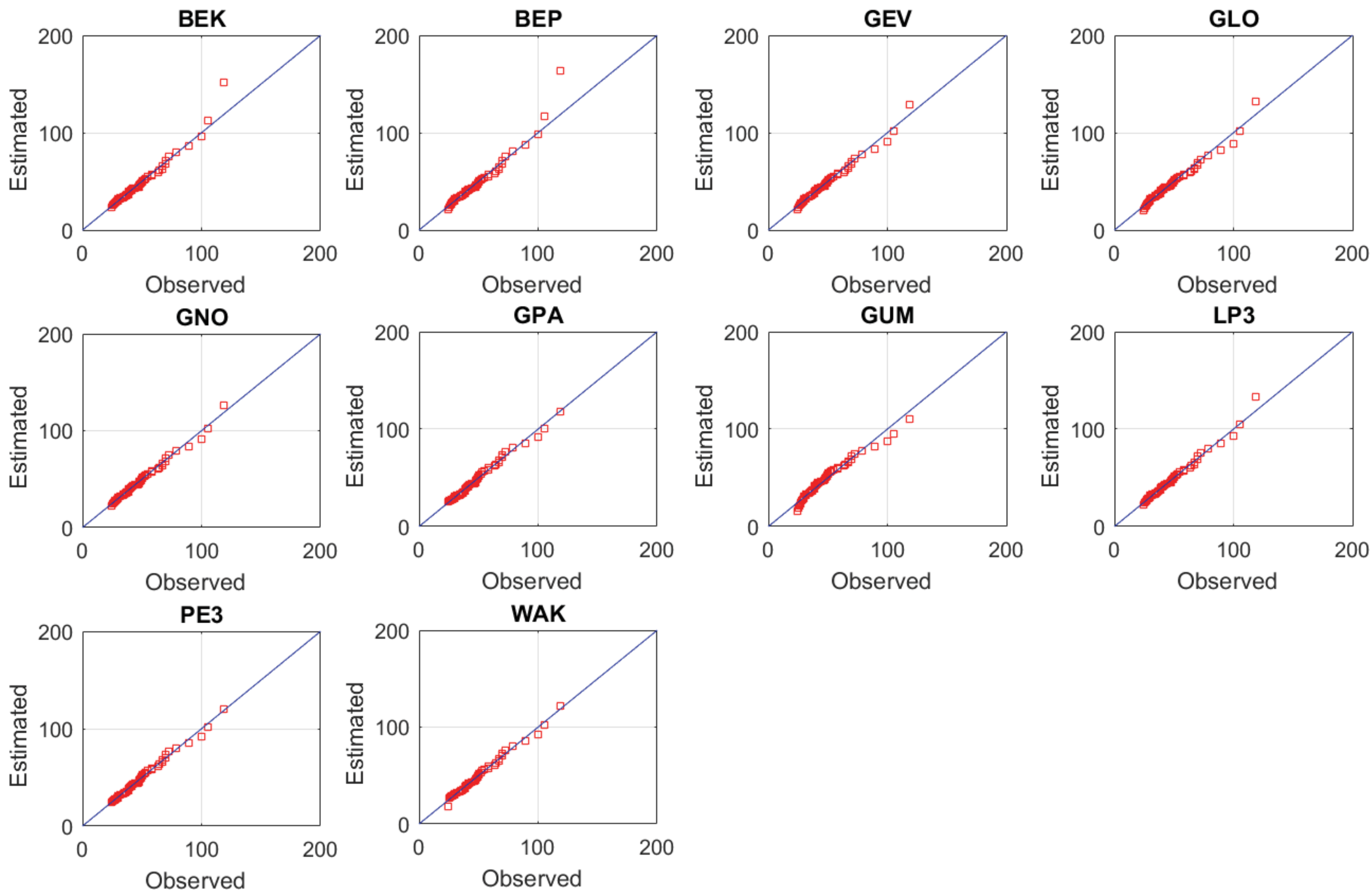

FIGURE 51 Q-Q PLOTS FOR 24HR RAINFALL DATA OF VICTORIA GONZALES HTS

APPENDIX 4 BOXPLOTS OF EXTRAPOLATED RIGHT-TAIL BOOTSTRAP DATA

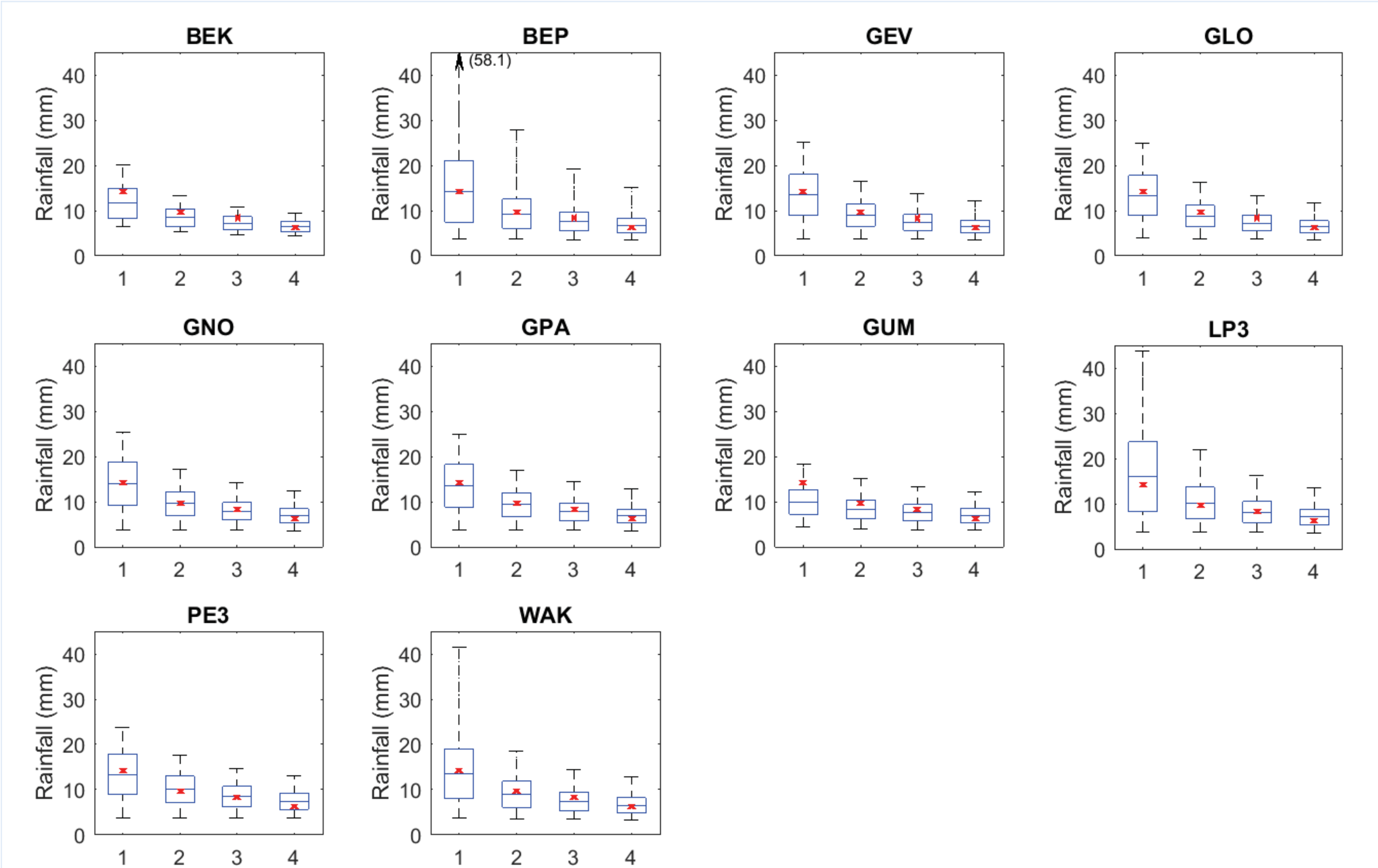

FIGURE 52 BOXPLOTS OF EXTRAPOLATED RIGHT-TAIL BOOTSTRAP DATA FOR 5MIN RAINFALL OF BLUE RIVER A

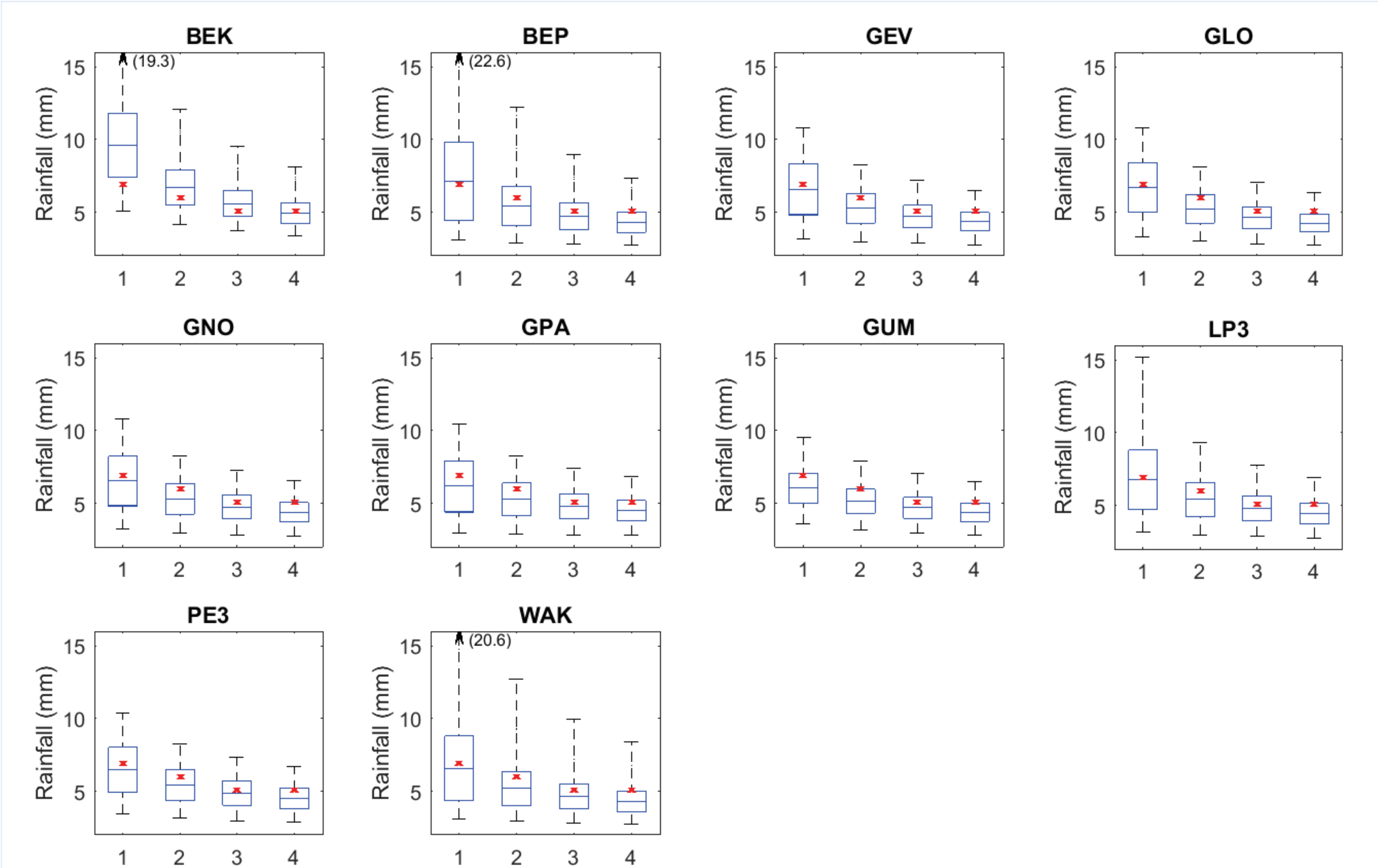

FIGURE 53 BOXPLOTS OF EXTRAPOLATED RIGHT-TAIL BOOTSTRAP DATA FOR 5MIN RAINFALL OF COMOX A

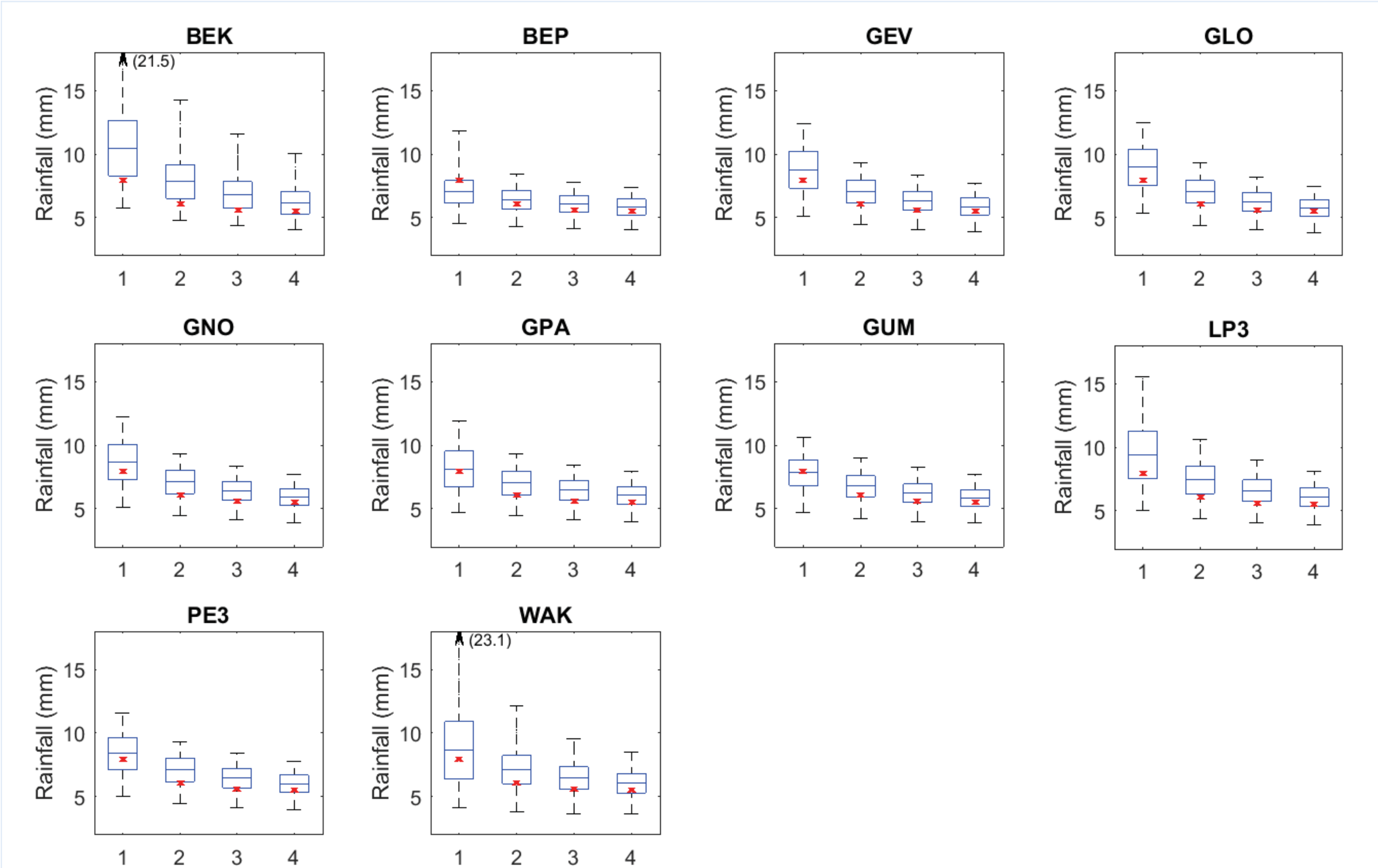

FIGURE 54 BOXPLOTS OF EXTRAPOLATED RIGHT-TAIL BOOTSTRAP DATA FOR 5MIN RAINFALL OF MISSION WEST ABBEY

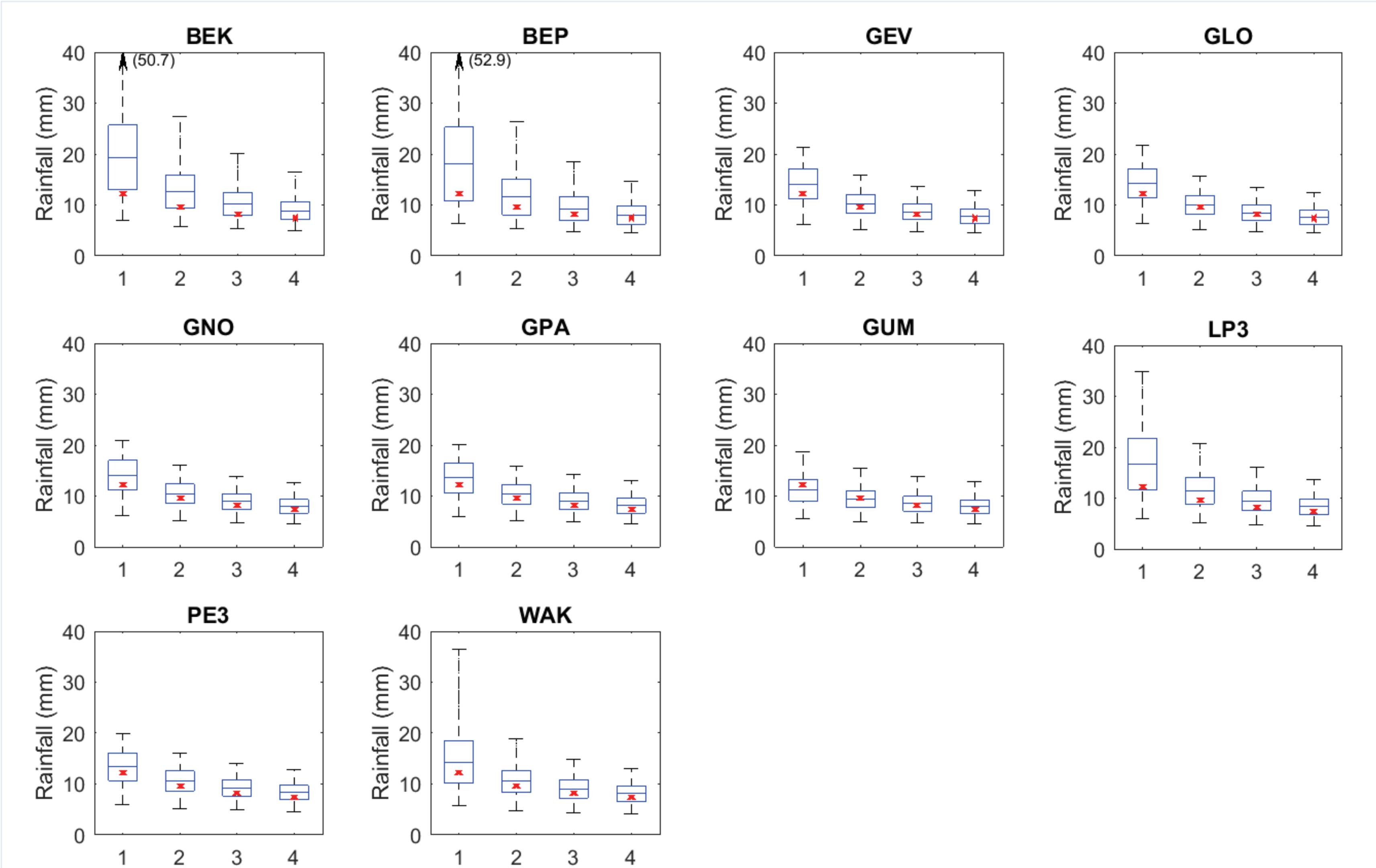

FIGURE 55 BOXPLOTS OF EXTRAPOLATED RIGHT-TAIL BOOTSTRAP DATA FOR 5MIN RAINFALL OF PENTICTON A

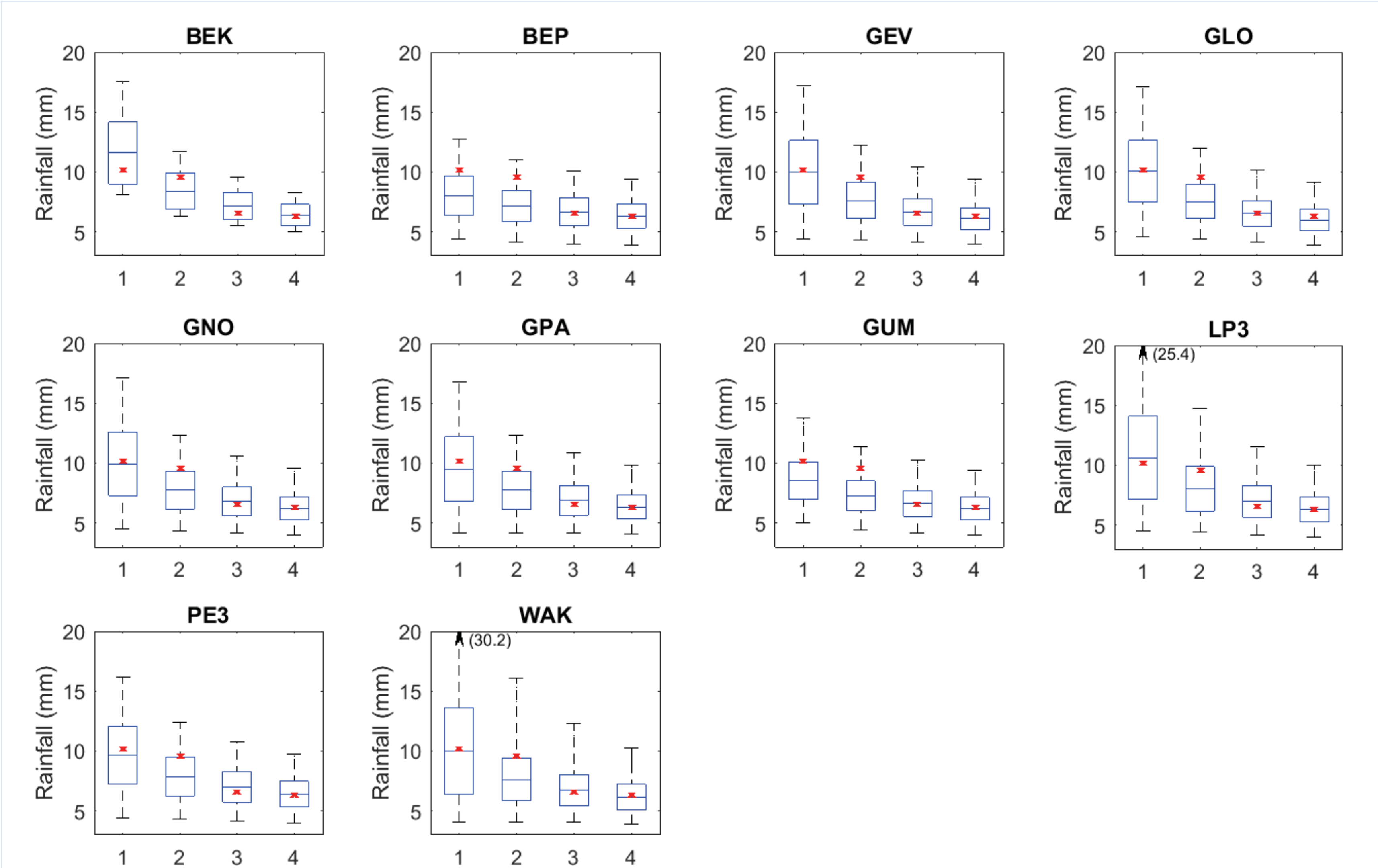

FIGURE 56 BOXPLOTS OF EXTRAPOLATED RIGHT-TAIL BOOTSTRAP DATA FOR 5MIN RAINFALL OF PITT POLDER

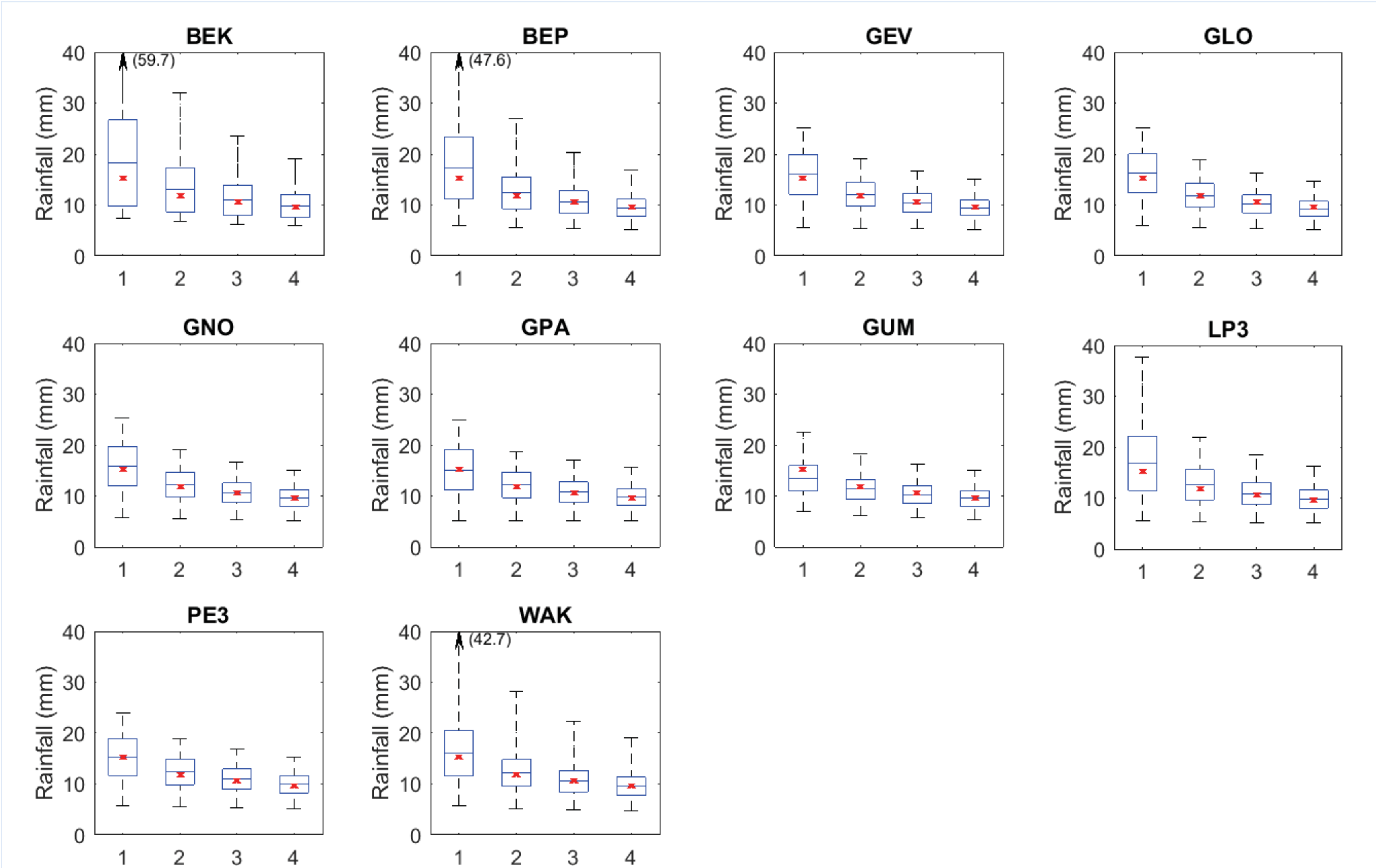

FIGURE 57 BOXPLOTS OF EXTRAPOLATED RIGHT-TAIL BOOTSTRAP DATA FOR 5MIN RAINFALL OF PRINCE GEORGE A

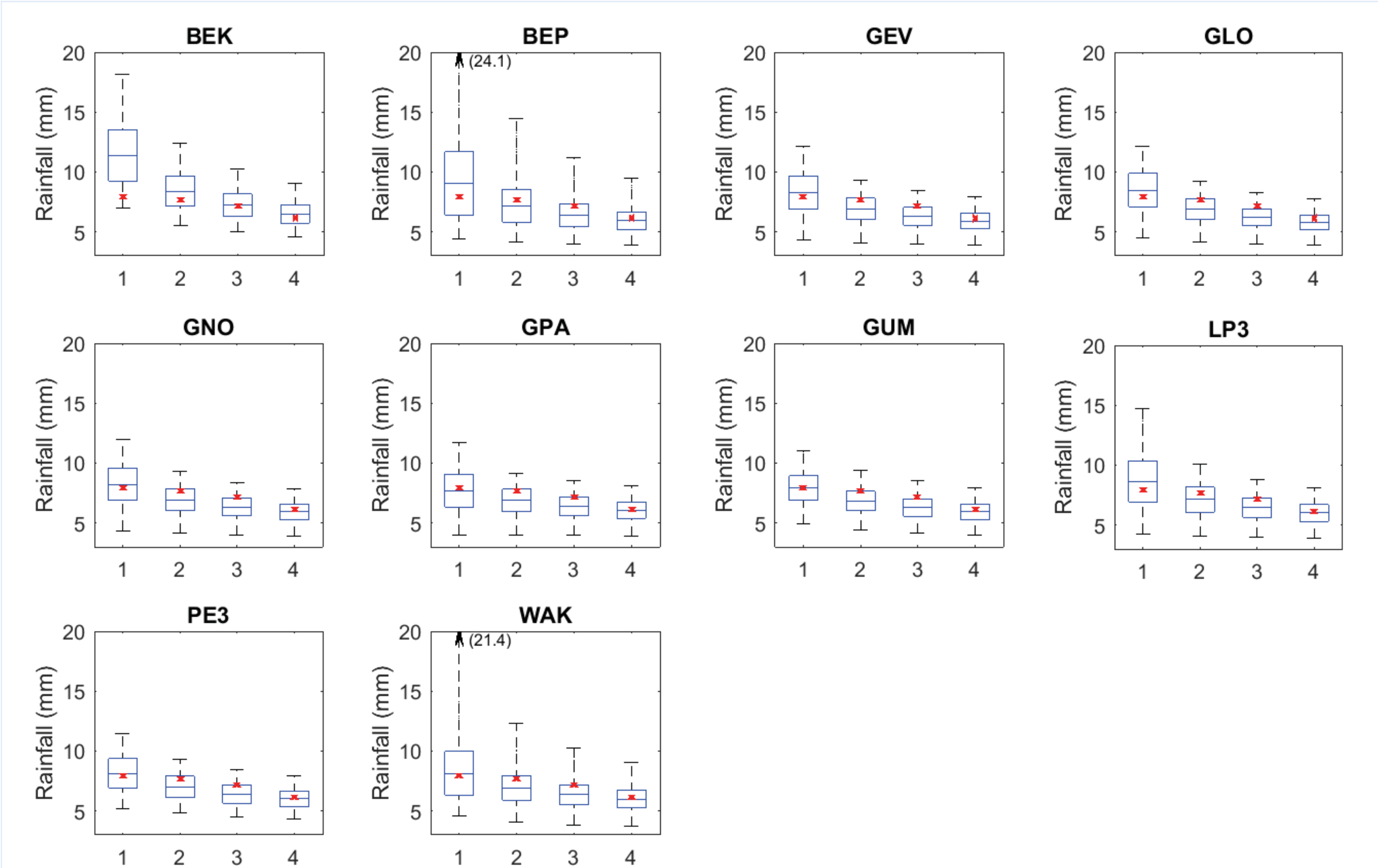

FIGURE 58 BOXPLOTS OF EXTRAPOLATED RIGHT-TAIL BOOTSTRAP DATA FOR 5MIN RAINFALL OF TERRACE PCC

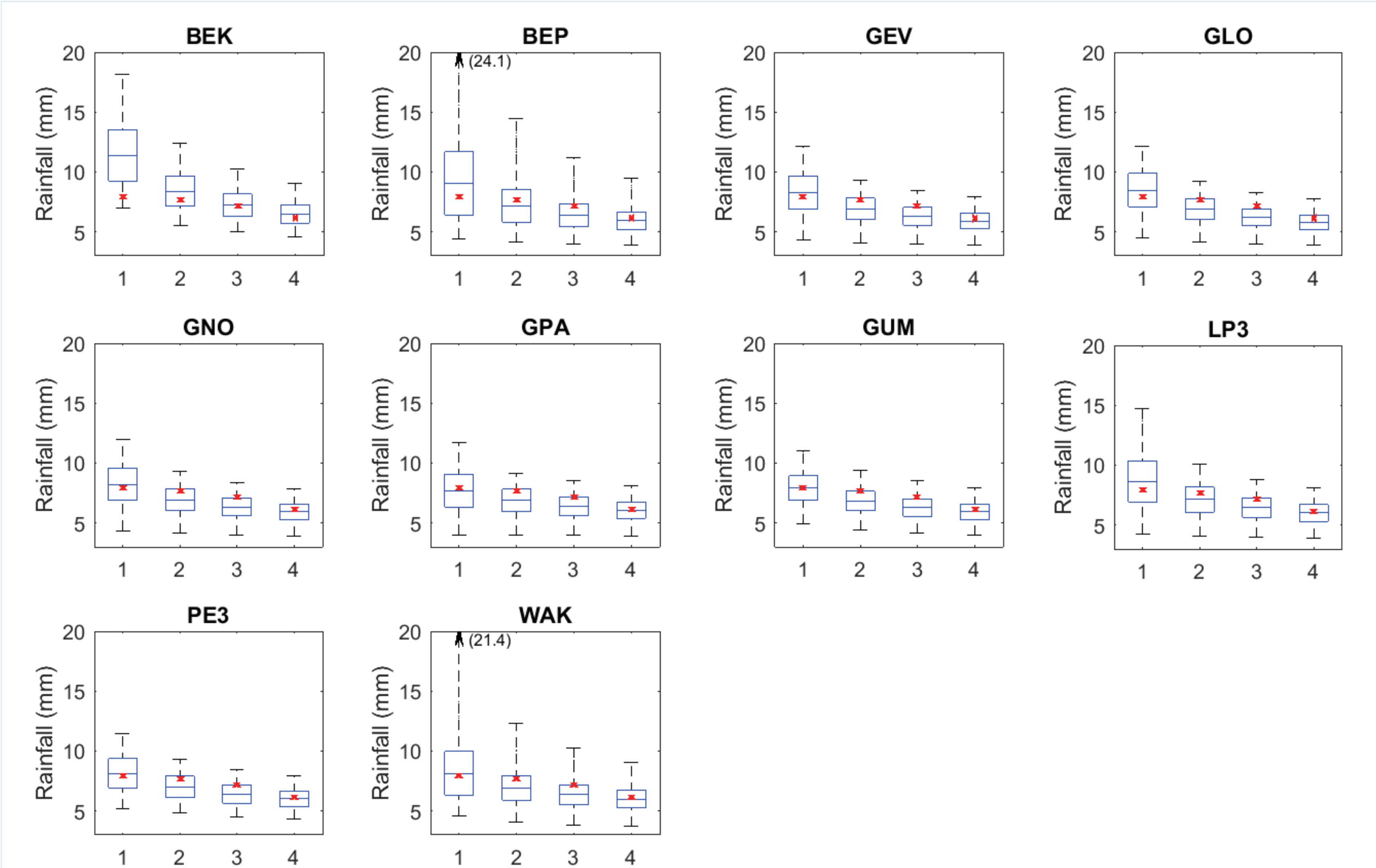

Figure 59 Boxplots of Extrapolated Right-Tail Bootstrap Data for 5min Rainfall of Tofino A

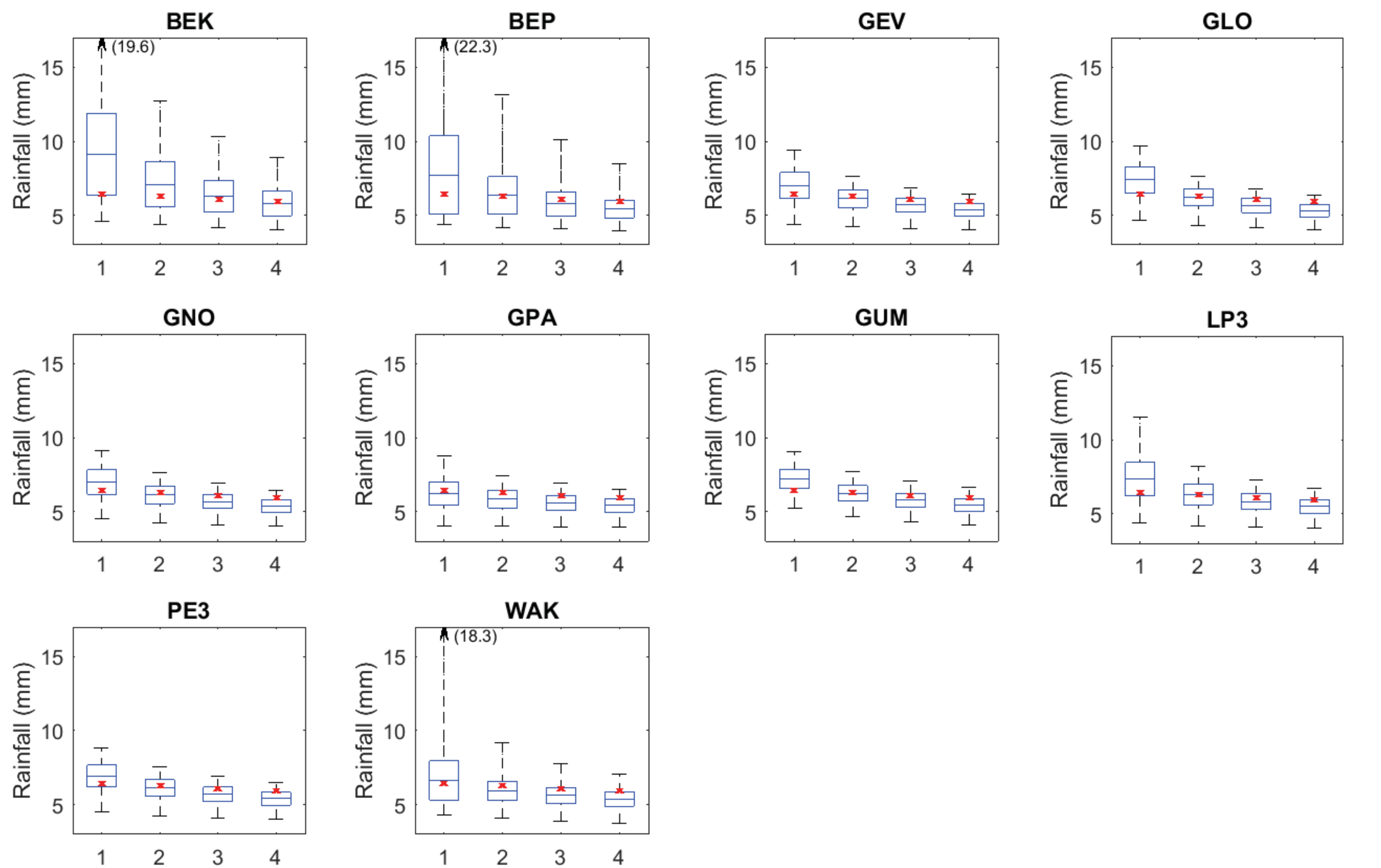

FIGURE 60 BOXPLOTS OF EXTRAPOLATED RIGHT-TAIL BOOTSTRAP DATA FOR 5MIN RAINFALL OF VANCOUVER INTL A

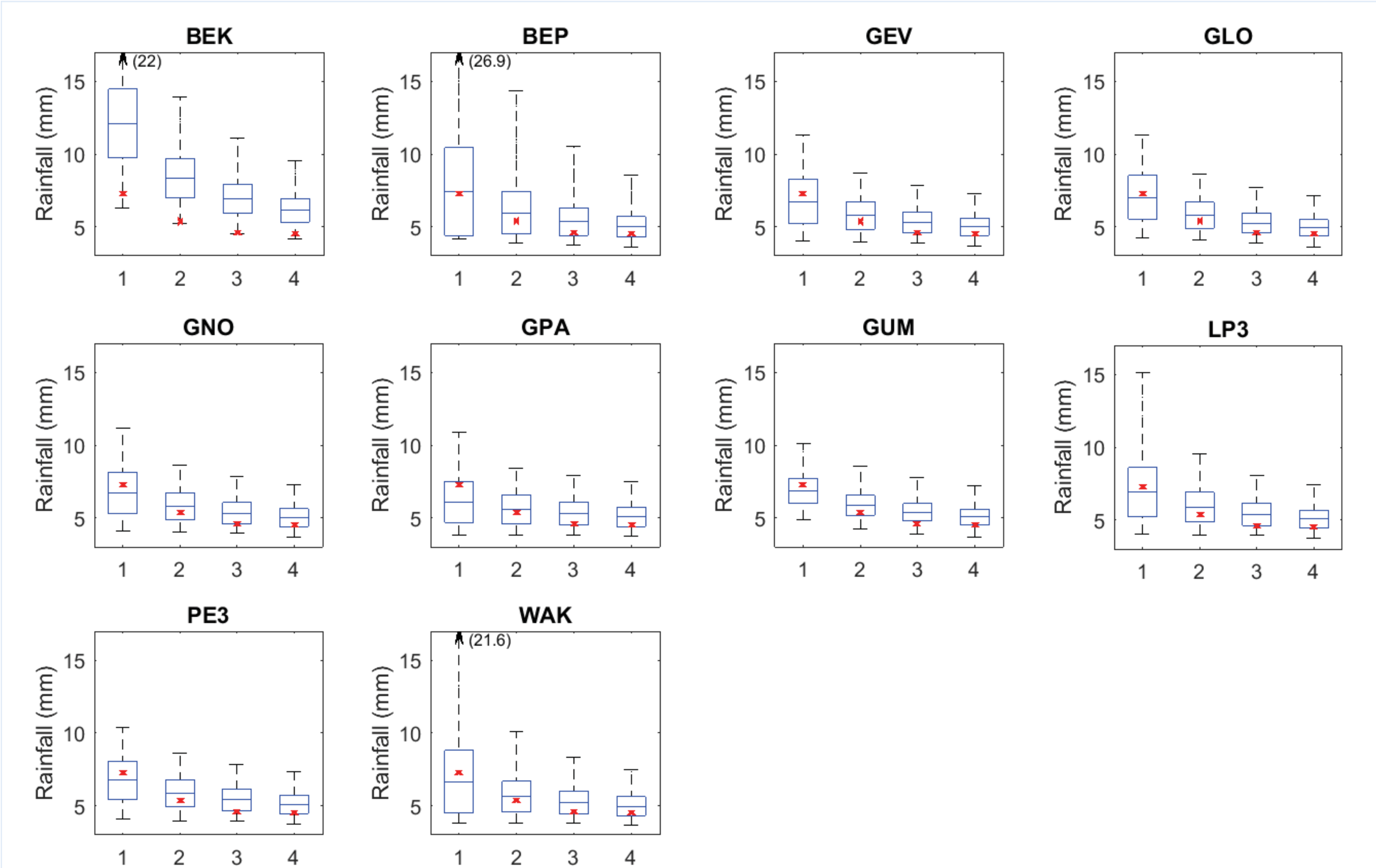

FIGURE 61 *BOXPLOTS OF EXTRAPOLATED RIGHT-TAIL BOOTSTRAP DATA FOR 5MIN RAINFALL OF VICTORIA INTL A*

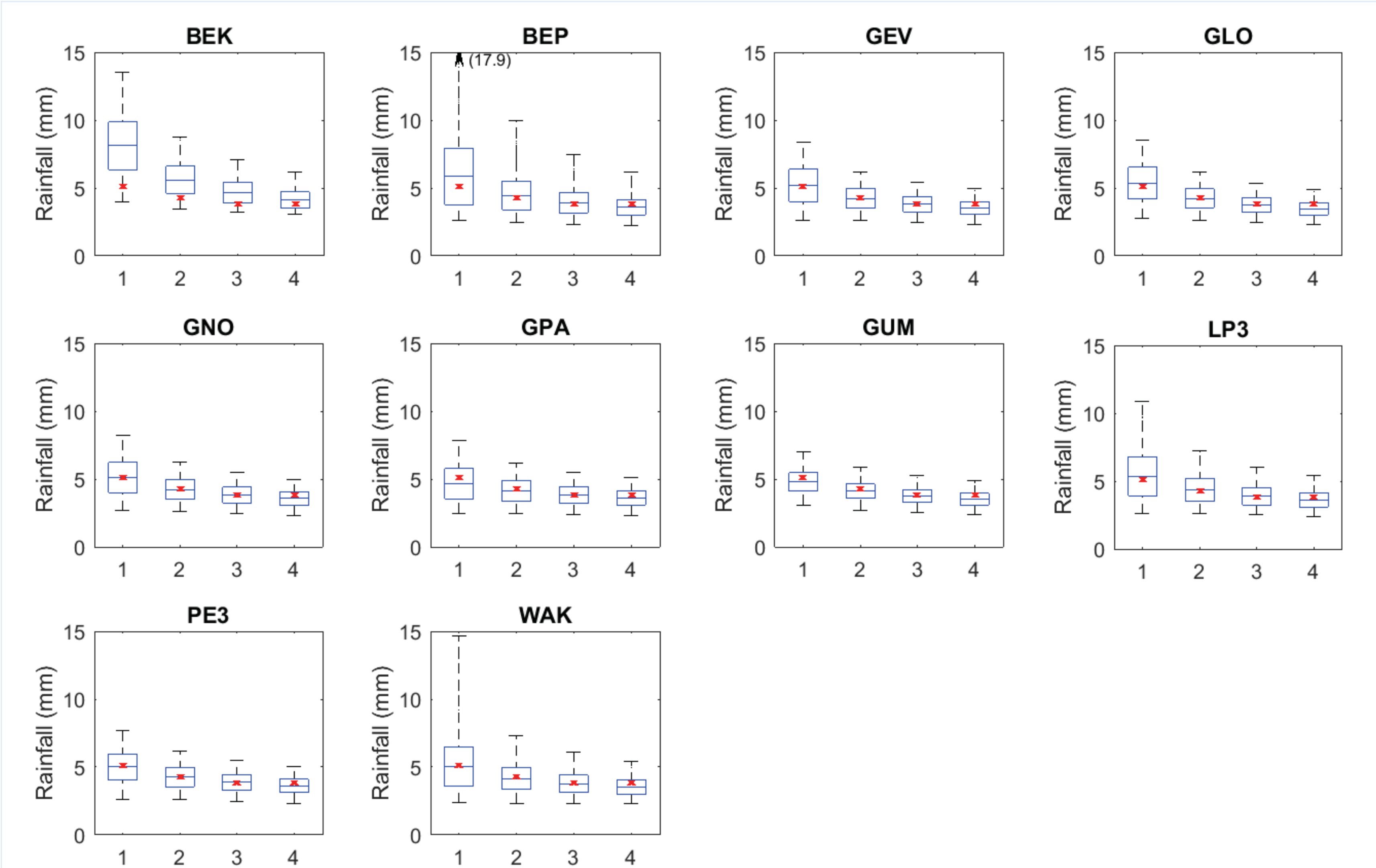

FIGURE 62 BOXPLOTS OF EXTRAPOLATED RIGHT-TAIL BOOTSTRAP DATA FOR 5MIN RAINFALL OF VICTORIA GONZALES

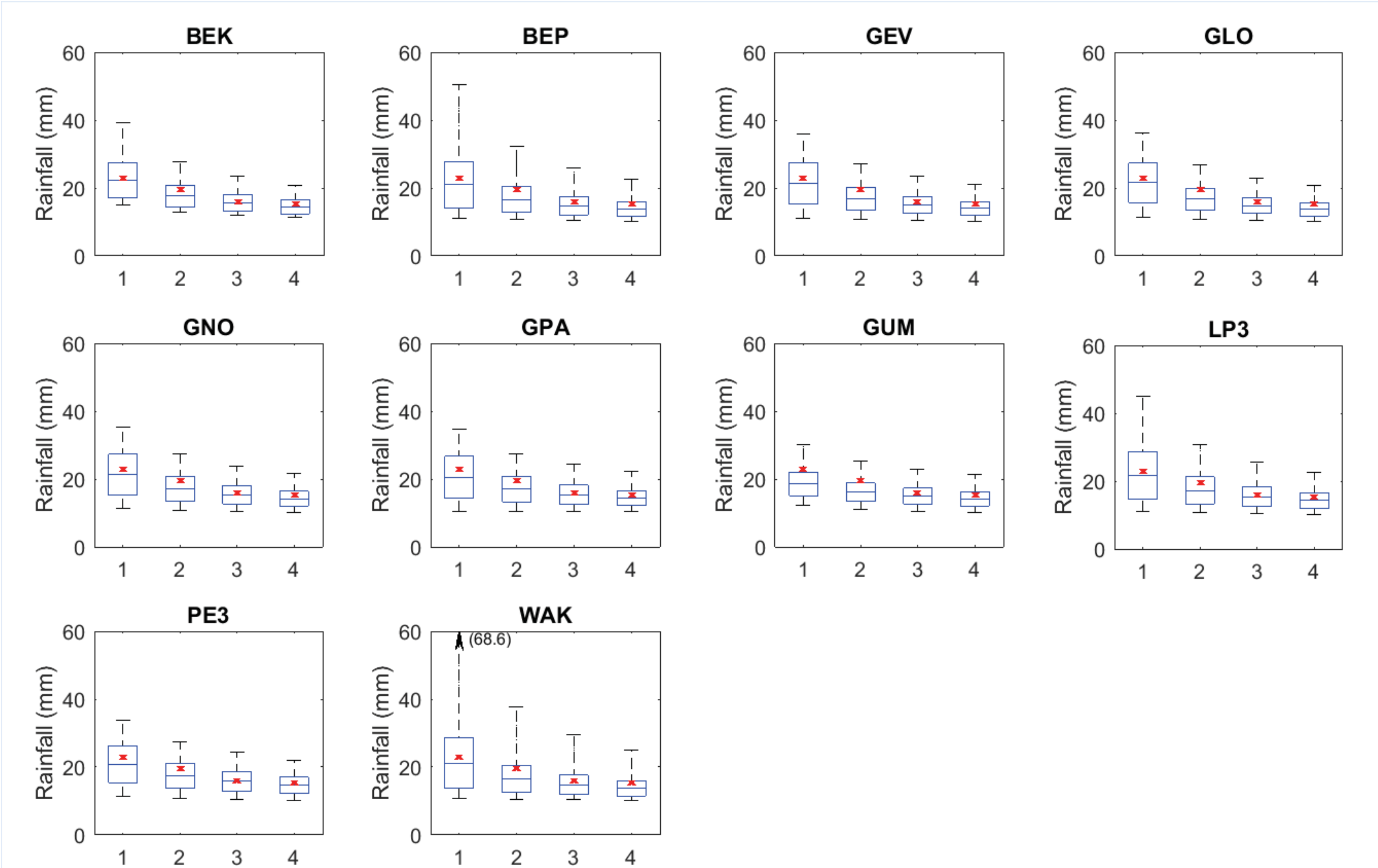

FIGURE 63 BOXPLOTS OF EXTRAPOLATED RIGHT-TAIL BOOTSTRAP DATA FOR 1HR RAINFALL OF BLUE RIVER A

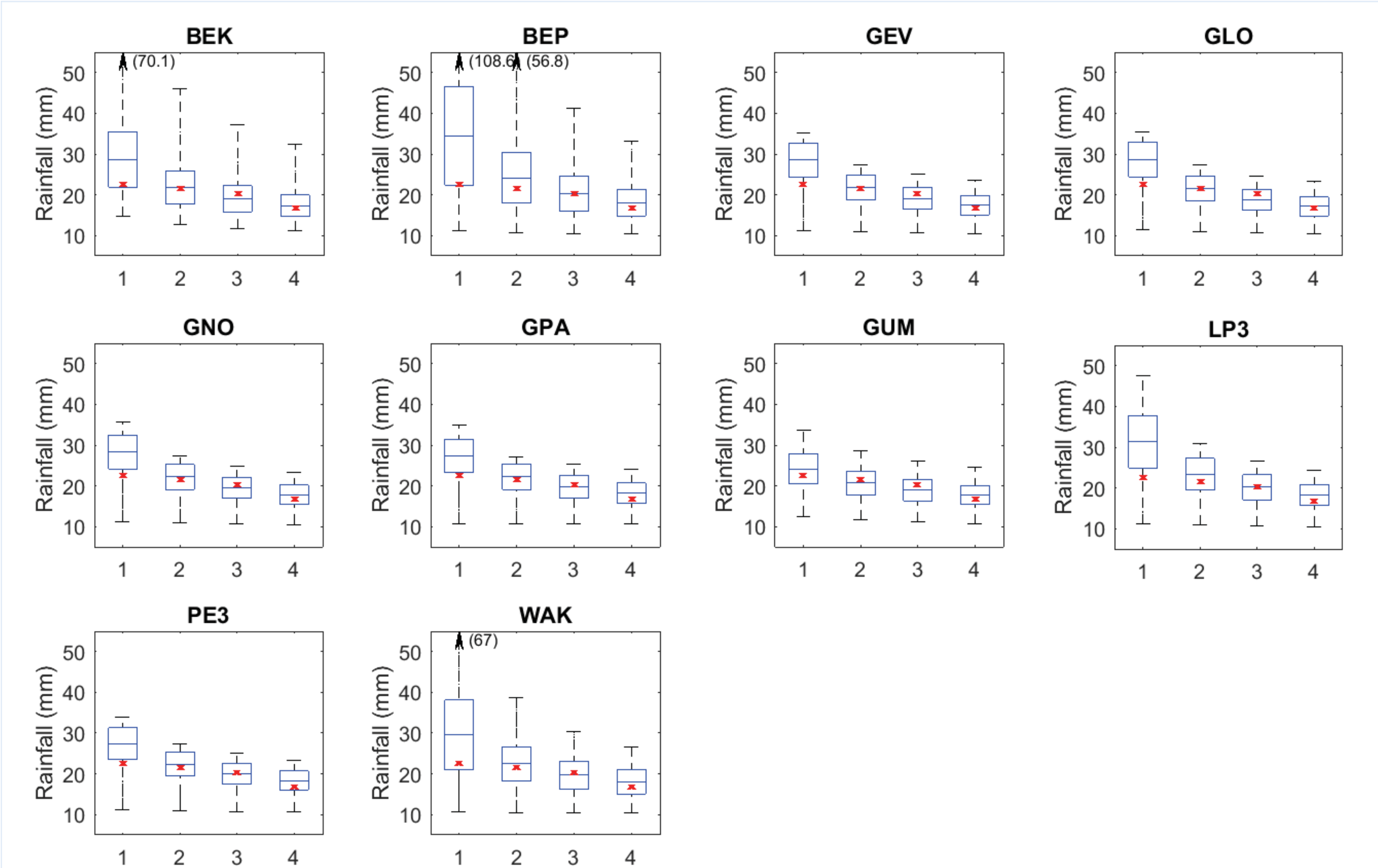

FIGURE 64 BOXPLOTS OF EXTRAPOLATED RIGHT-TAIL BOOTSTRAP DATA FOR 1HR RAINFALL OF COMOX A

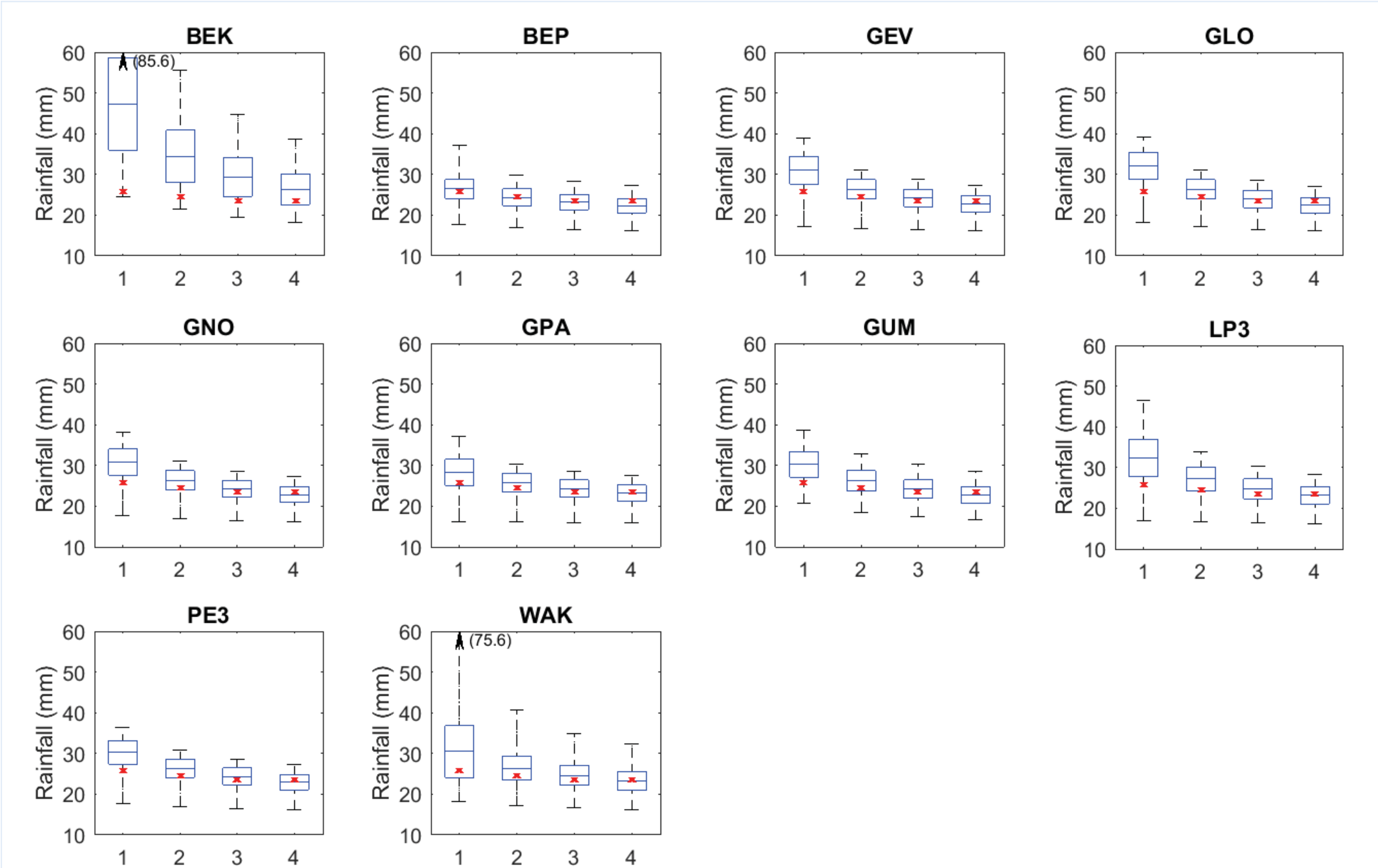

FIGURE 65 BOXPLOTS OF EXTRAPOLATED RIGHT-TAIL BOOTSTRAP DATA FOR 1HR RAINFALL OF MISSION WEST ABBEY

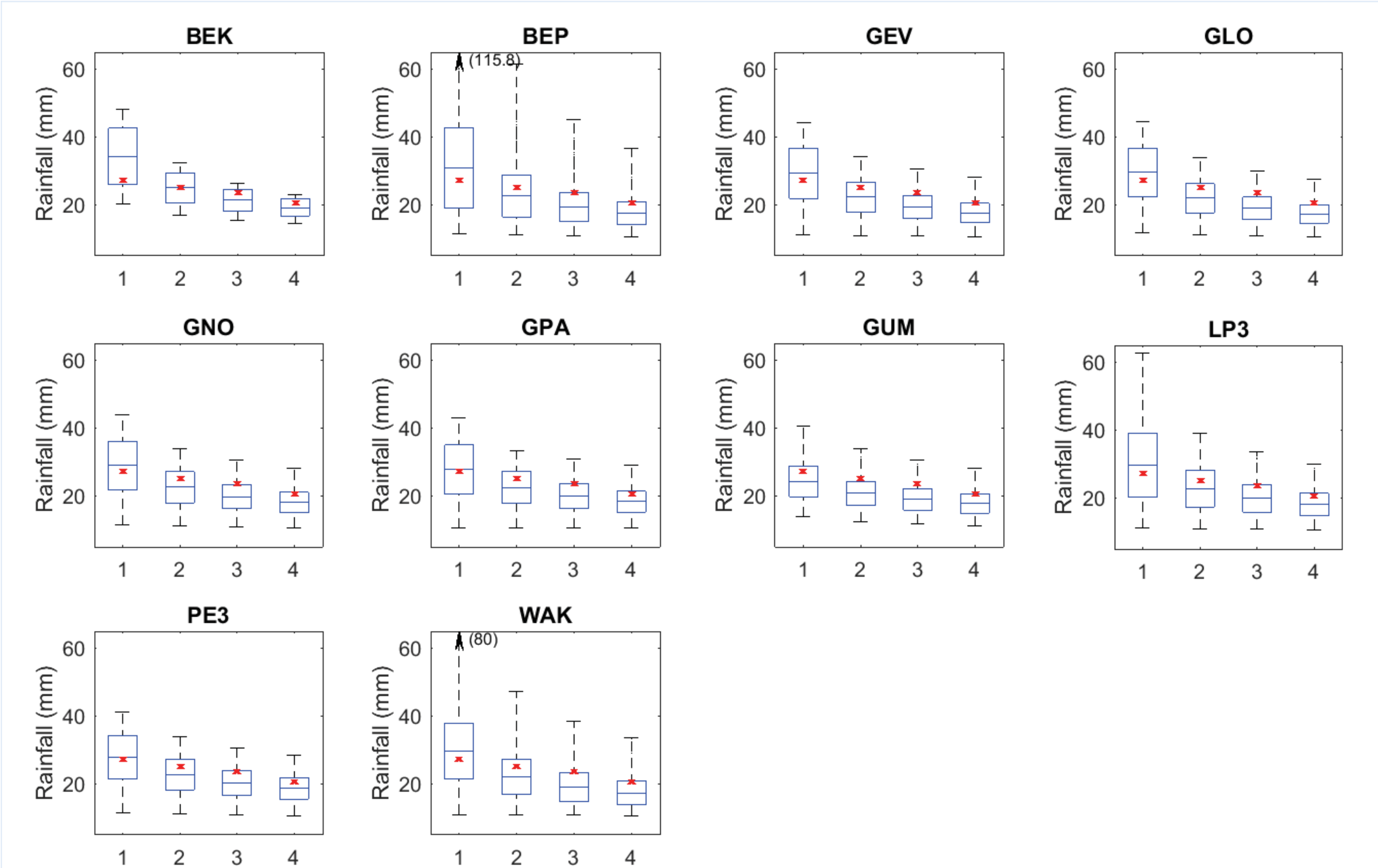

FIGURE 66 BOXPLOTS OF EXTRAPOLATED RIGHT-TAIL BOOTSTRAP DATA FOR 1HR RAINFALL OF PENTICTON A

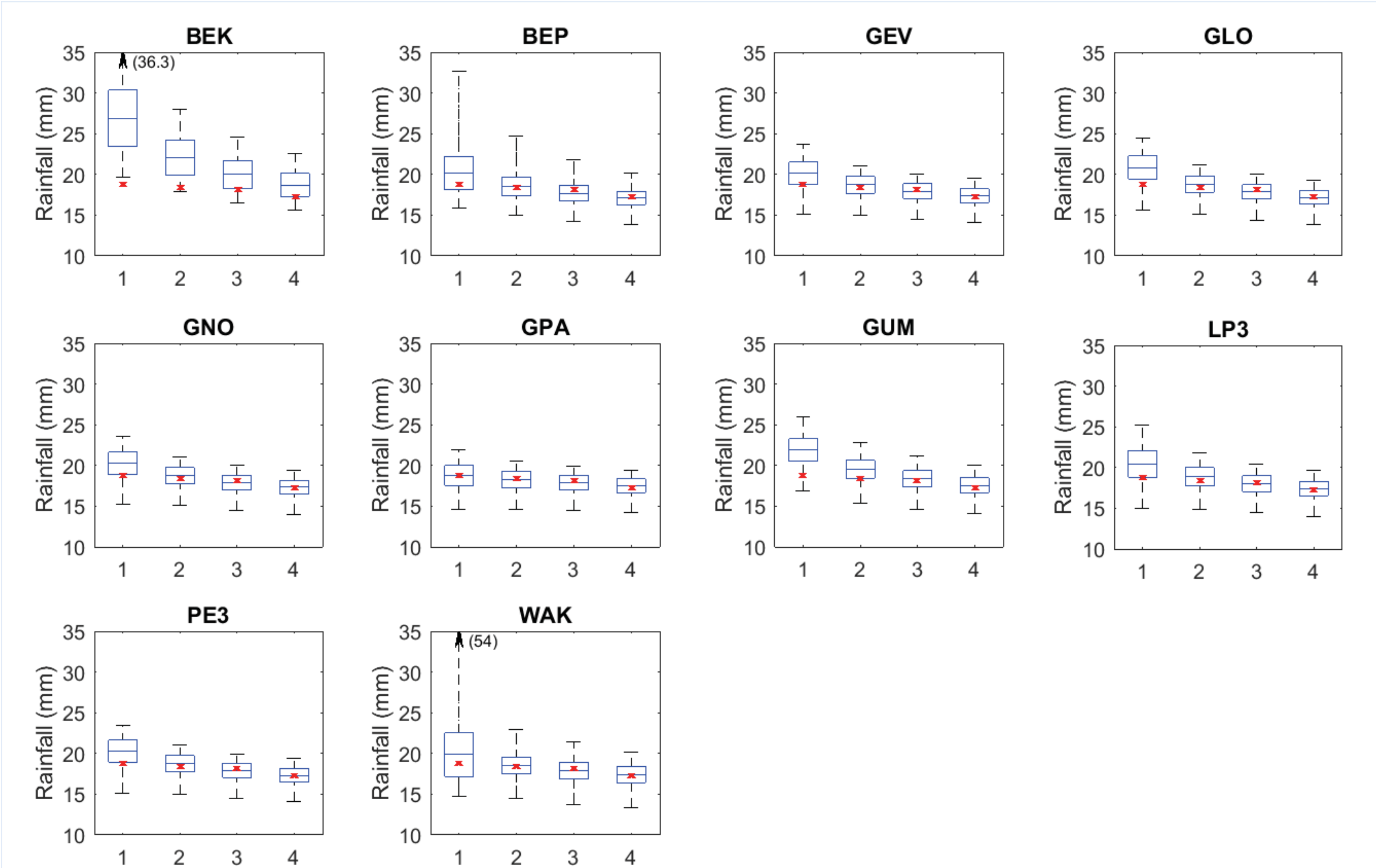

Figure 67 Boxplots of Extrapolated Right-Tail Bootstrap Data for 1hr Rainfall of Pitt Polder

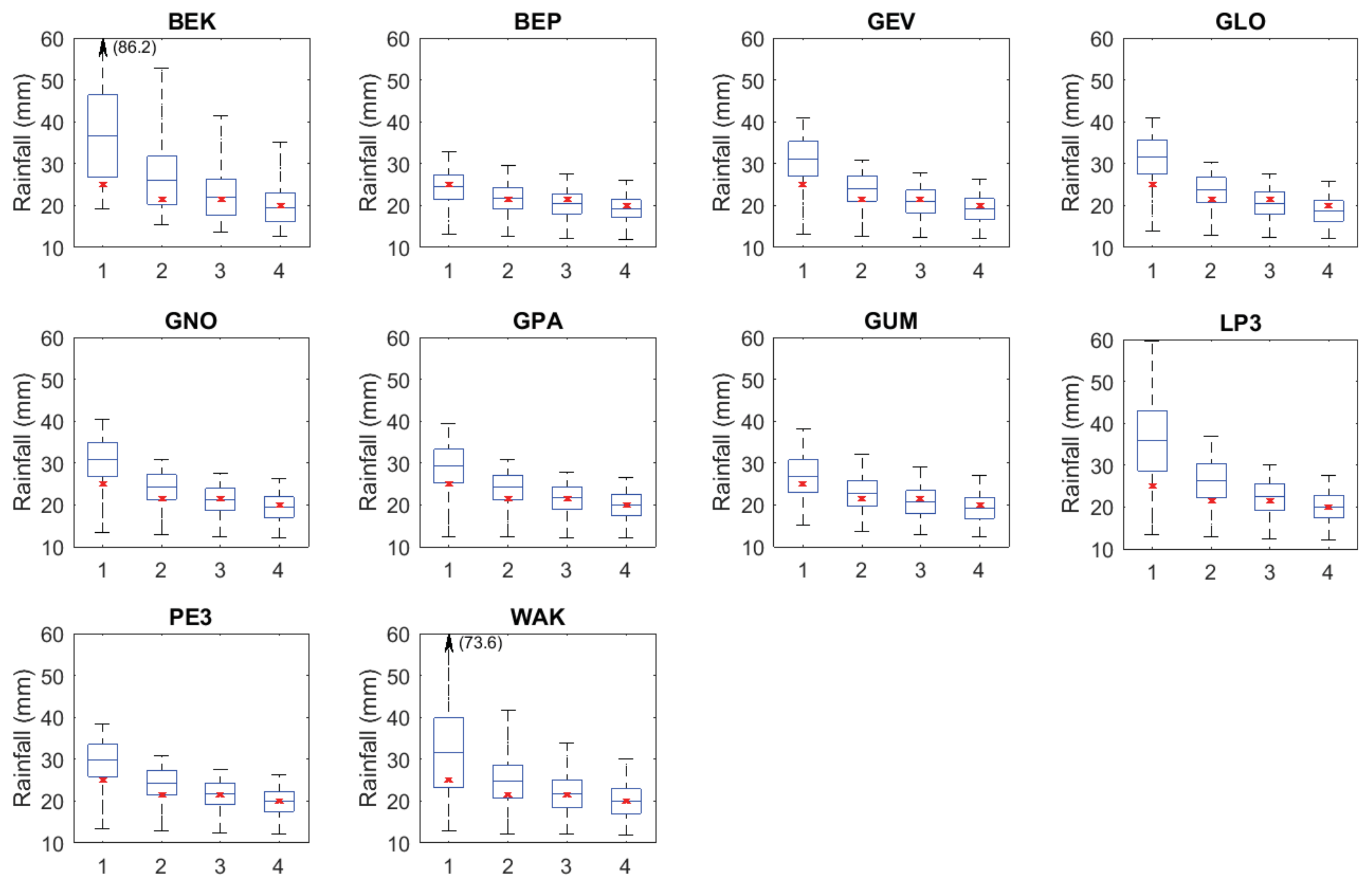

FIGURE 68 BOXPLOTS OF EXTRAPOLATED RIGHT-TAIL BOOTSTRAP DATA FOR 1HR RAINFALL OF PRINCE GEORGE A

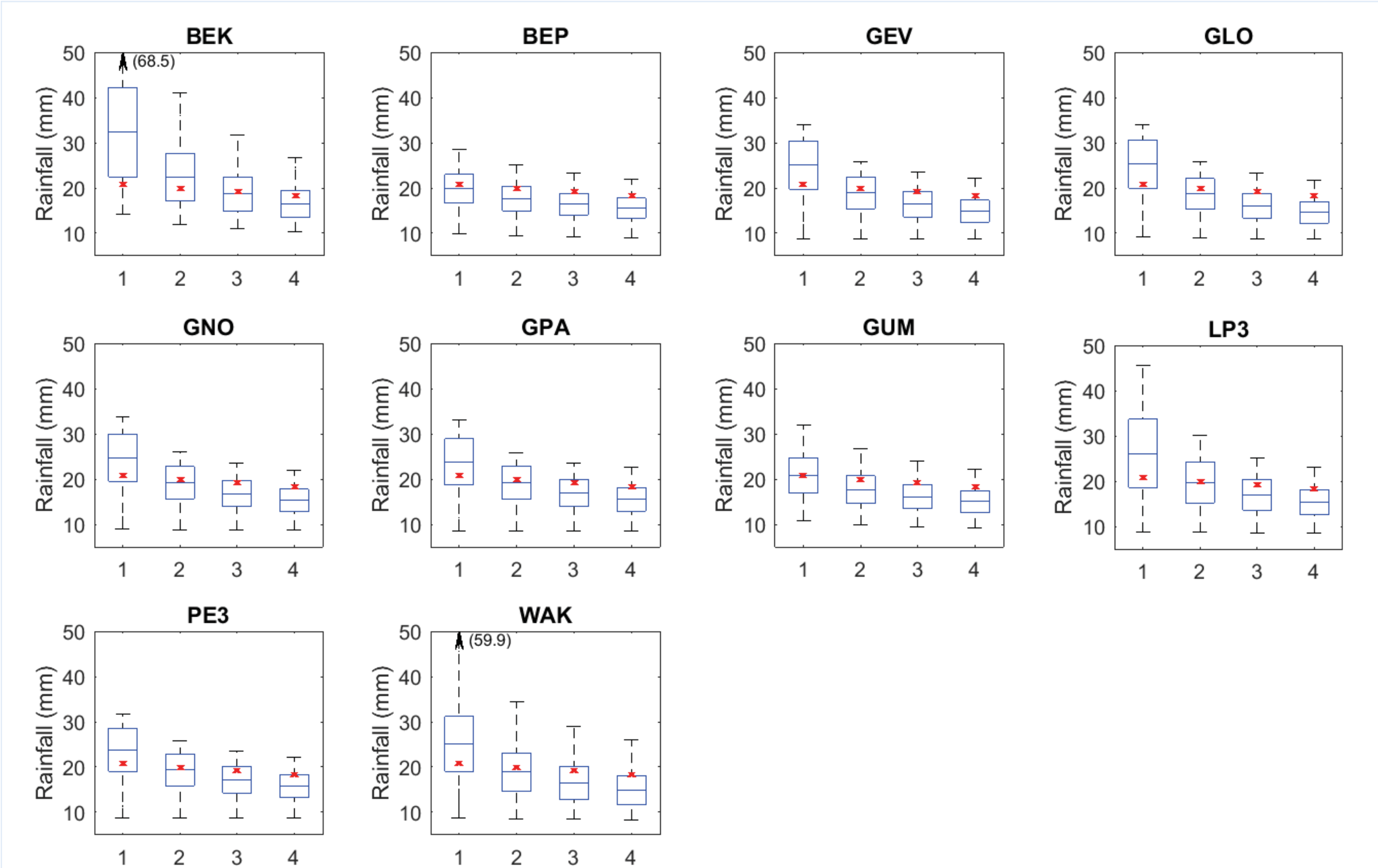

FIGURE 69 BOXPLOTS OF EXTRAPOLATED RIGHT-TAIL BOOTSTRAP DATA FOR 1HR RAINFALL OF TERRACE PCC

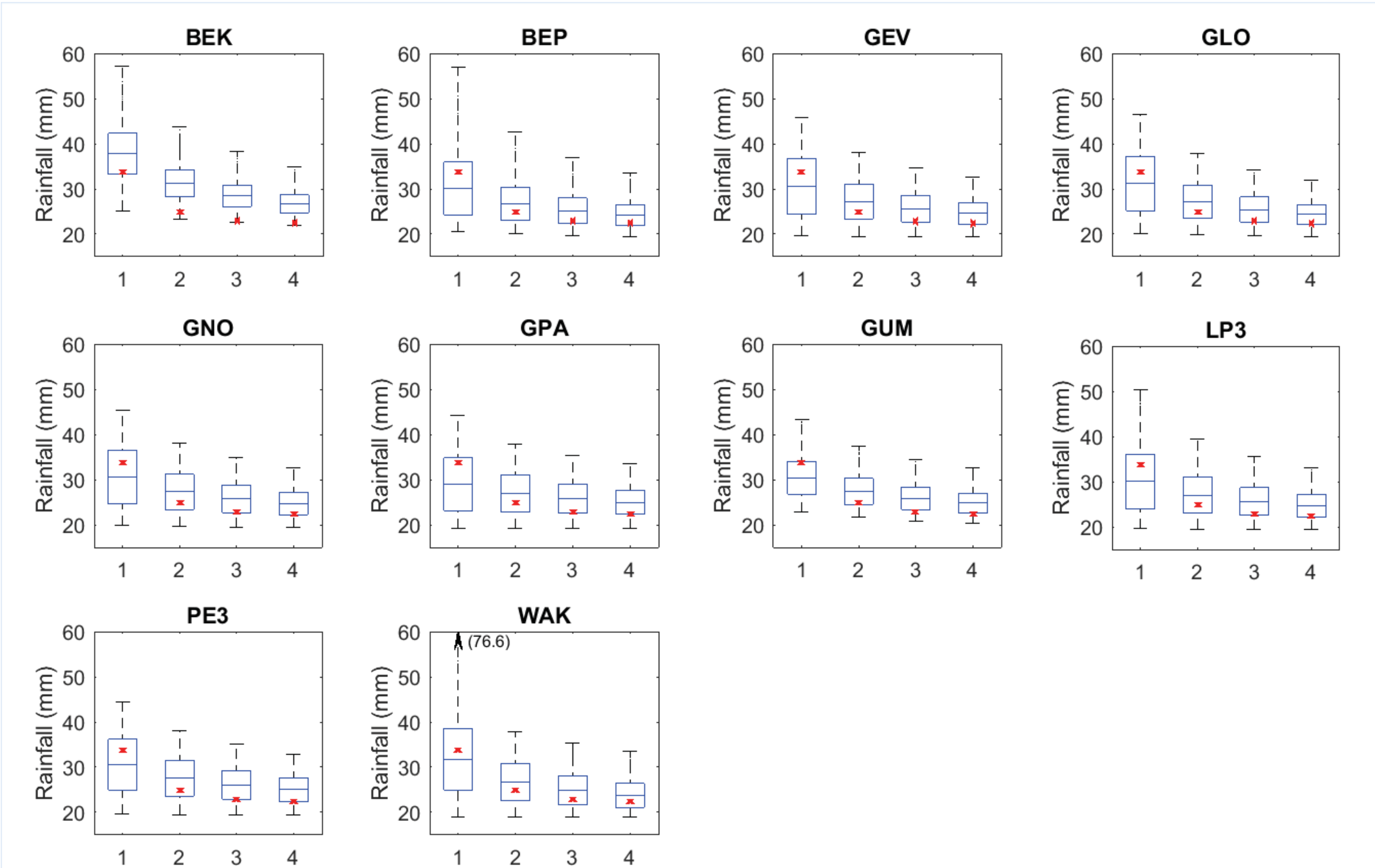

Figure 70   Boxplots of Extrapolated Right-Tail Bootstrap Data for 1hr Rainfall of Tofino A

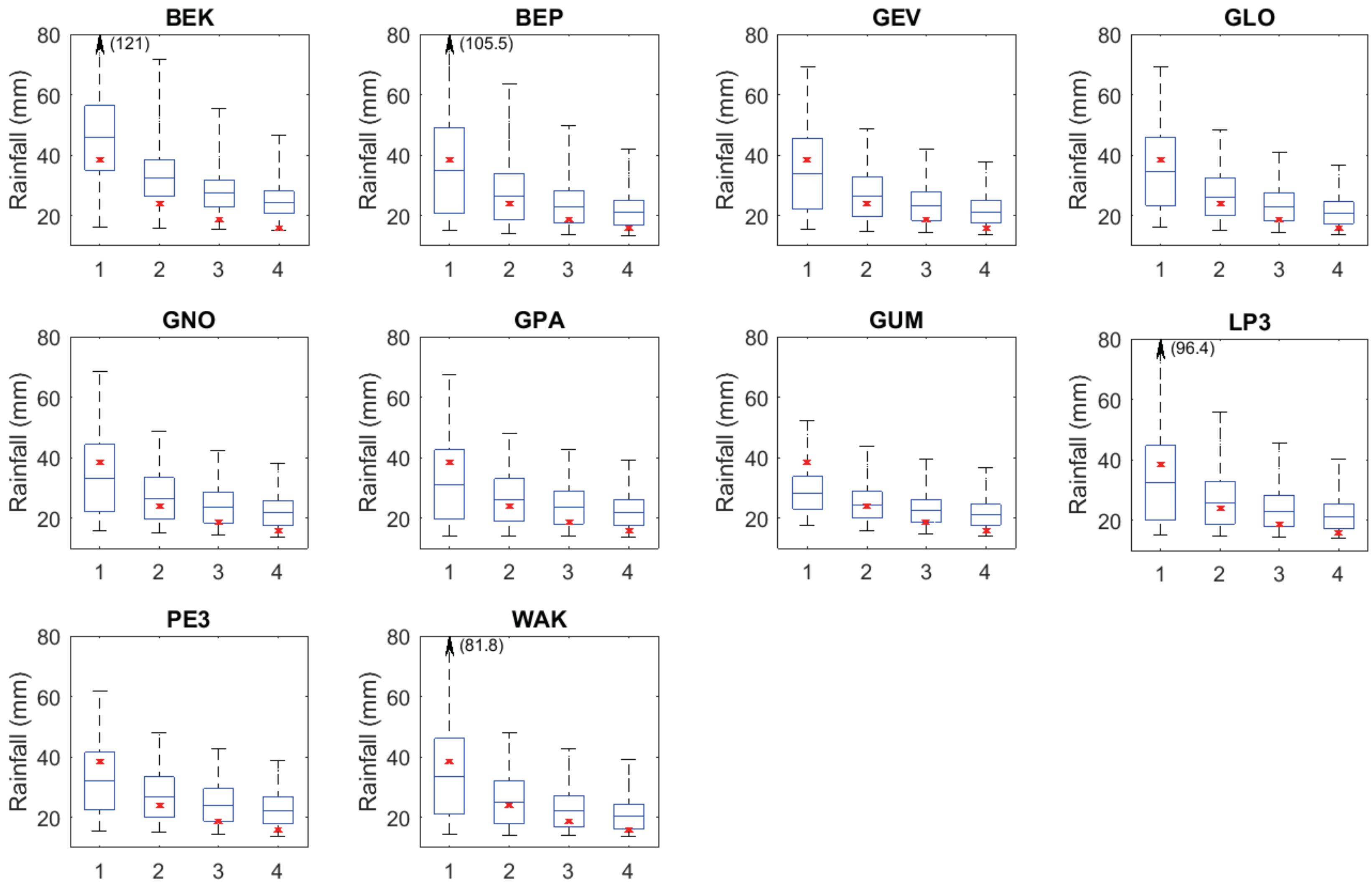

FIGURE 71 BOXPLOTS OF EXTRAPOLATED RIGHT-TAIL BOOTSTRAP DATA FOR 1HR RAINFALL OF VANCOUVER INTL A

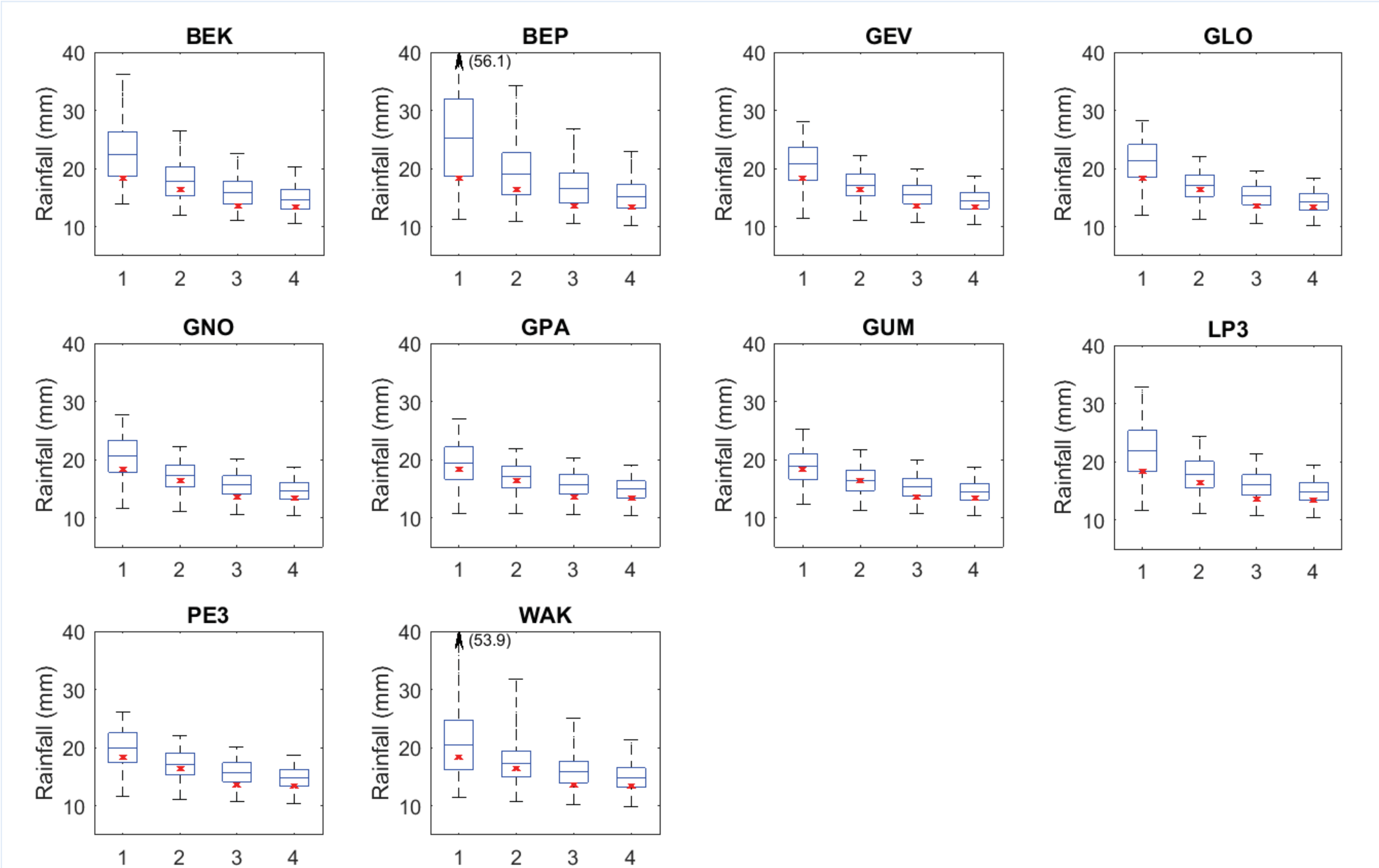

FIGURE 72 BOXPLOTS OF EXTRAPOLATED RIGHT-TAIL BOOTSTRAP DATA FOR 1HR RAINFALL OF VICTORIA INTL A

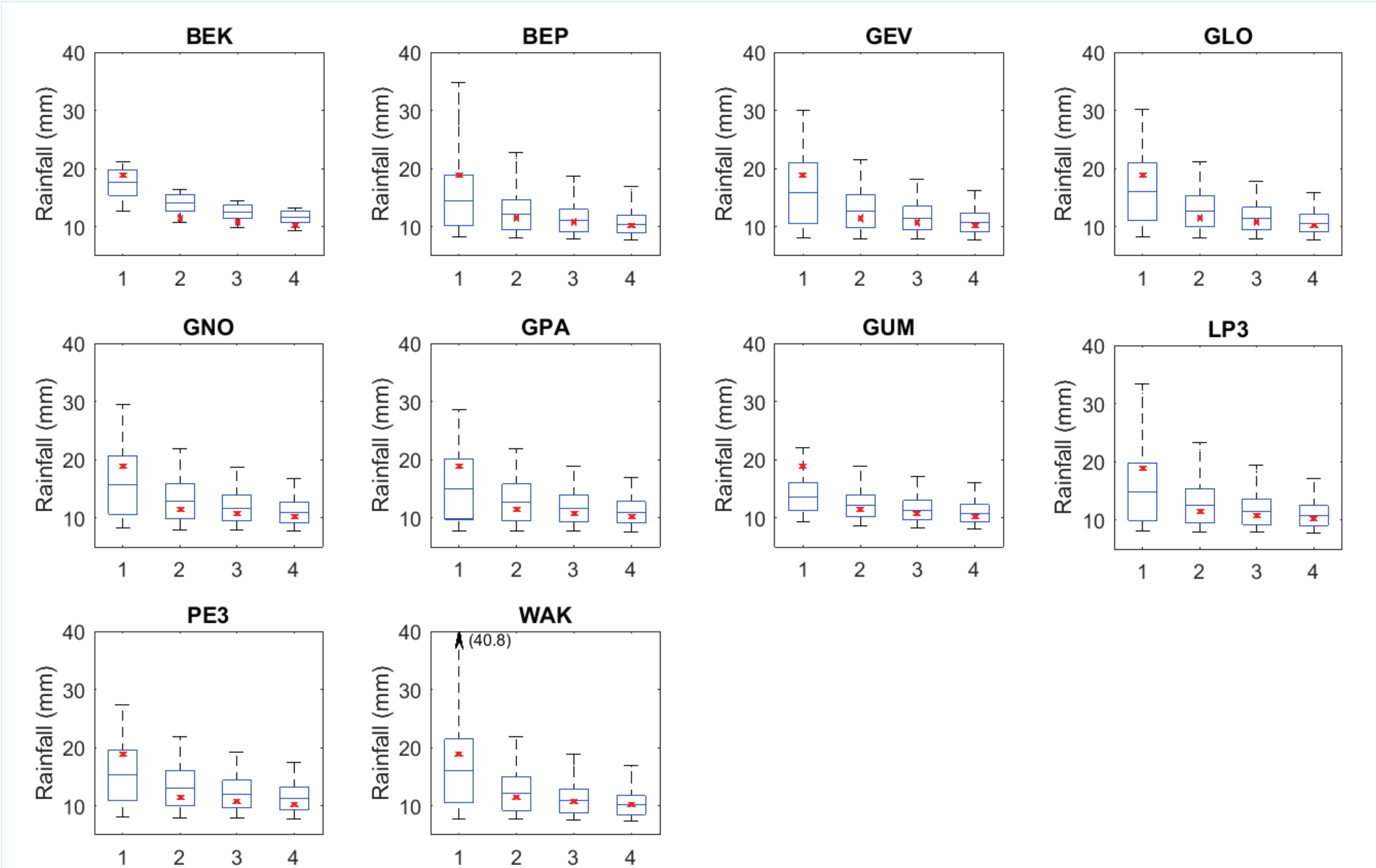

FIGURE 73 BOXPLOTS OF EXTRAPOLATED RIGHT-TAIL BOOTSTRAP DATA FOR 1HR RAINFALL OF VICTORIA GONZALES

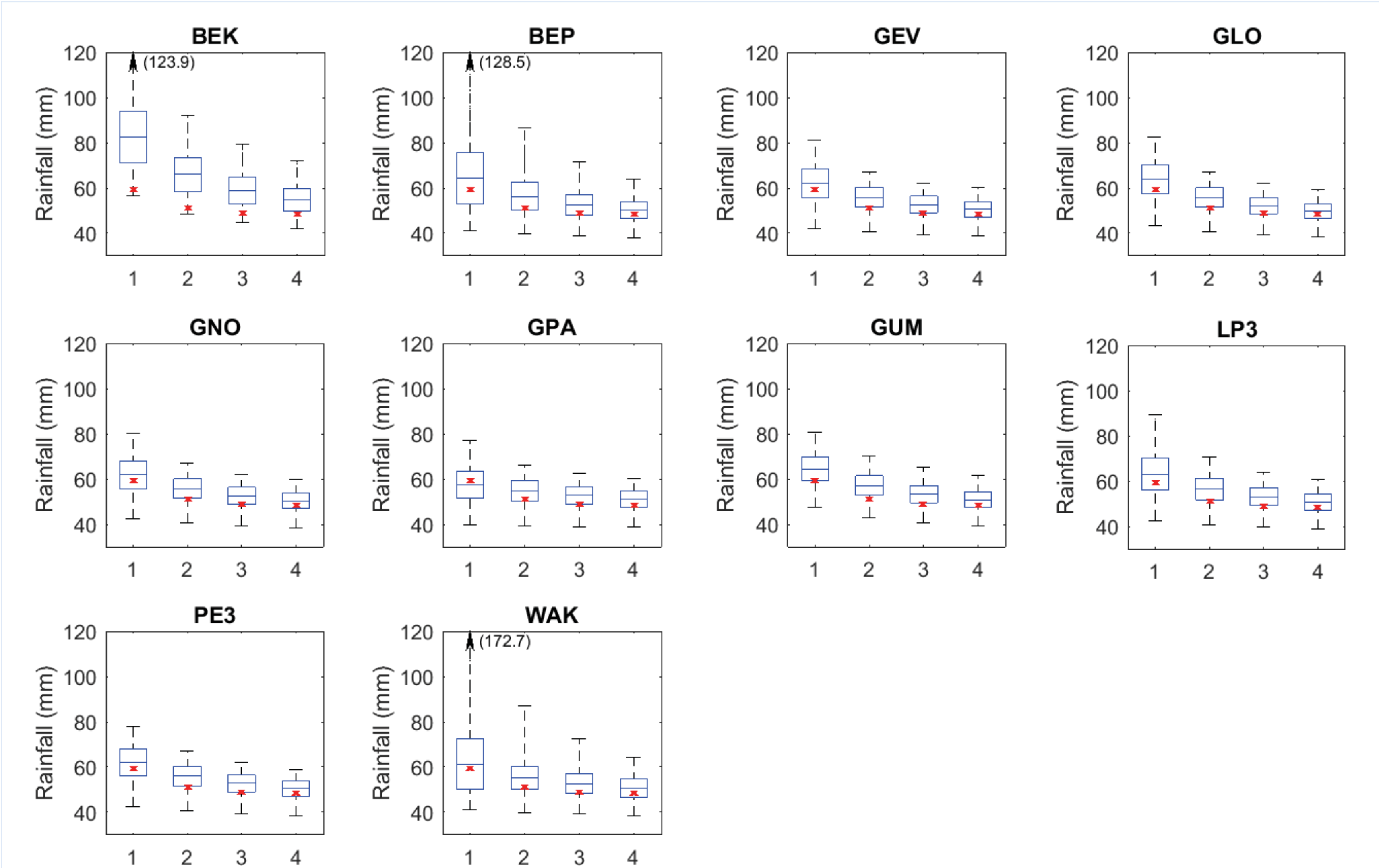

FIGURE 74 BOXPLOTS OF EXTRAPOLATED RIGHT-TAIL BOOTSTRAP DATA FOR 24HR RAINFALL OF BLUE RIVER A

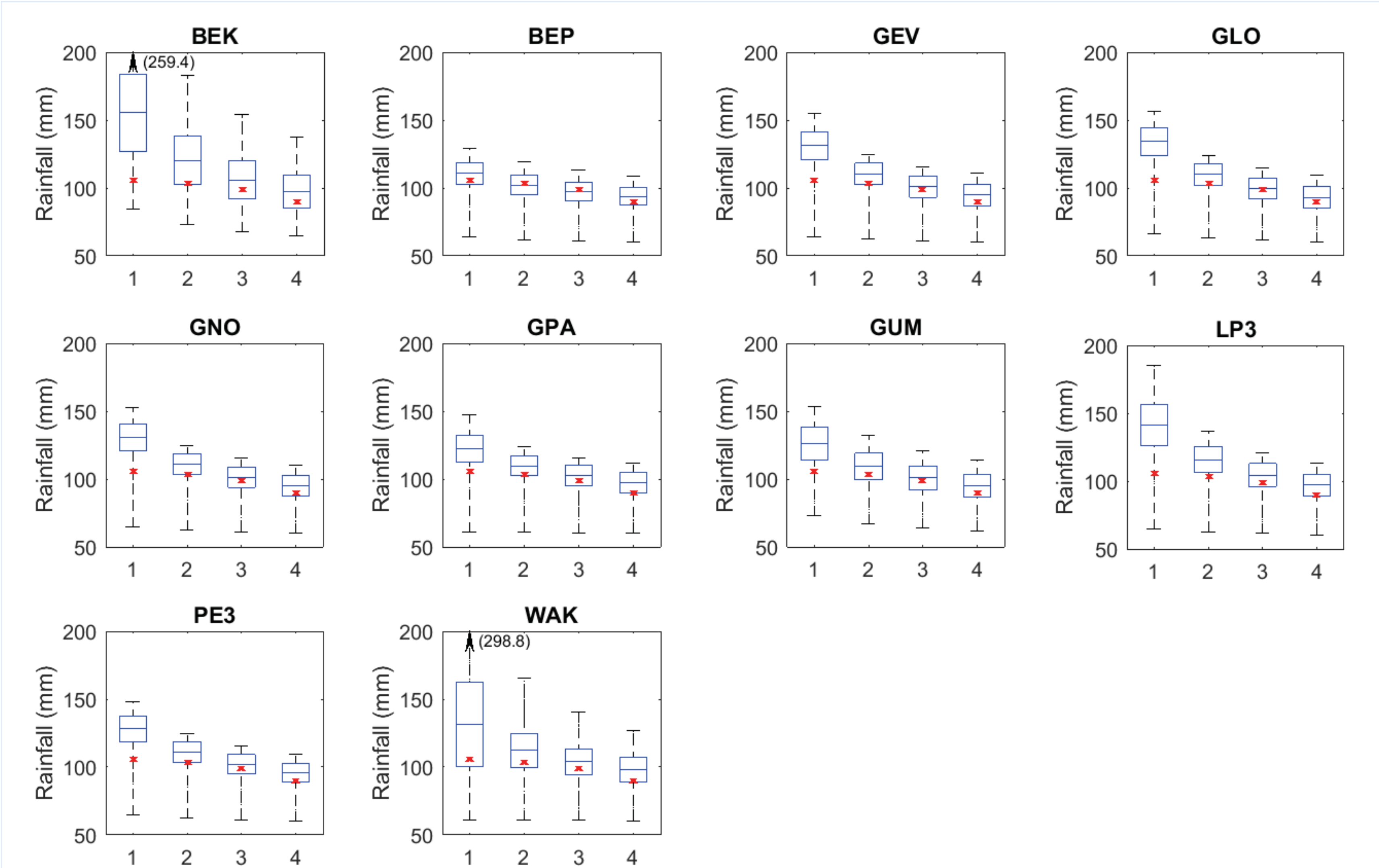

FIGURE 75 BOXPLOTS OF EXTRAPOLATED RIGHT-TAIL BOOTSTRAP DATA FOR 24HR RAINFALL OF COMOX A

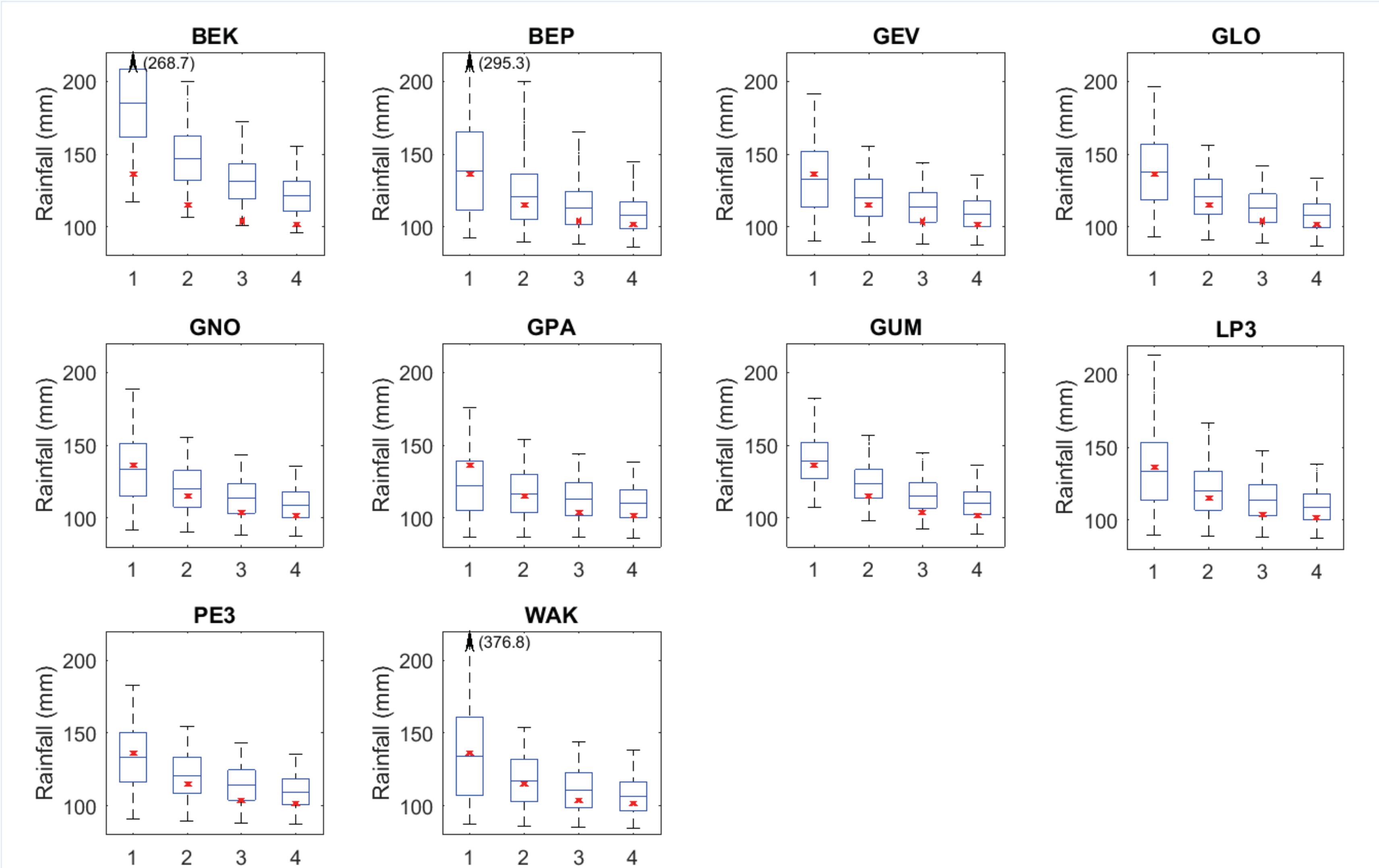

FIGURE 76 BOXPLOTS OF EXTRAPOLATED RIGHT-TAIL BOOTSTRAP DATA FOR 24HR RAINFALL OF MISSION WEST ABBEY

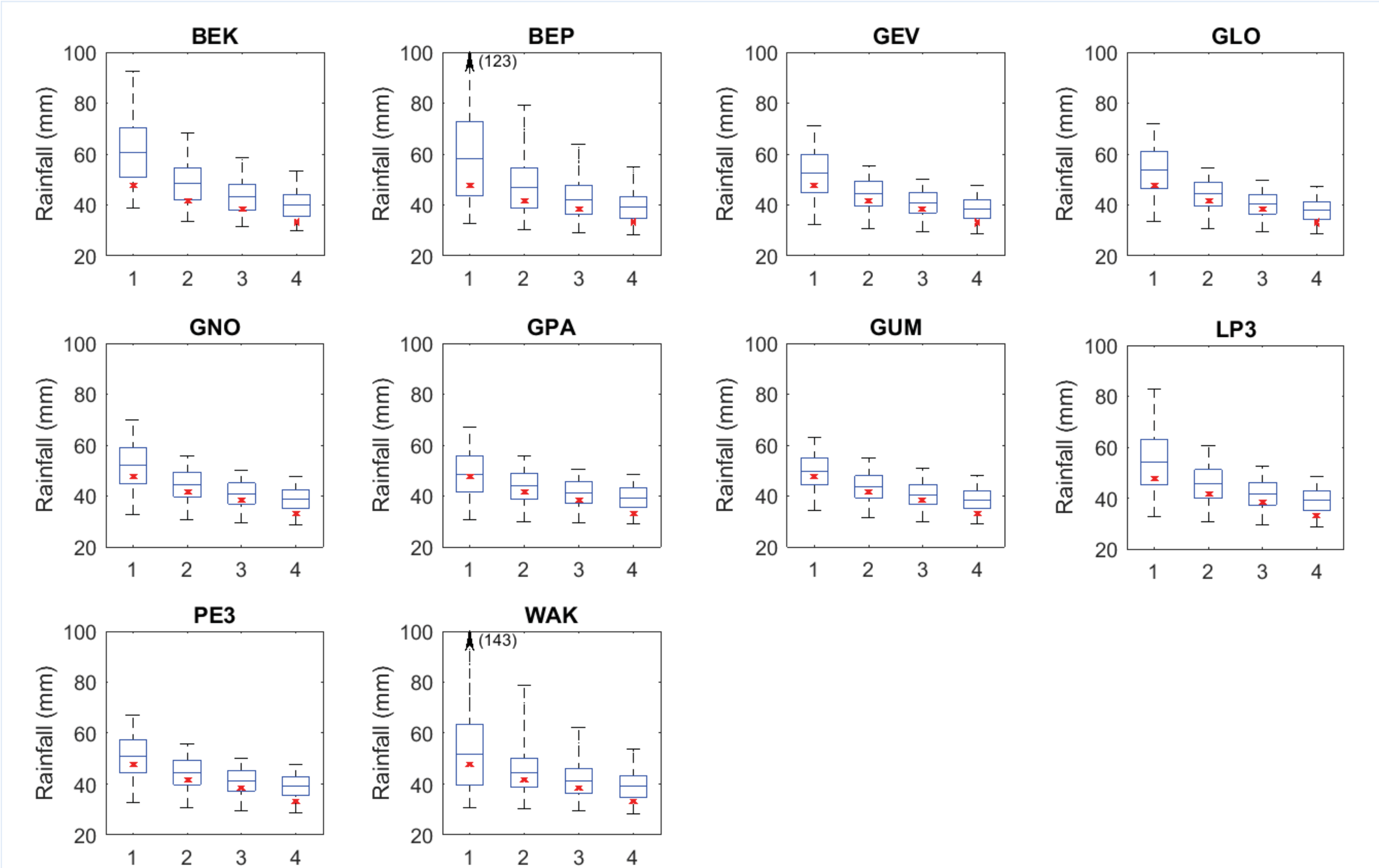

FIGURE 77 BOXPLOTS OF EXTRAPOLATED RIGHT-TAIL BOOTSTRAP DATA FOR 24HR RAINFALL OF PENTICTON A

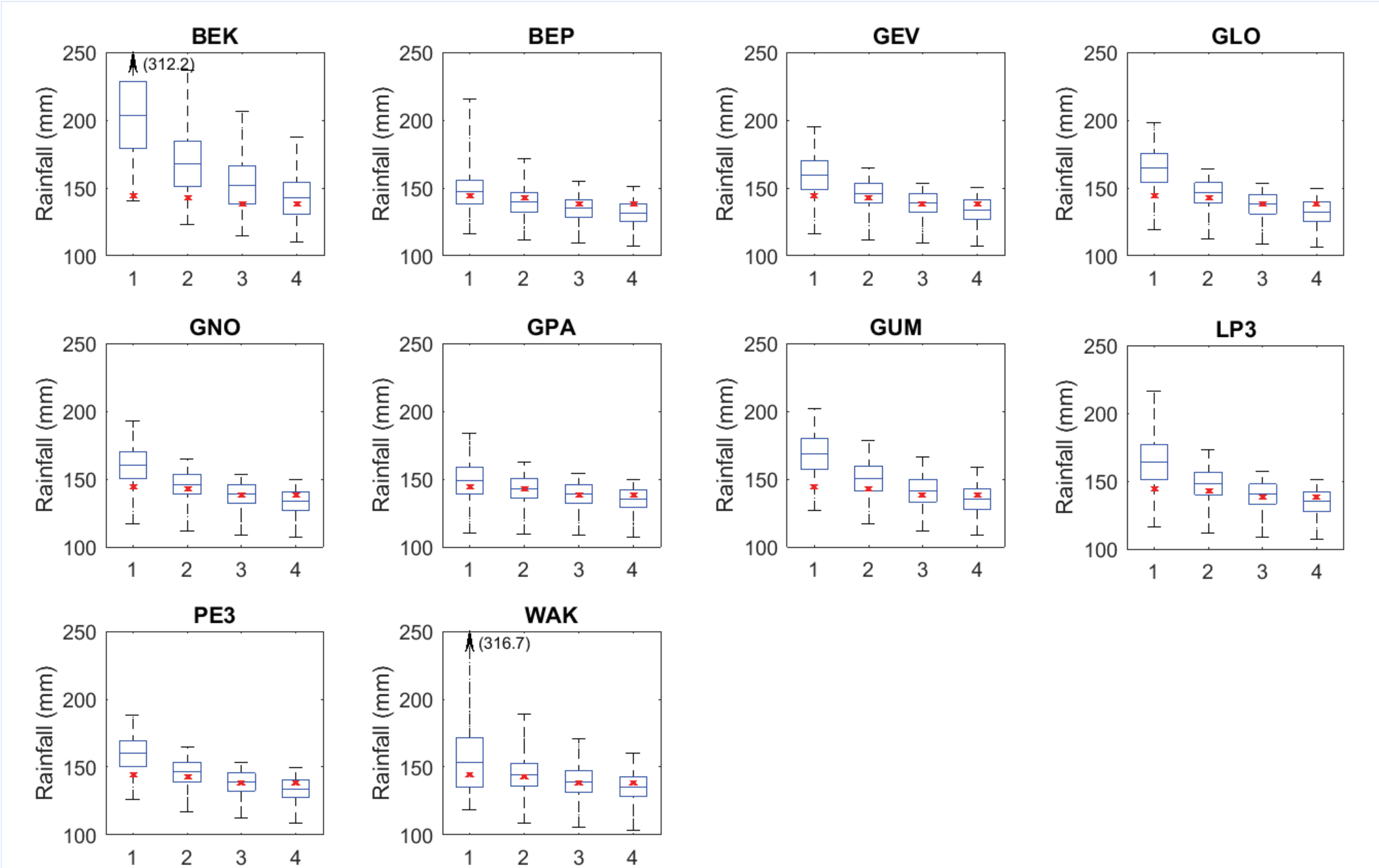

FIGURE 78 BOXPLOTS OF EXTRAPOLATED RIGHT-TAIL BOOTSTRAP DATA FOR 24HR RAINFALL OF PITT POLDER

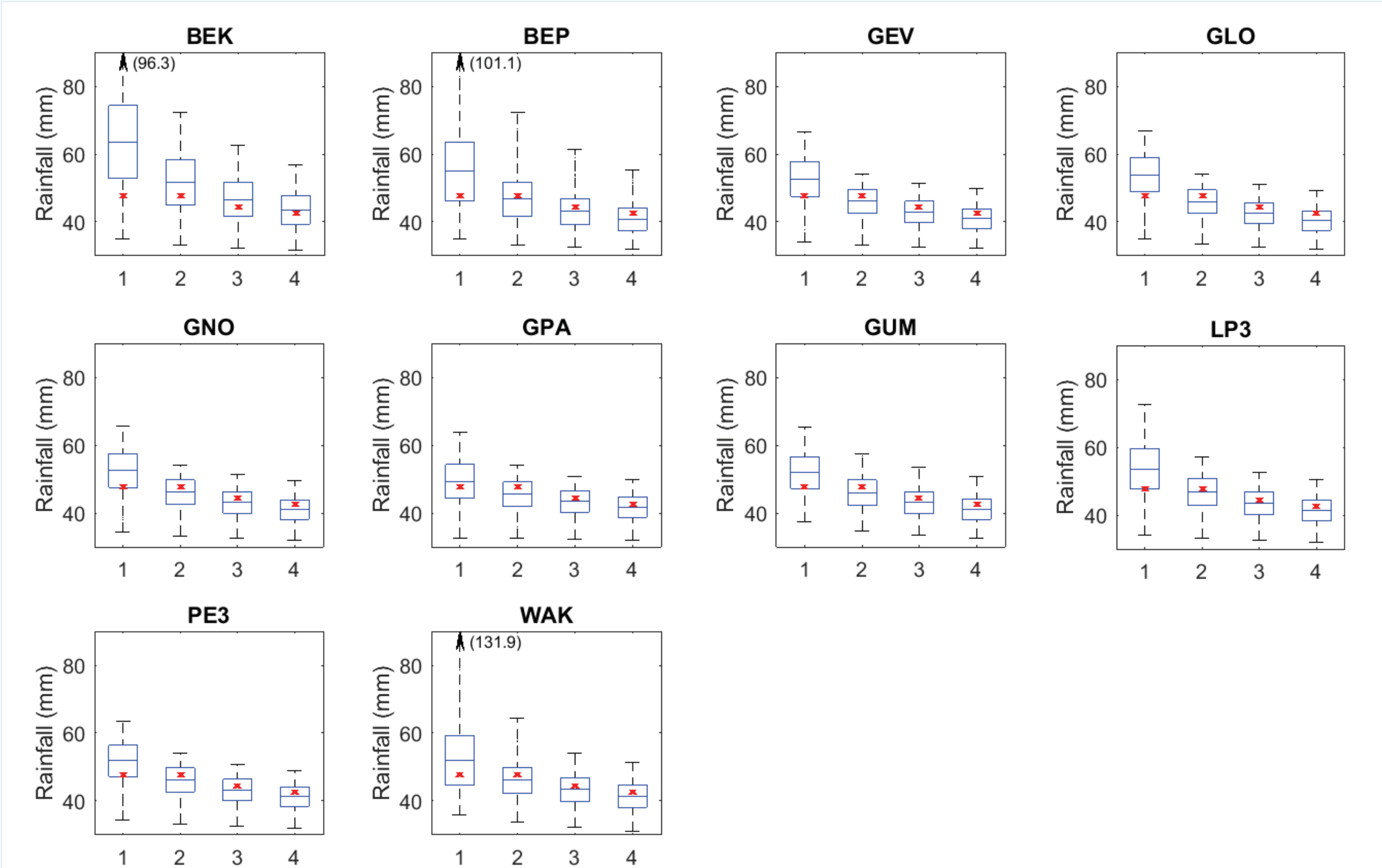

FIGURE 79 BOXPLOTS OF EXTRAPOLATED RIGHT-TAIL BOOTSTRAP DATA FOR 24HR RAINFALL OF PRINCE GEORGE A

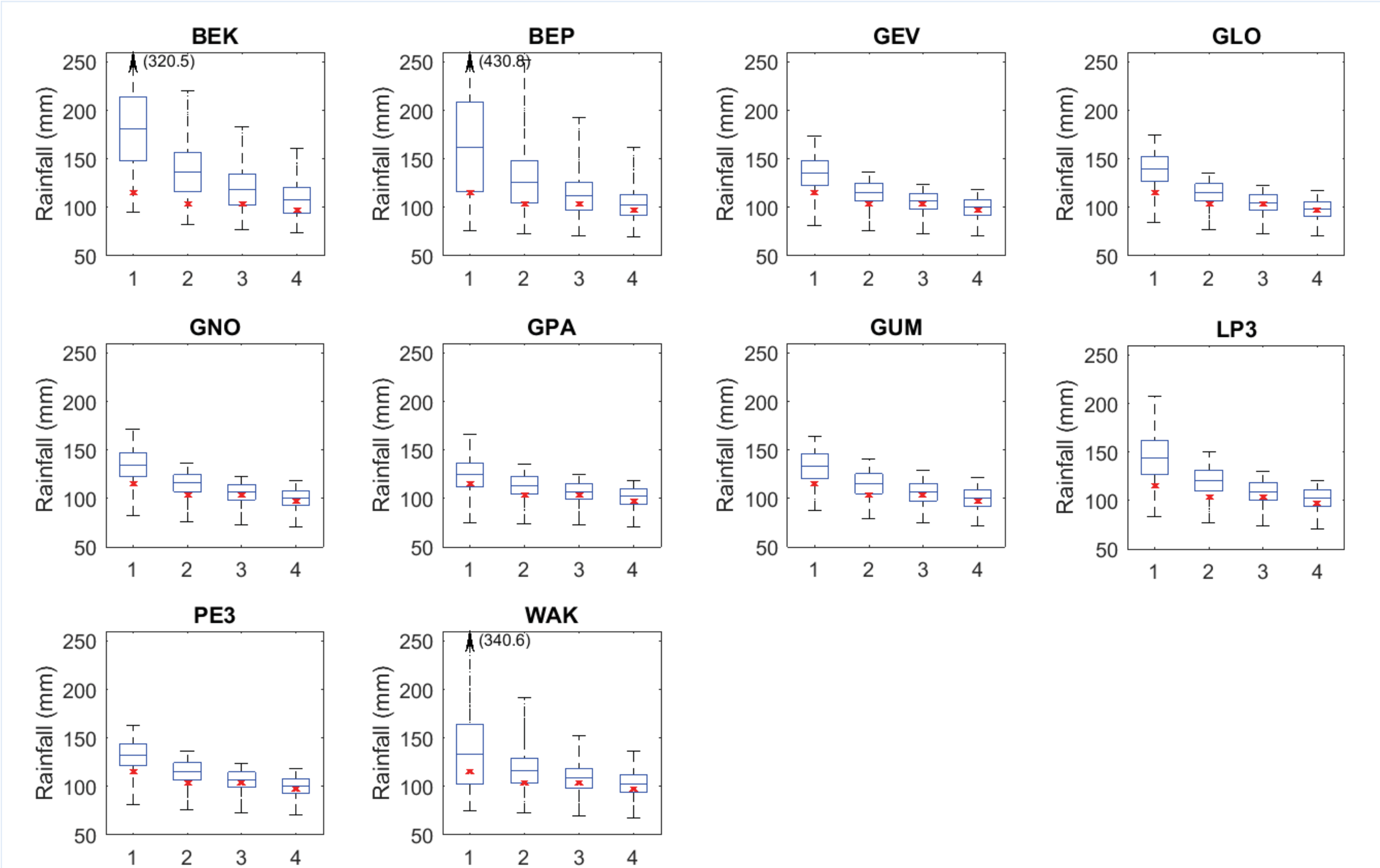

FIGURE 80 BOXPLOTS OF EXTRAPOLATED RIGHT-TAIL BOOTSTRAP DATA FOR 24HR RAINFALL OF TERRACE PCC

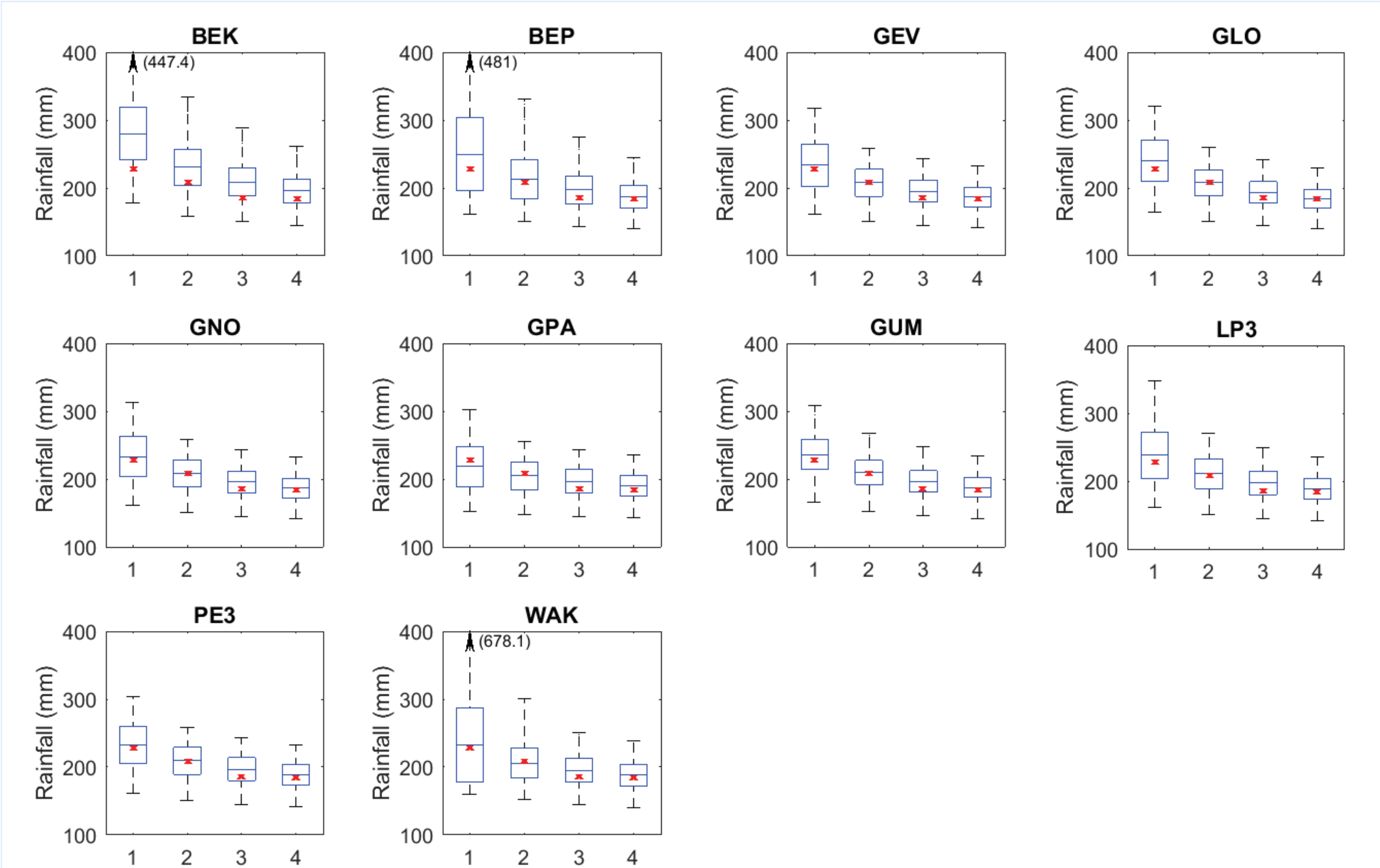

FIGURE 81 BOXPLOTS OF EXTRAPOLATED RIGHT-TAIL BOOTSTRAP DATA FOR 24HR RAINFALL OF TOFINO A

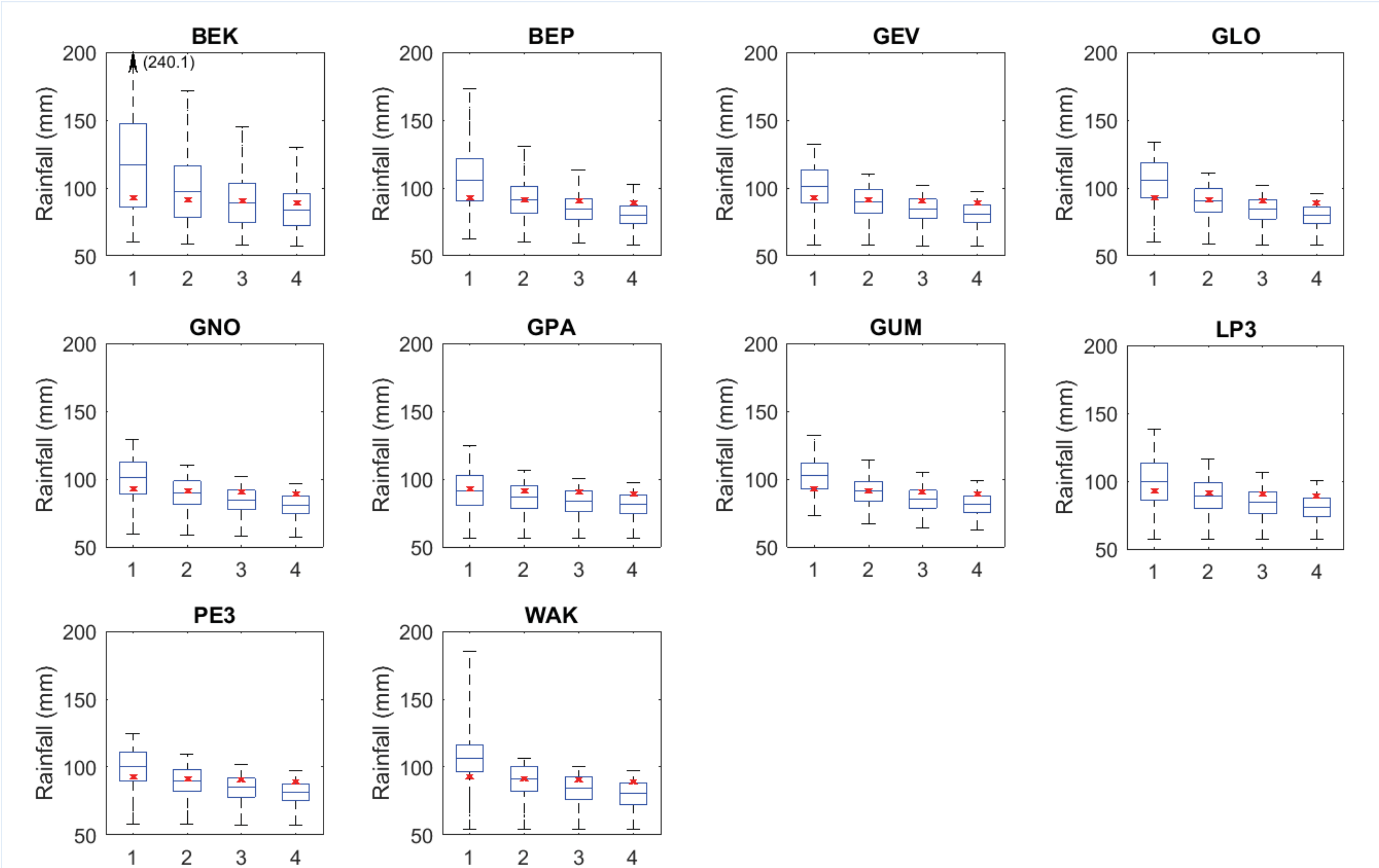

FIGURE 82 BOXPLOTS OF EXTRAPOLATED RIGHT-TAIL BOOTSTRAP DATA FOR 24HR RAINFALL OF VANCOUVER INTL A

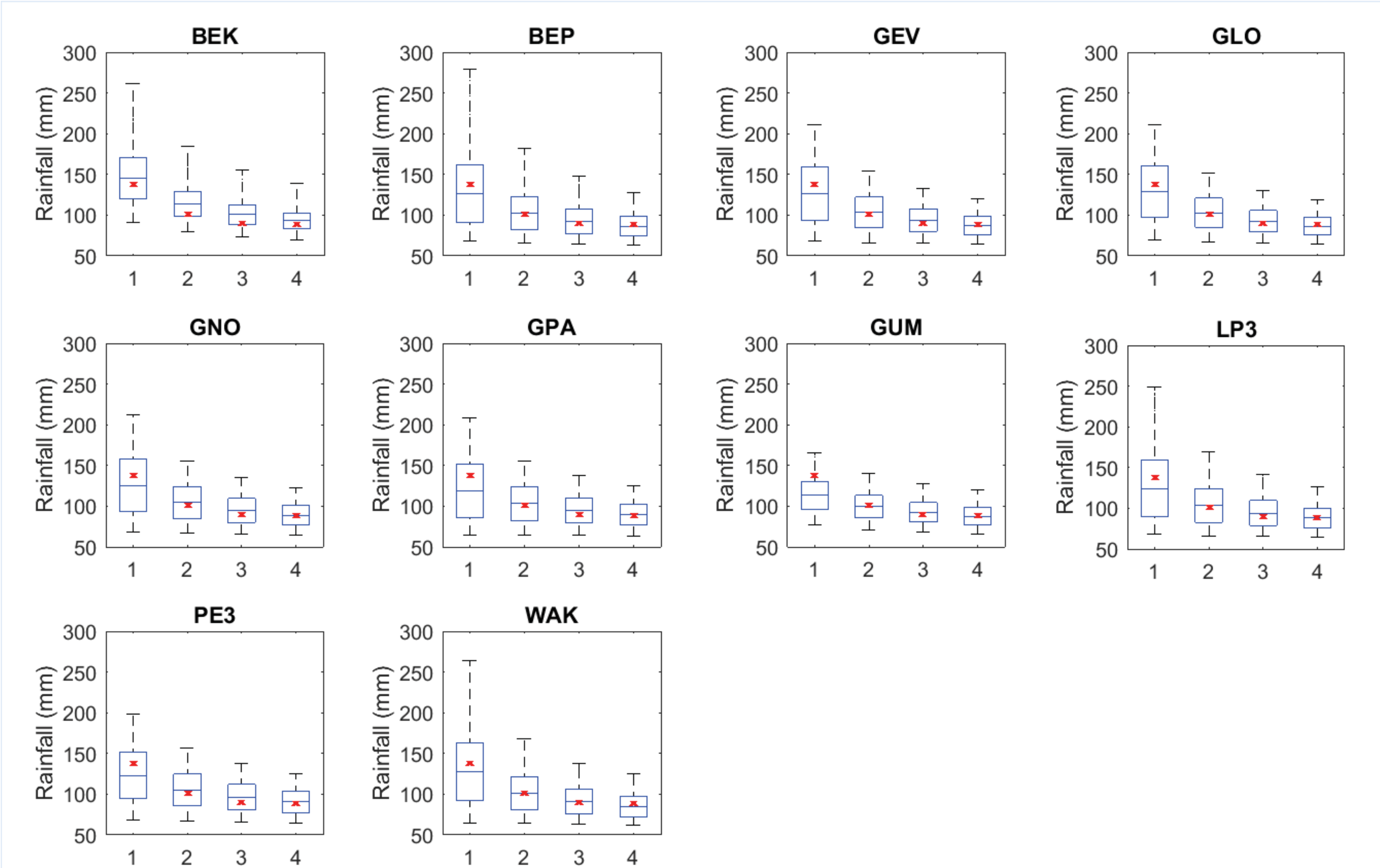

FIGURE 83 BOXPLOTS OF EXTRAPOLATED RIGHT-TAIL BOOTSTRAP DATA FOR 24HR RAINFALL OF VICTORIA INTL A

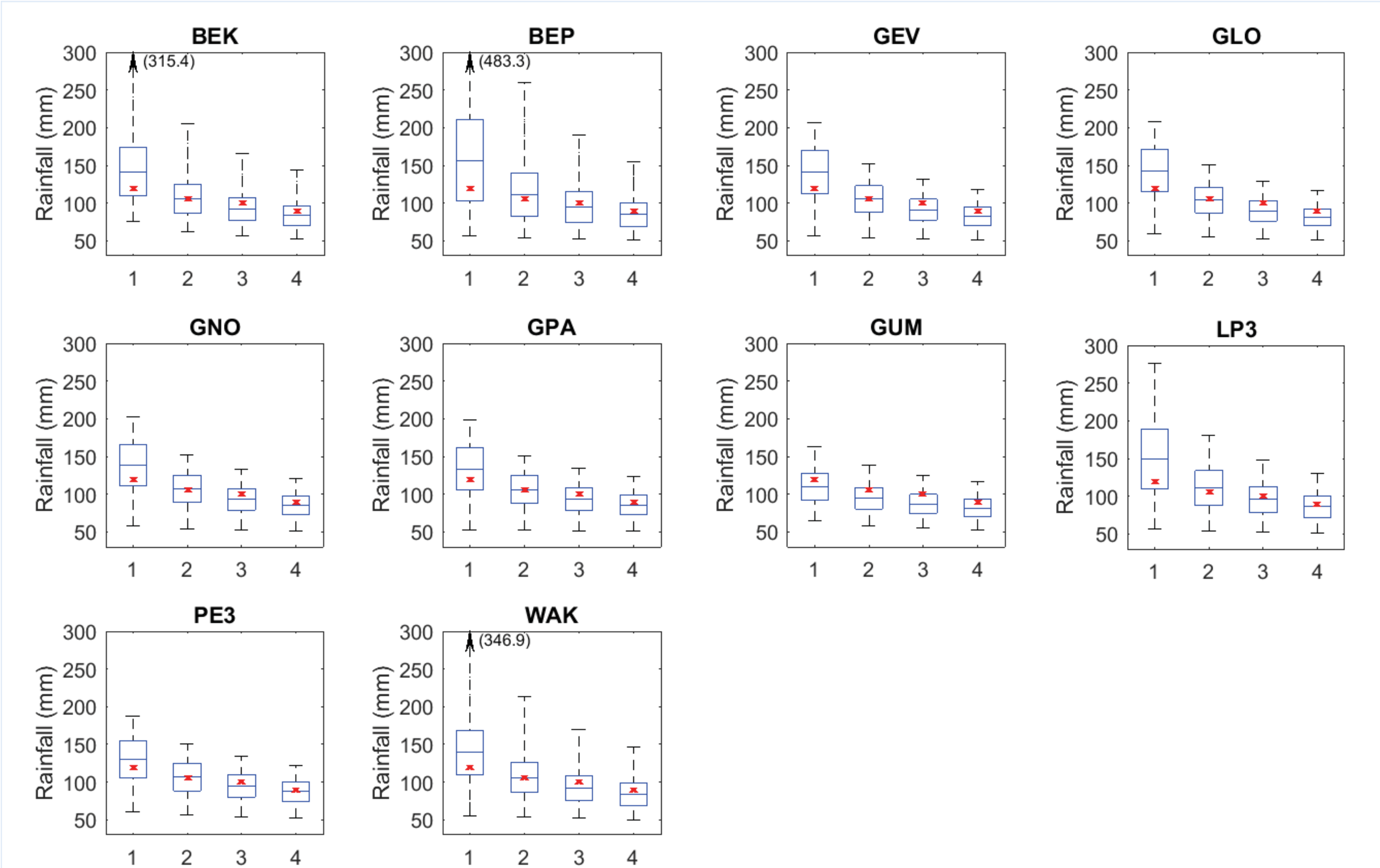

FIGURE 84 BOXPLOTS OF EXTRAPOLATED RIGHT-TAIL BOOTSTRAP DATA FOR 24HR RAINFALL OF VICTORIA GONZALES